

UNIVERSITY OF BIRMINGHAM

EXPLORING THE EFFECTS OF TRANSCRANIAL DIRECT CURRENT STIMULATION ON THALAMO-CORTICAL CONNECTIVITY; IMPLICATIONS FOR THERAPEUTIC INTERVENTIONS ON PROLONGED DISORDERS OF CONSCIOUSNESS

By

DAVIDE ALOI

A thesis submitted to the University of Birmingham for the degree of

DOCTOR OF PHILOSOPHY

The Centre for Human Brain Health (CHBH)

School of Psychology

College of Life and Environmental Sciences

University of Birmingham

26/05/2023

UNIVERSITY OF
BIRMINGHAM

University of Birmingham Research Archive

e-theses repository

This unpublished thesis/dissertation is copyright of the author and/or third parties. The intellectual property rights of the author or third parties in respect of this work are as defined by The Copyright Designs and Patents Act 1988 or as modified by any successor legislation.

Any use made of information contained in this thesis/dissertation must be in accordance with that legislation and must be properly acknowledged. Further distribution or reproduction in any format is prohibited without the permission of the copyright holder.

ABSTRACT

Prolonged disorders of consciousness (PDOC) are a medical condition characterised by heterogeneous brain atrophies. PDOC are clinically defined by an impairment of consciousness in one or more of its two components (i.e., awareness and wakefulness). Options for the rehabilitation of such disorders are limited, and restricted to disability management rather than treatment. Different neuroimaging studies revealed a subgroup of PDOC patients characterised by a lack of wakefulness and a partially (or fully) preserved awareness (i.e., Cognitive Motor Dissociation, CMD). Interestingly, the lack of behavioural responsiveness present in patients with CMD has been linked to a partial reduction of coupling in two key areas of the motor network, namely the thalamus and the primary motor cortex (M1). Recent evidence shows that Transcranial Direct Current Stimulation (tDCS) - a non-invasive brain stimulation technique - might have a potential therapeutic effect. This notwithstanding, the literature is highly inconsistent, and the neural basis of such putative therapeutic effects is still unknown.

This thesis proposes a new therapeutic direction that directly targets the mechanisms underlying the lack of responsiveness in PDOC. Using Dynamic Causal Modelling (DCM), I explored the effects of tDCS on motor-network dynamics during command-following in three functional Magnetic Resonance Imaging (fMRI) experiments conducted on healthy individuals. In Chapter 4, I administered a single session of M1-tDCS (*Experiment 1*) and of cerebellar-tDCS (*Experiment 2*). In Chapter 5, I investigated the effects of five M1-tDCS sessions paired with passive mobilisation (*Experiment 3)*. Additionally, in Chapter 6, I utilised magnetic resonance imaging (MRI) structural scans from the above experiments to model tDCS-induced electric fields and investigated the relationship between current density and connectivity changes following stimulation. Overall, I demonstrated that cathodal cerebellar-tDCS can selectively modulate thalamo-cortical connectivity during command-following in a polarity-specific manner (*Experiment 2*), while M1-tDCS reduced self-inhibition in the thalamus and M1 (*Experiment 1* and *3*, respectively). Therefore, I propose that the tDCS protocols used in this thesis could help sustain PDOC rehabilitation either by directly

modulating thalamo-cortical connectivity or by reducing thalamic and M1 self-inhibition. Moreover, the relationship between current density metrics and effective connectivity following tDCS suggests that considering stimulation parameters based on subjects' electric field models might help mitigate inter-individual differences in tDCS effectiveness. Lastly, I tested the methods employed throughout the thesis on a PDOC patient in a multi-session multi-modal tDCS study. It is noteworthy that the data collection was restricted to one patient due to the impact of COVID-19.

ACKNOWLEDGEMENTS

First and foremost, I would like to thank my supervisors, Dr Davinia Fernández-Espejo, and Dr Damian Cruse, for the constant guidance they have provided throughout my PhD, and for creating such a friendly and supportive environment in the lab.

To Antonio Incisa della Rocchetta and the staff of Wellington Hospital, thank you for your assistance with the data collection of the Raindrop project.

To all the members of the DoC lab, Leah, Consu and Damiano, who made the office a fun place to be; To Rodi, who always patiently answered my countless questions about EEG; To Sean, with whom I spent some very pleasant months sharing a flat (your reinterpretation of paella isn't that bad after all); To Roya and Melanie, with whom I shared endless hours in the MRI scanner. Huge thanks to my PhD buddy Sara, with whom I shared the joys and frustrations of the PhD. Without your help, I would still be running DCM analyses. To my friend Sabrina, we finally made it through this journey!

Thanks to Mike, who made Selly Oak a not-so-terrible place to live, and to my fellow countrymen Ale and Albe for all the trips and fun we shared during the first months in Birmingham.

I am extremely grateful to my parents and siblings, who were always there for me, even from afar and during difficult times. Thanks, Dad, for picking me up at the airport at the most random times. Mamma, grazie per avermi fatto bello. Thanks to my brother, with whom I shared many lockdown months, along with many, many glasses of Amaro del Capo, and post-curfew illegal spritz. A special thanks to my sister Clio for producing the cutest creature ever, who has brightened our days since day one.

To my ex-flatmate Enrico: I cannot count the laughs and adventures we had together. This experience wouldn't have been the same without you. I'll always be amazed at the fact that we managed to not kill each other during lockdown.

I would like to extend my gratitude to my lifelong friends, Edo, Feps, and Tommi, for the support they did not provide during the past years (cit.). I miss you all the time!

Lastly, I would like to thank the CHBH, for giving me the chance to meet my ‘media naranja’, Bianca.

"Per ogni fine c'è un nuovo inizio"

Antoine de Saint-Exupéry

TABLE OF CONTENTS

Page

ABSTRACT **1**
ACKNOWLEDGEMENTS **3**
TABLE OF CONTENTS **4**
LIST OF FIGURES **9**
LIST OF TABLES **12**
KEY ABBREVIATIONS **14**
LIST OF PUBLICATIONS **18**
INTRODUCTION TO DISORDERS OF CONSCIOUSNESS AND TRANSCRANIAL DIRECT CURRENT STIMULATION **1**
1.1. Consciousness 1
1.2. Nosology of Disorders of Consciousness 2
1.3. Behavioural assessment of PDOC 4
1.4. Cognitive-motor dissociation in PDOC patients 6
1.5. Additional methods for the detection awareness in PDOC patients: rs-fMRI and EEG 8
1.6. tDCS 12
THERAPEUTIC USE OF TRANSCRANIAL DIRECT CURRENT STIMULATION IN THE REHABILITATION OF PROLONGED DISORDERS OF CONSCIOUSNESS, **27**
2.1. Abstract 27
2.2. Introduction 28
2.3. Clinical effects of tDCS in PDOC 30
2.4. Target areas 39
2.5. Number of treatment sessions 41
2.6. Long term effects of tDCS 42
2.7. Effects of tDCS on brain function 44
2.8. Common Methodological Limitations 46
2.9. Integration of tDCS in current pathways of care for PDOC 59
2.10. Conclusions 65
GENERAL METHODS **68**
3.1. A brief introduction to Functional Magnetic Resonance Imaging 69
3.2. Experimental design and fMRI tasks 69
3.3. (f)MRI sequences 70
3.4. Additional methods used in the case study 70
3.5. tDCS montages and parameters 71
3.6. Behavioural data analysis 75
3.7. Brief overview on Bayesian statistics 75
3.8. Overview of the effective connectivity analyses in the current thesis 77
TDCS MODULATES EFFECTIVE CONNECTIVITY DURING MOTOR COMMAND FOLLOWING;

A POTENTIAL THERAPEUTIC TARGET FOR DISORDERS OF CONSCIOUSNESS 82
4.1. Abstract 82
4.2. Introduction 83
4.3. Material and methods 85
4.4. Results 100
4.5. Discussion 104
4.6. Conclusions 111
MULTI-SESSION TDCS PAIRED WITH PASSIVE MOBILISATION OF THE THUMB MODULATES THALAMO-CORTICAL COUPLING DURING COMMAND FOLLOWING IN THE HEALTHY BRAIN 113
5.1. Abstract 113
5.2. Introduction 114
5.3. Materials and Methods 116
5.4. Results 128
5.5. Discussion 137
5.6. Conclusions 141
EXPLORING THE RELATIONSHIP BETWEEN ELECTRIC FIELD CHARACTERISTICS AND TDCS-INDUCED CONNECTIVITY CHANGES IN THE MOTOR NETWORK 143
6.1. Introduction 143
6.2. Methods 145
6.3. Results 156
6.4. Discussion 162
TDCS COMBINED WITH PASSIVE MOBILISATION IN PDOC: A MULTI-MODAL MULTI-SESSION CASE STUDY 170
7.1. Introduction 170
7.2. Methods 172
7.3. Results 188
7.4. Discussion 201
GENERAL DISCUSSION 208
8.1. Summary of aims and results 208
8.2. Interpretation of results 210
8.4. Limitations of the Research 219
8.5. Conclusions and future directions 221
APPENDIX 225
Appendix A 225
Appendix B 229
Appendix C 234
Appendix D 239
Appendix E 243
REFERENCES 245

LIST OF FIGURES

Figure 1.1. Schematic representation of the taxonomy of Disorders of Consciousness……. 6

Figure 2.1. Comparison between conventional tDCS and HD-tDCS montages targeting the left DLPFC……... 40

Figure 2.2. Representation of the pathways of care for PDOC patients as proposed by the Royal College of Physicians (2020)..……... 63

Figure. 4.1. Experimental Design and tDCS montages……. 90

Figure 4.2. Analysis pipeline**.**…….. 93

Figure 4.3. Activation at Baseline.…….. 97

Figure 4.4. Effects of tDCS on brain activation during command following (Experiment 1).……. 101

Figure 4.5. Effects of tDCS on functional neural dynamics with M1 or the cerebellum as targets.…….. 102

Figure 5.1. Study Design and tDCS montage.……..... 119

Figure 5.2. Analysis pipeline.…….…… 123

Figure 5.3. Activation at baseline. Brain activation at the group level (RFX, 1-sample t-test) for the command-following task.…….….. 129

Figure 5.4. Effects of M1-tDCS on neural dynamics.…….…… 134

Figure 5.5. Effects of M1-tDCS on thalamo-M1 coupling.…… 135

Figure 6.1. fMRI protocol and analysis pipeline.…… 157

Figure 6.2. Median current density values for the 3 experiments.…….. 158

Figure 6.3. CCA results for *Experiment 3*, (Day5-MRI)..... 160

Figure 7.1. T1-weighted image of the patient..... 174

Figure 7.2. Experimental procedure..... 176

Figure 7.3. Brain activation results for the motor-imagery task (SMA ROI) and command-following task (SMA and M1 ROIs)..... 189

Figure 7.4. Results of the ERD analysis for the EEG command-following task, for the third (EEG baseline) and fourth (EEG post anodal tDCS) weeks of testing (i.e., anodal stimulation)..... 191

Figure 7.5. CRS-R results..... 193

Figure 7.6. The figure shows the effects of M1-tDCS on functional neural dynamics..... 194

Figure 7.7. Results of the seed-to-voxel connectivity analysis with the left PCC seed (reported in blue) for the resting-state session following the first anodal M1-tDCS (Day-1). 197

Figure 7.8. Motion tracking data (euclidean distance between the two motion tracking sensors) for the EEG command-following task of week 3 (EEG baseline) and week 4 (after anodal tDCS)..... 198

Figure 7.9. Results of the resting-state EEG analyses..... 200

Figure 8.1. Electrode locations in *Experiment 1* (first and second head models) and *Experiment 3* (third and fourth head models)..... 213

Figure B1. Brain activation during command following across trials..... 233

Figure C1. Effective connectivity on the pre-tDCS run on Day1-MRI session..... 236

Figure C2. Effects of M1-tDCS on behavioural metrics..... 237

Figure D.1. Additional PEB results for Experiment 3……... 240

Figure D.2. Axial views of the generated electric-field maps (V/m) for each participant, for Experiments 1, 2 and 3…….…….. 242

LIST OF TABLES

Table 2.1. *Overview of single session tDCS studies in PDOC*…… 32

Table 2.2. *Overview of multiple session tDCS studies in PDOC*……... 35

Table 2.3. *Demographics and aetiologies of VS and MCS patients included in the different studies*……. 51

Table 3.1. E*xperiments summary*……..…….…….…….. 73

Table 4.1. *Canonical activation during command-following*…….……. 95

Table 5.1: *Canonical activation during command-following*…….……... 131

Table 6.2. *Cross- and canonical loadings from the CCA analysis for Experiment 3 (Day5-MRI)*……... 159

Table 6.3. *Voxel-wise correlation analysis results*……..…….. 161

Table 7.1. *Brain activation during motor-imagery (Cathodal Day-1)*……..…… 174

Table 7.2. *Brain activation during command-following (Cathodal Day-1, before stimulation)*…….……... 190

Table 7.3. *Brain activation during passive-mobilisation*…….. 195

Table 7. 4. *Results for the seed-to-voxel correlation analyses (Anodal Day-1, post stimulation)*…….……... 196

Table B1. *Effect of M1-tDCS on brain activation*…….…..…….. 229

Table B2. *Effects of tDCS on behavioural metrics*……..……. 230

Table B3. *Blinding*……...…….. 232

Table C1. *Effects of tDCS on behavioural metrics (V2)*…… 234

Table D.1. *Electric-field medians and max values*……...…….… 239

Table E1. *Instructions of the tasks included in the case study*…….…….. 243

KEY ABBREVIATIONS

AAL: automatic anatomical labelling

ABI: acquired brain injury

AC-PC: anterior commissure posterior commissure

ANOVA: analysis of variance

BMA: bayesian model average

BMI: bayesian model inversion

BMR: bayesian model reduction

BOLD: blood-oxygenation level dependent

CB: cerebellum

CBI: cerebellar-brain inhibition

cb-tDCS: cerebellar tDCS

CCA: canonical correlation analysis

CF-fMRI: command-following fMRI

CMD: cognitive motor dissociation

CRS-R: coma recovery scale revised

CSF: cerebrospinal fluid

CV: canonical variate

CVA: cerebrovascular accident

DCM: dynamic causal modelling

DCN: deep cerebellar nuclei

DLPFC: dorsolateral prefrontal cortex

DMN: default mode network

DOC: disorders of consciousness

DTI: diffusion tensor imaging

DWI: diffusion weighted images

EEG: electroencephalography

E-field: electric field

e-LTP: early long-term potentiation

EMCS: emerging from minimally conscious state

EPI: echo-planar imaging

ERD: event-related desynchronisation

ERPs: event-related potentials

ERS: event-related synchronisation

FDR: false-discovery rate

FEM: finite-element model

FLAIR: fluid-attenuated inversion recovery

fMRI: functional magnetic resonance imaging

FOUR: full outcome unresponsiveness

FPN: fronto-parietal networks

FTPC: fronto-temporal-parietal cortices

FWE: family-wise error

FWHM: full-width-half-maximum

GCS: glasgow coma scale

GLM: general linear model

GOS-E: Glasgow outcome scale extended

HC: healthy controls

HD-EEG: high definition EEG

HD-tDCS: high definition tDCS

HRF: haemodynamic response function

ICU: intensive care unit

LIFU: low-intensity focused ultrasound

LIS: locked-in syndrome

l-LTP: late long term-potentiation

M1: primary motor cortex

MCS: minimally conscious state

MCS+: high-level MCS

MEP: motor-evoked potentials

MRI: magnetic resonance imaging

NCCs: neural correlates of consciousness

NIBS: non-invasive brain stimulation

OFC: orbitofrontal cortex

PDOC: prolonged disorders of consciousness

PEB: parametric empirical bayes

ROI: region of interest

RPE: rate of perceived exertion

rs-EEG: resting-state EEG

rs-fMRI: resting-state fMRI

RX: random effects

SMA: supplementary motor area

SPM: statistical parametric mapping

T1-w: T1-weighted

T2-w: T2-weighted

TBI: traumatic brain injury

tDCS: transcranial direct current stimulation

TE: echo time

tES: transcranial electrical stimulation

TH: thalamus

TMS: transcranial magnetic stimulation

ToCs: theories of consciousness

tPCS: transcranial pulsed-current stimulation

TR: repetition time

UWS: unresponsive wakefulness syndrome

VLPDC: ventrolateral prefrontal cortex

VOI: volume of interest

VS: vegetative state

WNSSP: Western Neuro Sensory Stimulation Profile

wPLI: weighted phase-lag index

wSMI: weights symbolic mutual information

LIST OF PUBLICATIONS

Below is a list of published work included in this thesis. Author contributions are also outlined.

Paper 1

Aloi, D., della Rocchetta, A. I., Ditchfield, A., Coulborn, S., & Fernández-Espejo, D. (2021). Therapeutic Use of Transcranial Direct Current Stimulation in the Rehabilitation of Prolonged Disorders of Consciousness. Frontiers in Neurology, 12, 632572. https://doi.org/10.3389/fneur.2021.632572

Author contributions:

Davide Aloi, Literature review, Writing –original draft, Writing –review & editing; Antonio Incisa Della Rocchetta: Literature review, Writing –review & editing; Sean Coulborn: Literature review, Writing –review & editing; Davinia Fernández-Espejo: Writing –original draft, Writing –review & editing;

The above publication forms the entire body of **Chapter 2**, as it was published.

Paper 2

Aloi, D., Jalali, R., Tilsley, P., Miall, R. C., & Fernández-Espejo, D. (2022). TDCS modulates effective connectivity during motor command following; a potential therapeutic target for disorders of consciousness. NeuroImage, 247, 118781. https://doi.org/10.1016/j.neuroimage.2021.118781

Author contributions: Davide Aloi: Formal analysis, Methodology, Writing –original draft, Writing –review & editing. Roya Jalali: Investigation, Methodology, Writing –original draft, Writing –review & editing. Penelope Tils- ley: Investigation, Methodology, Writing –review & editing. R. Chris Miall: Methodology, Writing –review & editing. Davinia Fernández-

Espejo: Visualization, Funding acquisition, Data curation, Formal analy- sis, Methodology, Supervision, Writing –original draft, Writing –review & editing.

The above publication forms the entire body of **Chapter 4**, as it was published.

Paper 3

Aloi, D., Jalali, R., Calzolari, S., Lafanechere, M., Miall, R. C., & Fernández-Espejo, D. (2022). Multi-session tDCS paired with passive mobilisation increases thalamo-cortical coupling during command following [Preprint]. BiorXiv. https://doi.org/10.1101/2022.11.22.517479

Author contributions: Davide Aloi: Investigation, Data curation, Formal analysis, Methodology, Writing – original draft, Writing – review & editing. Roya Jalali: Investigation, Methodology, Writing – review & editing. Sara Calzolari: Methodology, Writing – review & editing. Melanie Lafanechere: Investigation, Writing - review & editing. R. Chris Miall: Methodology, Writing – review & editing. Davinia Fernández-Espejo: Visualization, Funding acquisition, Data curation, Methodology, Supervision, Writing – original draft, Writing – review & editing.

The above preprint forms the entire body of **Chapter 5,** as it was published (in preprint).

*Note that an updated version of **Paper 3** was subsequently published on Neuroimage*:

Aloi, D., Jalali, R., Calzolari, S., Lafanechere, M., Miall, R. C., & Fernández-Espejo, D. (2023). Multi-session tDCS paired with passive mobilisation of the thumb modulates thalamo-cortical coupling during command following in the healthy brain. NeuroImage, 120145. https://doi.org/10.1016/j.neuroimage.2023.120145

Chapter 1

INTRODUCTION TO DISORDERS OF CONSCIOUSNESS AND TRANSCRANIAL DIRECT CURRENT STIMULATION

1.1. Consciousness

There is considerable debate regarding a precise definition and explanation of consciousness. It is even argued that fully comprehending consciousness requires relying on internal experiences, which are not fully explicable through current scientific methods, that only rely on external observation (Blumenfeld, 2023). This issue has been referred to as the "hard" problem of consciousness (Chalmers & Cruz, 2016). This notwithstanding, there is a significant body of scientific literature aimed at explaining the *neural correlates of consciousness* (NCCs), that is, the link between brain activity and consciousness. As pointed out by Seth & Bayne (2022), while NCCs have been extremely useful, in that they provided a "theory-neutral" methodological framework for researchers, they are limited by the difficulty of distinguishing the real neural correlates of consciousness from the neural prerequisites, and from the consequences of consciousness itself. To tackle such limitations, a plethora of theories of consciousness (ToCs) have been developed, aimed at identifying the explanatory connection between underlying neural mechanisms and various aspects of consciousness (Seth & Bayne, 2022). In the current thesis, however, I will leave aside the different ToCs that exist, to focus on consciousness from a more clinical angle. A useful way to conceptualise consciousness from such a clinical perspective is as a bi-dimensional construct, composed of two major components, wakefulness (also referred to as arousal) and awareness. The former refers to the level of alertness, whereas the latter refers to the content of consciousness itself (that is, the sensory, cognitive and affective experience) (Giacino et al., 2018; Laureys, 2005). As regards to neuroanatomical correlates, wakefulness and awareness rely on different brain structures. Wakefulness is associated with neuronal populations in the brainstem (reticular activating system), that project to cortical neurons directly (Di Perri et al., 2014) or indirectly through a thalamic relay (Laureys et al., 2009), with the hypothalamus also playing an important role in modulating different states of arousal (Stiefel et al., 2014). Conversely, awareness has most commonly been associated with fronto-parietal areas, as well as with the connectivity between fronto-parietal associative areas and the thalamic nuclei (Di Perri et al., 2014; Laureys et al.,

2009). Importantly, the classification of the different pathological conditions where consciousness is disrupted - i.e., Disorders of Consciousness (DoC) - is structured upon this two-dimensional aspect of consciousness.

1.2. Nosology of Disorders of Consciousness

Under most normal and pathological conditions, the two components of consciousness, awareness and wakefulness, are positively correlated: in order to be aware, one should also be awake - with dreaming being an exception (Laureys et al., 2009). Following a severe acquired brain injury (ABI) (either traumatic or not), this correlation might or might not be disrupted. For example, in a coma, the lack of awareness is given by the lack of wakefulness, with both components of consciousness being impaired. Clinically, a coma is established when there is a lack of eye-opening following stimulation (and spontaneously), in the absence of bilateral ptosis (Giacino et al., 2009; Laureys et al., 2009). Additionally, no voluntary motor behaviours are observed, with behavioural responses restricted to reflex activity only (Giacino et al., 2009). Normally, a coma results from a diffuse axonal injury following traumatic brain injury (TBI), or from lesions at the level of the brainstem, specifically around the reticular activating system (Giacino et al., 2009). Importantly, comatose patients who survive normally start to recover between 2-4 weeks (Laureys et al., 2009), with the more severe injuries normally resulting in a prolonged (i.e., > 28 days) DoC (PDOC). PDOC include vegetative state (VS) (Royal College of Physicians, 2020) - also named unresponsive wakefulness syndrome (UWS) (Laureys et al., 2010) - and minimally conscious state (MCS) (Giacino et al., 2002). The former disorder refers to the condition in which the above mentioned correlation between awareness and wakefulness is lost. In fact, VS/UWS patients are clinically defined by a presence of sleep-wake cycles (i.e., periods of spontaneous eyes-opening), but an overall lack of awareness (no behavioural response to verbal commands and no intelligible speech) (Royal College of Physicians, 2020). In summary, while arousal is substantially spared, VS/UWS patients show no voluntary or goal oriented behaviours (Giacino et al., 2009), and are therefore considered to be unaware of themselves and their surroundings (Jennet, 1972). Importantly, it has been arbitrarily decided that VS/UWS is considered to be “continuing” if the condition is still present for one month

after the ABI, and it is considered to be permanent when it is still present 6 months following a non-traumatic brain injury, or 12 months following a traumatic brain injury (Royal College of Physicians, 2020). Noticeably, while "continuing" does not imply irreversibility, permanent does, reflecting the observation that individuals who remained in a steady state of disrupted consciousness over a long period of time are unluckily to recover awareness (Royal College of Physicians, 2020).

On the other hand, MCS patients show presence of "inconsistent but discernible" behaviours that can be linked to awareness (i.e., the ability to follow simple commands, the ability to produce gestural or verbal yes or no answers, purposeful behaviours and intelligible verbalisation) (Giacino et al., 2002). Another important aspect of MCS patients is related to their ability to reproduce such behaviours, which is fundamental for differentiating purposeful movements from reflexive behaviours (Giacino et al., 2002). This notwithstanding, MCS patients are still unable to communicate in a consistent manner (Laureys et al., 2004). Additionally, MCS patients can be distinguished from those in a VS/UWS state by the presence of particular behaviours that are not random, but instead happen in response to appropriate external stimuli (Giacino et al., 2009). Noticeably, these behaviours tend to fluctuate across assessments, hence the appreciation of such signs must be replicated in multiple examinations (Giacino et al., 2009). Lastly, when, during clinical assessment, MCS patients show functional interactive communication, or functional use of at least two different objects, they are considered to be improving (Giacino et al., 2002). These "emerging" MCS patients are commonly referred to as MCS+ (Giacino et al., 2002).

With respect to the prognosis of VS/UWS and MSC patients, it should be noted that at 1 year post injury the latter patients show a much higher probability of recovery (around 50% will in fact achieve a moderate disability) as opposed to a lower 3% for VS/UWS patients (Giacino et al., 2009). Additionally, it is important to acknowledge that, differently from VS/UWS, MCS patients do not have strongly defined temporal parameters for recovery, and that they generally show a great heterogeneity in terms of the extent of functional recovery ultimately reached (Lammi et al., 2005).

In terms of brain lesions, MCS patients and VS/UWS patients present structural similarities and differences that are consistent with the fact that the two disorders differ by the level of

awareness rather than wakefulness (Schnakers et al., 2016). Patients normally present widespread lesions in both cerebral hemispheres, with brainstem areas being relatively spared (Fernandez-Espejo et al., 2011; Laureys et al., 2004). A diffusion tensor imaging (DTI) study reported a similar level of integrity within the brainstem of MCS and VS/UWS patients, but different levels of integrity within subcortical white matter and thalamus (Fernandez-Espejo et al., 2011). Importantly, this finding also highlights the fundamental role that the thalamus has in supporting awareness, and - as highlighted by (Schnakers et al., 2016) - is consistent with morphometry imaging studies that linked the level of thalamic atrophy to that of consciousness following brain damage (Lutkenhoff et al., 2013).

To conclude, it is important to mention that two other pathologies exist - namely locked-in syndrome (LIS) and brain death - that are not considered DOC, but are characterised by behavioural unresponsiveness, and must therefore be differentiated from MCS and VS/UWS (Giacino et al., 2009). In a LIS, patients are not cognitively impaired, however they are unable to produce speech, face or limb movements, due to a physical paralysis, normally caused by a lesion at the level of the ventral pons (Giacino et al., 2009; Laureys et al., 2009). On the other hand, brain death is characterised by an irreversible loss of consciousness and brain function, apneas, and lack of behavioural responsiveness to stimuli (Giacino et al., 2009).

1.3. Behavioural assessment of PDOC

PDOC diagnosis has historically been based on behavioural observation (Giacino et al., 2009). Several behavioural scales exist, aimed at assessing the level of consciousness, among which the Glasgow Coma Scale (GCS) (Teasdale & Jennett, 1974), the Full Outcome Unresponsiveness (Four) (Wijdicks, 2006), the Wessex Head Injury Matrix (Shiel et al., 2000), the Sensory Modality Assessment and Rehabilitation Technique (Gill-Thwaites & Munday, 2004) and the JFK Coma Recovery Scale-Revised (CRS-R) (Giacino et al., 2004). I will briefly discuss the widely used GCS, as well as the CRS-R, as it has been used in the case study presented in this thesis (Chapter 7), and it is also generally used as outcome measure in studies of transcranial direct current stimulation (tDCS) in PDOC (Chapter 2). The GCS scale was the first scale developed to specifically assess consciousness in critical care units (Teasdale &

Jennett, 1974). The scale is constituted of three different subscales - namely arousal (eye-response), motor responses and verbal responses - which scores are added up to a total score between 3 and 15. As noted by Giacino et al., (2009), the scale presents issues in terms of inter-rater reliability, as well as in determining the level of consciousness in patients with ocular trauma, tracheostomy or ventilatory support.

On the other hand, the CRS-R - a revision of the CRS tool originally published by (Giacino et al., 1991) - is aimed at differentiating the diagnosis between PDOC subtypes, while also serving as a prognostic evaluation tool (Giacino et al., 2004). In brief, the CRS-R includes six different subscales (auditory, visual, motor, oromotor, communication and arousal), with each subscale consisting of hierarchically-arranged items targeting behaviours mediated at the level of brainstem (i.e., reflexive activity), subcortical and cortical areas (i.e., cognitively mediated behaviours) (Gerrard et al., 2014). Importantly, the scoring is based on the presence or lack of behavioural responses to sensory stimuli administered by the examiner (Giacino et al., 2004). Noticeably, even though the scale has adequate inter-rater and test-retest variability, and can be used to discern patients in VS/UWS from those in MCS (Giacino et al., 2004), the error rate is still particularly high (30%-40%) (Giacino et al., 2018; J. Wang et al., 2020). As discussed more in depth in Chapter 2 (section 8.5), the high error rate in PDOC differential diagnosis using behavioural scales is likely linked to multiple factors, such as that patients' movements can be small and inconsistent, or the presence of lesions to motor, language and visual cortices, that may limit patients' ability to understand requests and produce appropriate motor responses (Laureys & Schiff, 2012). In the worst cases, misdiagnosis of VS/UWS patients happens due to the presence of cognitive-motor dissociation (Schiff, 2015a).

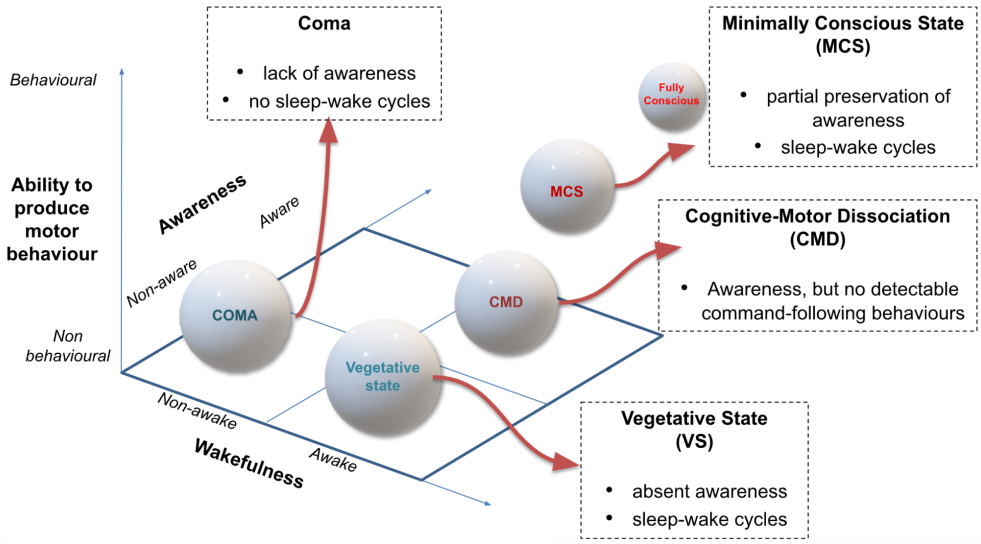


Figure 1.1. Schematic representation of the nosology of Disorders of Consciousness. Adapted from Owen et al., (2020).

1.4. Cognitive-motor dissociation in PDOC patients

As mentioned above, for a PDOC patient to classify as VS/UWS, they must be unaware, as clinically proven by a lack of behavioural responsiveness to external stimuli. However, in a landmark fMRI study, it was reported for the first time that a patient in VS/UWS (hence without evidence of behavioural responsiveness) could modulate their brain activity in response to the experimenter commands (Owen et al., 2006). Specifically, Owen and colleagues (2006) adopted a novel fMRI paradigm where they asked the patient to either imagine playing tennis, or to imagine moving around their house, and showed that the former command resulted in activation within the supplementary motor area (SMA), whereas the latter resulted into activation in parahippocampal areas. Interestingly, these patterns of brain activity were subsequently observed on healthy participants (Boly et al., 2007a). The "active" or "command-following" paradigm used by Owen et al. (2006) falls into the category of *mental imagery tasks*, and an adaptation of such a paradigm has been used in the case study reported in Chapter 7. Owen and colleagues' findings have been subsequently replicated using similar approaches (with both fMRI and EEG methods), and it has been established that around 14-20% of VS/UWS patients retain some level of cognitive capacity, reflected by brain activation in

response to commands, in the absence of motor responsiveness, as assessed with behavioural scales (Cruse et al., 2011; Kondziella et al., 2016; Monti et al., 2010). The above findings led to the proposal of the term cognitive-motor dissociation (CMD), to describe this specific syndrome of these "covertly aware" patients (usually VS/UWS or low MCS patients), characterised by a dissociation between bedside behaviour, which is absent, and laboratory investigations (Fernandez-Espejo et al., 2015; Fernández-Espejo & Owen, 2013; Schiff, 2015a). Importantly, though, it has been highlighted that the absence of brain activation following commands does not exclude the presence of consciousness, and, conversely, the presence of brain activation in motor-imagery tasks does not imply that such paradigms can be used to establish communication with the patient (Laureys & Schiff, 2012; Schiff, 2015a). In fact, as noted by Laureys & Schiff (2012), the absence of brain activity in response to commands from the experimenter can be due to many factors, such as test-dependent technological issues, patients' fluctuation in arousal or even the above mentioned perceptual sensory inadequacies (i.e., visual, auditory, language or working-memory functions). Leaving these limitations aside, it is fundamental to highlight that the correct identification of CMD is of paramount importance, as accurate assessment of consciousness in PDOC patients has direct implications in terms of care, prognosis and even end-of-life decisions (as discussed in Chapter 2, section 2 and 9).

An interesting aspect of CMD, which is also crucial for the understanding of the methodological choices in the experiments presented in Chapter 4-5 and 7, is that the dissociation between cognitive capacity and motor responsiveness has been linked to impairments in the structural connectivity between the thalamus and primary motor areas (Fernandez-Espejo et al., 2015). This observation is also backed up by the evidence that, in healthy individuals, motor execution is linked to increased activity in the thalamus and in the motor cortex, as well as to enhanced connectivity between those two areas, as compared to motor imagery (Fernandez-Espejo et al., 2015). Additionally, a recent study using fibre tractography reported diminished structural integrity in the white-matter fibres linking the thalamus and M1 in PDOC patients, as compared to healthy controls (Stafford et al., 2019a). This evidence suggests that such localised structural impairments in thalamo-cortical connectivity may constitute the basis of the reduced behavioural responsiveness characterising PDOC patients, with the important implication that the assessment of consciousness should not

rely exclusively on behavioural scales (Stafford et al., 2019a). Noticeably, similar observations regarding the importance of thalamo-cortical coupling with respect to the loss and recovery of awareness and complex behaviours were already made (Demertzi et al., 2015; Laureys et al., 2000).

As highlighted above, the empirical studies presented in the following chapters are also grounded on the mechanistic hypothesis that lack of behavioural responsiveness in some PDOC patients is linked to a decrease thalamo-cortical coupling. Therefore, it is reasonable to also hypothesise that interventions aimed at improving such connectivity patterns (as those presented in Chapters 4-5 and 7) could improve responsiveness, and re-establish some level of motor control in covertly aware patients (Fernandez-Espejo et al., 2015), which would in turn improve clinical management, patients' quality of life, and lower the chances of misdiagnosis (Chapter 2, section 9).

To provide a better understanding of the targeted networks in Chapters 4-5 and 7, a schematic representation of the cortico-thalamo-cortical and cortico-cerebellar-thalamic pathways is given in Figure A.1.

1.5. Additional methods for the detection awareness in PDOC patients: rs-fMRI and EEG

Differently from the fMRI experiments on healthy individuals reported in Chapter 4 and 5, the case study presented in Chapter 7 included additional fMRI and EEG protocols for the detection of consciousness, which were added to better characterise the therapeutic effects of tDCS. I will provide a brief overview below, which serves as background information for the case study reported in Chapter 7.

1.5.1. rs-fMRI

Since the discovery that a minority of UWS patients retain a certain level of awareness, as observed with mental-imagery fMRI tasks discussed in the previous section, there has been an

increase interest in finding alternative ways of detecting and quantifying signs of consciousness, mainly through resting-state fMRI (rs-fMRI), resting-state EEG (rs-EEG) and stimulus-based EEG tasks (Chennu et al., 2014).

Normally, the clearest way to prove the presence of signs of consciousness in an unresponsive patient would be using active tasks, where patients are asked to follow specific instructions (i.e., command-following tasks or mental imagery tasks). This notwithstanding, active paradigms are limited by PDOC patients' fluctuation of attention, aphasia and/or presence of sensory and motor deficits (Duszyk-Bogorodzka et al., 2022). Compared to stimulus-based tasks, rs-fMRI has then the advantage of not relying on attention, visual or auditory functions (Snider & Edlow, 2020), which makes it an appropriate method in those patients who are not able to engage with mental imagery tasks.

Over the past years, rs-fMRI has proven a valuable tool to study brain processes underlying consciousness (Sanz et al., 2021). Recent studies have unveiled a number of differences in rs-fMRI network derived metrics and dynamics between DOC patients and healthy controls (for a review see (Sanz et al., 2021; Snider & Edlow, 2020). Additionally, rs-fMRI can provide biomarkers with great clinical relevance, as indicated by various studies reporting correlations between measures derived from resting-state functional networks of PDOC patients and behavioural scores (B. Cao et al., 2019; Demertzi et al., 2015; Threlkeld et al., 2018). Despite the advantages of resting-state methods (both fMRI- and EEG-based methods discussed below) over task-based ones, it is important to highlight that resting-state patterns are not used to demonstrate covert awareness and command-following is normally preferred as ultimate evidence of consciousness. In fact, resting-state patterns are only evaluated on the basis of how much they resemble those patterns that are normally observed in healthy individuals or covertly-aware patients. Considering this, resting-state patterns might provide helpful information as to whether a brain has the capacity to sustain consciousness.

For example, recently there has been substantial research around impairments in the Default Mode Network (DMN) in PDOC. In brief, the DMN is a network that shows increased activity at rest as compared to during tasks requiring attention, and that can be easily identified with rs-fMRI (Vanhaudenhuyse et al., 2010). rs-fMRI studies have shown that the connectivity within the DMN in DOC patients is atypical and reduced, and that it correlates with the level of

awareness. Furthermore, it has been observed that recovery of consciousness is associated with restoration of normal patterns of connectivity within the DMN network (for a review see Bodien et al., (2017); Snider & Edlow, (2020).

1.5.2. EEG

As mentioned above, alongside fMRI methods, in Chapter 7, I also used high-density EEG to assess the presence of evidence indicating covert cognition, as well as to describe tDCS-induced changes in functional connectivity through EEG-derived graph-theory measures and EEG spectral power. Importantly, the following introduction on EEG applications in PDOC will not include a review of the findings from studies assessing the effects of tDCS in PDOC using such EEG techniques, as those will be discussed in Chapter 2, section 7. In brief, EEG is a non-invasive neuroimaging technique capable of measuring neuronal activity from electrodes placed on the scalp. EEG signals originate from neurons' inhibitory/excitatory postsynaptic potentials, which summate in the cortex and extend to the surface of the scalp (for a more detailed description of EEG methods and analyses see (Kumar & Bhuvaneswari, 2012) and (Subha et al., 2010).

Several features and parameters can be extracted from EEG time-series that have proven to have some clinical validity (i.e. differential diagnosis or prognostic value), among which power spectral density, functional connectivity measures, graph-theory metrics, evoked potentials and event-related synchronisation/desynchronisation (ERS/ERD) (for an in-depth review of EEG studies on PDOC see Wutzl et al., 2021).

Briefly, spectral power analysis is a method that allows quantification of the power of different frequencies in the EEG signal. Normally, EEG oscillations are divided into the following five frequency bands: delta (0.5-3 Hz), theta (4-7 Hz), alpha (8-13 Hz), beta (14-30 Hz) and gamma (above 30 Hz). Several studies investigating spectral power differences between UWS, MCS and healthy participants have observed differences in the alpha, delta and - although less consistently - theta bands (Wutzl et al., 2021). Specifically, relative power in the alpha band seems to be lower and relative delta power higher, in UWS patients as compared to MCS (Chennu et al., 2014; Lechinger et al., 2013; Lehembre et al., n.d.; Naro et al., 2018; Piarulli et

al., 2016; Stefan et al., 2018), with relative alpha power positively correlating with CRS-R scores, and relative delta power showing an opposite pattern (Chennu et al., 2014; Rossi Sebastiano et al., 2015; Sitt et al., 2014; Stefan et al., 2018). Lastly, alpha and delta powers also seem to represent good indicators of recovery in UWS patients (Babiloni et al., 2009; Stefan et al., 2018; O'Donnell et al., 2021).

EEG functional connectivity methods seek to quantify the relationship between brain areas, through various measures - such as correlation, coherence or information theory (Cao et al., 2022) - which rely on different aspects of the EEG signal (i.e. time or frequency) (for a review of the different functional connectivity measures see (Bastos & Schoffelen, 2016). Similarly to EEG power spectra analyses, EEG functional connections are normally quantified in the different frequency bands mentioned above. Overall, UWS patients present reduced functional connectivity, especially in central and posterior areas (King et al., 2013), with several studies reporting reduced functional connectivity in alpha and theta bands, and increased connectivity in the delta band (Höller et al., 2014; Sitt et al., 2014), in line with findings from spectral power analyses (Duszyk-Bogorodzka et al., 2022). In comparison to UWS patients, MCS patients have functional connectivity patterns more in line with those of healthy individuals, although with weaker connections in the alpha band, and stronger connections in the delta band (Chennu et al., 2014). Noticeably, the pattern of reduced connectivity in PDOC patients in the theta and alpha bands has been observed especially in fronto-parietal areas, which have been linked to preserved consciousness (Chennu et al., 2014; Sitt et al., 2014).

Connectivity networks derived from EEG functional-connectivity analyses can be described with graph-theoretical methods, which also help reduce the high-dimensionality typical of EEG data. Graph-theory refers to the study of networks, which are constituted by nodes and edges (connections between nodes). In EEG, nodes are typically electrodes, whereas edges are the connections between each pair of electrodes, as quantified by functional-connectivity measures. Graph-theory provides a plethora of measures for the quantification of different aspects of a network, ranging from measures describing its global integration (e.g. path length, connection density, modularity etc.) to those describing its local integration (node degree, clustering coefficient, node centrality etc.) (for more detail on graph-derived measures see (Bullmore & Sporns, 2009). Research on PDOC and EEG resting-state has reported differences

in several graph-derived measures between DOC patients and healthy controls - mainly related to reduced modularity and long-distance connectivity - among which reduced local and global efficiency in DOC patients as compared to healthy participants, reduced clustering coefficient in the alpha band, which was instead increased in the delta and theta bands, and finally increased characteristic path length in the alpha band (Chennu et al., 2014).

Interestingly, Chennu et al. (2014) also observed a significant correlation between measures of network efficiency in the alpha band and the level of awareness. Lastly (Stefan et al., 2018) were able to distinguish MCS patients from UWS using clustering coefficient and characteristic path lengths. Importantly, graph-theory metrics derived from resting-state EEG also have a good prognostic value, as reviewed by (Wutzl et al., 2021).

Lastly, in EEG motor-imagery tasks, individuals are asked to imagine themselves performing a movement (i.e. motor command, e.g. “try to move your right hand” or “open and close your right hand”). EEG motor-imagery tasks rely on the evidence that, when I imagine or plan a movement of a limb, modulations in sensorimotor cortex activity are reflected in EEG-detected changes in the oscillatory power in mu and/or beta bands occur, over central electrodes (Cruse et al., 2012). Specifically, a reduction in power over the scalp contralateral to the limb and an increase in power over the ipsilateral scalp are observed (Pfurtscheller et al., 2006, 2008; Pfurtscheller & Neuper, 2001). These reductions and increases in EEG power have been named ERD and ERS respectively. In line with what was found in several fMRI studies (discussed in section 1.4 above), EEG studies have also demonstrated that a minority of PDOC patients can modulate their brain activity in response to verbal commands (for a review see (Kondziella et al., 2016). For example, in a recent study by (Claassen et al., 2019), 16 out of 104 clinically unresponsive patients showed brain activation in an EEG motor-imagery task (i.e. cognitive-motor dissociation, section 1.4). Furthermore, the authors also observed that cognitive-motor dissociation is predictive of Glasgow Outcome Scale Extended (GOS-E) levels of 4 or above, therefore representing a good prognostic indicator. Findings from (Claassen et al., 2019) add up to the existing literature reporting diagnostic and prognostic utility of EEG and motor-imagery tasks (Cruse et al., 2011, 2012; Goldfine et al., 2011). Using similar methods, in another observational cohort study the authors reported that 27 (14%) out of 193 PDOC patients presented EEG evidence of CMD (Egbebike et al., 2022). Taken together, the above studies

indicate that EEG motor-imagery tasks might represent a good alternative to fMRI methods for the assessment of covert awareness in PDOC patients.

1.6. tDCS

Throughout this thesis, tDCS was utilised as the main intervention method in all of the studies presented. As such, an overview of tDCS is given below, focusing on its effects (sections 1.6.1-3) and the impact of brain lesions and atrophies on tDCS-induced current (section 1.6.4). Noticeably, the following paragraphs focus mainly on the effects of tDCS on motor areas - as M1 was the targeted area in 3 out of 4 studies included in the thesis - although the effects of tDCS over the cerebellum (targeted in *Experiment 2*) are also considered (section 1.6.3.4). Importantly, the paragraphs below draw mainly on the literature on healthy populations, as the effects of tDCS on PDOC are discussed thoroughly in Chapter 2.

1.6.1. Brief overview of tDCS

tDCS is a non-invasive brain stimulation (NIBS) technique - more specifically a transcranial electrical stimulation technique (tES) - that has been used for more than 20 years as a means to study brain functioning (Reinhart et al., 2017; A. Woods et al., 2016), and as a therapeutic tool for a number of psychiatric (Kekic et al., 2016) and neurological conditions (Flöel, 2014). As a matter of fact, beneficial effects of tDCS have been reported for various diseases, among which chronic depression, drug addictions, pain conditions, traumatic spinal cord injuries, stroke, epilepsy and disorders of consciousness (Flöel, 2014; Stagg & Nitsche, 2011; Chapter 2). In short, tDCS involves delivering a weak electrical current to the scalp (normally around 1-2mA), via two or more electrodes (A. Woods et al., 2016). Normally, a tDCS device is comprised of a stimulator, which allows to specify different stimulation parameters (e.g., current intensity, current duration, ramp off and ramp on periods and blinding) and an electrode assembly connected to the stimulator, which usually comprises rubber electrodes and a contact medium (e.g., saline solution or conductive paste), used to improve the conductivity of current to the scalp (A. Woods et al., 2016). In its simplest setup, tDCS is delivered using two

electrodes, an anode and a cathode, which respectively represent the positive and negative terminal of the battery within the stimulator (Reinhart et al., 2017).

In terms of the mechanisms of actions of tDCS, it has been suggested that tDCS alters the resting membrane potentials of the neuronal populations that are reached by the electrical stimulation field (Stagg et al., 2018). In particular, tDCS has sub-threshold effects, in the sense that it does not induce neuronal activity independently from the afferent inputs, but it rather increases or decreases cortical excitability (i.e., neuronal resting potentials), such that the affected neurons become more or less likely to generate action potentials in the presence of afferent activity (Stagg et al., 2018; Stagg & Nitsche, 2011; A. Woods et al., 2016). Therefore, tDCS is different from other NIBS methods (e.g., Transcranial Magnetic Stimulation), which have supra-threshold effects (that is, they elicit action potentials of the targeted neuronal populations) (Stagg et al., 2018). Finally, when considering tDCS effects on the brain, it is important to distinguish between immediate (or "acute") effects, and after-effects (or "neuroplastic effects").

Regarding the direction of acute effects, studies reported that applying anodal-tDCS over the motor cortex increases cortical excitability, with cathodal-tDCS showing an opposite effect (Bastani & Jaberzadeh, 2012; Horvath et al., 2015a; Monte-Silva et al., 2013a; Stagg et al., 2018; Yamaguchi et al., 2020). In their systematic meta-analysis, Bastani & Jaberzadeh (2012) highlighted that this effect was consistently reported by multiple studies on healthy individuals, although with a small effect size. Moreover, the authors also found that a similar effect was reported by studies on stroke patients.

Importantly, these acute effects have been normally studied in humans using Transcranial Magnetic Stimulation (TMS) protocols, where motor evoked potentials (MEP) elicited by TMS are recorded pre and post tDCS over M1, and used as an index of change in cortical excitability (Stagg et al., 2018). Noticeably, it has been observed that, at the tDCS intensities commonly used (between 1 and 2mA), the change in neuronal membrane potential is relatively low (between 0.2 and 0.5 mV), considering that for the generation of an action potential the membrane potential has to increase from around -70mV to -50mV, approximately (Opitz et al., 2016; Radman et al., 2009; Stagg et al., 2018). However, neuronal network simulation studies suggested that tDCS is still effective even despite such small changes, mainly due to

amplification, network-level alterations or changes in the timing of action potentials (Anastassiou et al., 2010; Carandini & Ferster, 2000; Stagg et al., 2018).

Even though this explanation of polarity-specific tDCS effects makes it easy to interpret and discuss findings from tDCS studies, it represents an oversimplification. In fact, the direction of the current injected by tDCS is greatly influenced by cortical folding, which can produce current inversions even in the areas under the electrodes, resulting in complex effects, due to a combination of areas being depolarised and other areas hyper-polarised (Rahman et al., 2013; A. Woods et al., 2016). At the microscopic level, this is caused by neurons having various orientations with respect to the induced electric field (Stagg et al., 2018).Overall, this aspect is of crucial importance as it is thought to be at the basis of the high inter-subject variability observed in the field (both on healthy individuals and patients) (Albizu et al., 2020), and it will be further discussed in this thesis (see section 6.4 below, Chapter 2, section 8.2 and Chapter 6).

In addition to current direction, changes in current intensity also result in changes in electric fields within the brain, and in neuronal excitability, which in turn might impact behavioural outcomes (Albizu et al., 2020). Adding an extra layer of complexity to the effects of tDCS is then the observation that intensity-dependent effects can be non-linear, especially when considering cathodal-tDCS (Batsikadze et al., 2013; Shilo & Lavidor, 2019; Vimolratana et al., 2023). In fact, studies assessing the neurophysiological and motor responses following cathodal-tDCS have reported conflicting results: low-intensity stimulations (1 mA) normally led to a reduction of cortical excitability, whereas stimulations at 2mA have been observed to increase cortical excitability (see Vimolratana et al., 2023). Overall, all the above factors must be taken into account both when interpreting results from tDCS studies, and they also highlight the importance of individualised tDCS protocols where the subject-specific neuroanatomical features are taken into account.

The content below is focused on M1-tDCS, as this is the main montage used in this thesis. However, I also provide a brief overview of cerebellar-tDCS, which was used in Chapter 4 (*Experiment 2*).

1.6.2. After-effects of tDCS

Differently from acute effects, neuroplastic effects are instead thought to be mediated by changes of synaptic efficacy, such as early and late long-term potentiation (e-LTP and l-LTP), rather than by modulation of membrane resting potentials (Stagg et al., 2018). Specifically, evidence from studies on the motor cortex indicates that such neuroplastic effects are mainly mediated by calcium-dependent plasticity, induced by tDCS at the level of glutamatergic synapses (particularly through NMDA receptors) through GABA reduction (Nitsche et al., 2005; Stagg, Best, et al., 2009; Stagg, Bestmann, et al., 2011; Stagg et al., 2018). In short, the changes in M1 cortical excitability following certain tDCS protocols might trigger synaptic plasticity, which in turn affects motor skill learning (Kumar et al., 2022).

Results from studies targeting the motor cortex in healthy individuals suggest that the duration of these effects depend on the specific tDCS protocol used, and range from a few minutes to more than 1 day (Monte-Silva et al., 2010, 2013a; Nitsche et al., 2003; Nitsche & Paulus, 2000, 2001; Stagg et al., 2018). Interestingly, these effects appear to be nonlinear, and highly influenced not only by the stimulation parameters (i.e., intensity and duration), but also by the amount of sessions and the interval between sessions (Agboada et al., 2020; Kronberg et al., 2017; Mosayebi Samani et al., 2020; Stagg et al., 2018). In particular, evidence suggests that, at least regarding anodal-tDCS, multiple stimulation sessions within specific time windows are needed to induce l-LTP-like plasticity changes in the motor cortex and prolong tDCS after effects (Agboada et al., 2020; Monte-Silva et al., 2013). Interestingly, a similar effect was not found using the same methods with cathodal-tDCS, which was unable to induce plastic changes even after multiple sessions (Mosayebi Samani et al., 2020).

Interestingly, there is only one study involving rs-fMRI and tDCS in PDOC patients (Cavaliere et al., 2016). In their study, the authors retrospectively evaluated functional connectivity patterns derived from rs-fMRI collected prior to one tDCS session over the left DLPFC in a group of MCS patients. The authors observed that patients who responded to the stimulation - that is, those who recovered at least one additional sign of consciousness that was not present before real tDCS - had higher functional connectivity prior to the stimulation in regions that normally co-activate with the left DLPFC, compared to non-respondent patients. Even though in their study (Cavaliere et al., 2016) targeted a different brain network and focused on MCS

patients rather than UWS, their findings are important in the context of the case study reported in Chapter 7, in that they show that rs-fMRI could be a valuable tool in detecting the neural underpinning of responsiveness to tDCS.

1.6.3. tDCS and motor function

While there are many meta-analyses assessing the effects of tDCS on cognitive functions, only a few have systematically investigated the impact of tDCS on motor function (i.e., motor skills, motor learning and motor performance) in healthy individuals (Patel et al., 2019). Additionally, many recent studies regarding the effects of tDCS on motor functions concern clinical populations rather than healthy individuals (Bastani & Jaberzadeh, 2012). For example, in the review of Bastani & Jaberzadeh (2012), only two out of 14 studies concerned healthy subjects, and were specifically focused on the effects of M1-anodal-tDCS on hand motor performance (Boggio et al., 2006; Hummel et al., 2010). Both studies reported a significant improvement in motor function following anodal-tDCS. Regarding motor skill learning, tDCS applied over the motor cortex (unilaterally or bilaterally) seems to induce long-lasting improvements, especially when the stimulation is concurrent to the training (rather than applied pre-training) (Reis & Fritsch, 2011). This was also backed up by recent reviews (Patel et al., 2019), although it has been pointed out that due to the great heterogeneity of methods used, both regarding tDCS protocols and motor tasks assessed, it remains difficult to make generalisation regarding tDCS effects on motor functions (Buch et al., 2017; Patel et al., 2019). On the other hand, in the meta-analysis of Hashemirad et al. (2016), focused on the effects of single and multiple sessions of anodal-tDCS on motor learning (specifically assessing studies using sequential finger tapping tasks and serial reaction time tasks), it was found that multiple tDCS sessions result in stronger improvements in motor learning, as compared to single sessions. As pointed out by (Patel et al., 2019), the current explanation for how tDCS enhances motor learning is that it causes changes in M1 excitability, which in turn leads to an augmentation of synaptic connections within the same region. However, the author also highlights that the evidence supporting such an hypothesis is still inconsistent.

Interestingly, tDCS has been found to lead to improvements not only in unimanual motor tasks as those mentioned above, but also regarding bimanual motor skills (Pixa & Pollok, 2018). Regarding motor performance, previous studies have reported improvements, especially regarding the Rate of Perceived Exertion (RPE), but only for submaximal graded exercises (i.e., tasks that do not require maximal force capacity) (see Angius et al., 2017). A tendency towards a reduction of fatigue was also observed (Patel et al., 2019). Even though a mechanistic understanding is still lacking, it has been proposed that such an effect of tDCS on RPE is caused by M1 needing less input to generate enough output to recruit a muscle, due to the increase in its excitability following tDCS (Angius et al., 2017). In line with this explanation is the idea that, in the absence of motor learning, anodal-tDCS' influence on motor behaviour (i.e., the maximum voluntary force produced) might be due to the increased firing rate of neuronal populations in the motor cortex (Orban de Xivry & Shadmehr, 2014). These last observations related to tDCS and motor performance are of particular interest in the context of this thesis, as the outcome of the proposed tDCS interventions is not to reinforce motor learning, but rather to facilitate movement execution (Chapter 4, 5 and 7).

Overall, the results from the above meta-analyses suggest that tDCS might lead to modest improvements in dexterity tasks, motor learning, and motor strength and fatigue in general, however due to several caveats in the literature (such as heterogeneity of methods), it remains difficult to draw definitive conclusions (Patel et al., 2019).

1.6.3.1. Single vs multiple tDCS sessions

For tDCS to have a therapeutic effect on PDOC patients, the improvements, whether in the motor or cognitive domain, should be long-lasting rather than transient. However, the positive effects of a single tDCS session are normally only short-lasting (Chapter 2; Zhang et al., 2021). Noticeably, the literature shows a trend towards greater therapeutic effect of multiple sessions of tDCS as compared to a single session. Importantly, this trend is not restricted to the PDOC population only, and meta-analyses on other neurological and psychiatric disorders report similar patterns, highlighting the need of multi-session interventions for achieving clinically meaningful improvements (Lefaucheur et al., 2017; Song et al., 2019). For instance, it was

recently observed that multiple-session treatments induce long lasting improvements in the order of months as compared to hours, with respect to phantom limb pain (Navarro-López et al., 2022).

A similar augmentative effect of multiple tDCS sessions was found also on healthy individuals. As mentioned above, in their meta-analysis, Hashemirad and colleagues (2016) reported a trend towards increased behavioural change and retention time for multiple sessions as compared to a single session. Similarly, the effects of tDCS on motor learning have been observed to be greater when tDCS is delivered over several days (Pixa & Pollok, 2018; Reis et al., 2009; Saucedo Marquez et al., 2013). A beneficial effect of multiple tDCS sessions have been observed even in healthy older participants, with respect to both manual dexterity (Rostami, Mosallanezhad, Ansari, Kidgell, et al., 2020) and lower extremity functional performance (Rostami, Mosallanezhad, Ansari, Ehsani, et al., 2020).

The above results could be explained drawing on the literature on the after-effects of tDCS applied to the motor cortex: normally, the after-effects of a single session last up to a few hours, hence falling in the range of e-LTP, and increasing the duration of the stimulation does not seem to extend such effects (Agboada et al., 2020). However, several studies have reported that, by repeating the intervention (with specific intervals), it is possible to prolong the after-effects of tDCS even up to 24h post intervention, suggesting that multiple sessions are able to induce l-LTP-like plasticity in the motor cortex (Agboada et al., 2020; Monte-Silva et al., 2013a). These findings are backed up by recent evidence on computational models of tDCS-induced cell assembly creation, where it was observed that l-LTP can be induced only with multiple sessions, which seems to boost the effects of tDCS on cell connectivity (Lu et al., 2019). According to the authors, multiple sessions are needed to produce stronger tDCS after-effects, however, similarly to what was found by (Agboada et al., 2020; Monte-Silva et al., 2013a), this happens only when appropriate pauses between sessions are used.

Overall, while evidence suggests that multiple sessions might be more effective than a single session, it must be noted that studies with designs that allow for a proper comparison between the effects of multiple versus single tDCS interventions are rare (Hashemirad et al., 2016b).

1.6.3.2. tDCS during task vs tDCS at rest

Aside from administering tDCS multiple times, it has been also suggested that combining the stimulation with a task might have a synergistic effect (Bolognini et al., 2009a). According to the authors, the main reason why such a combination might be more effective than administering tDCS alone, is that motor learning relies on similar mechanisms as brain stimulation (that is, through changes in excitability and synaptic efficacy).

In motor learning studies, this hypothesis is backed up by the evidence that applying tDCS during sequence learning rather than before, modulates learning learning, in a polarity-specific manner (i.e., with anodal-tDCS increasing it and cathodal-tDCS decreasing it) (Stagg, Jayaram, et al., 2011). Interestingly, the application of tDCS prior to motor learning led to a slower learning rate compared to sham-tDCS. The authors explain the anodal-tDCS and motor learning timing-dependent interaction in terms of metaplastic mechanisms (i.e., activity-dependent) and suggest also that the effects of anodal-tDCS on neuronal excitability are akin to those of motor learning. Noticeably, such an effect was not found for cathodal-tDCS, which led to reduced motor learning instead, suggesting that anodal- and cathodal-tDCS influence neural plasticity through different mechanisms (Stagg et al., 2011). A similar effect of tDCS on motor memory formation and retention was also found by (Galea & Celnik, 2009). Additionally, another study by (Koyama et al., 2015) found that dual-hemisphere M1 anodal-tDCS coupled with motor practice induced a consolidation of the movement examined (a ballistic thumb movement) which the authors did not observe in a preliminary experiment where tDCS was applied alone. Similar findings highlighting the state-dependent effects of tDCS have been observed even in non-motor domains (Dubreuil-Vall et al., 2019; Kadosh et al., 2010). Moreover, a similar augmenting effect was also found in a study combining postural training with M1 or bilateral cerebellar anodal-tDCS to improve postural control and balance of healthy participants with high risk of falling (Yosephi et al., 2018).

Interestingly, an fMRI study reported findings in line with the previously mentioned literature, showing an increased cortical activity in the motor cortex when pairing anodal-tDCS with a motor task, as compared with the motor task alone (Kwon & Jang, 2011). Furthermore, tDCS has been observed to impact also functional connectivity of large-scale brain networks in a brain state (i.e., task-dependent) and polarity-dependent way (Li et al., 2019), and not only the

activity of the targeted area. Crucially, the beneficial effects that tDCS coupled with motor training has on motor learning seem to be long-lasting on both healthy subjects (Reis & Fritsch, 2011), and on patients with chronic stroke (Ehsani et al., 2022; Jin et al., 2019), underlying the potential therapeutic benefit of such a coupling.

It must be noted that the effects of tDCS on plasticity seem to be deeply dependent on the nature of the task that is paired with the stimulation (i.e., on whether it relies on the same regions that are being targeted by the stimulation) (Antal et al., 2007; Nozari et al., 2014). This idea has also been consolidated by a recent study using a rotarod paradigm, in which it was found that anodal-tDCS applied during a task selectively enhances the activity of those neuronal populations engaged during the task itself, hence providing a first animal model of the neuronal mechanisms behind tDCS task-specific enhancement effect (Y. Wang et al., 2023).

Overall, the literature suggests that tDCS might enhance the response of neuronal populations to motor training (Bolognini et al., 2009a; Ehsani et al., 2022; Jin et al., 2019; Morrison-Ham et al., 2022), hence increasing the effects of motor practice through a priming-like effect. Importantly, however, the task coupled with tDCS must be a relevant one for the targeted behaviour.

1.6.3.3. tDCS during passive mobilisation

In PDOC patients, passive mobilisation could be more feasible compared to active tasks. Interestingly, studies on healthy participants found a comparable engagement of the motor regions for active and passive movements (Alary et al., 1998; Boscolo Galazzo et al., 2014; Jaeger et al., 2014; Lotze et al., 2003; Zhavoronkova et al., 2017). For instance, in their fMRI study, (Boscolo Galazzo et al., 2014) found that both active and passive movements led to activation of similar areas, namely the contralateral sensorimotor cortex, the supplementary motor area, the inferior parietal lobes, the thalamus and the cerebellum. Moreover, similar findings were obtained in the study of (Zhavoronkova et al., 2017), where the fMRI responses for active and passive movements of dominant and non-dominant hands were compared. However it was also observed that the clusters of activation had a smaller volume during the

passive movements as compared to the active ones. Interestingly, the same pattern was observed even with respect to active and passive movements of the lower limbs (i.e., active and passive stepping): both engage similar cortical and subcortical areas within the sensorimotor network, however the latter lead to a lower fMRI response (Jaeger et al., 2014).

Interestingly, research assessing MEPs through TMS reported findings in line with the above fMRI studies: in their study, Chye et al., (2010) assessed the effects of active and passive movements of forearm muscles, and observed similar changes in corticomotor excitability for both movements. Additionally, in a study involving repetitive passive movements of the thumb, it was observed that the modulation of M1 cortical excitability depends on the frequency at which passive mobilisation is administered (Sasaki et al., 2017).

Miyaguchi et al. (2013) also found a similar effect of active and passive movements on MEP amplitudes. Noticeably, in their study, the authors also compared the effects of different stimulation protocols, including, tDCS coupled with active movements and tDCS coupled with passive mobilisation, on MEPs. The authors found a significant difference in MEP amplitudes at 2' and 10' post stimulation, when comparing the tDCS plus active movements condition with the tDCS plus passive mobilisation one. However, no differences were observed in MEP amplitudes pre and post stimulation for the tDCS plus passive mobilisation condition.

Interestingly, only two studies were found that applied tDCS and passive mobilisation on clinical populations (Koh et al., 2017; Ochi et al., 2013). In their study (Ochi et al., 2013), applied concurrent tDCS plus robot-assisted arm training in chronic stroke patients. The authors compared two tDCS protocols, targeting the affected and unaffected hemispheres (with anodal and cathodal tDCS respectively), and found that both interventions led to improvements of the motor outcome measures considered. Similarly, (Koh et al., 2017) tested the effects of bilateral tDCS coupled with sensory modulation on chronic stroke patients, but found only a trend towards an improvement in voluntary movement.

However, it must be noted that the above two studies focused on the effects of tDCS coupled with passive mobilisation only, so while their findings are interesting, they are non informative for addressing the difference between tDCS coupled with active versus passive movements.

1.6.3.4. Cerebellar-tDCS

The cerebellum has an important role with respect to multiple motor and cognitive control functions (Grimaldi et al., 2016). It is in fact generally linked to voluntary motor initiation and control, as opposed to motor execution, which relies on cortical motor areas (Manto et al., 2012). Crucially, it has been observed that the cerebellum exerts an inhibitory influence over the motor cortex (Pinto & Chen, 2001), which has been referred to as cerebellar-brain inhibition (CBI) (Daskalakis et al., 2004). CBI happens in an indirect manner, specifically starting from the purkinje neurons (that is, GABAergic inhibitory neurons constituting the main output of the cerebellum), which have inhibitory projections to the deep cerebellar nuclei (DCN). The DCN have excitatory projections to the thalamus (mainly the ventral portion) which in turn exerts an excitatory effect on the motor cortex (Daskalakis et al., 2004).

The effects of cerebellar-tDCS (cb-tDCS) on CBI were tested for the first time through a TMS-tDCS protocol, by measuring MEPs after applying TMS first over the right cerebellum and 5ms later on the left motor cortex, and assessing the effect of different tDCS protocols on the those MEPs (Galea et al., 2009). Interestingly, the authors found a polarity-specific effect, with anodal cb-tDCS increasing CBI (possibly through an enhancement of purkinje cells excitability), whereas cathodal cb-tDCS reduced CBI. This findings were partially replicated by a more recent study, where it was found that the effect of anodal and cathodal cb-tDCS on CBI depends on the TMS intensity used to engage the cerebellar-thalamus-M1 axis: at higher TMS intensities both anodal- and cathodal-tDCS led to decreased CBI, whereas at lower intensities a polarity-dependent effect akin to that found in Galea et al. (2009) was found (Batsikadze et al., 2019). This notwithstanding, the above suggests that cb-tDCS might be used to enhance motor functions (Galea et al., 2009), and potentially as an alternative route to M1-tDCS for the modulation of the thalamo-cortical coupling in PDOC patients. As such, the effects of cb-tDCS on the motor network connectivity were tested on healthy participants in the study reported in Chapter 4 (*Experiment 2*), as a proof-of-concept for future applications of cb-tDCS in PDOC.

1.6.4. The impact of brain lesions and atrophies on tDCS-induced current

It is well established that tDCS-induced current is influenced by inter-individual differences in anatomical features such as scalp and skull thickness and shape, cortical thickness, and cortical density and volume (Evans et al., 2022). Studies have reported that differences in electrode placements can greatly impact both the distribution and direction of tDCS-induced electric current (Opitz et al., 2018; A. J. Woods et al., 2015). Additionally, electric field orientation seemed to affect the likelihood of neuronal firing in a whole-cell recording study (Radman et al., 2009). This is also confirmed by cortical excitability in healthy participants, which is influenced by current direction (Jacobson et al., 2012; Rawji et al., 2018), with MEPs in the motor cortex varying depending on the electrode montage (i.e., orthogonal montage or parallel montage relative to the motor cortex) (Rawji et al., 2018). According to (Albizu et al., 2020), the above suggests that the direction of current flow in the tDCS-induced electric field may strongly influence the effect of tDCS on behavioural outcomes.

TBI and non-TBI events can lead to great neuroanatomical changes, such as brain tissue displacements (Rosenfeld et al., 2007) or cerebrospinal fluid (CSF) abnormalities following brain atrophy (Du et al., 2022). Importantly, both factors can greatly impact current intensity and direction. For instance, following TBI, midline shifts - horizontal shifts of midline brain tissue, observable on axial images - often occur (Rosenfeld et al., 2007). Noticeably, midline shift and ventricle compression can also result from the intracranial pressure created by a cerebral edema following a non-traumatic hypoxic-ischemic event (Adhami et al., 2006; Ho et al., 2012). It is plausible that midline shift affects tDCS electrode placements that are based on common montages (as opposed to electrode placements based on subjects' MRI scans) due to the displacement of the targeted brain structures with respect to the scalp.

Anoxic events can also lead to important CSF changes. For instance, cerebral edemas that develop after an anoxic brain injury are largely composed by CSF (Du et al., 2022). In addition, lost brain tissue that is lost due to an atrophy is also normally replaced by CSF (Indahlastari et al., 2020). Importantly, both brain atrophies and CSF disorders result in an increase in brain water content (Cherian et al., 2018; Indahlastari et al., 2020). CSF changes highly affect tDCS-induced current conductivity due to its high electrical conductivity which causes electrical current to shunt, hence reducing the amount of current reaching the targeted areas. Importantly,

the effects of brain atrophies and CSF changes on tDCS-induced electric fields in PDOC have not been investigated. However, I can draw from the literature on the ageing brain and aphasic patients. For instance, (Mahdavi & Towhidkhah, 2018) investigated how cerebral shrinkage due to normal ageing or pathologic disease influences tDCS-induced current density distribution. The authors reported that reduced grey matter volumes decrease the magnitude of current density reaching the brain. The author links this to the increase in CSF volume - associated with ageing or to a loss of grey matter volume - which increases the scalp distance from the grey matter, reducing the amount of current delivered (Mahdavi & Towhidkhah, 2018). Indahlastari et al., (2020) investigated tDCS-generated electric fields in 587 healthy older adults' brains and found that the amount of tDCS current reaching the brain decreases as atrophies increase.

Similarly, (Laakso et al., 2015) found that electric field peak intensity was lower in the elderly than in young participants, due to older participants having higher CSF volumes. Interestingly, the authors also found that CSF volume explains 50% of the inter-individual variability in tDCS-induced electric fields within the motor cortex. Another study on five participants with age spanning five decades of life (from 43 to 85 years old), also confirmed a reduction of peak electric field with increasing age, among participants aged from 43 to 75 years old, with this relationship being reversed for the oldest participant (Thomas et al., 2018). In contrast with the studies discussed so far, (Unal et al., 2020) investigated the influence of brain atrophy on tDCS induced current in three patients with primary progressive aphasia, and found no relationship between amount of atrophy and brain current flow, which differences across patients fell within the distribution of anatomically typical subjects. Even though the previously mentioned study is limited by a small sample, it highlights the complexity of the relationship between brain atrophy and electric field induced by tDCS, and suggests the need for studies with a larger sample of patients.

Chapter 2

THERAPEUTIC USE OF TRANSCRANIAL DIRECT CURRENT STIMULATION IN THE REHABILITATION OF PROLONGED DISORDERS OF CONSCIOUSNESS[1,2]

2.1. Abstract

Patients with Prolonged Disorders of Consciousness (PDOC) have catastrophic disabilities and very complex needs for care. Therapeutic options are very limited, and patients often show little functional improvement over time. Neuroimaging studies have demonstrated that a significant number of PDOC patients retain a high level of cognitive functioning, and in some cases even awareness, and are simply unable to show this with their external behaviour - a condition known as cognitive-motor dissociation (CMD). Despite vast implications for diagnosis, the discovery of covert cognition in PDOC patients is not typically associated with a more favourable prognosis, and the majority of patients will remain in a permanent state of low responsiveness. Recently, transcranial direct current stimulation (tDCS) has attracted attention as a potential therapeutic tool in PDOC. Research to date suggests that tDCS can lead to clinical improvements in patients with a minimally conscious state (MCS), especially when administered over multiple sessions. While promising, the outcomes of these studies have been highly inconsistent, partially due to small sample sizes, heterogeneous methodologies (in terms of both tDCS parameters and outcome measures), and limitations related to electrode placement and heterogeneity of brain damage inherent to PDOC. In addition, we argue that neuroimaging and electrophysiological assessments may serve as more sensitive biomarkers to identify changes after tDCS that are not yet apparent behaviourally. Finally, given the evidence that concurrent brain stimulation and physical therapy can enhance motor rehabilitation, we argue that future studies should focus on the integration of tDCS with conventional

[1] As published in Frontiers in Neurology:

Aloi, D., della Rocchetta, A. I., Ditchfield, A., Coulborn, S., & Fernández-Espejo, D. (2021). Therapeutic Use of Transcranial Direct Current Stimulation in the Rehabilitation of Prolonged Disorders of Consciousness. Frontiers in Neurology, 12, 632572. https://doi.org/10.3389/fneur.2021.632572

[2] A number of papers on the effects of tDCS on PDOC were published after this review. Findings from such studies are discussed in Appendix A.

rehabilitation programmes from the subacute phase of care onwards, to ascertain whether any synergies exist.

2.2. Introduction

Prolonged Disorders of consciousness (PDOC) are heterogeneous medical conditions characterised by absent or limited awareness for at least 4 weeks after severe brain injury (Royal College of Physicians, 2020). Therefore, PDOC refers specifically to the vegetative (VS, also called unresponsive wakefulness syndrome) and minimally conscious states (MCS, including those emerging from this condition) (Laureys et al., 2009), and excludes acute conditions such as coma or cases where diagnosis has not been confirmed yet. PDOC diagnosis is based on clinical criteria, whereby the MCS differs from the VS by the fluctuating presence of reproducible behaviours that can be associated with awareness of the patient's self or of their environment. This includes the ability to follow simple commands, gestural or verbal yes/no responses, intelligible verbalisation, or some purposeful behaviours (see Giacino et al., 2002). These behaviours are not present in the VS, and patients are assumed to be entirely unaware of themselves and their environment as a result. Importantly, neuroimaging studies have demonstrated that a significant number of PDOC patients retain a high level of cognitive functioning, and in some cases awareness, but are unable to show this with their external behaviour. This condition has been recently named cognitive-motor dissociation (CMD; Shiff, 2015), and is typically revealed by the ability to follow commands in functional magnetic resonance (fMRI) or electroencephalography (EEG) motor imagery tasks. The discovery of covert command-following in some PDOC patients has wide implications for diagnosis and is sometimes associated with a more favourable prognosis. Specifically, recent evidence has shown that, when evident in the early stages (i.e., acutely, Edlow et al., 2017; Johr et al., 2020; or within the first year post injury, Pan et al., 2020), CMD may be a good predictor for a better outcome. In Edlow et al. (2017), three out of four patients identified with CMD recovered beyond a confusional state by 6 months (one died), as measured by the Glasgow Outcome Scale-Extended (GOSE). Similarly, Pan et al. (2020) reported that 15 out of 18 VS patients with CMD regained consciousness (compared to 5 out of 27 in a true VS) and 14 out of 16 MCS patients with CMD improved their CRS-R scores (compared to only 4 out of 17 MCS patients without CMD), at a 3-month follow-up. Finally, in a large study including 141 patients,

Johr et al. (2020) showed that patients presenting with potential clinical CMD (as assessed by the revised Motor Behavior Tool; Pincherle et al., 2019) exhibited much more favourable recovery trajectories across cognitive and functional domains than their PDOC counterparts.

Despite these encouraging possibilities, therapeutic options for PDOC patients are still very limited, and many patients show little functional improvement over time, or even progress to a permanent state of low responsiveness. In fact, national guidelines of care proposed by the Royal College of Physicians (RCP, 2020) do not recommend active rehabilitation in PDOC, but advise instead disability management, maintenance therapy, and responsiveness monitoring. Recently, transcranial direct current stimulation (tDCS) has attracted attention as a potential non-pharmacological rehabilitative tool for treatment of patients with PDOC. tDCS is a non-invasive brain stimulation technique that works by delivering a direct current from a stimulator through electrodes placed on the scalp, with the aim of modulating brain activity (Truong et al., 2018). When electric current reaches the brain, it creates an electric field that polarises or depolarises underlying neurons based on the field's magnitude and direction (Truong et al., 2018). These changes can impact cortical excitability and plasticity and influence cognitive functions as a result (Truong et al., 2018). Traditionally, tDCS was thought to affect only cortical areas. This would limit its application in PDOC, where subcortical and thalamo-cortical networks are known to play a crucial role (Schiff 2010). However, there is now growing evidence from both animal (Bolzoni et al., 2013) and human studies (Polanìa et al., 2011; Clements et al., 2014; Nonnekes et al., 2014), that tDCS can indirectly influence deeper structures too, when these are functionally connected to the cortical target region in a relevant cognitive function. In line with this, we have found evidence that anodal tDCS over the motor cortex and cathodal tDCS over the cerebellum lead to long-range changes in thalamo-cortical coupling when participants are engaged in a motor task (Chapter 4), and therefore has potential to target the specific mechanisms underlying CMD (Fernandez-Espejo et al., 2015). Moreover, as discussed elsewhere (Bikson and Dmochowski 2020), modelling and intra-cranial recordings have also shown that tDCS can also generate significant current in deeper regions to expect successful neuromodulations (Gomez-Tames et al., 2009; Datta et al., 2009; DaSilva et al., 2012; Opitz et al., 2016; Huang et al., 2017; Chhatbar et al., 2018). Importantly, tDCS is associated with a low risk to induce seizures and is highly portable and easy to deliver,

which makes it a particularly attractive option for PDOC patients, whether they are hospitalised or treated at home.

Several studies have reported short-term improvements in behavioural responsiveness of PDOC patients after tDCS (Thibaut et al., 2014; Angelakis et al., 2014; Naro et al., 2016; Thibaut et al., 2017; Huang et al., 2017; Zhang et al., 2017; Martens et al., 2018; Straudi et al., 2019, Zhang et al., 2020). While very promising, their outcomes have sometimes been inconsistent, partially due to small sample sizes, heterogeneous methodologies across studies (e.g., differences in montage, current intensity, or target area, amongst others) and variability in the outcome measures used (from behavioural scales to electroencephalographic recordings).

Here, we review findings in support of the use of tDCS as an intervention to support rehabilitation in PDOC, with a specific focus on CMD patients. We identify several areas for consideration when interpreting the outcomes of current literature of tDCS on PDOC and propose ways to address these to increase robustness of conclusions in future research. We also review whether the use of neuroimaging data can help identify tDCS changes that are not behaviourally evident. Finally, we argue that tDCS can be integrated with routine care programmes to maximise its beneficial effects.

2.3. Clinical effects of tDCS in PDOC

A total of 20 studies have investigated the effects of tDCS stimulation in the level of consciousness of PDOC patients. Among these, nine considered effects of a single-session of tDCS (Thibaut et al., 2014; Naro et al., 2015; Naro et al., 2016; Bai et al., 2017; Bai et al., 2018; Martens et al., 2019; Thibaut et al., 2019; Carrière et al., 2020; Martens et al., 2020) and the remaining 11 involved multiple tDCS sessions (5-20) (Angelakis et al., 2014; Estraneo et al., 2017; Thibaut et al., 2017; Huang et al., 2017; Zhang et al., 2017; Martens et al., 2018; Cavinato et al., 2019; Straudi et al., 2019; Wu et al., 2019; Guo et al., 2019; Zhang et al., 2020) (see **Tables 2.1** and **2.2**). While the majority of the studies used a double-blind, sham-controlled randomised crossover design, a small number used (double-blind, sham-controlled) randomised non-crossover designs (Wu et al., 2019; Zhang et al., 2017), open-label sham-controlled designs (Angelakis et al., 2014, Bai et al., 2018), or open-label without a sham

condition (Straudi et al., 2019; Guo et al., 2019; Zhang et al., 2020). All used anodal stimulation as the active condition. The duration of the stimulation was typically around 20 minutes, at amplitudes between 1-2mA. Sample sizes ranged from 10 to 45 patients and included either MCS only or both VS and MCS patients.

Table 2.1. *Overview of single session tDCS studies in PDOC.*

Author	**Patients**	**Type of study**	**tDCS montage**	**Stimulation parameters (intensity, electrode size, duration)**	**Immediate post-stimulation evaluations**	**Follow up**	**Dependant measure**	**tDCS elicited changes**
Thibaut et al., 2014	25 VS, 30 MCS.	Double-blind sham-controlled randomised crossover.	Anode: left DLPFC; Cathode: right supraorbital region.	1mA, 35cm^2, 20 min	Immediately post-stimulation.	12 months.	CRS-R.	● Increased CRS-R scores in MCS only. ● At the individual level, 13 MCS patients and 2 VS patients showed signs of consciousness which were not observed before active tDCS nor after sham tDCS.
Naro et al., 2015	20 HC, 10 VS, 12 MCS, 2 EMCS, 1 LIS.	Double-blind sham-controlled randomised crossover.	Anode: OFC; Cathode: Cz.	1mA, 25cm^2 (Anode), 35cm^2 (Cathode), 10 min.	Immediately and 60' post-stimulation.	-	CRS-R, TMS and MEPs.	● No effects on CRS-R scores in any clinical group ● Increased cortical excitability in HC and MCS patients ● Increased M1 excitability and premotor-motor connectivity in 4 VS patients (no group effects).
Naro et al., 2016	10 HC, 10 VS, 10 MCS.	Double-blind sham-controlled randomised crossover.	Anode: medial cerebellum; Cathode: left buccinators muscle.	Oscillatory tDCS: rectangular waves changing polarity at 5Hz, between 0 and 2mA per electrode, 16cm^2, 10 min.	Immediately, after 30' and after 60' post-stimulation.	-	CRS-R, EEG: absolute power spectra (POW), coherence (COH).	● Increased CRS-R scores in MCS only. ● Increased absolute power spectra and coherence in the fronto-parietal network increased in HC and MCS.

Bai et al., 2017	9 VS, 7 MCS.	Double-blind sham-controlled randomised crossover.	Anode: left DLPFC; Cathode: right supraorbital.	2mA, 25cm^2, 20 min.	Immediately post-stimulation	-	TMS-EEG (global mean field amplitude).	● Changes in excitability in temporal and spatial domains that are different between MCS and VS.
Bai et al., 2018	9 VS, 8 MCS.	Sham controlled crossover.	Anode: L-DLPFC; Cathode: right supraorbital area.	2mA, 25cm^2, 20 min.	Immediately post-stimulation	-	CRS-R, EEG: coherence.	● No effects in CRS-R scores ● Modulations of fronto-parietal coherence in MCS: increase in theta band and decrease in gamma band coherence.
Martens et al., 2019	4 VS, 6 MCS.	Double-blind, sham-controlled randomised crossover trial study.	Anodal: M1 (C3 or C4); Cathode: supraorbital area (contralateral).	2mA, 35cm^2 , 20 min.	Immediately post-stimulation	-	CRS-R.	● No effects in CRS-R scores.
Thibaut et al., 2019	5 VS, 7 MCS, 1 MCS+, 1 LIS	Double-blind, sham-controlled randomised crossover pilot study.	Multichannel: 2 Anodes: L/R DLPFC; 2 Cathodes: L/R M1.	1ma, 20 min.	Immediately post-stimulation	-	MAS, CRS-R, EEG: relative power band and wPLI.	● No effects in CRS-R scores. Four patients (1 VS, 2 MCS and 1 EMCS) showed reduced spasticity in finger flexors although no group level effect was observed. ● Increased connectivity (wPLI) values in beta-2 EEG band, higher relative power in theta band, and higher connectivity in beta band in responders.
Carrière et al., 2020	13 MCS /MCS+.	Double-blind, sham-controlled randomised crossover pilot study.	Anode: L-DLPFC; Cathode: right supraorbital region.	1mA, 35cm^2 , 20 min.	Immediately post-stimulation	-	CRS-R HD-EEG: connectivity (wPLI, wSMI) and power.	● No effects in CRS-R scores. Higher relative power l in the alpha band (central regions) and theta band (frontal and posterior regions). Higher wSMI connectivity between left and right parietal regions, and higher fronto-parietal wPLI.

								NB. both EEG effects are uncorrected for multiple comparisons.
Martens et al., 2020	17 VS, 23 MCS, 6 MCS+.	Double-blind sham-controlled randomised crossover trial.	Multichannel: Anodes: F3, F4, CP5 and CP6 (bilateral fronto-parietal areas); Cathode: FP2, FPz (prefrontal) and O1, Oz (occipital).	1mA per anode, 3.14cm^2, 20 min.	10’ post-stimulation.	-	CRS-R, EEG: relative band power and LZW complexity.	● No effects in CRS-R scores. ● Increase in EEG complexity for low-frequency bands (1-8 Hz). ● Changes in CRS-R scores negatively correlated with LZW complexity for those bands.

CRS-R, Coma recovery scale revised; DLPFC, dorsolateral prefrontal cortex; EEG, electroencephalography; EMCS, exit-minimally conscious state; HC, healthy controls; HD-EEG, high-definition EEG; LIS, locked-in syndrome; LZW, Lempel-Ziv-Welch; M1, motor cortex; MAS, Modified Ashworth Scale; MCS, minimally conscious state; MCS+, high-level MCS; OFC, orbitofrontal cortex; TMS, transcranial magnetic stimulation; VS, vegetative state; wPLI: debiased weighted phase lag index.

Table 2.2. *Overview of multiple session tDCS studies in PDOC.*

Author	Patients	Type of study	tDCS montage	Stimulation parameters (intensity, electrode size, duration)	Number of sessions	Immediate post-stimulation evaluations	Follow up	Dependant measure	tDCS elicited changes
Angelakis et al., 2014	7 VS, 3 MCS.	Open-label, sham-controlled, case series trials.	Anode: L-DLPFC or L-M1; Cathode: right orbit.	1mA / 2mA, 25cm^2, 20 min.	15 (5 1mA, 5 2mA, 5 sham).	Immediately after each week's last stimulation session.	12 months	CRS-R.	● CRS-R scores increased in 3 MCS patients and 1 VS patient. The VS patient who showed a clinical improvement was diagnosed as MCS- at a 12-month follow-up.
Estraneo et al., 2017	7 VS, 6 MCS.	Double-blind sham-controlled randomised crossover.	Anode: L-DLPFC; Cathode: right supraorbital region.	2mA, 35cm^2, 20 min.	20 (5 anodal, 5 sham).	Immediately after the first stimulation session and two hours after the last weekly stimulation.	3 months	CRS-R, EEG: background activity (visual classification by 2 clinicians).	● No effects in CRS-R scores. ● Some MCS patients with short time post-injury showed small increases in CRS-R total score. ● EEG changes occurred in conjunction with small clinical improvements.
Thibaut et al., 2017	16 MCS.	Double-blind sham-controlled randomised crossover.	Anode L-DLPFC; Cathode: right supraorbital region.	2mA, 35cm^2, 20 min.	10 (5 anodal, 5 sham).	Immediately post-stimulation in all sessions	1 week	CRS-R.	● CRS-R scores increased in chronic MCS patients. The effects were present both at day 5 as well as 1 week after the last stimulation.
Huang et al., 2017	33 MCS.	Double-blind sham-controlled randomised crossover.	Anode: posterior parietal cortex (Pz). Cathode: right supraorbital region.	2mA, 20 min.	10 (5 anodal, 5 sham).	Immediately post-stimulation in all sessions	5 days	CRS-R.	● CRS-R scores increased in 9 MCS patients.

Zhang et al., 2017	real tDCS: 5 VS, 8 MCS. Sham tDCS: 6 VS and 7 MCS.	Double-blind sham-controlled randomised, non-crossover.	Anode: L-DLPFC; Cathode: right supraorbital region.	2mA, 35cm^2, 20 min.	20, twice a day for 10 days.	Immediately after last stimulation session for each condition	Directly after	CRS-R, EEG: auditory odd-ball paradigm, amplitude and latency (auditory ERP, p300).	● Increased CRS-R scores increased in MCS only. ● Significant increase in P300 amplitude (but not in latency) in MCS patients.
Martens et al., 2018	22 MCS.	Double-blind sham-controlled randomised crossover.	Anode: L-DLPFC; Cathode: right supraorbital region. Cathode right supraorbital region	2mA, 35cm^2, 20 min.	40 (20 anodal, 20 sham) for 4 weeks.	Immediately after last stimulation session for each condition	3 months	CRS-R.	● No group effects on CRS-R scores. ● At the individual level, 6 patients showed new signs of consciousness at the end of the 20 sessions of active tDCS, that were not present after the sham sessions. ● No improvements present at a 12-month follow-up.
Cavinato et al., 2019	12 VS, 12 MCS.	Double-blind sham-controlled randomised crossover.	Anode: L-DLPFC; Cathode: contralateral deltoid.	2mA, 35cm^2, 20 min.	20 (10 anodal over 2 weeks, 10 sham over 2 weeks).	Immediately after last stimulation session for each condition.	Directly after	CRS-R, WNSSP, EEG: coherence and power spectra.	● No effects on CRS-R scores. ● MCS patients showed an increase in WNSSP score, in power and coherence in frontal and parietal EEG bands. ● VS patients showed an increase in frontal coherence in the delta band but no changes in power spectra.

Straudi et al., 2019	10 MCS.	Open-label pilot study.	2 anodes: bilateral M1; Cathode: Nasion.	2mA, 16cm^2, 40 min.	10 over 2 weeks.	Immediately after each week's last stimulation session	3 months	CRS-R, EEG: relative band power.	● Increased CRS-R scores in 8 out of 10 MCS patients. ● In MCS patients, the alpha upper band at the parietal site was increased after 5 stimulation sessions out of 10.
Wu et al., 2019	9 VS, 7 MCS.	Double-blind sham-controlled randomised, non-crossover.	Anode: L-DLPFC or R-DLPFC; Cathode: corresponding contralateral supraorbital area.	2mA, 35cm^2, 20 min.	10 anodal or sham over 2 weeks.	Immediately after each week's last stimulation session.	3 months	CRS-R, GOS-E, EEG: connectivity (PLV).	● No effects on CRS-R scores. ● L-DLPFC tDCS led to increased excitability of the prefrontal cortex. ● R-DLPFC tDCS only elicited activation in the right frontal lobe and no increases in region-to-region connections.
Guo et al., 2019	5 VS, 6 MCS.	Open-label pilot study.	HD-tDCS (4x1-ring) Anode: 1 electrode over the precuneus; Cathode: 4 electrodes surrounding the anode (each placed 3.5 cm radially from the anode).	2mA, 20 min.	28 anodal over 14 consecutive days (twice a day).	Immediately after the 2nd , 14th , and last sessions.	-	CRS-R, EEG: coherence.	● Increased CRS-R scores in all MCS patients and 3 VS patients. ● Reduced coherence in the delta band, for frontal inter-hemisphere, central inter-hemisphere and between the central and parietal region.

Zhang et al., 2020	15 VS, 20 MCS.	Open-label study.	HD-tDCS (4x1-ring) Anode: 1 electrode over the precuneus; Cathode: 4 electrodes surrounding the anode (each placed 3.5 cm radially from the anode).	2mA, 20 min.	28 anodal over 14 consecutive days (twice a day).	Immediately after the 2^{nd} , 14^{th} , and last sessions.	-	CRS-R; EEG: clustering coefficient and global efficiency based on dwPLI.	● Increased CRS-R scores in 11 MCS patients and 5 VS patients. ● Increased average clustering coefficient values in the beta and gamma bands for MCS patients only. ● Decreased global efficiency values in the delta band and increased values in the beta band for MCS patients only.

CRS-R, Coma recovery scale revised; DLPFC, dorsolateral prefrontal cortex; dwPLI: debiased weighted phase lag index; EEG, electroencephalography; ERP, event-related potential; GOS-E, Glasgow Outcome Scale-extended; M1, motor cortex; MCS, minimally conscious state; PLV, phase-locking value; VS, vegetative state; WNSSP, Western Neuro Sensory Stimulation Profile;

2.4. Target areas

The most commonly targeted area was the left DLPFC (12 studies; Thibaut et al., 2014; Angelakis et al., 2014; Thibaut et al., 2017; Estraneo et al., 2017; Bai et al., 2017; Zhang et al., 2017; Martens et al., 2018; Bai et al., 2018; Thibaut et al., 2019; Cavinato et al., 2019; Wu et al., 2019; Carrière et al., 2020). A small number of studies investigated other areas such as the motor cortex (Angelakis et al., 2014; Straudi et al., 2019; Martens et al., 2019), cerebellum (Naro et al., 2016), right DLPFC (Wu et al., 2019; Thibaut et al., 2019), orbitofrontal cortex (OFC) (Naro et al., 2015), posterior parietal cortex (Huang et al., 2018), or bilateral fronto-parietal areas (Martens et al., 2020). In addition to these standard tDCS montages, two studies (Guo et al., 2019; Zhang et al., 2020) applied a more recent method known as high-definition tDCS (HD-tDCS) over the precuneus, for 14 consecutive days. See **Figure 2.1** for an example of a canonical and a HD-tDCS montage).

All studies except Bai et al. (2017) used the Coma Recovery Scale Revised (CRS-R; Giacino et al., 2004) as one their main outcome measures. This is currently the gold-standard for diagnosis in PDOC. Out of these 19 studies, 10 did not report significant changes in behavioural responsiveness at the group level following tDCS (Naro et al., 2015; Estraneo et al., 2017; Bai et al., 2018; Martens et al., 2018; Martens et al., 2019; Cavinato et al., 2019; Thibaut et al., 2019; Wu et al., 2019; Carrière et al., 2020; Martens et al., 2020). Interestingly however, eight of these reported significant EEG changes (see section below).

In contrast, nine studies reported significant changes in CRS-R scores after tDCS, although those changes were limited to MCS patients only (with the exception of Zhang et al. (2020) who also observed increased CRS-R scores in VS patients, although this increase was significantly lower to the one observed in MCS patients). Among these studies, three targeted the left dorsolateral prefrontal cortex (L-DLPFC) (Thibaut et al., 2014; Thibaut et al., 2017; Zhang et al., 2017), one the cerebellum (Naro et al., 2016), one targeted both M1 and the L-DLPFC (Angelakis et al., 2014), one bilateral M1 (Straudi et al., 2019), one the posterior parietal cortex (Huang et al., 2017), and two the precuneus (Guo et al., 2019; Zhang et al., 2020).

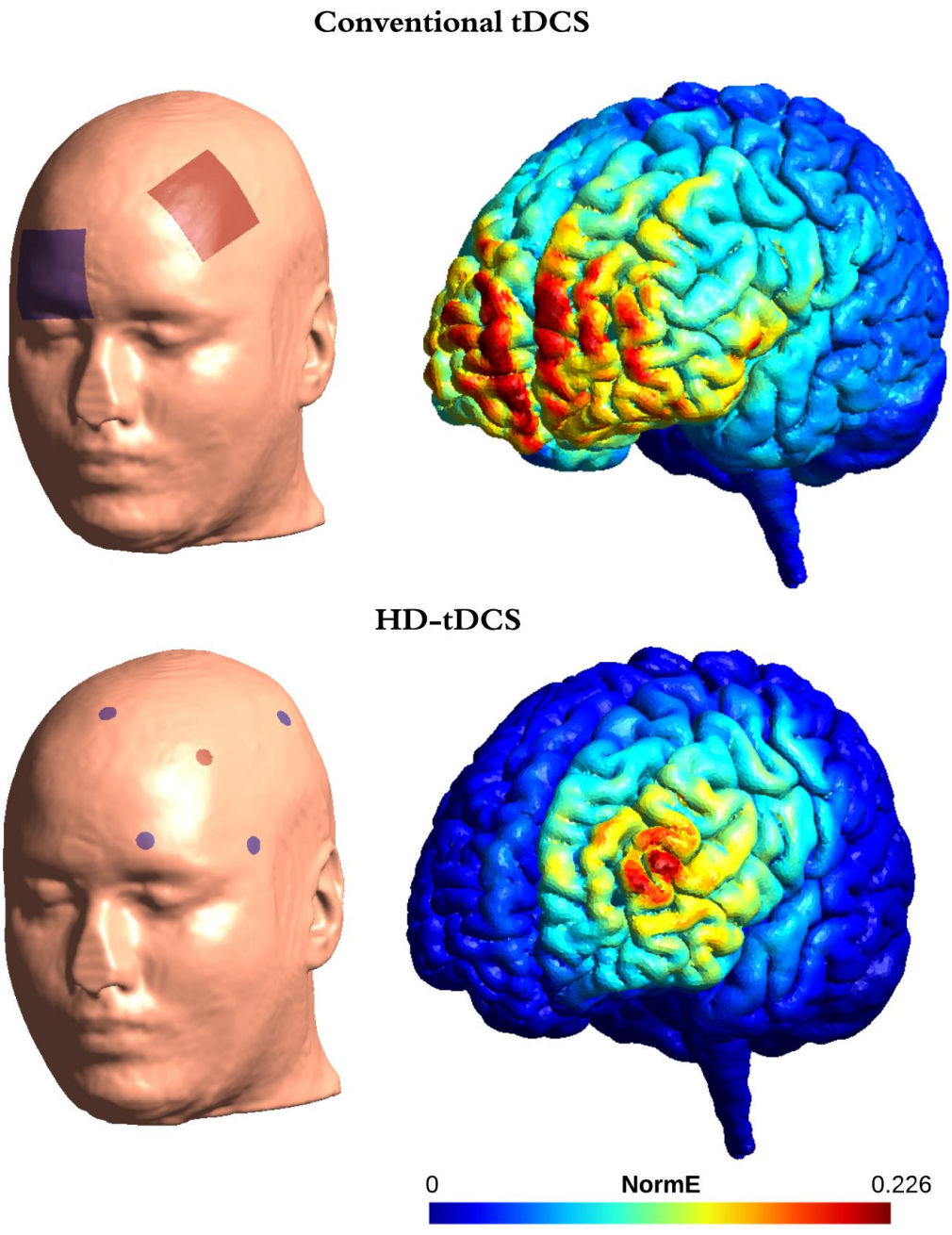


Figure 2.1. Comparison between conventional tDCS and HD-tDCS montages targeting the left DLPFC. The top two inset displays the most commonly used montage to target the DLFC with conventional tDCS: active electrode (anode) placed over F3 and the reference electrode (cathode) over Fp2. The bottom two insets display the equivalent HD-tDCS montage: active electrode over F3 and 4 reference

electrodes, placed at FP1, FZ, C3 and F7. For each montage, the left inset represents the location of each electrode on a three-dimensional head model and the right inset represents the simulated electric field on a standard brain. Red colours represent higher fields. We used Simnibs3.2.2 on the “Ernie" head model with the current intensity for the active electrode set at 1mA.

2.5. Number of treatment sessions

Seven of the nine studies reporting clinical changes after tDCS, delivered multiple stimulation sessions: two studies used five sessions (Thibaut et al., 2017; Zhang et al., 2017), two used 10 sessions (Angelakis et al., 2014; Straudi et al., 2019), one used 20 sessions (Zhang et al., 2017) and two used 28 sessions (Guo et al., 2019; Zhang et al., 2020). Note that the latter two studies used HD-tDCS.

The only two single session studies that reported significant increases in patients’ CRS-R scores were Thibaut et al. (2014) and Naro et al. (2016). The former assessed the effects of 20 minutes of 1mA anodal tDCS over the L-DLPFC on 25 VS patients (6 traumatic and 19 nontraumatic) and 30 MCS patients (19 traumatic and 11 nontraumatic) and found that 43% of MCS patients showed some clinical improvements as measured by CRS-R. The same group effect was not found within VS patients, with only two patients showing post anodal tDCS-related improvements. A similar pattern was found in Naro et al. (2016), where an improvement in CRS-R scores (in the motor and arousal sub-scales) was observed in MCS patients only, and not VS, after 10 minutes of anodal tDCS at 2mA over the cerebellum.

More recent studies typically included multiple sessions with the aim of increasing the effects of stimulation. For example, Huang et al. (2017) administered five daily sessions of anodal tDCS at 2mA, for 20 minutes each, over the posterior parietal cortex in a sample of 33 MCS patients and found that 27% of them improved in their CRS-R scores. This included the appearance of new behaviours such as reproducible command-following, visual pursuit, intentional communication, object recognition, and intelligible verbalisation. While these represented a clear clinical improvement, the new behaviours remained consistent with a diagnosis of MCS in all cases. Moreover, these improvements were not present anymore at a 5-day follow-up. Other multiple session studies obtained similar results. For example, in

Angelakis et al. (2014), five sessions of anodal tDCS at 1mA and five sessions at 2mA, over the L-DLPFC or M1, led to CRS-R increases in all three MCS patients included in their study, and one VS patient out of 7. Similarly, Thibaut et al., (2017), reported a two-point increase in CRS-R scores after five sessions of anodal L-DLPFC tDCS in a sample of chronic MCS patients (> 5 months post injury). Interestingly, this effect was still present a week after receiving the last stimulation session. A further study including 20 tDCS sessions over the L-DLPFC (twice a day for 10 days) showed improvements in CRS-R scores in the MCS but not the VS patients assigned to the real stimulation group (Zhang et al., 2017). In addition to these, Martens and colleagues (2018), who also targeted the L-DLPFC, found a moderate effect size at the end of 4 weeks of 20 daily home-based tDCS sessions, although this effect only approached statistical significance. Using a different target (anodes on the left and right M1 and cathode on the nasion), Straudi et al. (2019) found on average two points improvement in eight out of 10 chronic MCS patients (time post injury between 1 and 19 years), after 10 sessions of tDCS. Finally, the only two studies administering HD-tDCS, reported improvements in the CRS-R scores of all (six) MCS patients (Guo et al., 2019) and in 11 out of 20 MCS patients and in 5 out of 15 VS patients (Zhang et al., 2020), after 28 sessions targeting the precuneus over 14 consecutive days. Collectively, these studies suggest that multiple tDCS sessions may be more effective than a single session in PDOC.

2.6. Long term effects of tDCS

To date, we still have very little evidence in support (or otherwise) of a long-term therapeutic value of tDCS in this group. In fact, the above changes in CRS-R are typically registered shortly after stimulation (within one hour). Only eight studies included follow-up measurements post-tDCS: at 12 months (Angelakis et al., 2014; Thibaut et al., 2014), three months (Estraneo et al., 2017; Martens et al., 2018; Wu et al., 2019; Straudi et al., 2019), seven days (Thibaut et al., 2017), and five days (Huang et al., 2018). Among these, only Angelakis and colleagues (2014) and Straudi and colleagues (2019) found a lasting treatment effect. In the former, at one-year follow-up, one out of seven VS patients progressed to MCS, while four VS patients remained stable as VS, and two VS patients died. In contrast two out of three MCS patients regained consciousness and one remained MCS. In the latter, eight out of 10 MCS patients showed an

overall clinical improvement of two points in the total CRS-R score at three months post-tDCS, as compared to their first assessment. It is worth highlighting here that Straudi et al. (2019), did not include sham or other control conditions, which limits the interpretation of their results. Overall, even though transient post stimulation effects are scientifically informative - in that they are suggestive of greater potential effects when stimulation protocols are refined - they would only have a real therapeutic value if they last days, weeks or months (Parkin et al., 2015). Crucially, there is currently not enough evidence in support of long-lasting effects of tDCS even in healthy participants, or other clinical groups, when tDCS is administered at rest (that is, not coupled to a task). Indeed, most studies report effects that last a few minutes (Nitsche & Paul, 2000; Jamil et al., 2017; Hassanzahraee et al., 2020) to just a couple of hours (Nitsche & Paul, 2001; Labruna et al., 2016). This calls into question whether the above reported long term changes in CRS-R can indeed be attributed to tDCS or to the normal clinical progression of the patients.

In contrast, there is evidence that tDCS can lead to longer lasting effects when coupled to a task. For example, several studies in healthy volunteers have demonstrated increases in numerical performance or motor learning that can last days or even months post-stimulation (Kadosh et al., 2010; Galea and Celnik, 2009; Koyama et al., 2015). Rroji et al. (2015) shed light on the mechanisms of these changes by showing that anodal tDCS over M1 coupled with motor practice (ballistic thumb flexion movements with the non-dominant hand) improved long-term (1 week follow-up) but not short-term retention (30 minutes and one day follow-up). This supports the idea that tDCS augments synaptic plasticity through long-term potentiation-like processes. In clinical groups, a pilot study on three chronic post-stroke aphasic patients showed that tDCS administered for two weeks (5 times per week) and coupled to naming training had beneficial effects in picture naming, that lasted up to 21 weeks after the end of stimulation (Vestito et al., 2014). There are evident challenges associated with delivering tDCS during a task in PDOC, as many of these patients by definition cannot engage in purposeful behaviour. However, due to the clear benefits of such an approach, this is an exciting avenue that could drastically improve the effects of tDCS in CMD patients who are able to voluntarily follow commands, albeit not behaviourally.

2.7. Effects of tDCS on brain function

To date, no study has assessed tDCS changes using active fMRI/EEG paradigms. However, Zhang et al. (2017) used EEG to investigate auditory event-related potentials (ERPs) changes in a passive paradigm (i.e., a task that does not require the patient's active participation) and found that tDCS increased P300 amplitude but not latency in MCS patients. Consistently with behavioural studies, the authors also observed that P300 waves appeared more frequently in MCS patients than in VS ones.

A much larger number of studies have focused on metrics derived from resting-state EEG recordings, such as power or different indexes of connectivity. For example, Naro et al. (2016) assessed EEG connectivity of fronto-parietal networks (FPN) and found that anodal tDCS over the cerebellum modulated power in theta and gamma bands and increased coherence within the FPN in both VS and MCS patients. Importantly, these modulations correlated with increases in CRS-R scores only in MCS patients. Similar results were found by Bai et al. (2018), who also assessed EEG coherence of the FPN and observed an increase in the theta band and a decrease in the gamma band coherence in MCS patients only after L-DLPFC tDCS. In a multi-session study, Cavinato et al. (2019) found an increase in power and coherence of frontal and parietal alpha and beta bands in MCS patients following multiple anodal tDCS on the L-DLPFC. Interestingly, in VS patients tDCS led only to local changes in slow frequencies of anterior brain regions, suggesting a lack of integration of fronto-parietal functional networks.

More recently, Thibaut et al. (2019) reported increased connectivity values in beta-2 EEG band (18–30 Hz) at the group level after multi-channel tDCS over left and right DLPFC. Importantly, they also identified higher relative power in theta band (4-8 Hz) and connectivity in beta band in tDCS responders (i.e., patients presenting a decrease in hypertonia in at least 2 joints after active but not sham tDCS) as opposed to non-responders. Similarly, Estraneo and colleagues (2017) reported more normalised patterns in background EEG activity (according to the classification criteria proposed by Bruno et al. 2012) in those patients whose CRS-R score improved after tDCS. Wu et al. (2019) observed a trend towards higher EEG functional connectivity in frontal areas after two weeks of tDCS over the right and left DLPFC. More recently, Carrière et al. (2020) assessed weighted phase-lag index (wPLI), symbolic mutual Information (wSMI), and EEG power bands changes following anodal tDCS over the L-

DLPFC in 13 MCS patients. They observed higher wSMI connectivity between left and right parietal regions, and higher fronto-parietal wPLI connectivity, although these changes only appeared when uncorrected for multiple comparisons. Additionally, tDCS led to higher relative power at the group level in the alpha band (central regions) and theta band (frontal and posterior regions), but also at uncorrected statistics only. In their pilot study, Straudi and colleagues (2019) found that multiple sessions of bilateral anodal tDCS over M1 led to modulations in resting-state EEG alpha bands that correlated with improvements in consciousness. Lastly, a study that investigated changes in EEG relative band power and connectivity following multi-channel anodal tDCS over fronto-temporal areas found an increase in EEG complexity for 1-8 Hz bands (Martens et al., 2020). Moreover, increases in the difference between pre-tDCS CRS-R scores and post-tDCS CRS-R scores negatively correlated with EEG complexity for those bands.

While most EEG studies focused on connectivity and power band analyses, a small number of them assessed changes in cortical excitability instead. To this end, Bai et al. (2017) combined TMS with EEG after delivering anodal tDCS over the L-DLPFC. They found that tDCS can indeed modulate cortical excitability in PDOC patients and identified differences in temporal and spatial domains between MCS and VS. Additionally, Naro et al. (2015) used motor-evoked potentials (MEPs) to investigate the effect of anodal tDCS over the OFC and found boosts on cortical excitability in MCS patients and some VS patients.

Collectively, EEG studies suggest a trend towards increased functional connectivity following tDCS in MCS patients, which are more pronounced in patients who show behavioural responses to the stimulation. Interestingly, previous studies have associated recovery of consciousness with restoration of long-range connectivity (for a review see Bodien et al., 2017). It is thus possible that the reported changes in resting state EEG are indexing subclinical improvements, which suggests that further optimisation of stimulation parameters may be needed to allow for these to translate into clinically measurable ones. However, as previously argued by Bestmann and colleagues (2015), we do not yet have a good understanding of how the physiological effects of tDCS relate to its impact on behaviour. This may delay the development of more effective treatments and promote mechanistic inferences that are not plausible.

2.8. Common Methodological Limitations

A number of limitations could be explaining the variable success of tDCS in PDOC to date. While not aiming to provide an exhaustive list, some of the most important considerations are:

2.8.1. Selection of targets

As can be appreciated in our description above (see also **Tables 2.1** and **2.2**), there is a high heterogeneity in the specific tDCS montage used across the different studies included in this review. This is likely due to the absence of a broadly accepted theory of consciousness that can explain the (full or partial) absence of awareness in PDOC (Zhao et al., 2019; Maillé and Lynn, 2020), and can provide a mechanistic framework for the selection of targets for stimulation.

This notwithstanding, most studies targeted the left DLPFC, and provide different justifications for this choice. For example, some selected this region on the basis of its role in integrating motor control and behaviour, and its involvement in decision-making (Zhang et al., 2018). Others refer to its connectivity with the default mode network and bilateral fronto-parietal networks (Thibaut et al., 2014) linked with self- and external awareness respectively (Vanhaudenhuyse et al., 2010). Studies targeting the OFC allude to its role in translating integrated information into behaviour (Naro et al., 2015), and those selecting the precuneus base this on its role in consciousness recovery (Guo et al., 2019; Zhang et al., 2020).

We have argued elsewhere (Chapter 4) that the field needs better mechanistic models to inform the selection of targets for stimulation in PDOC. In the absence of a unified theory of consciousness, we have previously proposed to focus on external responsiveness instead by targeting motor areas (Chapter 4). Some studies have targeted M1 or the cerebellum on the basis of their strong connections with the thalamus, and the central role of this structure in arousal regulation (Zhang et al., 2018; Straudi et al., 2019). We suggest that thalamic modulations via motor regions would likely result in modulations of behavioural responsiveness instead. Indeed, we have provided evidence that tDCS over M1 and cerebellum

can indeed modulate such connections in healthy volunteers and elicit neural changes associated with behavioural responses to commands (Chapter 4).

It is important to note here that VS and MCS patients are characterised by different severity in their patterns of injury. Specifically, MCS patients show less severe white matter and thalamic damage (Fernández-Espejo et al., 2010, 2011) as well as less extensive atrophies in basal ganglia (Lutkenhoff et al.,2014). Many of the suggested mechanisms of action proposed to explain the selection of targets in PDOC rely on modulations of cortico-subcortical networks and therefore, these differences in damage could explain why tDCS appears to benefit only MCS patients.

2.8.2. Electrode placement and inter-individual anatomical differences

Alongside challenges to identify a mechanistically informed target, there are also important considerations related to ensuring that the tDCS montage adequately targets the selected area in patients with very severe injuries and altered neuroanatomy. In line with most clinical tDCS research, studies in PDOC typically identify the location of the electrodes on the scalp by using EEG caps or manual measurements based on the 10-20 international electroencephalography system. While practical, this method is known to lack accuracy even in healthy volunteers, due to inter-subject brain variability. For example, in a recent study (De Witte et al., 2018), the authors compared the localisation of the DLPFC achieved with the 10-20 EEG system versus MRI-guided neuronavigation and found that these varied significantly. These errors can only be expected to increase in PDOC patients, whose brains are characterised by gross abnormalities, such as brain atrophies, that are highly heterogeneous across patients, and lead to important anatomical and physiological changes (Zhang et al., 2017). Seminal post-mortem studies showed that, while some abnormalities such as diffuse axonal injury or thalamic damage seem to appear in many patients, there was also high heterogeneity in the patterns of damage and the specific focal injuries observed (Jennet et al., 2001, Jellinger 2013). It is thus possible that in many of the patients investigated to date, current was simply not reaching the target areas, or not at enough intensity.

Inter-individual anatomical differences are particularly important when using high-definition tDCS (HD-tDCS), an increasingly popular approach in the tDCS literature that we anticipate will quickly become popular in PDOC too. HD-tDCS can achieve higher spatial precision as compared to conventional tDCS, by circumscribing the current flow to the area of the small electrodes used (Morya et al., 2019). This method was designed to overcome limitations related to the poor spatial resolution of conventional tDCS, whereby due to the use of large electrodes, the electrical current being applied to the brain does not only reach the targeted area but also other surrounding regions (Morya et al., 2019). The diffuse nature of conventional tDCS makes it difficult to link observed effects (whether neural or behavioural) to the region originally being targeted and limits the effectiveness of tDCS for therapeutic uses. To our knowledge, only two studies assessed HD-tDCS in PDOC patients (Guo et al., 2019; Zhang et al., 2020), but we expect this to increase in coming years. However, it is important to note that as spatial specificity increases, so does the need of using robust and reliable current flow models to plan the location of the electrodes on the scalp to achieve an accurate targeting of the regions of interest (Rawji et al., 2018). In fact, even in healthy volunteers, individual responses to tDCS can vary greatly due to differences in scalp and skull thickness or shape (Opitz et al., 2018), cortical thickness, density or volume (Filmer et al., 2020), or neurochemical factors (Wassermann et al., 2002). This has prompted the development of models that can be personalised to the individual anatomy of each participant (via structural MRI images) and can identify the best montage and doses to achieve the desired intensity in the target area (Evans et al., 2020). However, while recent years have seen a steep rise in the development of such models, and many are now available as part of commercial applications, these are based on healthy anatomy and tissue properties and have not been validated in severely injured brains. Although it is currently possible to use a patient's MRI data to create current models that take into account their specific neuroanatomy (and injury), in addition to focal injury, PDOC patients may have diffuse brain lesions that can greatly affect the microstructure of the remaining tissue and affect conductance.

The use of healthy models of current distribution to localise the best electrode placement for conventional and HD-tDCS may thus likely result in targeting the wrong anatomical region for many patients. In the specific case of HD-tDCS this can lead to even worse results than conventional (less focussed) tDCS. Therefore, we believe that the field needs the development

of specific models that can incorporate individual differences in tissue abnormalities to aid the choice of montage and maximise the effects of tDCS across patients. We could further argue that such models are necessary before HD-tDCS can successfully be applied to PDOC patients.

In fact, it is only by gaining a deeper understanding of the observed variability in tDCS responsiveness - that is, understanding why tDCS is effective in some patients and not in others - that we can develop more effective, patient-focused protocols. Going forwards, the field needs studies to include neuroimaging methods within their protocols with the aim of identifying biomarkers that can help make predictions about responsiveness to stimulation protocols. In trials where the use of neuroimaging is not possible or feasible, we recommend a careful selection of candidate patients on the basis of absence of focal injuries in the target region(s) and nearby areas, as well as no gross abnormalities that result in region shifting. On the basis of the differences in subcortical damage discussed in section 1 above, we would argue that the selection criterion should go beyond focal cortical lesions to also include a relative preservation of the networks that tDCS intends to modulate with any given montage. While together, these requirements would clearly result in a reduced number of eligible patients, they would also result in better targeting and a better characterisation of causality in the reported effects of tDCS. In our opinion, this is essential for the field to move forwards.

2.8.3. Small sample sizes and heterogeneity of methods

As mentioned above, the majority of the studies in this review used small sample sizes; an average 20.7 (± 12.6) patients, that usually included both VS and MCS. In addition to this, patients' aetiology is often varied with most studies including both traumatic and non-traumatic patients (for more details see **Table 2.3**). Moreover, as it is evident above, there is a great heterogeneity in the methods used (i.e., tDCS setups, number of sessions, outcome measures etc.). All together, these issues make comparisons across studies futile. While sample sizes and heterogenous patients are typical in the broader PDOC field, and inherent to conducting research with this very challenging clinical population, adopting more standard methods would facilitate meta-analyses, and perhaps the combination of data across multiple centres. This would allow us to achieve a better understanding of the variability in responsiveness to tDCS observed in PDOC patients.

Table 2.3. *Demographics and aetiologies of VS and MCS patients included in the different studies.*

Author	**VS patients' characteristics**	**VS patients' aetiologies**	**MCS patients' characteristics**	**MCS patients' aetiologies**	**Aetiology of VS patients who showed clinical improvements**	**Aetiology of MCS patients who showed clinical improvements**
Single-session studies						
Thibaut et al., 2014	N: 25; Gender: 9 females, 16 males; Mean age: 42 ± 17; BI onset: 24 ± 48 months.	6 TBI 9 anoxic 9 nontraumatic (5 CVA, 4 SH)	N: 30; Gender: 7 females, 23 males; Mean age: 43 ± 19; BI onset: 43 ± 63 months.	19 TBI, 4 anoxic, 6 non-traumatic (3 CVA, 3 SH, 1 mixed traumatic ischemic).	**2 VS patients:** both SH	**13 MCS patients:** 5 TBI, 4 anoxic, 2 CVA, 2 SH.
Naro et al., 2015	N: 12; Gender: 7 females, 5 males; Mean age: 54.4 ± 11.3; BI onset: 23± 21.5 months.	5 TBI, 7 anoxic.	N: 10; Gender: 5 females, 5 males; Mean age: 55.6 ± 15.9; BI onset: 13.9 ± 9.4 months.	5 TBI, 5 anoxic.	**4 VS patients:** all anoxic.	**All MCS patients:** 5 TBI, 5 Anoxic.
Naro et al., 2016	N: 10; Gender: 7 females, 3 males; Mean age: 51 ± 10; BI onset: 25 ± 24 months.	6 TBI, 4 anoxic.	N: 10; Gender: 5 females, 5 males; Mean age: 56 ± 17; BI onset: 14 ± 10 months.	3 TBI, 7 anoxic.	-	**All MCS patients.**
Bai et al., 2017	N: 9; Gender: 2 females, 7 males;	2 TBI, 4 anoxic,	N: 7; Gender: 3 females, 4 males;	2 TBI, 3 anoxic,	-	-

	Mean age: 45.8 ± 15.2; BI onset: 11.3 ± 6.8 months.	2 haemorrhagic, 1 ischemic.	Mean age: 47 ± 13.4; BI onset: 15.4 ± 11.5 months.	2 haemorrhage.		
Bai et al., 2018	N: 9; Gender: 2 females, 7 males; Mean age: 44.8 ± 14.5; BI onset: 11.4 ± 6.9 months.	3 TBI, 4 anoxic, 2 haemorrhagic.	N: 8; Gender: 4 females, 4 males; Mean age: 43.2 ± 14.9; BI onset:12.6 ± 8.7 months.	4 TBI, 1 anoxic, 3 haemorrhagic.	-	-
Martens et al., 2019	N: 4; Gender: 1 female, 3 males; Mean age: 57.5 ± 19.6; BI onset: 3.1 ± 3.7 months.	1 TBI, 3 non-TBI.	N: 6; Gender: 1 female, 5 males; Mean age: 43.5 ± 20.8; BI onset: 8.9 ± 13.1 months.	5 TBI, 1 non-TBI.	**1 VS patient:** non-TBI.	**1 MCS patient:** 1 TBI.
Thibaut et al., 2019	N: 5; Gender: 3 females, 2 males; Mean age: 44.6 ± 12.1; BI onset: 9.4 ± 2.4 months.	3 TBI, 2 cardiac arrest	N: 7; Gender: 4 females, 3 males; Mean age: 38.5 ± 15.1; BI onset: 47.2 ± 35.5 months. 1 EMCS patient: male, aged 61, 10.6 months post BI.	3 TBI, 3 haemorrhagic stroke, 1 cardiac arrest EMCS patients: haemorrhagic stroke.	**1 VS patient:** Cardiac arrest	**2 MCS patients**: 1 TBI, 1 haemorrhagic stroke. **1 EMCS:** haemorrhagic stroke
Carrière et al., 2020	-	-	N: 11; Gender: 3 females, 8 males; Mean age: 46 ± 14 BI onset: 8.4 ± 6.3 months.	3 TBI, 3 cardiac arrest. 4 aneurysm,	-	**3 MCS patients:** 1 TBI, 1 cardiac arrest,

				1 meningitis.		1 aneurysm.
Martens et al., 2020	N: 17; Gender: 9 females, 8 males; Mean age: 50.7 ± 12.8; BI onset: 7.7 ± 7.1 months.	2 TBI, 15 non-TBI.	N: 23 MCS; Gender: 6 females, 17 males; Mean age: 45.7 ± 15.9; BI onset: 61.8 ± 82.6 months. 6 EMCS patients: 3 females, aged 43.3 ± 16.3, 25 ± 24.8 months post BI.	12 TBI, 11 non-TBI. EMCS patients: all TBI.	-	**3 MCS patients:** 2 TBI, 1 non-TBI. **1 EMCS:** TBI
Multiple session studies						
Angelakis et al., 2014	N: 7; Gender: 2 females, 5 males; Mean age: 41.1 ± 12.5; BI onset: 62.4 ± 39.6.	3 TBI, 4 anoxic.	N: 3; Gender: 1 female, 2 males; Mean age: 39 ± 12.3 BI onset: 21.3 ± 18.9 months.	2 TBI, 1 postoperative stroke.	**1 VS patient:** TBI	**All MCS patients:** 2 TBI, 1 postoperative stroke
Estraneo et al., 2017	N: 7; Gender: 3 females, 4 males; Mean age: 49.6 ± 24.5; BI onset: 13.8 ± 18 months.	1 TBI, 4 anoxic, 2 vascular.	N: 6 Gender: 3 females, 3 males; Mean age: 60.3 ± 13.2; BI onset: 27.16 ± 27 months.	2 anoxic, 4 vascular.	**2 VS patients:** 1 anoxic, 1 vascular.	**3 MCS patients:** 1 anoxic, 2 vascular.

Thibaut et al., 2017	-	-	N: 16; Gender: 7 females, 9 males; Mean age: 43.3 ± 15.15; BI onset: 78.25 ± 97.6 months.	11 TBI, 2 anoxic, 3 cardiac arrest	-	**9 MCS patients:** 5 TBI, 1 anoxic, 2 cardiac arrest.
Huang et al., 2017	-	-	N: 33; Gender: 13 females, 20 males. Mean age: 57 ± 11; BI onset: 6 ± 5 months.	20 TBI, 13 non-TBI.	-	No individual data provided.
Zhang et al., 2017	N: 11; Gender: 6 females, 5 males; Mean age: 60 ± 17.5; BI onset: 4.5 ± 3.5 months.	4 TBI, 3 anoxic, 3 haemorrhagic,	N: 15; Gender: 5 females, 10 males; Mean age: 42.7 ± 18.3; BI onset: 6.2 ± 4.4 months.	8 TBI, 2 ischemic, 4 haemorrhagic, 1 anoxic.	-	**8 MCS patients:** 4 TBI, 3 haemorrhagic, 1 ischemic.
Martens et al., 2018	-	-	N: 22; Gender: 6 females, 16 males; Mean age: 41.9 ± 12.5; BI onset: 106.3 ± 84.5 months.	10 TBI, 8 cardiac arrests, 3 aneurysm, 1 anoxic.	-	**6 MCS patients.**
Cavinato et al., 2019	N: 12; Gender: 5 females, 7 males; Mean age: 47.1 ± 16.2; BI onset: 80.28 ± 99.36 months.	2 TBI, 5 anoxic, 3 CVA,	N: 12; Gender: 5 females, 7 males; Mean age: 47.1 ± 16.2; BI onset: 64.2 ± 38.4 months.	6 TBI, 2 anoxic, 1 CVA,	-	Number of patients not specified.

		3 SH.		1 SH.		
Straudi et al., 2019	-	-	N: 10; Gender: 3 females, 7 males; Mean age: 35.4 ± 12.6; BI onset: 66 ± 64.8 months.	All TBI.	-	**8 MCS patients.**
Wu et al., 2019	N: 9; Gender: 3 females, 6 males; Mean age: 51.5 ± 11.1; BI onset: 102 ±61.5 months.	4 TBI, 1 anoxic, 4 haemorrhagic.	N: 7; Gender: 2 females, 5 males; Mean age: 42.6 ± 20.9; BI onset: 210.3 ± 189.6 months.	2 TBI, 2 anoxic, 3 haemorrhagic.	-	**1 MCS patient:** TBI
Guo et al., 2019	N: 5; Gender: - Mean age: 49.9 ± 9.7; BI onset: 5.2 ± 1.9 months.	2 TBI, 3 haemorrhagic.	N: 6; Gender: - Mean age: 55.5 ± 14.4; BI onset: 3.6 ± 1.1 months.	All haemorrhagic.	**3 VS patients:** 1 TBI, 2 haemorrhagic.	**All MCS patients.**
Zhang et al., 2020	N: 15; Gender: 3 females, 12 males; Mean Age; 51 ± 9.6; BI onset: 1.94 ± 3.42 months.	4 TBI, 11 haemorrhagic.	N: 20; Gender: 10 females, 10 males; Mean Age; 52.3 ± 16.9; BI onset: 3.3 ± 2.97 months.	4 TBI, 16 haemorrhagic.	**5 VS patients:** **1 TBI,** **4 haemorrhagic.**	**11 MCS patients:** **3 TBI** **8 haemorrhagic.**

BI, brain injury; CVA, cerebrovascular accident; EMCS, emerging from minimally conscious state; MCS, minimally conscious state; SH, subarachnoid haemorrhage; TBI, traumatic brain injury; VS, vegetative state;

2.8.4. tDCS polarity and control condition

Due to constraints in resources and time availability, and other challenges that are also inherent to PDOC research, the majority of tDCS studies are focused on the effects of one polarity (typically anodal stimulation) and used sham to control for placebo effects. While the introduction of sham-controlled designs represented the first solid evidence in support of the effectiveness of tDCS, this approach is not without its limitations. Indeed, there is increasing evidence that current methods for sham stimulation do not always guarantee that participants and experimenters are unaware of the stimulation delivered (i.e., Filmer et al., 2020). More importantly, the lack of a control polarity or stimulation site limits the attribution of the resulting effects to the modulation of a particular brain region or network (used as target) instead of a broader generic effect over the brain or peripheral nerves (Parkin et al., 2015). Although this may seem a scientific rather than clinical consideration, it can be argued that it is necessary to achieve a good understanding of the networks that modulate specific clinical effects in order to develop more effective stimulation protocols that can be targeted to the needs of specific patients.

Moreover, the choice of anodal stimulation as therapeutic is based on the assumption that this polarity has excitatory effects over neuronal populations, with cathodal tDCS typically having inhibitory effects. Following this assumption, enhanced or reduced behaviours are often explained by increased or decreased activity in specific cortical regions. Nevertheless, as uncovered by Bestmann and colleagues (2015), this view might be over simplistic, as different cell morphologies and cortical folding of brain tissues have a profound influence on the net effects of stimulation.

2.8.5. Challenges of using clinical scales to assess responses to tDCS

It can be argued that for tDCS to have clinical significance as a therapeutic option it should lead to changes that can be assessed with current diagnostic scales (such as the CRS-R). However, it is also true that these scales are not sensitive to covert changes in cognitive functioning or awareness (Owen et al., 2016). On the one hand, clinical scales mainly rely on motor outputs, which can be highly inconsistent and limited in PDOC, due to lesions in motor cortices (Fernandez-Espejo et al., 2015; Pincherle et al., 2019; Stafford et al., 2019; Wang et

al., 2020). In addition, the presence of injury in language and visual cortices may also interfere with the patients' ability to understand the instructions and show appropriate responses (Schnakers et al., 2009). Furthermore, the presence of tracheostomy, altered reflexes, or arousal fluctuations (Schnakers et al., 2009; Owen et al., 2016) adds further difficulties to detect clinical signs of awareness. In the most severe cases, the presence of CMD – whereby patients are by definition unable to produce motor behaviours, may mask such changes entirely. These difficulties are at the root of the high rates of misdiagnosis that are typically present in this population (Schnakers et al., 2009) and suggest that clinical assessments may not be well suited to reliably capture changes after tDCS.

It is thus possible that the challenges inherent to clinical assessments explain some of the inconsistencies in the above results. Recently developed clinical scales aimed at detecting subtle motor behaviours that may indicate residual cognition (and therefore a possible CMD) may offer a superior alternative to identify the effects of tDCS (Pincherle et al., 2019; Pignat et al., 2016). In addition, there is vast evidence that active fMRI and EEG paradigms (i.e., where patients are required to voluntarily follow commands) can successfully identify preserved but covert cognitive abilities and awareness in PDOC, in many instances before such changes become apparent clinically (see Fernández-Espejo and Owen, 2013 for a review). It is therefore possible that active electrophysiological / neuroimaging paradigms may be able to more accurately detect tDCS-induced effects on consciousness as compared to behavioural evaluations. However, while active tasks provide a definite answer that a patient can follow commands covertly and therefore are aware, they are also very cognitive demanding and may also fail to detect awareness in patients who are affected by language or working memory impairments. A recent study provided an alternative to active paradigms by focusing on the passive processing of the patients' peri-personal space; the multisensory-motor space that surrounds one's body (Noel et al., 2019). The authors found that certain EEG measures off peri-personal space were associated with preserved measures of neural complexity, suggesting a possible CMD. To further support this, peri-personal space metrics did not correlate with CRS-R (Noel et al., 2019). While confirmation of CMD in an individual patient requires a positive response in an active task, measures of peri-personal space offer a promising tool to detect sensorimotor changes mediating crucial self-environment interactions after tDCS.

2.8.6. Challenges in using electrophysiological and neuroimaging studies

As can be appreciated in the summary above, the EEG metrics used across the different tDCS studies in PDOC is striking: three studies included coherence measures, six studies performed power spectral analyses (absolute power spectra or relative power spectra), one study used auditory ERPs, another used global mean field amplitude, a further study calculated the Lempel-Ziv-Welch complexity, and finally three investigated EEG connectivity at the electrode level using different connectivity measures (wPLI, wSMI and phase-locking value). This heterogeneity creates challenges when assessing whether results are consistent across studies or otherwise. Leaving the effects of tDCS aside, EEG assessments of awareness in PDOC have also been characterised by a complex variety of protocols, measures, and analysis pipelines (Bai et al., 2020), and beyond active tasks that can provide a proxy for covert command-following, the field has yet to agree on gold-standard measures of consciousness using EEG. While no study has used fMRI to characterise the effects of PDOC yet, it is important to highlight that the above considerations about heterogeneity of approaches and measures also apply to this technique (Berlingeri et al., 2019).

It is also worth noting that the majority of EEG studies activity successfully identified changes in at least one of the measures considered, even when no significant changes in CRS-R were observed. Although this may speak for an increased sensitivity as a biological marker, we believe that it cannot currently be ruled out that false positives may partially explain the discrepancy between CRS-R and EEG findings in some of the studies included in this review instead. With this in mind, while we strongly believe that imaging and electrophysiology methods can shed light on the effectiveness of tDCS in low responsive patients such as those in PDOC, we also think that the field needs to work towards developing standardised outcome measures that can enable comparisons across studies.

Studies have used both active and passive tasks to successfully assess patients' residual consciousness. However, similarly to studies using EEG, neuroimaging studies also present a great deal of heterogeneity of paradigms used to evaluate consciousness. In addition to this, the majority of these studies included a relatively small group of patients, and often lacked comparisons with healthy controls (for a meta analysis see Berlingeri et al., 2019). To further

evaluate and support the diagnostic value of fMRI paradigms in PDOC patients, systematic replications of these studies are crucial.

2.9. Integration of tDCS in current pathways of care for PDOC

The pathway for care of PDOC patients proposed by the RCP (2020) is composed of five different phases. This pathway is not linear, and patients can be moved up and down at any point during their care. For tDCS to make the jump from research studies into routine clinical care, it would need to be integrated into existing pathways. Importantly, several areas of study are still required before there is sufficient evidence to support the design of effective tDCS interventions in PDOC, and we will review these in detail below. Notwithstanding this, here we review RPC pathways to provide a tentative framework to discuss the feasibility and potential uses for tDCS when integrated into current procedures.

The first phase refers to the acute care in the hospital ward and identifies as main priorities the confirmation of the origin of the disorder of consciousness (DOC) and the identification of the level of preservation of the primary neurological pathways. During this phase, if the DOC persists, the RCP suggests the following three steps, after three days, 2 weeks and four weeks respectively: assessment for interim advice, review and evaluation to eliminate treatable causes and, lastly, referral to specialist PDOC neurorehabilitation units. The second phase refers to the subacute / post-acute stage, which starts 4 weeks after injury (Giacino et al., 2018) and involves early proactive management. In this phase the patient's DOC is considered prolonged (they are henceforth referred to as PDOC) and they are transferred to a specialist PDOC neurorehabilitation service for usually 2-4 months. During these, the patient's medical condition is stabilised, assessments of responsiveness are carried out and a care programme is set up. In the third phase, the patient is under continued active management with specialist PDOC monitoring. This phase lasts until the patient either recovers and is transferred to a specialist rehabilitation unit, or it becomes likely that they will remain in VS or MCS. In the latter case, their clinical status would be considered chronic (Giacino et al., 2018). Importantly, the RCP (2020) states that if the patient shows signs of change at this stage, they should be moved back to the second phase. The fourth phase (chronic PDOC) corresponds to long-term

care, in the patient's own home or in a nursing home setting. The fifth and final phase refers to end-of-life care.

To our knowledge, no study has explored the feasibility of delivering tDCS on DOC patients in the very acute setting (intensive care unit, ICU) or early stages of the subacute phase (phase 2). While administering tDCS at the ICU may not be possible, we argue that future studies should focus on the administration of tDCS in the initial stages of subacute care (4 weeks after injury), to assess its potential for improving clinical diagnosis and assisting rehabilitation (**Figure 2.2**). By increasing patients' responsiveness, the clinical team would more easily recognize signs of awareness, and thus tDCS could help lower the chances of misdiagnosis as a result. Moreover, tDCS could be helpful in revealing covert signs of awareness even when motor behaviours are absent. For example, as reviewed above, Naro and colleagues (2015) assessed residual connectivity in PDOC patients using EEG, and showed that tDCS over the OFC is able to uncover M1 excitability and premotor-motor connectivity in some VS patients, indicating they could potentially have CMD. While CMD can only be confirmed with neuroimaging methods, these are typically expensive and require experts to analyse and interpret the data. If tDCS can indeed identify signs of a potential CMD, this could be used to triage patients for referral for specialised neuroimaging studies. tDCS could therefore be a powerful tool for improving DOC differential diagnosis, when coupled with current behavioural scales (i.e., CRS-R) and electrophysiological methods. Decreasing the chance of misdiagnosis, either by improving detection of CMD in a patient or by differentiating between VS and MSC, is crucial for developing an adequate care plan. In fact, accurate assessment of consciousness has profound implications for patient care, as it is informative for prognosis and guides treatment decisions (such as end-of-life care decisions).

On the other hand, tDCS could improve the success of functional rehabilitation of PDOC in phases two and three. As mentioned above, tDCS is able to enhance motor learning in healthy participants and can aid in the recovery of motor functions in patients with brain lesions (for a review see Ammann et al., 2016). There is also evidence that concurrent brain stimulation and physical therapy can help motor rehabilitation (for a review see Bolognini et al., 2009). In fact, according to Bolognini and colleagues (2009), tDCS would augment the response of neural networks to motor training and, in turn, reinforce its long-term effects. Importantly, PDOC

patients receive intensive physical therapy daily, as part of their management, from the second phase of care onwards. To our knowledge, there are no studies assessing the effects of combined tDCS and physical therapy in PDOC. Nevertheless, we can draw on the literature on other neurological diseases to assess the feasibility of using such methods during the early stage of treatment. For example, it has been observed that bi-hemispheric tDCS (anodal over the affected motor cortex and cathodal over the unaffected one) increases the gain of motor function induced by constraint-induced movement therapy in poststroke patients (Bolognini et al., 2011). Moreover, a study by Bornheim and colleagues (2020) assessed the effects of repetitive tDCS (5 sessions) during the first month after stroke, while patients remained in the neurovascular unit, and observed that when administered prior to rehabilitation, tDCS led to clinically significant improvements in both functional motor outcomes and somatosensory functions. Similarly, Sattler and colleagues (2015) showed that five consecutive daily sessions of anodal tDCS combined with radial nerve stimulation promotes motor hand recovery in the acute phase after ischemic stroke in the rehabilitation unit. Importantly, patients included in this study had their stroke within a maximum of two weeks before starting stimulation. With a patient group more directly related to PDOC (moderate to severe traumatic brain injuries, TBI), Ulam and colleagues (2015) assessed cumulative effects of 10 anodal tDCS sessions on both EEG oscillations and neuropsychological tests while patients were undergoing neurorehabilitation during the acute to subacute stages (approximately 7 ± 4 weeks). Although no cognitive gains were observed, tDCS successfully induced changes in brain oscillations in several frequency bands that suggested an increase in cortical excitability in such patients. Importantly, these changes correlated with improvements in performance.

Taken together, tDCS studies in stroke and TBI, demonstrated that tDCS can accelerate and improve functional recovery while paired with conventional rehabilitation. Moreover, they proved the safety and feasibility of administering repetitive tDCS in the subacute stages after brain injury. We believe this is an exciting area for development in future PDOC studies. The field urgently needs evidence that tDCS can indeed add to the effects of routine clinical interventions. Literature on stroke and TBI suggests this is a research avenue worth pursuing. In addition to these earlier stages, the beneficial effects of tDCS could be investigated also in combination with the routine care during the fourth phase (the long-term care, or chronic stage) at patients' homes, rehabilitation centres or nursing homes. Martens and colleagues (2018)

showed that tDCS can be appropriately used by patients' relatives and caregivers after proper training and can lead to some clinical improvements that may have an impact on the quality of life of patients or caregivers. While these are promising results, and in our opinion offer strong support for the feasibility of this approach, the field still lacks evidence in support of long-term effects even after repeated sessions at home. As we have argued in earlier sections, tDCS is particularly well suited for home delivery due to its portability and safety. Therefore, we think that further research should focus on this stage, where patients would not typically receive any other intervention, to corroborate whether tDCS can offer an alternative to improve their quality of life.

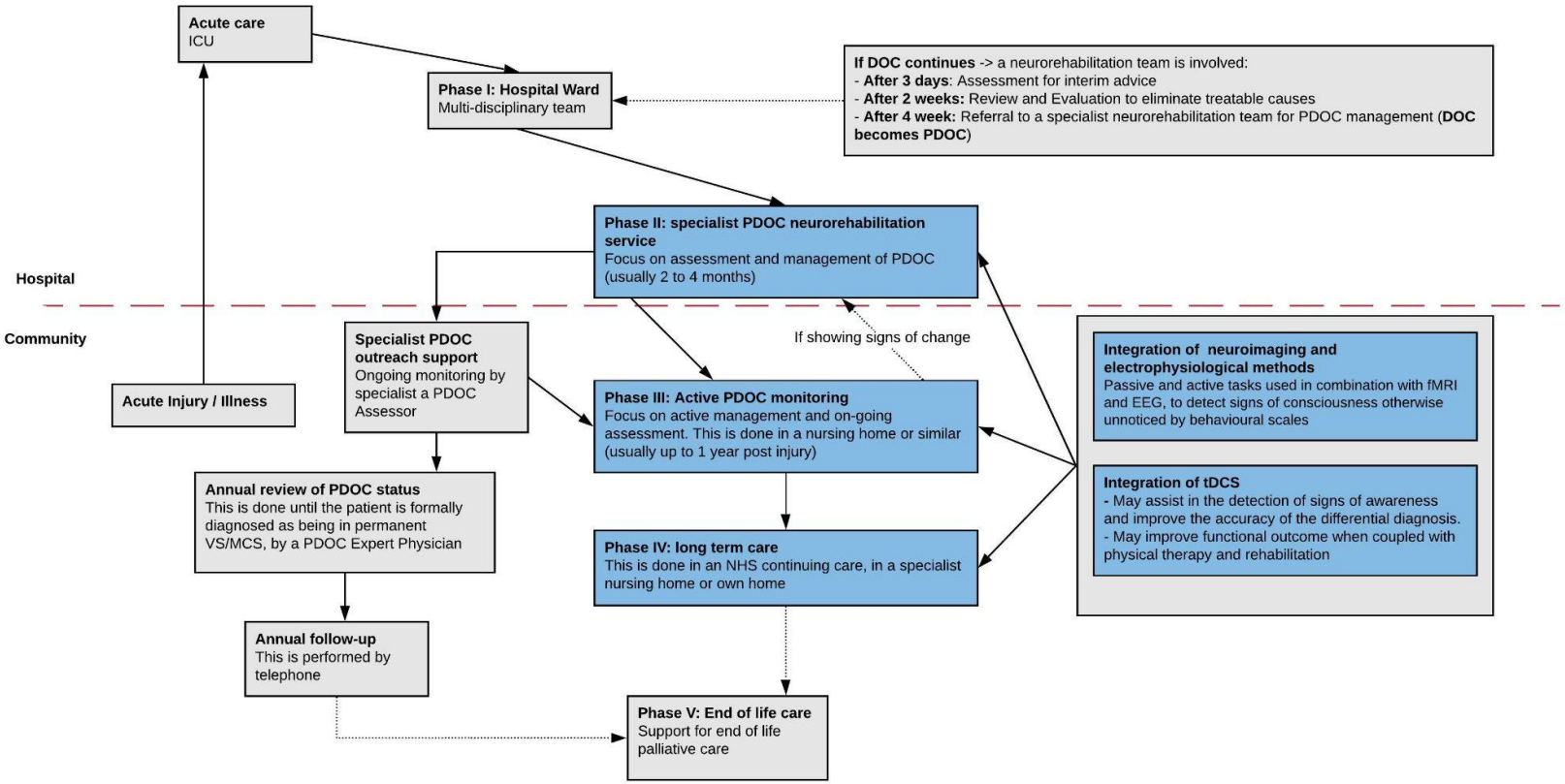

Acute care
ICU
Phase I: Hospital Ward
Multi-disciplinary team
If DOC continues -> a neurorehabilitation team is involved:
- After 3 days: Assessment for interim advice
- After 2 weeks: Review and Evaluation to eliminate treatable causes
- After 4 week: Referral to a specialist neurorehabilitation team for PDOC management (DOC becomes PDOC)
Phase II: specialist PDOC neurorehabilitation service
Focus on assessment and management of PDOC (usually 2 to 4 months)
Hospital
Community
If showing signs of change
Specialist PDOC outreach support
Ongoing monitoring by specialist a PDOC Assessor
Acute Injury / Illness
Phase III: Active PDOC monitoring
Focus on active management and on-going assessment. This is done in a nursing home or similar (usually up to 1 year post injury)
Integration of neuroimaging and electrophysiological methods
Passive and active tasks used in combination with fMRI and EEG, to detect signs of consciousness otherwise unnoticed by behavioural scales
Integration of tDCS
- May assist in the detection of signs of awareness and improve the accuracy of the differential diagnosis.
- May improve functional outcome when coupled with physical therapy and rehabilitation
Annual review of PDOC status
This is done until the patient is formally diagnosed as being in permanent VS/MCS, by a PDOC Expert Physician
Phase IV: long term care
This is done in an NHS continuing care, in a specialist nursing home or own home
Annual follow-up
This is performed by telephone
Phase V: End of life care
Support for end of life palliative care

Figure 2.2: Representation of the pathways of care for PDOC patients as proposed by the Royal College of Physicians (2020), with suggestions for the role that tDCS and neuroimaging/electrophysiological methods could play in each of the stages. Reproduced and amended from Royal College of Physicians (2020).

2.10. Conclusions

In conclusion, there is consistent evidence that tDCS can lead to neural changes and measurable clinical improvements in a subset of MCS patients. Moreover, research to date suggests that the use of multiple stimulation sessions can further enhance the clinical effects of tDCS in this group (with 2 single-session vs six multiple-session studies leading to changes in CRS-R score). However, research has been highly heterogeneous in their specific choice of stimulation parameters, montages, protocols, and outcome measures, and it is yet not possible to draw any conclusions about what factors may explain why some patients respond and others do not as a result. In addition to this, studies have typically used relatively small sample sizes. While it is important to recognise that achieving large sample sizes of PDOC patients in single centres is a challenge, we should also acknowledge that tDCS is well-known for leading to highly heterogeneous responses and very large samples are required to obtain reliable and reproducible effects. We therefore think that the field urgently needs multi-centre studies that are appropriately powered to assess the effect of individual differences in the responses elicited by tDCS in PDOC. Crucially, these studies should include appropriate assessments to capture potential long-term effects of tDCS, which are required for any intervention to be clinically useful.

Furthermore, we have argued that the use of electrophysiological and neuroimaging techniques, alongside conventional behavioural assessments of consciousness may identify covert changes after stimulation but may also support the characterisation of inter-individual differences, and, in turn, lead to the development of more patient-specific stimulation protocols. Specifically, the field needs the development of current flow models that consider patients' specific neuroanatomy and lesions and can be used to find the best electrode placement to achieve the desired effects in each individual patient. Such models would also be crucial to stratify patients who are more likely to respond to tDCS. We argue that this step of individualising treatments is imperative to the application of tDCS in clinical settings.

Finally, there is robust evidence that tDCS can lead to much stronger and long-lasting effects when paired with a task that can engage the networks of interest. We believe that this supports its integration into existing rehabilitation programmes and physical therapy to exploit potential

synergies, and that studying whether such synergies exist should be a priority for future studies. Should this be demonstrated, we argue that its implementation is feasible from the second phase of the national pathways of care recommended by the RCP (i.e., subacute stage of rehabilitation), where patients have the greatest potential for improvement. In addition to this, we believe it is crucial to assess the role of tDCS in the chronic phases of injury with a focus on improving patients' quality of life.

Note that the appendix to this chapter can be found at the end of the thesis (Appendix A), where I reviewed more recent papers on tDCS and PDOC.

Chapter 3

GENERAL METHODS

This thesis is structured around three empirical fMRI studies on healthy individuals (Chapters 4-6) and an fMRI case study on a single PDOC patient (Chapter 7). Specifically, Chapter 4 reports two experiments that focus on the effects of a single session of M1-tDCS (*Experiment 1*) and cerebellar-tDCS (*Experiment 2*) on the effective connectivity of the motor network. Chapter 5 explores the effects of multiple sessions of M1-tDCS coupled with passive mobilisation on the previously mentioned network (*Experiment 3*). Chapter 6 investigates the relationship between current density metrics computed from MRI-derived electric field models, and changes in thalamocortical connectivity following tDCS, using structural MRI and fMRI effective-connectivity data from the three above mentioned experiments. Lastly, Chapter 7 investigates the effects of multiple sessions of M1-tDCS on behavioural responsiveness, and brain activity and connectivity in a PDOC patient with UWS. The case study used an experimental design akin to that of *Experiment 3*, but, noticeably, behavioural assessments to monitor patient's functioning were used, as well as additional fMRI and EEG motor-imagery and resting-state tasks, to better characterise the effect of the stimulation on covert awareness and brain dynamics. The methods used across the chapters (including additional methods in the case study) are summarised below. Any differences across the studies - i.e., MRI scanner parameters and sequences, tDCS montages and protocols, experimental designs and analysis pipelines - are highlighted.

3.1. A brief introduction to Functional Magnetic Resonance Imaging

The current thesis is largely comprised of neuroimaging experiments based on fMRI methods, which were used to 1) quantify brain activation in response to specific tasks (section 3.2), 2) characterise changes in brain effective connectivity during command-following (section 3.8) and 3) characterise changes in resting-state functional connectivity (section 3.4). fMRI is a non-invasive neuroimaging technique that relies on magnetic fields to create high-resolution images of brain metabolism. These metabolic changes detected by fMRI can result from task-induced changes in cognitive state or from spontaneous processes in the resting brain (Glover, 2011).

3.2. Experimental design and fMRI tasks

The four fMRI experiments included in this thesis (that is, *Experiments 1,2* and *3* in Chapters 4-5 and the case study in Chapter 7) share the same sham- and polarity-controlled, randomised, blind, crossover experimental design. In particular, in each experiment, all participants completed all three tDCS conditions (anodal, cathodal and sham), and performed the fMRI tasks both before and after each stimulation. However, in *Experiment 3* and the case study, participants underwent five tDCS sessions per condition (instead of a single session) and two fMRI scans (during the first and fifth tDCS sessions of each condition).

Regarding the fMRI tasks, all the fMRI experiments in the thesis used the same task to characterise the effects of tDCS on motor-network effective connectivity during behavioural command-following. In such a task, participants are asked to perform simple thumb movements every time they hear an auditory cue (i.e., a "beep"). In the case study, however, the command-following task was slightly modified to make it less demanding to the patient, by substituting the "beep" cues with the instruction "try to move your thumb". Importantly, in *Experiments 1-3* an MRI-compatible joystick was used to record the onset, speed and acceleration of each thumb movement. Note that this device was not used in the case study due to the difficulty of adapting such a device to account for patients' limb rigidity.

In addition, the fMRI protocol in the case study included a motor imagery task (adapted from (Owen et al., 2006) for the detection of the patients' residual covert cognition, and a resting-state task to explore intrinsic connectivity changes following tDCS.

3.3. (f)MRI sequences

The four experiments present some differences regarding the MRI scanners used to collect the data, as well as the MRI structural and functional sequences (see **Table 3.1** for more details around similarities and differences across the studies). Data in *Experiments 1* and *2* were collected with a Philips Achieva 3T MRI system at the Birmingham University Imaging Centre (BUIC); in *Experiment 3* Siemens Magnetom Prisma 3T at the Centre for Human Brain Health (CHBH) wa used, and in the case study a and Siemens Skyra Magnetom 3T at the Wellington Hospital were used. Noticeably, in *Experiment 2*, the field of view (FOV) for the fMRI sequence was increased to ensure a full coverage of the cerebellum, which led to longer repetition time (TR) as compared to that of *Experiment 1*.

T1-weighted images were used in the empirical chapters for coregistration purposes. Moreover, in Chapter 6, those were used to model electric-fields induced from tDCS, at the individual level. In *Experiment 3*, in addition to the T1-weighted images, T2-weighted scans were also collected. These were used in Chapter 6 to achieve a more accurate tissue segmentation and ultimately improve the MRI-derived electric field models (Van Hoornweder et al., 2022).

3.4. Additional methods used in the case study

As highlighted in section 1.6.2, in the case study reported in Chapter 7, in addition to the above fMRI protocols, active-task and resting-state EEG methods were also used to assess the residual cognition and to characterise changes in brain dynamics in response to the stimulation. In particular, a motor-imagery task was used to assess the presence of covert awareness (see Chapter 1, section 6.2). In the task, the patient was asked to perform a thumb movement every

time they heard an auditory stimulus ("try to move your right thumb"), and ERDs were computed and used as a proxy for covert awareness.

Moreover, several graph-metrics, as well as EEG power spectrum and functional connectivity measures, were also computed. These metrics have been reported to have diagnostic and/or prognostic value (O'Donnell et al., 2021). Lastly, patient's behavioural responsiveness was evaluated at several time points during each testing week, specifically before each testing week, before and after each tDCS session at bedside and before each fMRI session. The assessment was performed using the CRS-R scale discussed in section 1.3.

3.5. tDCS montages and parameters

tDCS protocols for each study are summarised in **Table 3.1**. In all experiments, a minimum of 1-week between conditions was present to allow for post-tDCS-effects washout. In all experiments, each tDCS session was 20 min long, with 30 seconds ramp-up at the beginning of the stimulation and 30-seconds ramp-down at the end. During sham sessions only 30 seconds of stimulation were delivered to ensure proper blinding. In all experiments 5x5cm2 electrodes were used, which were secured with self-adhesive bandages and electro-conductive paste to increase conduction. Noticeably, while in *Experiment 1* and *2* the stimulation was administered at rest (that is, not paired with a task), in *Experiment 3* and in the case study the stimulation was paired with passive mobilisation of the thumb, to engage the targeted network during the stimulation (see section 5.2).

In *Experiment 1*, *3* and in the case study, the target of the stimulation was the left motor cortex (with the return electrode being placed on the right orbitofrontal cortex), and the intensity of the stimulation was set at 1mA. Noticeably, while in *Experiment 1* the left motor hotspot was located via a TMS procedure, in *Experiment 3* and in the case study a manual procedure was used instead (i.e., using a 10-20 cap and locating C3 for the left motor cortex and Fp2 for the right orbitofrontal region). This decision was made based on the fact that using a TMS procedure to locate the motor cortex in each of the 15 tDCS sessions included in *Experiment 3* and in the case study would have been extremely laborious. Additionally, in the case study,

TMS was also avoided due to the risk of seizures (Stultz et al., 2020). On the other hand, in *Experiment 2* the right cerebellum was targeted - which was identified using the inion as a reference landmark - and the return electrode was placed on the right buccinator muscle. The intensity of the stimulation in *Experiment 1*, *3* and in the case study was set at 1mA, whereas in *Experiment 2* the intensity was set at 1.85mA (as recommended by Jalali et al., 2018).

Lastly, while in *Experiment 1* and *2* all tDCS sessions were carried out within the MRI scanner, in *Experiment 3* and in the case study only the first and last stimulation sessions of each condition were performed in the MRI scanner, whereas the other sessions occurred in a designated cubicle in *Experiment 3,* or at the patients' bedside in the case study.

Table 3.1. *Experiments summary.*

Experiment	Chapter	Participants	Stimulation protocol summary	Target localisation procedure	MRI scanner	fMRI parameters	Structural MRI acquisition details
Experiment 1	4	21 (13 women, 8 men; mean age 23 ± 4 years)	M1-tDCS (1mA) administered at rest. Single session.	M1 was located using a TMS procedure.	Philips Achieva 3T; 32-channel coil.	160 volumes per run, 34 slices, TR = 2000 ms, TE = 35 ms, matrix size = 80 × 80, voxel size = 3 × 3 × 3 mm, no gap, flip angle = 79.1°, SENSE acceleration factor = 2.	- T1-w image: TR = 7.4ms, TE = 3.5 ms, matrix size = 256 × 256 x 208 mm, voxel size = 1 × 1 × 1 mm, and flip angle = 7°.
Experiment 2	4	21 (14 women, 7 men, mean age 27 ± 4 years)	Cerebellar-tDCS (1.85mA) administered at rest. Single session.	The right cerebellum was located manually (3 cm lateral from the inion).	Philips Achieva 3T; 32-channel coil.	119 volumes per run, 46 slices, TR = 2700 ms, TE = 35 ms, matrix size = 80 × 80, voxel size = 3 × 3 × 3, no gap, flip angle = 79.1°, SENSE acceleration factor = 2.	- T1-w image: TR = 7.4ms, TE = 3.5 ms, matrix size = 256 × 256 x 208 mm, voxel size = 1 × 1 × 1 mm, and flip angle = 7°.
Experiment 3	5	22 (16 women, 6 men; mean age 25 ± 4 years)	M1-tDCS (1mA) coupled with passive mobilisation (administered by a device), five sessions.	M1 was located using a 10-20 EEG cap.	Siemens MAGNETOM Prisma 3T; 64-channel.	198 volumes per run, 63 slices, TR = 1620 ms, TE = 35 ms, matrix size = 84 x 84, voxel size = 2.5 x 2.5 x 2.5 mm, no gap, flip angle = 71°, iPAT acceleration factor = 3.	- T1-w image: TR = 2000 ms, TE = 2.03 ms, matrix size = 256 x 256 x 208, voxel size = 1 x 1 x 1 mm, and flip angle = 8°.

							- T2-w image: TR 3200 ms, TE 408ms, matrix size = 256 x 256 x 208, voxel size 1 x 1 x 1 and flip angle = 8°.
Case study	7	1 (male, 27 years old)	M1-tDCS (1mA) coupled with passive mobilisation (administered manually), five sessions.	M1 was located using a 10-20 EEG cap.	Siemens Skyra Magnetom 3T; 32-channel coil.	225 volumes (command-following task) / 200 volumes (motor-imagery task) / 170 volumes (resting state). 63 slices, TR = 1770 ms, TE = 35 ms, matrix size = 84 x 84, slice thickness = 2.5 x 2.5 x 2.5 mm, no gap, flip angle = 71°, iPAT acceleration factor = 3.	- T1-w image: TR = 4000 ms, TE = 2 ms, matrix size = 208 x 256 x 256, voxel size = 1x1x1mm.

3.6. Behavioural data analysis

Even though the current thesis focused on the changes in brain activity and connectivity following tDCS, a few behavioural data analyses were carried out as well. In particular, in *Experiments 1-3*, the efficacy of the tDCS blinding protocol was analysed, using data of surveys collected after each tDCS session. Moreover, in *Experiment 1-3*, the effects of tDCS on several motion-tracking metrics derived from the data collected with the MRI-compatible joystick (i.e., effects of tDCS on thumb movements' onsets, acceleration and velocity) were assessed. Lastly, in the case study, motion tracking time series collected during the tDCS sessions at bedside were visually inspected, as well as the results of the CRS-R assessments, to evaluate the presence of changes that could be related to the active tDCS sessions.

Noticeably, there was an important difference between the motion tracking data analyses in *Experiments 1-2* and *Experiment 3*. Specifically, in *Experiment 1-2*, a frequentist statistical approach was used, whereas in *Experiment 3* a Bayesian approach was adopted. The reason for using Bayesian statistics in the motion-tracking analysis of *Experiment 3* was to improve consistency with the fMRI effective-connectivity analyses, which are also based on a Bayesian framework (as discussed in sections 3.7-8 below).

3.7. Brief overview on Bayesian statistics

In *Experiment 3*, Bayesian statistical procedures (specifically Bayesian repeated measures ANOVAs) were used to evaluate tDCS-related differences in motion tracking metrics related to the command-following task. Moreover, the Dynamic Causal Modelling (DCM) and Parametric Empirical Bayes (PEB) used to model motor-network causal architecture from fMRI data, and estimate tDCS-induced effective-connectivity changes, are also built upon a bayesian framework (Friston et al., 2003; Zeidman et al., 2019; Zeidman et al., 2019). Frequentist statistics focus on probabilities around data in the long run: one normally begins by assuming that a null hypothesis is true before collecting the data, and then quantifies how likely the collected data is under the null hypothesis (Fornacon-Wood et al., 2022). In other words, the focus is on quantifying the probability of obtaining another dataset that is as extreme

as the one observed, given the null hypothesis. This probability is referred to as *p-value*. Importantly, in Frequentist statistics the collected dataset is only one of the many potential datasets that could have been collected regarding the same question. Here lies a first conceptual difference between Frequentist and Bayesian statistics: in the latter the data is considered as fixed, and hypotheses and parameters are treated in terms of probability distributions. On the other hand, in Frequentist statistics probabilistic statements are not made about hypotheses or parameters: they can be made only about the data (Fornacon-Wood et al., 2022). Another key distinction between Frequentist and Bayesian statistics is that, in Frequentist statistics we have no prior knowledge surrounding parameters before collecting the data, and the results of statistical analyses are based exclusively on the collected data. Instead, in Bayesian statistics this assumption is substantially relaxed, and it is acknowledged that we might have some prior knowledge about the parameter. In Bayesian terminology, this prior knowledge is a probability distribution referred to as *prior* (Fornacon-Wood et al., 2022). Priors are then refined once the data becomes available, hence the summary of what is known after observing the data (also known as *posterior distribution*) uses a combination of the prior information and the observed data. The mathematical equation enclosing the above ideas is referred to as Bayes' Theorem:

$$p(\theta|Data) = \frac{p(Data|\theta) \cdot p(\theta)}{p(Data)}$$

where $p(\theta|Data)$ refers to the posterior distribution, $p(Data|\theta)$ to the likelihood (i.e., the probability of the observed data being generated from a particular scenario), $p(\theta)$ to the prior, and finally $p(Data)$ to the model evidence. A discussion of each component of the above theorem is outside the scope of this paragraph, but it is worth noting that one of the main advantages of Bayesian inference over Frequentist statistics is that the posterior distribution can be used to compute the probability of different hypotheses or models (Fornacon-Wood et al., 2022). Taking one step further, Bayesian statistics also allows for comparing two rival models through the so-called *Bayes factor*, which quantifies the relative predictive performance (that is, relative of one model to another) of competing models (van den Bergh et al., 2020).

For instance, in the Bayesian alternative of a Frequentist ANOVA, instead of comparing variances, one contrasts the predictive performance of several competing models *M* (e.g., a null model describing the dependent variable using a single grand average, and an alternative model describing the dependent variable using both an overall average and the effect of an independent variable) (van den Bergh et al., 2020). Following this approach, one is then able to quantify the performance of an alternative model over a null model (and vice versa) through Bayes factors. This approach was adopted in section 5.3.8 to study the effects of different tDCS conditions on motion tracking metrics.

As mentioned above, the DCM framework also relies on a Bayesian inference to quantify uncertainty about the parameters (that is, connection strengths and directions) before and after observing neuroimaging data (K. J. Friston et al., 2003; Zeidman, Jafarian, Corbin, et al., 2019b). The Bayesian approach to the DCM carries several advantages, among which: 1) it allows the incorporation of prior knowledge about parameters (that is, the underlying assumptions in the models), 2) it escapes the multiple comparison issue, 3) it allows to quantify uncertainty around parameters (fundamental to assess the reliability of a model), and 4) it allows to incorporate hypothesis testing and model comparisons through Bayesian Model Reduction and Averaging (BMR and BMA, respectively) (Friston et al., 2003; Zeidman et al., 2019; Zeidman et al., 2019).

3.8. Overview of the effective connectivity analyses in the current thesis

There are a number of methods to quantify brain connectivity from fMRI BOLD data (K. J. Friston, 2011). Overall, two broad classifications exist: functional and effective connectivity methods. The former describes the extent of statistical interdependence or correlation between the BOLD signal of different brain regions, while the latter depicts causal interactions (that is, how information is exchanged) within networks (Kahan & Foltynie, 2013). Effective connectivity methods therefore complement functional connectivity ones, by quantifying the influence of one region over another (Friston, 2009; Friston et al., 2003). One key difference is that in functional connectivity approaches, inferences are made at the level of the BOLD signal (which will be referred to as *y*), whereas in effective connectivity methods inferences

are made at the level of the underlying neuronal activity (which will be denoted as *z*) (K. Friston, 2009; Kahan & Foltynie, 2013). Note that, in the case of fMRI, this distinction is of paramount importance, as the fMRI BOLD signal only constitutes an indirect measure of the underlying neuronal activity *z*, which therefore represents a so-called hidden state variable (K. Friston, 2009). It follows that, to move from *y* to *z*, one needs to build (plausible *enough*) models of how *y* may arise from *z*. These models are referred to as the "generative models" (Friston, 2009; Friston et al., 2003).

In the present thesis, to build (and evaluate) single-subject models of effective connectivity, the Dynamic Causal Modelling (DCM) framework was used (K. J. Friston et al., 2003), specifically focusing on four brain regions left M1, left SMA, left thalamus, and right cerebellum.

The DCM - in its deterministic version - assumes that, given the neuronal activity of a set of interconnected brain regions (represented as a vector *z*), the rate of change of neuronal activity of each region (ż) is caused solely by 1) experimental inputs (e.g., stimuli introduced by the experimenter), and 2) the region's afferent connections (K. Friston, 2009, 2009; Kahan & Foltynie, 2013). Note that afferents can either arrive from distant regions (extrinsic connections) or the region itself (intrinsic connection). Consequently, under those assumptions, if we were to remove both afferents and inputs to a region, ż would be zero (i.e., no change in activity over time) (Kahan & Foltynie, 2013). The neuronal model of the DCM is parametrised by the strength of the intrinsic and extrinsic connections among the regions, that is, the parameters in the equation describing *z* encode the strength of the connections, and how connections change in response to external stimuli. In substance, the DCM tries to estimate those parameters (K. Friston, 2009). Note that, similarly to a more standard general linear model (GLM) used to model brain activity in response to stimuli, the DCM also relies on convolution models with haemodynamic and observation parameters to specify how neuronal activity is mapped into BOLD time series (y) (Friston, 2009; Friston et al., 2003). In that sense, the DCM can be also considered as a generalisation of the convolution model used in the GLM, with the most important difference that the DCM also includes afferents (as opposed to including experimental inputs only) (Kahan & Foltynie, 2013).

To summarise, the principal aim of the DCM framework is to find the parameters (i.e., coupling between regions) that best renders some fMRI data (K. Friston, 2009). This is achieved through a procedure named Bayesian Model Inversion (BMI), that, for each parameter a posterior probability density of its mean and standard deviation are provided (K. J. Friston et al., 2003). During such an estimation, the model is also scored by assigning to it a model evidence, which substantially represents the trade-off between model accuracy (how well the model fits the data) and model complexity (how parsimonious the model is in terms of number of parameters used) (K. Friston, 2009). Model evidence is a fundamental component of the DCM: first, it allows us to evaluate a model (as explained above), and second, it allows us to perform hypothesis testing at the within and between subject level (Zeidman, Jafarian, Seghier, et al., 2019).

In the empirical chapters of this thesis, after having built all single-subject DCMs (first-level analysis), the PEB framework was used to move to group-level inferences (e.g., to determine, at the group-level, which couplings increased/decreased for one tDCS condition compared to another) (Zeidman, Jafarian, Seghier, et al., 2019). Simply put, the PEB allows us to quantify commonalities and differences across subjects, hence enabling hypothesis testing (Zeidman, Jafarian, Seghier, et al., 2019).

Importantly, PEB is a hierarchical framework, in that it allows to estimate multiple levels of variability in the data, with parameters at the lowest level representing subject-specific effects, and those at the highest level representing population-level effects (Zeidman, Jafarian, Seghier, et al., 2019). To give a practical example, in Chapter 5, this hierarchical approach was used to: model connectivity during the command-following task (first-level DCM), then to model changes between before and after tDCS (first-level PEB), then the increases/decreases between two tDCS conditions (second-level PEB), subsequently these second-level PEBs were fed into third-level PEBs encoding the differences between the first and last stimulation day, and finally the group averages.

With this PEB-of-PEBs approach, variability in coupling strengths at each level can influence the subsequent level, until hypotheses are tested at the last level, by using a procedure called Bayesian Model Comparison (BMC). In short, BMC compares the evidence for different variations of the parameters (i.e., switching them on and off in different combinations). This

procedure of comparing full and reduced models is called Bayesian Model Reduction (BMR), which works by progressively "pruning" parameters from the full model and assessing whether the parameter contributed to the model evidence (Zeidman, Jafarian, Seghier, et al., 2019). Lastly, parameters from the best models identified through BMR are averaged using Bayesian Model Averaging (BMA), in order to determine group-level connection strengths, and thresholded at a posterior probability of > 95% or > 99% (Zeidman, Jafarian, Seghier, et al., 2019).

Chapter 4

TDCS MODULATES EFFECTIVE CONNECTIVITY DURING MOTOR COMMAND FOLLOWING; A POTENTIAL THERAPEUTIC TARGET FOR DISORDERS OF CONSCIOUSNESS[3]

4.1. Abstract

Transcranial direct current stimulation (tDCS) is attracting increasing interest as a potential therapeutic route for unresponsive patients with prolonged disorders of consciousness (PDOC). However, research to date has had mixed results. Here, we propose a new direction by directly addressing the mechanisms underlying lack of responsiveness in PDOC, and using these to define our targets and the success of our intervention in the healthy brain first. We report 2 experiments that assess whether tDCS to the primary motor cortex (M1-tDCS; Experiment 1) and the cerebellum (cb-tDCS; Experiment 2) administered at rest modulate thalamo-cortical coupling in a subsequent command following task typically used to clinically assess awareness. Both experiments use sham- and polarity-controlled, randomised, double-blind, crossover designs. In Experiment 1, 22 participants received anodal, cathodal, and sham M1-tDCS sessions while in the MRI scanner. A further 22 participants received the same protocol with cb-tDCS in Experiment 2. We use Dynamic Causal Modelling of fMRI to characterise the effects of tDCS on brain activity and dynamics during simple thumb movements in response to command. We found that M1-tDCS increased thalamic excitation and that Cathodal cb-tDCS increased excitatory coupling from thalamus to M1. All these changes were polarity specific. Combined, our experiments demonstrate that tDCS can successfully modulate long range thalamo-cortical dynamics during command following via targeting of cortical regions. This

---

3

As published in Neuroimage:

Aloi, D., Jalali, R., Tilsley, P., Miall, R. C., & Fernández-Espejo, D. (2022). TDCS modulates effective connectivity during motor command following; a potential therapeutic target for disorders of consciousness. *NeuroImage*, *247*, 118781. https://doi.org/10.1016/j.neuroimage.2021.118781

suggests that M1- and cb-tDCS may allow PDOC patients to overcome the motor deficits at the root of their reduced responsiveness, improving their rehabilitation options and quality of life as a result.

4.2. Introduction

Transcranial direct current stimulation (tDCS) is a non-invasive brain stimulation technique that is gaining popularity as a therapeutic option for complex clinical conditions for which no other alternatives are available (A. Liu et al., 2018). Among these, a paradigmatic case is that of prolonged disorders of consciousness (PDOC), such as the vegetative (VS) and the minimally conscious state (MCS). PDOC are characterised by catastrophic disabilities that are in many cases permanent (The Multi-Society Task Force on PVS, 1994), and the small number of therapies available have demonstrated very limited success at improving outcome (Thibaut et al., 2019). In response to this, over the last 5 years the field has seen a sharp rise in tDCS trials on PDOC (Bourdillon et al., 2019). These have typically targeted the left dorso-lateral prefrontal cortex (DLPFC), in an attempt to restore some residual level of awareness, but have only had mixed success. While several studies reported the emergence of new behaviours indicative of awareness in subsets of PDOC patients following tDCS (see e.g.(Thibaut et al., 2014a), many others have failed to elicit any clinical changes or indeed led to undesired changes (Martens et al., 2020). Individual responses to tDCS are well known for their heterogeneity even in healthy populations (Parkin et al., 2015), and we can expect an even higher variability in PDOC, where the specific aetiology and mechanisms of damage result in marked differences in brain atrophy and tissue microstructure across patients. However, in this particular case, we argue that these difficulties are further exacerbated by our limited understanding of how conscious awareness is supported in the brain, which precludes the identification of effective targets for stimulation. Indeed, while we know that consciousness requires sustained rich neural dynamics in fronto-parietal and thalamo-cortical networks (Demertzi et al., 2019; Luppi et al., 2019), the specific pattern of activity that would need to be restored in PDOC patients and how this can inform the selection of stimulation targets remains an elusive question.

Here we propose a different approach, wherein we switch the focus from the consciousness disorder itself to the patients' ability to produce voluntary behavioural responses (Schiff, 2015a). In doing so, we target a cognitive process that is much better understood, not only in terms of its neurophysiology but also which specific tDCS modulations can maximise behavioural changes (Parkin et al., 2015). In addition, recent voices have emphasised the importance of addressing the fundamentals of any tDCS intervention in well-controlled studies in healthy individuals before a clinical application with meaningful effects can be produced and clinically tested (Parkin et al., 2015). In line with this, we thus focus on characterising tDCS responses in the healthy brain, while keeping our methods translatable to PDOC patients. Clinical assessments of PDOC use the patient's ability to follow commands as a proxy measure for their awareness. Crucially, it is well known that a significant number of PDOC patients retain a much greater deal of awareness than can be expected from their clinical diagnosis and are simply unable to demonstrate this with overt purposeful (motor) responses in response to commands (Fernández-Espejo & Owen, 2013; Schiff, 2015a). We have recently shown that this lack of behavioural responsiveness is associated with specific impairments within the motor system that result in reduced excitatory coupling between the thalamus and the primary motor cortex (M1) (Fernandez-Espejo et al., 2015; Stafford et al., 2019a). On this basis we hypothesise that interventions to enhance the flow of information between the thalamus and motor cortices will provide patients with a renewed level of control over their external behaviour and increase their behavioural responsiveness as a result.

In this study, we use dynamic causal modelling (DCM) of fMRI data to explore whether tDCS can indeed modulate motor thalamo-cortical coupling during simple voluntary responses to command in the healthy brain. We report two separate experiments targeting M1 and the cerebellum respectively. While there is strong evidence that tDCS applied to M1 (henceforth referred to as M1-tDCS) leads to local polarity-specific changes in M1 excitability (Nitsche & Paulus, 2000) and BOLD signal (Stagg, O'Shea, et al., 2009), little is known about whether it can also influence coupling between other nodes of the motor network. Similarly, there is evidence that cerebellar tDCS (cb-tDCS) is able to modulate cerebellar brain inhibition (CBI) (Galea et al., 2009b), the natural inhibitory tone the cerebellum exerts over M1. Given that the cerebellum is structurally connected to M1 via a thalamic relay, it would follow that the previously reported effects of cb-tDCS on CBI should be mediated by the thalamus. However,

no studies have directly investigated how cb-tDCS affects the coupling in this cerebellar-thalamo-M1 axis. Furthermore, no study to date has assessed the effects of either M1- or cb-tDCS on the activity and dynamics of the motor network during simple motor command-following. We hypothesised that: (a) anodal M1-tDCS will increase excitation in the motor network and lead to an increased excitatory output from thalamus to M1 during command-following (Experiment 1); and (b) cathodal cb-tDCS will reduce inhibition in the thalamus and also result in increased excitation from thalamus to M1 (Experiment 2). Previous research has identified a relative structural preservation of M1-striatal-thalamic and dentate-thalamic pathways in PDOC patients (Stafford et al., 2019a). This suggests that both pathways may be viable routes to target the thalamus in this group.

4.3. Material and methods

4.3.1. Participants

Forty-nine right-handed healthy volunteers participated in the study (15 men, 34 women; mean age 25 ± 4 years). We recruited all participants from the University of Birmingham, using the local Research Participation Scheme and advertisements across campus. We pre-screened all participants before recruitment to confirm their eligibility to safely take part in MRI and tDCS experiments. All reported no previous history of neurological and/or psychiatric disorders, no personal or family history of epilepsy, no use of psychoactive drugs, and had normal or corrected vision. Additionally, we instructed them to be well hydrated and well slept, with no alcohol or coffee consumed during the 24 hours prior to the testing session, to be in keeping with brain stimulation safety regulations (Antal et al., 2017a). The University of Birmingham's Science, Technology, Engineering and Mathematics Ethical Review Committee approved the study and all participants gave written informed consent prior participation. We compensated participants with £110 or the equivalent in course credits.

Experiment 1 included 26 participants (8 male, 18 female; mean age 23 ± 4 years), from whom 22 completed all 3 sessions. We further discarded data from one participant due to failure to

comply with the task instructions, resulting in a final sample of 21 to be included in the analysis (8 male, 13 female; mean age mean: 23 ± 4 years).

Experiment 2 included 23 participants (7 male, 16 female; mean age: 27 ± 4 years), from whom 22 completed all 3 sessions. We excluded one further participant due to an acquisition error in one of the sessions that resulted in corrupted files. The final sample consisted of 7 males and 14 females, aged 27 ± 4 years. One participant took part in both Experiments (with a gap of over 7 weeks between them).

4.3.2. General Experimental procedure

Both experiments used sham- and polarity-controlled, randomised, double-blind, crossover designs. All participants completed anodal, cathodal, and sham stimulation sessions, while in the MRI scanner. These were scheduled at least 7 days apart (Experiment 1: mean 12 ± 10; Experiment 2: mean 13 ± 7), and in a counterbalanced order. Both the participants and the researchers conducting the data analyses were blind to the polarity in each session.

In their first testing session participants provided informed consent for the study and completed the Edinburgh handedness inventory (Oldfield, 1971a). Additionally, before each session, we pre-screened participants to confirm MRI and tDCS safety. After completing these steps, we set up the electrodes in a designated room (see below), and took the participants to the MRI scanner, where we completed the setup of the tDCS system and provided the participants with a joystick to record their responses in the fMRI task (see below). We used the MRI Intercom system to communicate with participants during the experiment. Before and after the stimulation, participants performed an fMRI motor command-following task where they were instructed to execute discrete simple thumb movements (abduction-adduction) with their right hand in response to auditory cues (see fMRI paradigm below).

Finally, to test whether our protocol achieved adequate blinding, participants completed a post-tDCS perceptual scale of their perceived sensations and/or discomfort after each session, and indicated whether they thought they received actual stimulation or sham.

4.3.3. Electrical Stimulation

In both experiments we administered tDCS in the MRI scanner using an MR-compatible NeuroConn DC-Stimulator MR (neuroCare Group GmbH, Germany). We used 5x5 cm^2 electrodes with electro-conductive paste to improve conduction and secured them in place using self-adhesive bandage.

Experiment 1. In line with previous studies targeting M1 (Nitsche & Paulus, 2000), in the anodal sessions we placed the target electrode (anode) centred on the left motor hotspot, as identified by TMS prior to the first MRI session, and oriented approximately at a 45° angle with respect to the midline. We placed the reference electrode (cathode) on the contralateral supraorbital region. We reversed this montage for the cathodal sessions. Half of the sham sessions replicated the anodal montage and the other half the cathodal montage. We used a Magstim BiStim^2 TMS stimulator paired with Brainsight TMS navigation system (Rogue Research Inc) to identify the motor hotspot in each participant in the first stimulation session, following standard methods (Rossini et al., 2015).

Experiment 2. We placed the target electrode on the right cerebellar cortex (3 centimetres lateral to the inion, oriented parallel to the midline) and the return electrode on the right buccinator muscle (Galea et al., 2011). The montage was reversed for cathodal sessions. As above, half of the sham sessions replicated the anodal montage and the other half the cathodal montage.

In both experiments, we used Brainsight to record the coordinates for the target electrode in the first session and used them to locate the electrode position for the subsequent sessions to ensure consistent placement.

During anodal and cathodal sessions, we delivered 20 minutes of stimulation, with 30 seconds of ramp-up and ramp-down periods. During sham, we delivered 30 seconds of stimulation before ramping down to give the sensation of active stimulation, and according to well established protocols to ensure blinding (A. Woods et al., 2016). In Experiment 1 we stimulated at an intensity of 1mA, as this typically induces tDCS canonical excitatory versus inhibitory effects for anodal and cathodal stimulation respectively (Nitsche & Paulus, 2000; Parkin et al., 2015). In Experiment 2, we stimulated at an intensity of 1.85mA as previously recommended

(Jalali et al., 2018b). In both studies, we delivered stimulation at rest, without the participant engaging in any motor (or other type of) task, as performing a task during stimulation would not be feasible in PDOC patients themselves.

4.3.4. MRI acquisition

We acquired all data on a Philips Achieva 3T system, with a 32-channel head coil, at the Birmingham University Imaging Centre (BUIC).

Experiment 1: fMRI acquisition parameters were as follows: 160 volumes per run, 34 slices, TR = 2000ms, TE = 35ms, matrix size = 80 × 80, voxel size = 3x3x3mm, no gap, and flip angle = 79.1°, SENSE acceleration factor = 2. Additionally, we acquired a high-resolution, T1-weighted MPRAGE image, for anatomical co-registration, with the following parameters: TR = 7.4ms, TE = 3.5ms, matrix size = 256x256mm, voxel size = 1x1x1mm, and flip angle = 7º.

Experiment 2: fMRI acquisition parameters were as follows: 119 volumes per run, 46 slices, TR = 2700ms, TE = 35ms, matrix size = 80x80, voxel size = 3x3x3, no gap, flip angle = 79.1°, SENSE acceleration factor = 2. High-resolution, T1-weighted MPRAGE images were also acquired for Experiment 2, with the following parameters: TR = 7.4ms, TE = 3.5ms, matrix size = 256x256, voxel size = 1x1x1, and flip angle = 7°.

In both Experiments we collected other anatomical data as well as resting state fMRI before, during, and after stimulation, but we did not analyse these within the current study, and we will report them in separate papers.

4.3.5. fMRI paradigm

We instructed participants to perform a thumb adduction-abduction movement as fast as they could in response to auditory cues (beeps). The use of a simple task enables both the direct translation of this paradigm to PDOC patients as well as the study of tDCS-induced activation changes independent of modulations of performance. We presented the beeps in blocks cued

by the word ‘move’ and interspersed with blocks in which the participant was instructed to rest (cued by the word ‘relax’). Each ‘move’ block included 7 beeps presented at a variable interstimulus interval (range 2-3 seconds), in order to avoid prediction effects. The task included 8 blocks of each type, each with a duration of 20 seconds, and for a total duration of 5 minutes and 20 seconds. We instructed the participants to maintain fixation on a white cross displayed in the centre of a black screen throughout the full duration of the task. This, as well as the instructions at the start of the task (“Start moving your thumb as quickly as you can every time you hear a beep. Stay still when you hear "relax". Make sure you keep looking at the fixation cross at all times”) were presented via a digital system (Barco F35 AS3D, Norway) that projected the image onto a mirror fixed to the head coil at a visual angle of ~10°. We delivered all auditory cues with an MR-compatible high-quality digital sound system incorporating noise-attenuated headphones (Avotec Silent Scan®). During ‘move’ blocks, we recorded thumb movements with an MRI compatible joystick (FORP-932, Current designs INC., PA USA), using 1200 Hz sampling frequency of x and y positions. To facilitate use of the joystick inside the MRI bore, the device was connected to the interface in the control room through an optical cable. For each session, we stabilised the joystick on the participant's torso and stabilised their right thumb using tape. To ensure accurate recordings, we calibrated the joystick before starting the experiment in each session. We used MATLAB 2015b on a Windows 7 computer to deliver all task stimulus and record motion tracking. See **Figure 4.1**.

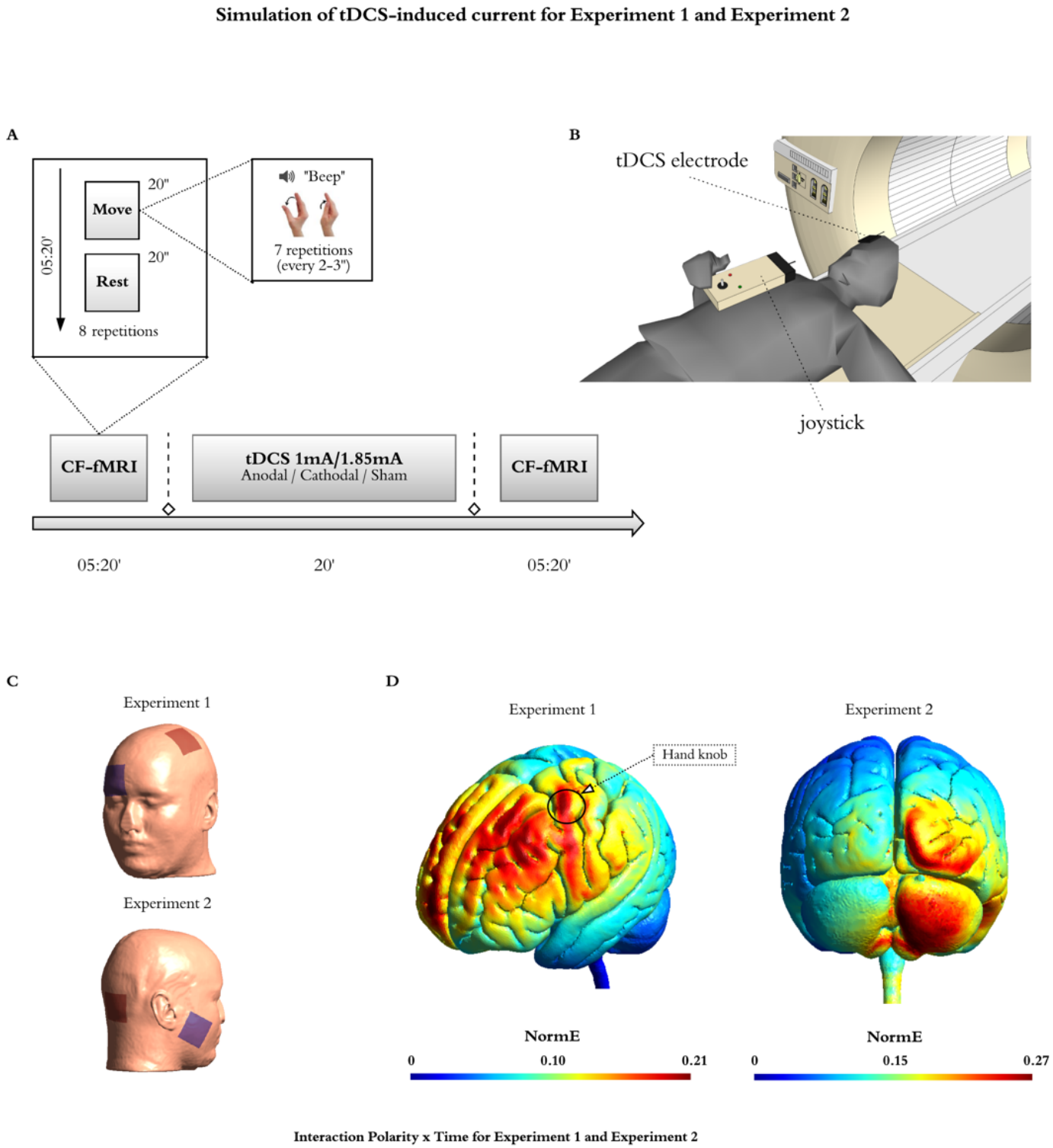


Figure. 4.1. Experimental Design and tDCS montages. Experimental design. (A) Participants performed a simple behavioural command following task in the MRI scanner (CF-fMRI) before and

after receiving 20 minutes of tDCS, whereby they move their right thumb in response to auditory cues (beeps). The task alternated 8 blocks of movement interspersed with rest blocks (all blocks were 20 seconds long for a total of 5 minutes 20 seconds). The beginning of each block was cued by the auditory words 'move' (movement blocks) or 'relax' (rest blocks). In each 'move' block the participants were instructed to perform 7 discrete thumb adduction-abduction movements as fast as they could in response to beeps that appeared at intervals ranging from 2-3 seconds, and while keeping their gaze fixated on a fixation crossed displayed in the centre of a black screen. Their movements were recorded with an MRI compatible joystick, using 1200 Hz sampling frequency of x and y positions (B). All participants received anodal, cathodal, and sham stimulation sessions in a counterbalanced order at least 7 days apart. In Experiment 1, we used a montage that targeted the left primary motor cortex (M1) with the reference electrode over the contralateral supraorbital region, and delivered our stimulation at 1mA (C, top inset). We used TMS to identify the best placement (motor hotspot) of the active electrode in each participant. In Experiment 2, our montage targeted the right cerebellar cortex, with a reference electrode over the right buccinator muscle, and delivered our stimulation at 1.85mA (C, bottom inset). (D) Computational model showing the electric field distributions in Experiment 1 (left) and Experiment 2 (right), as calculated with SimNIBS3.2.2 on the MNI standard head model. For the purpose of this simulation, in Experiment 1, we placed the active electrode on C3 to approximate the location of the motor hotspot in our participants (marked as hand knob in the figure), and the passive electrode on Fp2 . In Experiment 2, we placed the active electrode on I2 and the passive electrode over the right buccinator muscle. Note that this model does not consider individual differences in the position of the electrodes or the different tissue compartments across individual participants and therefore it should be interpreted as an estimate of the canonical field distribution to be expected with our montages.

4.3.6. fMRI preprocessing and GLM analysis

We used SPM12 on MATLAB 2015b (www.fil.ion.ucl.ac.uk/spm) for the preprocessing and analysis of both fMRI datasets. Each dataset was analysed independently but following the same pipeline, as described here. We first followed a standard spatial pre-processing, including realignment, co-registration between the structural and functional data sets, spatial normalisation, and smoothing with an 8mm fwhm Gaussian kernel). Additionally, in order to remove potential undesirable effects of physiological noise or participant's motion in the

activation maps, we performed single-subject independent component analysis (ICA) (Beckmann & Smith, 2004) and then applied FMRIB's ICA- based X-noiseifier (FIX) (Griffanti et al., 2014; Salimi-Khorshidi et al., 2014, p.) to identify artefactual components and remove them from our fMRI data. We first classified manually all components from a subset of datasets (18 in Experiment 1 and 23 in Experiment 2), ensuring an even coverage of all possible combinations of sessions, times, and polarities. Then, we used these manual labels to train a classifier for each of the studies that we then applied to the remaining datasets in that study. In order to test the accuracy of the automatic component classification, two of the authors (D.F-E for Experiment 1 and D.A. for Experiment 2) independently classified a number of components in the training set (8 datasets for Experiment 1 and 10 datasets for Experiment 2) and cross-checked their manual classification against the automatic classifications performed by FIX. There was a 100% match for 'bad' components between the manual and automatic classification lists.

We performed single-participant fixed-effect analyses using a general linear model in which we modelled each scan to belong to the motor execution (i.e. blocks of thumb movements) or the rest condition. The model also included the realignment factors as effects of non-interest to account for residual motion-related variance. We used high-pass filtering with a cut-off period of 80 seconds to remove slow-signal drifts from the time series. We then set linear contrasts to obtain estimates of the effects of interest for each subject, polarity, and time. Finally, in order to test the effects of tDCS on brain activation, we performed a second level full factorial analysis with polarity (anodal, cathodal, and sham) and time (before and after tDCS) as factors (total number of sessions = 126 for Experiment 1 and 126 for Experiment 2). When the interaction was significant, we also performed the corresponding pairwise interactions to study the direction of the effects. We report statistically significant voxels as being those that survive an uncorrected $p<.0001$ at the voxel level, on the following regions of interest: left supplementary motor area (SMA), left precentral gyrus, left thalamus, and right cerebellar lobes IV-V and VIII (Stoodley et al., 2012), using WFU PickAtlas. We did not include spurious activation, defined as a contrast returning a single significant voxel. We obtained these regions of interest from the Automated Anatomical Labeling atlas (Maldjian et al., 2003). In Experiment 1, we had to exclude one participant from the ANOVA due to an acquisition error in one of the sessions that resulted in the most superior slices of the brain being cropped (losing

a small section of M1). Note however that this issue did not affect the VOI analyses for the DCM (see section below) and therefore this participant was included in the DCM analyses. See full analysis pipeline in **Figure 4.2**.

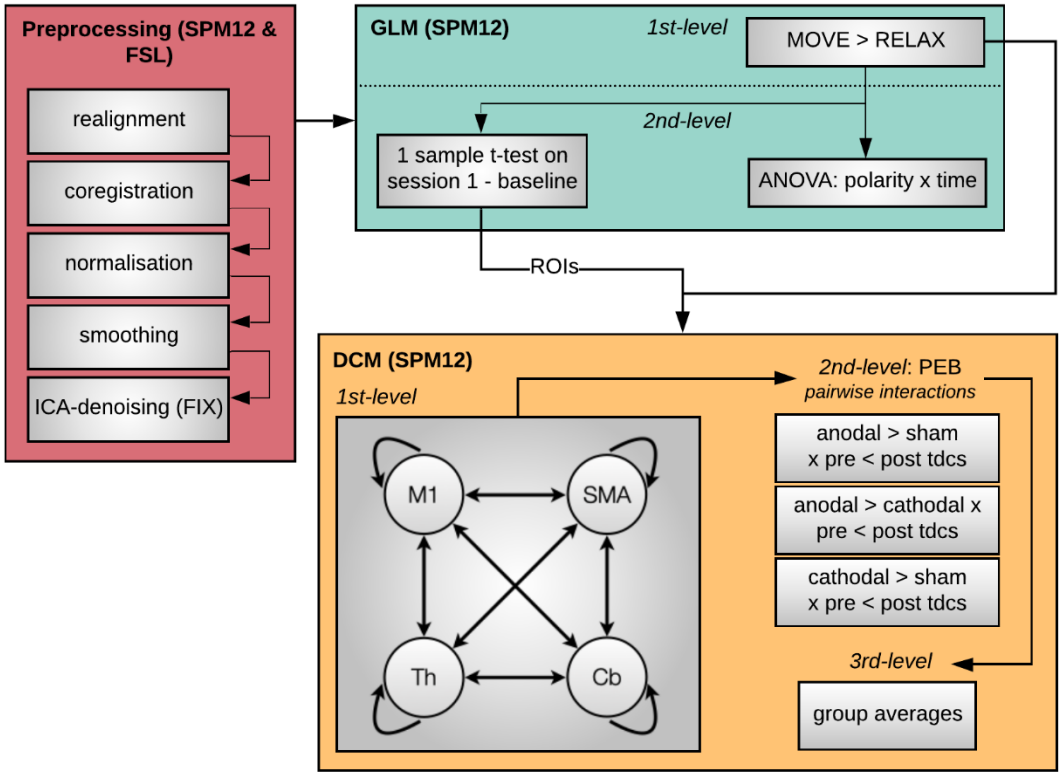


Figure 4.2. Analysis pipeline. We followed a standard pre-processing protocol (red panel), followed by fixed-effect general linear model analysis to model the effect of thumb movements in each individual participant (1st-level, green panel). We then conducted a second level full factorial analysis to test the effects of tDCS on brain activation (green panel). In addition, we performed a second-level one-sample t-test on the pre-stimulation run acquired in the first chronological session for each participant to characterise the canonical activation in the task, and define coordinates for the subsequent dynamic causal modelling (DCM) analyses. Finally, we used DCM to assess the effects of tDCS on the causal dynamics within our network of interest (yellow panel). We first built and estimated a fully connected model including left M1, left SMA, left thalamus, and right cerebellum in each participant. Then we applied Parametric Empirical Bayes (PEB) to model each of the three pairwise interactions between

polarity and time (i.e., interaction between pre-/post-tDCS and either anodal/cathodal, cathodal/sham, anodal/sham) in each participant (2nd-level, yellow panel). Finally, we created a 3rd-level PEB for each pairwise interaction modelling the average effect across participants. Note that we conducted data analysis for each Experiment individually but following the same protocol, as described above.

4.3.7. DCM analysis

4.3.7.1. Region selection and timeseries extraction

DCM is a framework for Bayesian modelling of brain dynamics, which allows the inference of hidden (unobserved) neuronal states from measured brain activity (Zeidman, Jafarian, Corbin, et al., 2019b). First, to obtain the canonical pattern of activity on our task for the group in each experiment, we performed second-level one-sample t-tests on the individual contrasts corresponding to the pre-stimulation run acquired in the first chronological session for each participant (**Figure 4.3**). In the resulting map, we identified the group peak of activation for the clusters corresponding to the left M1, SMA, left thalamus, and right cerebellum at an uncorrected $p<0.001$ (in bold in **Table 4.1**). These group-derived coordinates then served as a starting point for searching a nearby local maximum in each individual run. Each of these run-specific local maxima was constrained to be a maximum of 15mm away from the group level peak for the left M1, SMA, and right cerebellum ROIs and a maximum of 9mm away for the left thalamus ROI, and had to exceed a liberal statistical threshold of $p<0.05$ (Zeidman, Jafarian, Corbin, et al., 2019b). The differences in the allowed distance from the group peak accommodated for differences in size of the anatomical boundaries of each region. As recently recommended, when this threshold failed to produce a peak for that region, we iteratively reduced the threshold in 0.05 increments until reaching 0.25. When no peak could be found even at this threshold, we used the original group derived coordinates, as typically done (Zeidman, Jafarian, Seghier, et al., 2019). Note that we only used these liberal thresholds for the identification of coordinates to extract our timeseries (feature selection) but not for any statistical analyses. Having identified individual peak coordinates for each run, we extracted timeseries from 4mm radius spherical volumes of interest centred on them.

Table 4.1. *Canonical activation during command-following*

	Region	Cluster P	Cluster size	Peak P	T	MNI coordinates
		FWE-corrected	*in mm3*	*uncorrected*		*[x;y;z]*
Experiment 1	*M1*	<0.001	6264	<0.001	6.770	**[-33;-13;62]**
				<0.001	6.767	[-33;-19;56]
		0.966	81	<0.001	4.751	[-15;-4;68]
		0.903	162	<0.001	4.704	[-57;5;29]
		0.927	135	<0.001	4.324	[-54;5;14]
	SMA	<0.001	6426	<0.001	8.703	**[0;-7;65]**
	Thalamus	0.260	864	<0.001	6.330	**[-12;-22;5]**
	Cerebellum	0.022	2187	<0.001	7.137	**[15;-55;-22]**
Experiment 2	*M1*	0.326	702	<0.001	5.066	**[-24;-19;74]**
		0.983	81	<0.001	4.565	[-54;5;14]
		0.983	81	<0.001	4.251	[-15;-4;68]
		0.195	918	<0.001	4.107	[-42;-19;56]
				<0.001	4.085	[-36;-28;65]
				<0.001	3.957	[-33;-25;53]
		0.983	81	<0.001	3.795	[-39;-7;47]
		0.997	27	<0.001	3.606	[-33;-22;47]
	SMA	<0.001	5481	<0.001	7.087	**[-3;-4;65]**
				<0.001	6.178	[-12;-4;74]
				<0.001	5.345	[-9;-1;53]
	Thalamus	0.505	513	<0.001	4.352	**[-18;-16;14]**

				<0.001	4.153	[-9;-22;5]
	Cerebellum	0.003	3024	<0.001	8.799	**[12;-55;-25]**
				<0.001	7.671	[18;-49;-19]
				<0.001	5.159	[24;-43;-31]
		0.001	3915	<0.001	7.285	[24;-58;-46]
				<0.001	7.255	[12;-73;-46]
				<0.001	6.467	[6;-67;-31]

Results from the random effect group analyses on the brain activation during thumb movements to command in the baseline run for the first session. Results survived a threshold of uncorrected $p<0.001$. We highlight in bold the coordinates that we subsequently used as a starting point to search for individual coordinates to extract time series for the DCM. Abbreviations: FWE, family wise error; MNI, Montreal Neurological Institute; M1, primary motor cortex; SMA, supplementary motor area.

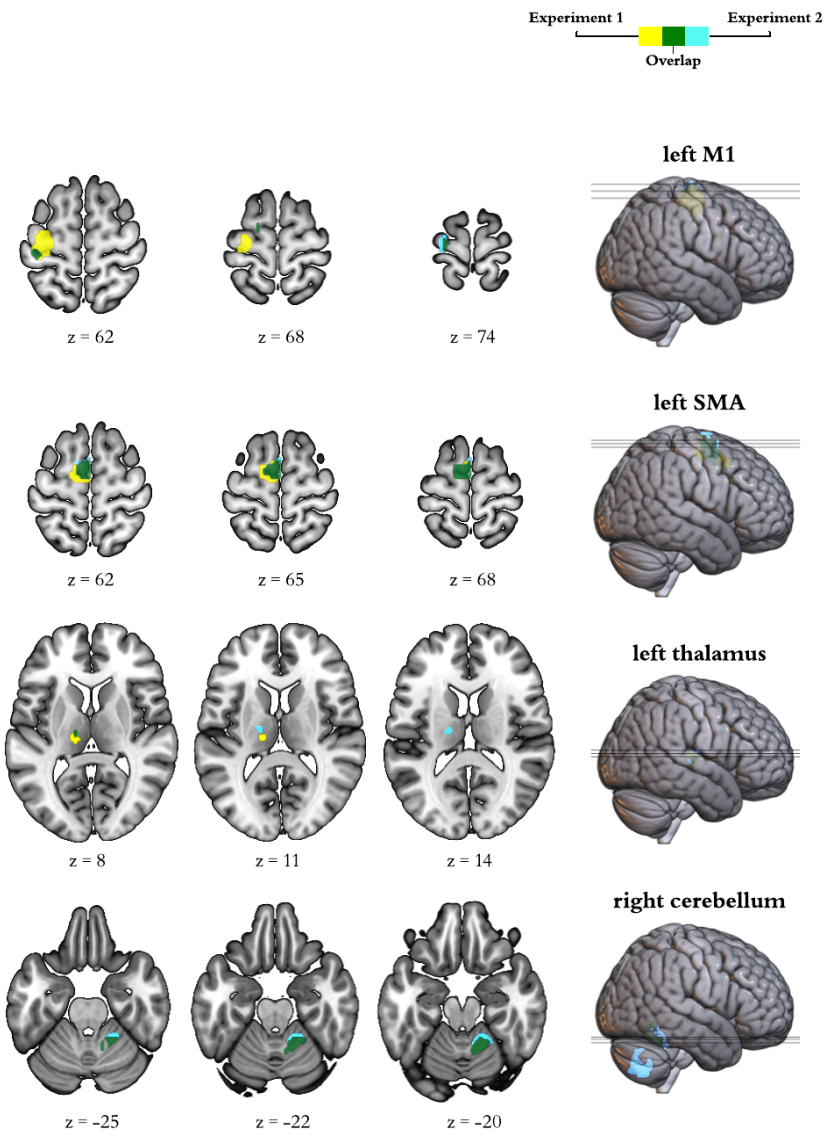


Figure 4.3. Activation at Baseline. Brain activation during command following in the pre-stimulation run corresponding to the first session for each participant. The insets display group general linear model differences between 'move' and 'rest' blocks in Experiment 1 (yellow) and Experiment 2 (light blue). The overlap across experiments appears in green. For display purposes, activation maps are shown at an uncorrected $p<0.001$ and rendered on a standard template (152 template in MRIcroGL). z indicates the Montreal Neurological Institute z coordinate.

4.3.7.2. Individual level DCM specification and definition of model space.

With the above extracted timeseries, we specified individual dynamic causal models using the deterministic model for fMRI, one-state per region, bilinear modulatory effects, and mean-centred inputs. We started with a 4-node fully connected model in which all self- and between region connections were switched on. The effect of thumb movements entered the model as modulatory input on the self-connection of each region, as this is recommended to improve both parameter identifiability and biological interpretability (Zeidman, Jafarian, Corbin, et al., 2019b). In addition to the intrinsic connections and modulatory inputs above, DCM requires the specification of driving inputs, which briefly 'ping' specific regions in the network at the onset of each block. In order to determine the best set of inputs for our data, we first created DCMs that included driving inputs to all 4 regions in our model and applied Parametric Empirical Bayes (PEB) to prune any parameters that were not contributing to the model evidence. Briefly, PEB is a hierarchical Bayesian framework for group-level modelling of effective connectivity, that allows the evaluation of both group effects and between-subject variability over DCM parameters (see (Zeidman, Jafarian, Seghier, et al., 2019) for a full description). For this step, we created a second-level PEB modelling the commonalities across all 6 sessions for each participant. These were then fed to a third-level PEB that modelled the commonalities across the group. In addition to the constant encoding the group mean, we included sex, age, and the score in the Edinburgh Handedness Inventory as nuisance regressors (all mean-centred). Finally, we used Bayesian Inference to invert the model for each subject and estimate the parameters that maximise explanation of data while minimising complexity. For this, we used Bayesian Model Reduction (BMR) to search over the reduced models followed by Bayesian Model Average (BMA) to calculate the average connectivity parameters (Zeidman, Jafarian, Seghier, et al., 2019). We used a 95% posterior probability threshold for free-energy (i.e., comparing the evidence for all models where a particular connection / input is on, versus those where it is off). This step indicated strong support (>99% posterior probability) for including driving inputs to cortical regions (M1, and SMA) only (see results for full details) and therefore we re-defined DCMs for all of our participants using these parameters. Our final model therefore included all self- and between-region connections, modulatory inputs to each self-connection, and driving inputs to M1 and SMA.

4.3.7.3. PEB ANOVAs

To test the effects of tDCS on the model parameters (connections and task modulations), we first created 3 second-level PEB models in each participant, which encoded the following pair-wise interactions: (1) greater increases after anodal stimulation as compared to sham (pre-tDCS < post-tDCS x anodal > sham sessions) and (2) greater increases after anodal stimulation as compared to cathodal (pre-tDCS < post-tDCS x anodal > cathodal), and (3) greater increases after cathodal stimulation as compared to sham (pre-tDCS < post-tDCS x cathodal > sham). Note that these contrasts also encode the opposite effects: e.g., PEB 1 can also be interpreted as greater decreases in sham as compared to anodal (pre-tDCS > post-tDCS x anodal < sham). Each subject specific PEB model was then entered into one of 3 third-level PEBs that encoded the commonalities across the group (mean) for each pairwise interaction, as well as sex, age, and handedness score.

We then used BMR and BMA to prune connections that do not contribute to the model evidence and estimate the parameters across all models for each of the connections that remain switched on. We thresholded our BMA results at a posterior probability > 95% (which is equivalent to a Bayes factor of 3) (Zeidman, Jafarian, Seghier, et al., 2019).

4.3.8. Motion tracking

We performed motion data analysis using a custom script on MATLAB 2017b. First, we calculated the Euclidean distance of the x-y position and applied a low-pass 15Hz filter to the data. We then identified the onset and end of the movement by looking at abrupt changes in the signal, using the matlab function *findchangepts*, which, given a vector x with N elements (in our case containing motion tracking data) returns the index at which the mean of x changes most significantly. We used the first and last change detected by *findchangepts* to determine when each movement started and ended. We excluded movements where no changes were detected, which could be due to participants not responding to the task or to the joystick not recording data. In Experiment 1, this resulted in the removal of 5 datasets from the motion tracking analysis, due to the joystick malfunctioning during recording in at least one of three sessions. Lastly, we calculated velocity and acceleration at each timepoint between the

beginning and end of each movement and obtained the mean velocity and peak acceleration for the trial. Additionally, we calculated reaction time defined as the time occurring between the auditory stimulus (beep) and the onset of the movement. Finally, we averaged these values across each run and computed a 2 (pre- vs post-tDCS) x3 (polarity) repeated measures ANOVA to check for any effect of tDCS on behaviour.

4.3.9. Blinding

In order to assess whether our blinding protocol was successful, in each Experiment, we used McNemar's test to assess whether the number of correct judgments across the group about whether they had received tDCS or not was different between real stimulation and sham stimulation sessions.

4.4. Results

4.4.1. Experiment 1 - Effects of M1-tDCS on brain activation and dynamics

See the canonical task activation at baseline in **Table 4.1** and **Figure 4.3**.

Our factorial analysis on the individual activation maps revealed a significant interaction between polarity (anodal, cathodal, and sham) and time (pre-, post-tDCS) on the left thalamus only (uncorrected $p<0.001$; see **Table B1** and **Figure B1** in **Appendix B**). Subsequent pairwise interactions revealed cathodal stimulation increased activity in this area as compared to sham. However, there were no significant differences between polarities and further reducing the threshold to uncorrected $p<0.005$ also revealed a cluster of increased activity in the thalamus for anodal as compared to sham. See Supplementary **Table 1** and **Figure 1** in **Appendix B,** for the positive effect of the task across all sessions in this ANOVA.

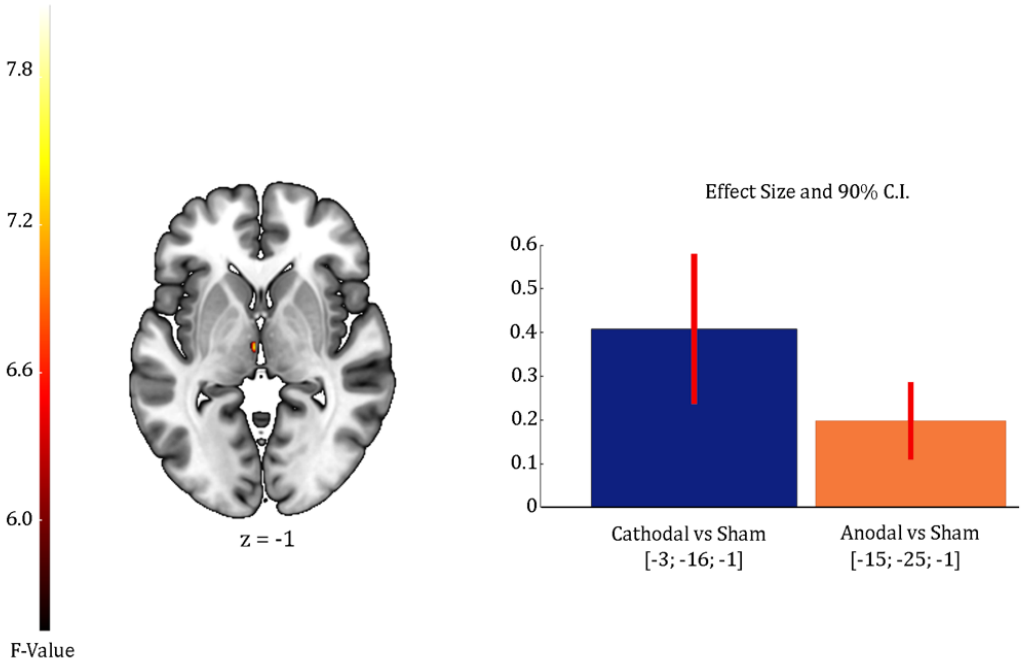


Figure 4.4. Effects of tDCS on brain activation during command following for Experiment 1. The brain inset displays the 2nd-level (group) general linear model (GLM) interactions between polarity (anodal, cathodal, sham) and time (pre-, post-tDCS) in the contrasts modelling brain activation during command following. For display purposes, activation maps and plots are shown at an uncorrected $p<0.005$ and rendered on a standard template (152 template in MRIcroGL). The colour bar represents the F value for the interaction in the GLM. z indicates the Montreal Neurological Institute z coordinate. Bar plots show the estimated effect size and 90% confidence intervals at the peak voxel for each pairwise contrast: greater activation after anodal stimulation as compared to sham (orange), and greater activation after cathodal stimulation as compared to sham (blue).

Our DCM analyses revealed that anodal stimulation of M1 reduced self-inhibition in the thalamus and led to a more inhibitory output from cerebellum to M1, compared to both sham and cathodal stimulation. Additionally, as compared to sham, anodal stimulation increased inhibition in all outputs from M1 to the rest of the network but reduced inhibition from cerebellum to thalamus, as well as in SMA and cerebellar self-connections. These changes were however not polarity specific. In turn, cathodal stimulation increased excitation from thalamus to SMA, both as compared to sham and to anodal stimulation. Additionally, as compared to sham, cathodal stimulation led to an increase in inhibition from both M1 and

cerebellum to SMA, an increase in excitation from thalamus to M1, and a reduction in self-inhibition in SMA. In terms of task modulations, cathodal M1 stimulation increased the modulatory input from the task on M1 (i.e., increased M1 self-inhibition) both as compared to anodal stimulation and sham, and decreased the modulatory input from the task on SMA as compared to anodal stimulation (see **Figure 4.5**).

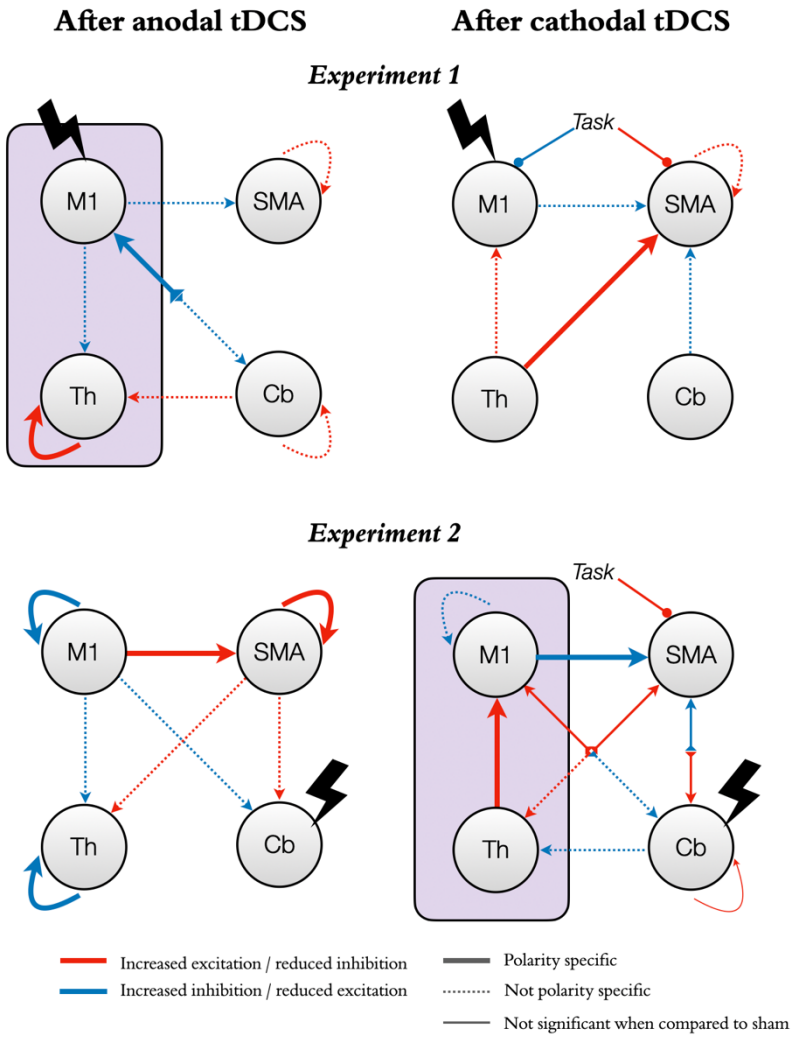


Figure 4.5. Effects of tDCS on functional neural dynamics with M1 or the cerebellum as targets. The figure shows the effects of tDCS on functional neural dynamics for the two experiments (Experiment 1, top panels; Experiment 2, bottom panels). The left and right panels represent changes after anodal and cathodal stimulation respectively. Red arrows indicate changes in the direction of

increased excitation (or reduced inhibition). Blue arrows indicate changes in the direction of increased inhibition (or reduced excitation). Note that self-connections are always inhibitory and thus red indicates a reduction in inhibition rather than an excitatory role per-se. Similarly, modulatory inputs from our command following task on each region increase (blue) or decrease (red) the region's inhibitory tone. Thick lines represent changes that are significant both as compared to the opposite polarity and to sham. Thin lines represent changes that are only significant as compared to the opposite polarity. Dashed lines represent changes that are only significant as compared to sham (not polarity specific). The purple boxes highlight our hypotheses for the M1-thalamus axis: anodal M1-tDCS (top left panel) reduced self-inhibition in the thalamus while cathodal cb-tDCS (bottom right panel) increased excitation from thalamus to M1, both in a polarity specific manner.

4.4.2. Experiment 2 - Effects of cb-tDCS on brain activation and causal dynamics

In terms of brain activity during command following, our factorial analysis revealed no significant interactions between polarity and time (pre- vs post-tDCS) in any of the ROIs. See Supplementary **Table 1, Appendix B,** and **Figure 1, Appendix B**, for the positive effect of the task across all sessions in this ANOVA.

In terms of effective connectivity, as predicted, cathodal stimulation led to increased excitation from thalamus to M1 both as compared to sham and anodal stimulation. In addition, it increased M1 self-inhibition as compared to sham but to a lesser extent than anodal stimulation. Finally, it increased inhibition from M1 to SMA both as compared to sham and anodal stimulation (**Figure 4.5**). When compared directly with anodal stimulation, cathodal cb-tDCS also decreased cerebellar self-inhibition and increased excitation from thalamus to SMA. Additionally, cathodal stimulation increased inhibition from M1 to cerebellum and from cerebellum to thalamus, and increased excitation from SMA to both thalamus and cerebellum, and from cerebellum to M1, as compared to sham. However, none of these changes were significant when compared with anodal stimulation. Finally, cathodal cb-tDCS decreased the effect of the task on SMA both as compared to sham and anodal stimulation. In contrast, anodal stimulation, when compared to sham and cathodal stimulation, led to increased self-inhibition in M1 and thalamus, reduced self-inhibition in SMA, as well as increased excitation from M1

to SMA. Additionally, anodal stimulation increased excitation from SMA to thalamus and cerebellum, and increased inhibition from M1 to cerebellum when compared to sham, but these changes were not polarity specific (i.e., did not reach statistical significance in the comparison between anodal and cathodal stimulation).

4.4.3. Experiments 1 and 2 - Effects of tDCS on behaviour

As expected, we did not find any interactions (polarity x time) for any of the metrics considered in neither Experiment 1 nor 2 (i.e., reaction time, mean velocity, and peak acceleration). In Experiment 2 only, we found a small main effect of time on average reaction times, which was 0.02 seconds (20 ms) faster in the second run as compared to baseline (pre-: 0.30s ± 0.04; post-tDCS: 0.28s ± 0.04; $p<0.001$ uncorrected, η_p^2 0.5). See **Appendix B Table 2** for full statistical information for all main effects, interactions, and post hoc tests.

4.4.4. Experiments 1 and 2 - Blinding

We found no significant differences in the number of times that sham and active stimulation sessions were perceived as real in either experiment, suggesting that participants' experiences did not differ between active and sham stimulation sessions and blinding was successful (see Supplementary **Table 3, Appendix B**).

4.5. Discussion

Efforts to use tDCS as a therapeutic intervention in PDOC have had mixed success to date. While some studies showed very promising clinical improvements, many others failed to show any effects even after repeated sessions (Chapter 2). The field is thus unable to reach a consensus about whether tDCS would or would not be a feasible therapeutic avenue for this patient group as a result. Most research to date has focused on targeting the left frontal cortex, in an attempt to engage non-specific networks involved in arousal and awareness. Here, we

propose a new therapeutic direction that directly addresses the neural mechanisms that support measurable changes in behavioural responses after tDCS at the level of functional thalamo-cortical coupling within the motor network (Fernandez-Espejo et al., 2015).

Our results provide the first evidence that tDCS over motor areas can distally modulate brain activity and causal dynamics in thalamo-cortico-cerebellar loops (beyond the immediate target area of stimulation) during behavioural command following, even when the stimulation is delivered at rest. In Experiment 1, anodal stimulation over M1 increased task-induced activation of the thalamus. Our DCM analyses revealed that this is likely explained by reduced thalamic self-inhibition. In Experiment 2, cathodal cerebellar stimulation did not lead to changes in task-induced activity but instead led to increased excitatory influence from thalamus to M1. Taken together, these experiments demonstrate that it is possible to influence thalamo-cortical coupling indirectly via targeting surface (easily accessible) regions in the motor network. More importantly, they suggest that this could be a viable route to elicit clinically relevant changes in PDOC. Indeed, we designed our command-following task to emulate the approach that is routinely used in clinical settings to assess awareness after severe brain injury; namely asking the patient to perform a discrete movement in response to a verbal command (Fernandez-Espejo & Owen, 2013). This resulted in a task that was insensitive to potential tDCS modulations of behaviour in healthy participants but allowed us to study the neural effects of tDCS independently of performance, permitting us to draw more direct comparisons to the PDOC population. Specifically, our task deviated from those typically used in the motor learning literature (e.g., (Hamada et al., 2014; Hannah et al., 2019) in three crucial points: the use of a very small number of trials (approximately 80-90% less), variable cue intervals to avoid prediction effects, and no feedback to participants. Further, we delivered stimulation at rest to increase the translatability of our results to unresponsive PDOC patients. It is important to highlight that the aim here was not to improve motor control in the healthy brain. Instead, we built upon convincing evidence that the thalamus is greatly inhibited in PDOC due to both structural and functional damage (Fernandez-Espejo et al., 2010, 2011; Schiff, 2010), resulting in less cortical excitation (Schiff, 2010). Our focus thus lay on compensating for this thalamic over-inhibition instead of enhancing normal function. We have previously shown that increased thalamic activity and excitation, as well as increased excitatory thalamus-M1 coupling facilitates the production of motor responses to command in tasks like the one we

used here (Fernandez-Espejo et al., 2015). We now show that anodal tDCS over M1 and cathodal tDCS over the cerebellum can each modulate these dynamics, albeit in different ways, and we propose that they may allow PDOC patients to overcome motor control deficits at the root of their diminished behavioural responsiveness (Fernandez-Espejo et al., 2015; Stafford et al., 2019a). This in turn would allow more patients to demonstrate their true level of awareness, especially in those affected by so-called cognitive motor dissociations (Schiff, 2015a). Alongside ensuring that each patient receives an appropriate diagnosis, this increased responsiveness can also have important implications for prognosis by facilitating patients' engagement with rehabilitation (Elliott & Walker, 2005). Moreover, regaining some level of control over their thumb would facilitate the use of assistive devices (including those for communication), which could have an enormous impact on their quality of life. Indeed, to further increase the clinical relevance of our study, we focused on thumb movements, as they are affected by spasticity in fewer PDOC patients and with less severity as compared to other fingers (B. Zhang et al., n.d.).

Importantly, our results suggest two potential routes to target the thalamo-M1 axis, providing some flexibility to adapt the tDCS montage to the specific pattern of injuries present in each individual patient. Crucially, while many PDOC patients present localised structural damage to the white matter fibres connecting thalamus and M1 (Fernandez-Espejo et al., 2015; Stafford et al., 2019a), this damage is partial instead of a complete deafferentation (Stafford et al., 2019a). This suggests the remaining pathways may be amenable to therapeutic intervention. In contrast, the white matter pathways connecting the cerebellum with the thalamus appear relatively preserved (Stafford et al., 2019a), suggesting that this may be a feasible route into the thalamus in the majority of PDOC patients. We have previously argued that the relative preservation of this pathway, in the context of damage to the thalamus and the white matter fibres connecting thalamus to M1, may be contributing to excessive thalamic inhibition (Stafford et al., 2019a). As discussed above, our current results show that cathodal cb-tDCS may be able to successfully counteract this. It is important to acknowledge here that, while both anodal M1 and cathodal cb-tDCS successfully modulated thalamic activity, there were differences in their respective effects over M1 activity and the thalamo-M1 dynamics. Furthermore, cathodal M1-tDCS also led to changes in thalamo-M1 coupling in the desirable direction (increased coupling), alongside increases in thalamic activity. This adds further

support to the now well accepted notion that the two polarities do not always result in opposing effects (Parkin et al., 2015). We include below discussion of potential compensatory mechanisms that may explain these effects, but we cannot rule out that cathodal M1-tDCS may also have therapeutic effects in some PDOC patients. We also note the possibility of simultaneous anodal-M1 and cathodal-cerebellar stimulation, although we have not tested this montage. In any case, further studies in PDOC patients themselves are required to test which of these modulations has greater therapeutic effect and for which specific patients. More broadly, while our results provide a robust proof-of-principle for the use of motor tDCS in PDOC, the specific dose, duration, and number of sessions required to induce reliable neural and behavioural changes in PDOC patients needs to be established. Further, the effects of tDCS are highly variable across individuals (Filmer et al., 2019) and this heterogeneity can only be expected to be greater in PDOC patients, due to individual differences in brain damage affecting thalamo-cortical regions and their structural connectivity (Fernandez-Espejo et al., 2011; Lant et al., 2016; Stafford et al., 2019a). We report here group effects and thus our results cannot be interpreted in terms of M1 or cerebellar tDCS resulting in less (or more) individual variability as compared to other available interventions (e.g., DLPFC). Indeed, an exploration of individual tDCS differences and their relationship to individual brain structure and white matter connectivity is beyond the scope of the current study but remains a crucial area of further investigation. By focusing on specific circuits that have a mechanistic role in PDOC, we believe our study provides a framework to study individual effects in a robust way.

To our knowledge, only 3 studies have targeted motor areas with tDCS in PDOC (Martens et al., 2019; Naro et al., 2016a; Straudi et al., 2019), in sharp contrast with the many others that have focused on the DLPFC, and currently represents the main direction in the field. These 3 motor studies included a combined total of 40 patients (14 VS and 26 MCS). Their small sample sizes, key differences in specific montages and stimulation parameters, alongside the focus on behaviour instead of neural markers, preclude us from drawing direct comparisons with our study. In addition, while we are satisfied that we were able to identify the optimal location of the electrodes on the scalp to target the desired regions in our study, this is a much more challenging task in patients with severe brain injury, where large macrostructural changes will affect the relative position of the brain structures of interest in respect to the scalp. Nevertheless, PDOC studies provided preliminary evidence that M1 and cerebellar tDCS are

well tolerated in this patient group and can indeed lead to specific improvements in motor responsiveness in a subset of patients (as indexed by increases in the motor and auditory CRS-R subscales).

Beyond the immediate implications for the rehabilitation of PDOC patients, our results speak for the ability of tDCS to influence long-range dynamics in the motor network during movement execution. The field of non-invasive brain stimulation has recently been tainted by a certain level of scepticism towards the effectiveness of tDCS, with some questioning whether it is indeed capable of modulating brain function at all (Filmer et al., 2019). The increasing number of well controlled imaging and electrophysiological studies has provided reassurance that tDCS can indeed modulate cortical regions under the electrodes. In the specific case of M1 stimulation, this is now well established. Here, we take this argument one step further, demonstrating that it can also lead to widespread distal modulations of cortico-subcortical loops when participants are engaged in a relevant cognitive task, and that such modulations do not require the participant to engage with the said task while receiving the stimulation itself. Specifically, our predicted changes to thalamo-cortical dynamics induced by anodal M1-tDCS (as discussed above), are consistent with, and expand, the now widely reported effects on M1 excitability (Nitsche & Paulus, 2000) as well as more recently described changes to BOLD signal (Baudewig et al., 2001; Jang et al., 2009; Stagg, O'Shea, et al., 2009) and functional connectivity at rest (Cummiford et al., 2016; Polania et al., 2012; Sankarasubramanian et al., 2017). In contrast, the effect of cerebellar tDCS on neural dynamics is much less understood. As discussed above, cathodal cb-tDCS increased thalamic afferent excitation over M1. In contrast, anodal stimulation led to increased self-inhibition in both M1 and thalamus. These findings demonstrate that tDCS is able to modulate cerebellar-brain inhibition (CBI) in a polarity specific manner, in agreement with previous electrophysiological reports (Galea et al., 2009), as well as a recent report of local increased activation in the dentate nuclei after cathodal cb-tDCS during simple finger tapping (Küper et al., 2019). Furthermore, for the first time, we provide a window into the specific functional dynamics mediating these effects.

Interestingly, against our prediction, cathodal tDCS over M1 also led to an increase in thalamic activation and in excitation from thalamus to M1, as compared to sham. These changes further support the already described complex effects that characterise this polarity (Parkin et al.,

2015). Specifically, cathodal tDCS is known to produce more inconsistent behavioural results than anodal stimulation, although these inconsistencies are more common in cognitive than motor studies (Jacobson et al., 2012). Interestingly, our cathodal M1-tDCS also increased the modulatory effect of the task over M1 (i.e., led to greater M1 inhibition during the move blocks), but this was not accompanied by reductions in motor performance in the task. We believe this suggests that the thalamic changes reflect a compensatory mechanism to overcome cortical inhibition caused by cathodal M1-tDCS and to maintain an acceptable level of motor performance. This is in line with earlier animal models suggesting sustained effects of tDCS that are characterised by the system trying to compensate and normalise its activity to baseline levels (see (Reato et al., 2010a) as discussed in (Jackson et al., 2016). Similarly, in Experiment 2, cathodal stimulation over the cerebellum led to the expected increases in excitatory output from thalamus to M1, but also an unexpected increase in M1 self-inhibition. Once again, tDCS did not alter behavioural performance and thus we believe this cortical reduction also compensated for the excess excitation coming from the thalamus. Alongside determining whether these changes have a therapeutic effect, neuroimaging studies of tDCS in PDOC will help elucidate whether the effects of cathodal M1-tDCS and anodal cb-tDCS are indeed compensatory or can alter behaviour when a motor deficit is present. In either case, in showing polarity specific modulations for some but not all our results, our study speaks for the complexity of the effects of tDCS (Filmer et al., 2019) and suggests that other active control conditions alongside polarity should be included in future studies.

Several limitations need to be acknowledged. First, the distribution of the current generated by conventional tDCS is characterised by very low spatial accuracy and can reach a widespread area beyond the intended target. As seen in the simulations provided in Figure 1, our montages are no exception to this. Our simulations suggest that the delivered current did not reach the thalamus with either montage. Therefore, our reported effects for this structure are likely to be explained by modulations of network connectivity. However, simulations suggest that M1-tDCS generated similar levels of current in SMA to that of M1 itself, and thus we cannot rule out that some of our effects are mediated by SMA. In contrast, our modelled current distribution for cb-tDCS extended beyond cerebellum into occipital and ventral temporal regions. These areas are not associated with our motor command-following task and are therefore not likely to have driven our effects. In either case, while the lack of spatial specificity does not limit the

potential clinical application of tDCS in PDOC, it should be considered when making inferences about causal links between elicited effects and specific brain areas. Future studies should consider using a montage targeting non motor regions to make stronger causal inferences about the role of specific areas. Additionally, high-definition tDCS (HD-tDCS) can achieve higher spatial precision (Morya et al., 2019).

However, as we have previously argued (Chapter 2), the increased spatial precision of this method requires careful consideration of individual brain structure and tissue properties, especially in patients with severe brain damage, which might limit clinical applications of HD-tDCS in PDOC. Second, the effects of tDCS are highly dependent on the state of the target brain networks during stimulation (Li et al., 2019), and are more effective when paired with a relevant task (Bolognini et al., 2009b). Using a task during stimulation also partially overcomes the above limitations in spatial accuracy in ensuring that the effects are maximal for the intended areas (amongst all areas receiving current). Additionally, while we encouraged our participants to remain awake and monitored them during the 20 minutes of tDCS, the lack of behavioural outputs inherent to rest scans precluded us from verifying their wakefulness levels. It is thus possible that some of our participants experienced variable levels of wakefulness that could result in further individual differences in their brain states.

However, as discussed above, PDOC patients are unable to voluntarily engage in behavioural tasks and delivering the stimulation at rest remains the most feasible option. Future studies should consider alternative ways to modulate brain states when designing tDCS interventions for this challenging patient group (e.g., see (*Exploring the Neural, Behavioural, and Clinical Effects of Transcranial Direct Current Stimulation in Patients with a Prolonged Disorder of Consciousness; Protocol for a Double-Blind Randomised Crossover Feasibility Study*, 2020). Third, in Experiment 2, we increased our FOV to ensure a full coverage of the cerebellum for all participants, and this required a longer TR. The resulting reduced temporal resolution that resulted may have affected our sensitivity to detect BOLD changes, compared to *Experiment 1* (Zeidman, Kazan, Todd, et al., 2019). We note that when all trials were included (e.g., see **Figure 1, Appendix A**) the activation patterns were similar across both experiments, but this difference in sensitivity should be considered when making comparative arguments about effectiveness across our two montages. Importantly, DCM provides a more complete and

sensitive account of differences in regional activation and their interactions, and can thus more reliably detect group differences (Schuyler et al., 2010). Future studies with larger cohorts are required to clarify whether our proposed montages can elicit robust changes at the GLM level also.

4.6. Conclusions

In summary, our results indicate that tDCS can successfully modulate long-range thalamo-cortical dynamics underlying behavioural responsiveness during command following. It is yet to be tested whether these effects can be replicated in PDOC patients themselves and whether this will result in measurable clinical effects. However, our methodology can be directly applied to investigate this, and in doing so, it opens new avenues to explore the mechanisms of tDCS interventions in this challenging population.

Note that the appendix to this chapter can be found at the end of the thesis (Appendix B).

Chapter 5

MULTI-SESSION TDCS PAIRED WITH PASSIVE MOBILISATION OF THE THUMB MODULATES THALAMO-CORTICAL COUPLING DURING COMMAND FOLLOWING IN THE HEALTHY BRAIN[4]

5.1. Abstract

Therapeutic options for patients with prolonged disorder of consciousness (PDOC) are limited. PDOC patients often exhibit a dissociation between their retained level of (covert) cognitive ability and their (overt) behavioural responses (cognitive-motor dissociation; CMD). This is linked to reduced coupling between thalamus and the primary motor cortex (M1). We have recently shown that a single session of tDCS over M1 delivered at rest can reduce thalamic self-inhibition during the type of command following tasks routinely used to assess awareness in PDOC. Here, we build upon this by exploring whether pairing tDCS with a concurrent passive mobilisation protocol (designed to be feasible in PDOC) can further influence thalamo-M1 dynamics and whether these changes are enhanced after multiple stimulation sessions. Specifically, we used Dynamic Causal Modelling (DCM) on functional magnetic resonance imaging (fMRI) data from 22 healthy participants to assess tDCS changes on effective connectivity within the motor network during command-following. We found that a single anodal tDCS session (paired with passive mobilisation of the thumb) decreased self-inhibition

4

As published in BiorXiv:

Aloi, D., Jalali, R., Calzolari, S., Lafanechere, M., Miall, R. C., & Fernández-Espejo, D. (2022). *Multi-session tDCS paired with passive mobilisation increases thalamo-cortical coupling during command following* [Preprint]. BiorXiv. https://doi.org/10.1101/2022.11.22.517479

An updated version of this paper was published in a peer-reviewed journal: Aloi, D., Jalali, R., Calzolari, S., Lafanechere, M., Miall, R. C., & Fernández-Espejo, D. (2023). *Multi-session tDCS paired with passive mobilisation of the thumb modulates thalamo-cortical coupling during command following in the healthy brain.* NeuroImage, 120145. https://doi.org/10.1016/j.neuroimage.2023.120145

in M1, with five sessions further enhancing this effect. In addition, anodal tDCS increased thalamo-M1 excitation as compared to cathodal stimulation, with the effects maintained after 5 sessions. In turn, cathodal tDCS had opposing effects on these connections after one session but became more similar to anodal after 5. Together, our results suggest that pairing anodal tDCS with passive mobilisation across multiple sessions may facilitate behavioural command-following in PDOC patients with CMD. More broadly, they offer a mechanistic window into the neural underpinnings of the cumulative effects of multi-session tDCS.

5.2. Introduction

Prolonged disorders of consciousness (PDOC), including the vegetative/unresponsive wakefulness state (VS) and the minimally conscious state (MCS) are catastrophic neurological conditions for which an effective therapeutic approach has yet to be found. In recent years, several studies have used transcranial direct current stimulation (tDCS) in an attempt to induce clinical improvement in VS and MCS patients (Chapter 2). However, despite some promising results(Angelakis et al., 2014; W. Huang et al., 2017; Martens et al., 2018; Naro et al., 2016b; Straudi et al., 2019; Thibaut et al., 2014b, 2017; R. Zhang et al., 2020; Y. Zhang et al., 2017), the outcome of these trials has been mixed and inconsistent, making it difficult to draw meaningful conclusions about the effectiveness of tDCS in PDOC (Chapter 2). Part of this variability corresponds to well-known limitations present in the broad tDCS literature, such as the effect of inter-individual differences in brain anatomy (Ridding & Ziemann, 2010), or a lack of standardisation of protocols that leads to heterogeneity of stimulation parameters across studies. In addition, PDOC originates from different aetiologies, resulting in heterogeneous patterns of brain injury across patients (Pozeg et al., 2021; Y. Zhang et al., 2017). However, as we have previously argued (Aloi et al., 2021, 2022b), a key consideration in this patient group refers to the lack of an accurate and precise definition of the neural basis of consciousness (Zhao et al., 2019), which complicates the identification of effective targets for neuromodulation.

In an earlier tDCS study (Chapter 4), we switched the focus from the consciousness disorder itself to the patients' (lack of) responsiveness or ability to produce voluntary motor responses.

While behavioural responsiveness, and specifically command-following, is the main clinical indicator of awareness in diagnostic examinations of PDOC, it is now well established that it does not accurately reflect the level of cognitive functioning in many patients who are partially (or in some cases fully) aware but lack voluntary motor control (Fernandez-Espejo & Owen, 2013; Schiff, 2015a). This condition is known as cognitive-motor dissociation (CMD) (Schiff, 2015a) and is associated with reduced thalamo-cortical coupling owing to selective structural impairments in the pathways connecting the thalamus and primary motor cortex (M1) (Fernandez-Espejo et al., 2015; Stafford et al., 2019b). In our previous study, we showed in the healthy brain that a single session of tDCS over M1 delivered at rest can successfully modulate thalamo-cortical dynamics during a subsequent behavioural command-following task (Chapter 4), suggesting a potential route to improve responsiveness in PDOC.

While our earlier results are encouraging, it is well known that tDCS leads to most reliable behavioural effects when paired with a task that can successfully engage the target network (Kadosh et al., 2010; Galea & Celnik, 2009; Koyama et al., 2015; Li et al., 2019). In fact, it is thought that tDCS reinforces the pattern of the underlying brain network activity (Abellaneda-Pérez et al., 2020; Dubreuil-Vall et al., 2019; Li et al., 2019), and thus, its effects on brain function are dependent on the ongoing neuronal state. Additionally, clinical work has shown that concurrent stimulation and physical therapy help promote motor rehabilitation, as tDCS appears to enhance the response of neural networks to the therapy, optimising plastic changes as a result (Bolognini et al., 2009b). Crucially, most PDOC patients (excluding those at the high end of the MCS spectrum) are by definition unable to execute voluntary external responses, and thus unable to take part in a command-following task. For this reason, existing studies in this patient group have delivered tDCS at rest. However, the literature suggests that passive mobilisation may lead to an engagement of the motor areas similar to active movements (Alary et al., 1998; Boscolo Galazzo et al., 2014; Jaeger et al., 2014; Lotze et al., 2003; Zhavoronkova et al., 2017) and could thus be an alternative to the use of a command-following task during tDCS. Importantly, PDOC patients typically receive regular passive mobilisation as maintenance therapy for the clinical management of their spasticity (*Prolonged Disorders of Consciousness Following Sudden Onset Brain Injury*, 2020). Therefore, a protocol involving passive mobilisation is clinically applicable in PDOC.

In addition, it is well-known that a single session of tDCS may not be sufficient to induce noticeable behavioural changes (Hashemirad et al., 2016a). In contrast, multiple sessions can lead to more significant improvements, possibly due to a potentiation of the functional connectivity between the regions activated during learning (Floyer-Lea & Matthews, 2005). The PDOC literature is consistent with this, with studies using several stimulation sessions showing more robust clinical improvements (Martens et al., 2018; Thibaut et al., 2014b, 2017).

Therefore, in this study, we used dynamic causal modelling of fMRI data to explore single- and multi-session effects of tDCS over M1 paired with passive mobilisation of the thumb on thalamo-cortical coupling during command-following. We focused on characterising the mechanisms and effects of tDCS on a well-controlled study in healthy individuals, while keeping our protocol and methods translatable to clinical practice in PDOC. We hypothesised that: (a) the combination of neurostimulation and passive mobilisation will enhance thalamo-cortical coupling beyond what we have previously reported when administering stimulation at rest (Chapter 4), and (b) such enhancement will be greater after multiple stimulation-mobilisation sessions.

5.3. Materials and Methods

5.3.1. Participants

Twenty-four right-handed healthy volunteers took part in the study (16 women, 8 men; mean age 24 ± 3 years), of whom 22 completed all three weeks of testing and were therefore included in the analyses (16 women, 6 men; mean age 25 ± 4 years). We recruited participants using advertisements across campus as well as the local Research Participation Scheme. All participants completed a pre-screening protocol to ensure eligibility to safely participate in MRI and tDCS experiments. They all reported no history of psychiatric or neurological disorders, no personal or family history of epilepsy, no use of psychoactive drugs, and normal or corrected vision. We instructed participants to come to the sessions well rested and hydrated, and not to consume coffee or alcohol within the 24 hours before each session, as per tDCS safety regulations (Antal et al., 2017b). The University of Birmingham's Science, Technology, Engineering, and Mathematics Ethical Review Committee approved the study and all

participants gave written informed consent. We compensated participants with £220 or the equivalent in course credits.

5.3.2. Experimental Procedure

We used a sham- and polarity-controlled, randomised, blind, crossover design. Our protocol involved 3 testing weeks in which participants received either anodal, cathodal, or sham tDCS, in a counterbalanced order (**Figure 5.1A**). Each week included 5 consecutive daily sessions of stimulation of the same polarity (i.e., one polarity per week). There was at least 1 week break between each polarity (mean days: 9 ± 15). Participants were blind to the polarity being used in each session. Before the first testing session, participants provided informed consent and completed the Edinburgh handedness inventory (Oldfield, 1971b). Each week, we delivered the first and fifth sessions of stimulation in the MRI scanner (we will refer to these as Day1-MRI and Day5-MRI sessions respectively), where participants also performed a command following task before and after the stimulation (this resulted in 12 fMRI runs of the task per participant). We delivered the second, third, and fourth tDCS sessions in a designated cubicle (we will refer to these as Day2-Lab, Day3-Lab, and Day4-Lab sessions). We screened participants to reconfirm MRI safety before each MRI session and to comply with tDCS safety requirements before every stimulation session. After confirming safety, we set up the tDCS electrodes in the MRI control room before each MRI session, or directly in the testing cubicle before each lab session. Once we had completed the tDCS setup, we gave participants an MRI-compatible joystick (FORP-190 932, Current designs INC., PA USA) to record their responses during an fMRI motor command-following task (CF-fMRI) and to deliver the passive mobilisation. For the MRI sessions, we placed the joystick on the participant's torso and secured their right thumb to the handle using tape. The joystick was connected to the interface through an optical cable. During the lab sessions we secured the joystick on a desk while the participant was sitting on a chair. In the MRI sessions, participants completed the CF-fMRI task before and after tDCS (paired with passive mobilisations). In the lab sessions, participants only received the stimulation/mobilisations but did not have to perform the task. We used a 1200 Hz sampling frequency of x and y positions to record movements during CF-fMRI. To ensure accurate recordings, we calibrated the joystick at the start of each session.

We used a Windows 10 Desktop PC and Matlab 2017b to deliver the stimuli and record the motion tracking data. In the MRI sessions, we presented all visual stimuli via a digital system (VPixx PROPIxx) that projected the image onto a mirror fixed to the head coil, with a visual angle of ~10°. We delivered auditory cues using the SOUNDPixx MRI stereo audio system coupled with disposable noise-attenuating (about 29db+) ear tips (MRIaudio INC), and used an intercom system to communicate with participants during the scanning sessions. In the lab sessions we used an Iiyama 24'' desktop monitor and provided participants with both earplugs and 3M ear defenders (35 dB).

After all sessions, participants received a post-tDCS perceptual scale where they rated the sensations and/or discomfort they perceived and indicated whether they thought they received real stimulation or sham.

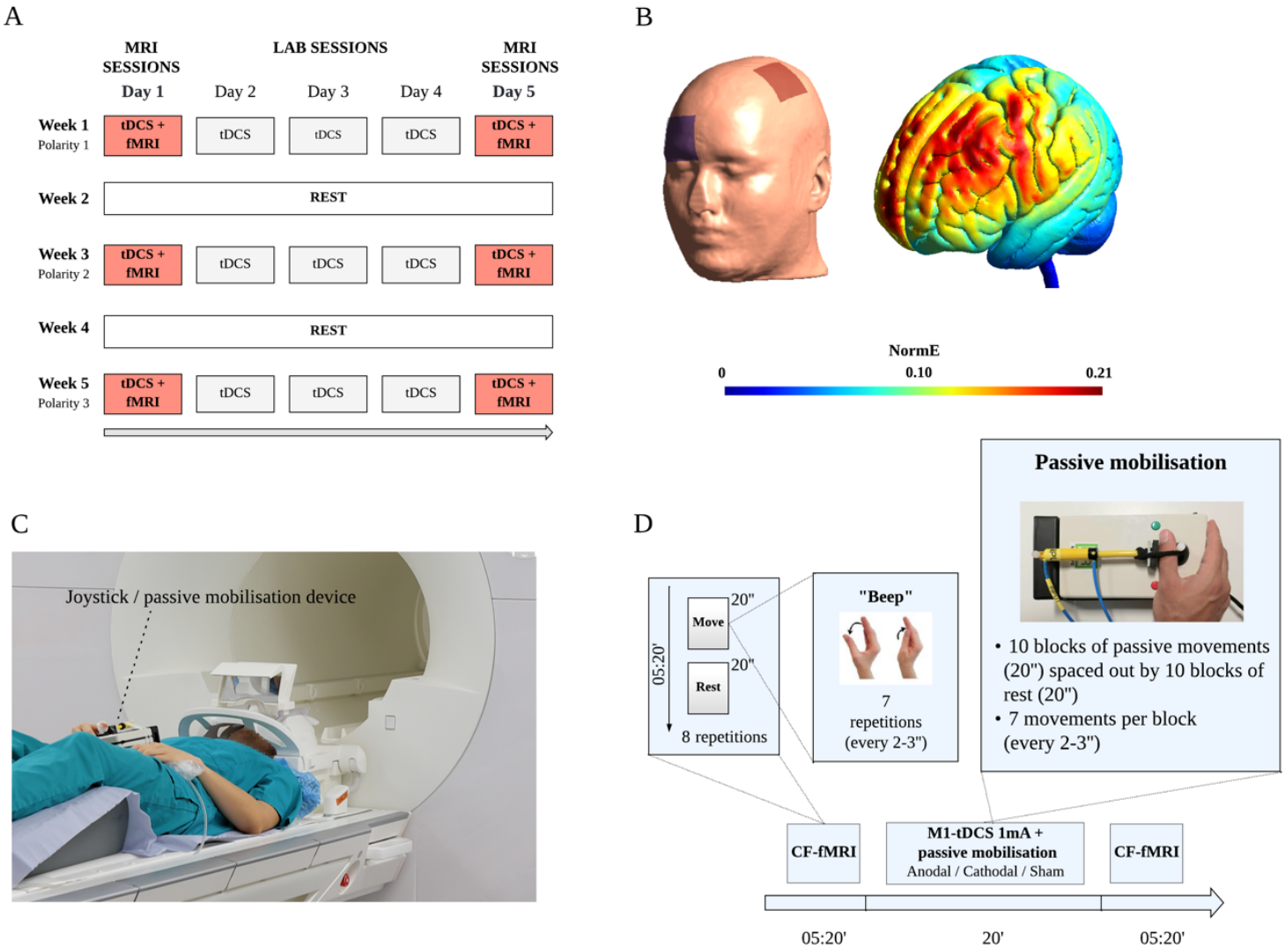


Figure 5.1. Study Design and tDCS montage. (A) Schedule of events for all participants. Note that tDCS was coupled with passive mobilisation of the thumb in all sessions. (B) tDCS montage (left) and simulation of current spread (electric field) on the MNI standard head model (right), as calculated with SimNIBS3.2.2. We placed the target electrode on C3 (M1) and the reference electrode on Fp2 for the simulation and set up the current to 1mA. Note that this simulation does not consider inter-individual differences in the position of the electrodes or the different tissue compartments across participants and therefore it should be interpreted as a rough estimate of the canonical field spread that is expected with our montage. (C) MRI setup. We recorded participant movements during the command-following (CF-fMRI) task with an MRI compatible joystick, which we also used to deliver passive mobilisation during

tDCS. (D) MRI session. Participants performed the CF-fMRI task before and after receiving 20 minutes of tDCS coupled with passive mobilisation of the thumb.

5.3.3. Electrical Stimulation

To administer the stimulation, we used a NeuroConn DC-STIMULATOR-MR for the MRI sessions and a DC-STIMULATOR for the lab sessions (neuroCare Group GmbH, Germany). We used 5x5 cm2 electrodes with a thin layer of electro-conductive Ten20® paste to increase conductivity in both MRI and lab sessions. We secured the electrodes on the scalp using self-adhesive tape. We placed the target electrode over the left M1 and the reference electrode over the right orbitofrontal area (see **Figure 5.1B** for a graphical representation of the montage and simulation of the current spread). To achieve this, we used a standard 10–20 system EEG cap to mark the position of C3 and Fp2 and place the active and reference electrodes respectively. Specifically, for anodal stimulation we placed the anode over C3 and the cathode over Fp2 and we reversed this for cathodal sessions. We used the anodal montage in half of the sham sessions, and the cathodal montage in the other half.

In the anodal and cathodal sessions, we stimulated for 20 minutes at 1mA, with 30 seconds ramp-up and 30 seconds ramp-down. Sham stimulation lasted only 30 seconds - also with 30 seconds ramp-up and 30 seconds ramp-down - to give the feeling of active stimulation, in line with well-established protocols used to ensure blinding (A. J. Woods et al., 2016a).

5.3.4. MRI acquisition

We acquired all MRI data on a Siemens MAGNETOM Prisma 3T system, with a 64-channel head coil, at the Centre for Human Brain Health (University of Birmingham). We used the following fMRI parameters: 63 slices, TR = 1620ms, TE = 35ms, matrix size = 84x84x63, voxel size = 2.5x2.5x2.5, no gap, flip angle = 71° and iPAT acceleration factor = 3. We collected 198 volumes for each run of the command-following task.

In addition to the functional scans, we also acquired a high-resolution T1-weighted MPRAGE image, used for anatomical co-registration, using the following parameters: TR = 2000ms, TE = 2.03ms, matrix size = 256x256x208, voxel size = 1x1x1mm, and flip angle = 8°.

We also collected diffusion tensor imaging data, fMRI data during stimulation, and resting state fMRI before and after the stimulation. However, we will analyse and report these in separate papers.

5.3.5. fMRI paradigm

We used the same paradigm described in (Chapter 4), whereby we instructed participants to perform a simple thumb movement (adduction-abduction), as fast as possible, in response to an auditory cue (beep) (**Figure 5.1C** and **5.1D**). Participants completed this task before and after tDCS stimulation. The use of a simple task that emulates the command following tasks typically used as part of clinical assessments, enables us to translate our methods to PDOC patients, as well as to study the effects of tDCS on the brain independently of modulations of task performance. We presented the beeps in 8 blocks of 20 seconds, for a total duration of 5 minutes and 20 seconds. Each active block started with the word “move”, and alternated with blocks in which participants were instructed to rest (cued by the word “relax”). Each active block included 7 beeps, which appeared at a variable interstimulus time, ranging from 2 to 3 seconds, to avoid prediction effects. Additionally, we instructed participants to maintain their gaze fixated on a white cross displayed in the centre of a black screen throughout the full duration of the tasks. At the beginning of each run of the task, we displayed the following written instructions: “Start moving your thumb as quickly as you can every time you hear a beep. Stay still when you hear ‘relax’. Make sure you keep looking at the fixation cross at all times”.

5.3.6. Passive mobilisation

In all sessions (MRI and Lab), we passively moved the participant's right thumb during the 20 minutes of tDCS stimulation. For this, we used a custom made system that involved a piston attached to the MRI-compatible joystick (**Figure 5.1D**) used to record participants’ responses in the CF-fMRI task. The piston was connected to an air compressor through plastic tubes. We used a Jun-Air Compressor Sj-27 placed in the MRI control room during the MRI sessions,

and a Bambi BB24 air compressor (24 litres) in the lab sessions. To open and close the airflow and move the piston, we used an electrically-operated valve, controlled with a Matlab script. In order to achieve a full range of movement (i.e., full abduction-adduction of the thumb), we secured the piston to the participant's thumb using a rubber band. This set-up was the same for both MRI and lab sessions. We delivered passive movements in blocks of 20 seconds, with 7 movements per block (with a variable time interval of 2-3 seconds), and 20 seconds rest between blocks, to emulate the timings in the command-following task. The total number of passive movements administered during the 20 minutes of stimulation was 210 (i.e., 30 blocks of passive movements and 30 blocks of rest). Importantly, we fitted participants with noise attenuating earphones both in the MRI and the lab sessions, to prevent them from hearing any noise produced by the air-compressor and piston, and being able to anticipate the passive movements as a result (see experimental procedure). Note that the scanner noise provided further masking. We also instructed participants to keep their gaze at a fixation cross throughout. Additionally, in the MRI scanner participants were laying in a supine position and could not see their thumb moving, ensuring no visual feedback.

5.3.7. fMRI preprocessing and DCM analysis of the command-following task

5.3.7.1. fMRI preprocessing

We used SPM12 on MATLAB 2015b for the preprocessing of the fMRI data and followed a standard pipeline, similar to our earlier study (Chapter 4). This included realignment, co-registration between the structural and functional scans, spatial normalisation, and smoothing with an 8mm FWHM Gaussian Kernel.

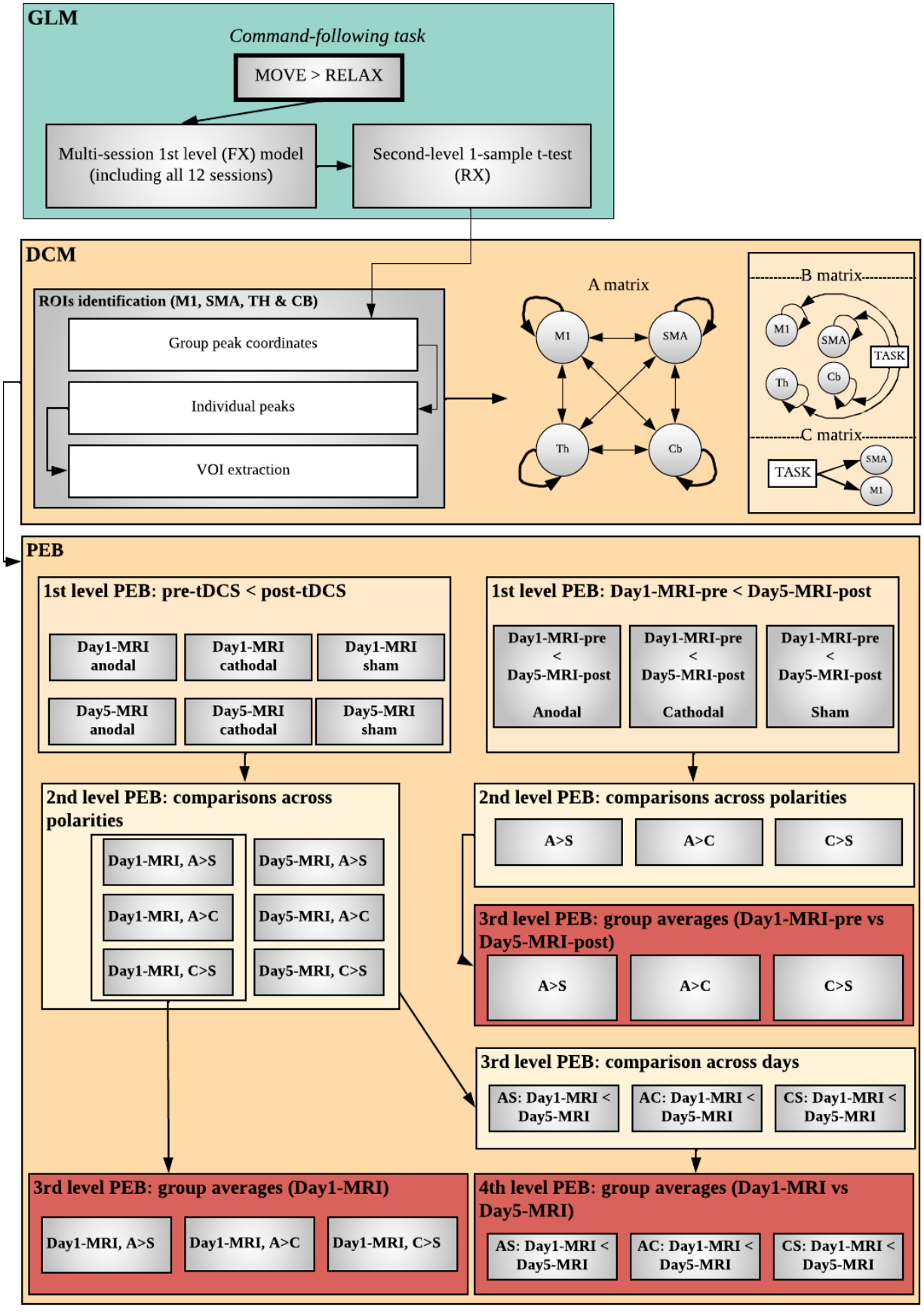

GLM
Command-following task
MOVE > RELAX
Multi-session 1st level (FX) model (including all 12 sessions)
Second-level 1-sample t-test (RX)
DCM
ROIs identification (M1, SMA, TH & CB)
Group peak coordinates
Individual peaks
VOI extraction
A matrix
M1
SMA
Th
Cb
B matrix
TASK
C matrix
PEB
1st level PEB: pre-tDCS < post-tDCS
Day1-MRI anodal
Day1-MRI cathodal
Day1-MRI sham
Day5-MRI anodal
Day5-MRI cathodal
Day5-MRI sham
1st level PEB: Day1-MRI-pre < Day5-MRI-post
Day1-MRI-pre < Day5-MRI-post Anodal
Day1-MRI-pre < Day5-MRI-post Cathodal
Day1-MRI-pre < Day5-MRI-post Sham
2nd level PEB: comparisons across polarities
Day1-MRI, A>S
Day1-MRI, A>C
Day1-MRI, C>S
Day5-MRI, A>S
Day5-MRI, A>C
Day5-MRI, C>S
2nd level PEB: comparisons across polarities
A>S
A>C
C>S
3rd level PEB: group averages (Day1-MRI-pre vs Day5-MRI-post)
A>S
A>C
C>S
3rd level PEB: comparison across days
AS: Day1-MRI < Day5-MRI
AC: Day1-MRI < Day5-MRI
CS: Day1-MRI < Day5-MRI
3rd level PEB: group averages (Day1-MRI)
Day1-MRI, A>S
Day1-MRI, A>C
Day1-MRI, C>S
4th level PEB: group averages (Day1-MRI vs Day5-MRI)
AS: Day1-MRI < Day5-MRI
AC: Day1-MRI < Day5-MRI
CS: Day1-MRI < Day5-MRI

Figure 5.2. Analysis pipeline. We followed a standard pre-processing protocol (not displayed), followed by general linear model analyses to obtain single-subject and group activation across all runs (GLM - panel). We then built and estimated DCMs for each participant and run (see DCM panel for a description of our model space). Finally, we used Parametric Empirical Bayes (PEB) to test group differences in effective connectivity (PEB panel). Abbreviations: GLM, general linear model; DCM, dynamic causal modelling; FX, fixed-effects; M1, primary motor cortex; SMA, supplementary motor area; TH, thalamus; CB, cerebellum; VOI, volume of interest; PEB, parametric empirical bayes; AS, anodal greater than sham; AC, anodal greater than cathodal; CS, cathodal greater than sham; A, anodal; C, cathodal; S, sham.

5.3.7.2. Region selection and time series extraction

DCM uses Bayesian modelling to infer effective connectivity among brain areas from measured brain activity (Zeidman, Jafarian, Corbin, et al., 2019c); that is, given a specific network architecture, DCM models how information propagates through different regions to produce the observed data (Kahan & Foltynie, 2013). We followed a similar pipeline to our previous study (Chapter 4): First, we identified the canonical pattern of activity on our command-following task at the group level (Figure 2, green box). To this end, we first built a multi-session 1st-level fixed-effects (FX) model for each individual subject, including all 12 command-following task runs (pre and post stimulation x Day-1/5 sessions x 3 testing weeks) and modelling the contrast corresponding to the move vs rest blocks across sessions (non-weighted average). Then, we performed a second-level random-effects (RX) 1-sample t-test on the individual contrasts to assess the group effects. In the resulting map, we identified the group peak of activation for the following motor regions of interest (ROI) obtained from the AAL atlas: left precentral gyrus (M1), left supplementary motor area (SMA), left thalamus (TH), and right cerebellar lobes IV-V and VIII (CB). We thresholded results using a family-wise error (FWE) corrected $p<0.05$ (see coordinates in bold in Table 1). The resulting group-derived coordinates then acted as a starting point for identifying, in each individual run, the nearest local maxima. We constrained the search of the individual peaks within a sphere centred on the group peak and with a size of 13 mm radius for the left SMA, M1 and right cerebellum, and 7mm for the left thalamus. The difference in the allowed distance from the group coordinates accommodated for the differences in the regions' anatomical sizes. Individual peaks had to

exceed a liberal statistical threshold of uncorrected p<0.05 (Zeidman, Jafarian, Corbin, et al., 2019c). When no peak was found for a specific run at p<0.05, we iteratively relaxed the threshold in 0.05 increments until reaching p = 0.25. When no peak could be found at this threshold, we used the group coordinates instead (Zeidman, Jafarian, Seghier, et al., 2019). It is important to mention that we only used these thresholds to identify the individual peak coordinates used for the feature selection (i.e., the extraction of the time series) but not for any statistical analyses. Once we identified the individual peak coordinates for each run, we extracted time series from 4mm radius spherical volumes of interest centred on them.

5.3.7.3. Individual level DCM specification and definition of model space

After the extraction of the time series, we specified dynamic causal models (**Figure 5.2**, DCM panel) at the individual level with a deterministic model for BOLD signal and the following parameters: one state per region, bilinear modulatory effects, and mean-centred inputs. DCM requires the specification of 3 matrices modelling the connectivity within- and between-regions (A matrix), the modulations of effective connectivity due to experimental conditions (B matrix), and driving inputs (C matrix), which briefly 'ping' specific regions in the system at the onset of each block (Zeidman, Jafarian, Corbin, et al., 2019c).

We defined our model space using the same parameters to those in our earlier study (Chapter 4): a fully connected A matrix (i.e., a model in which all self- and between region connections are switched on) including left M1, left SMA, left thalamus and right cerebellum, a B matrix including the effect of the motor task as modulatory input on all self-connections, and a C matrix modelling driving inputs to cortical regions only (M1 and SMA).

5.3.7.4. tDCS effects on effective connectivity

With the above DCMs, we employed Parametric Empirical Bayes (PEB) to remove the parameters that were not contributing to the model evidence, and to evaluate group effects and between subject variability (Zeidman, Jafarian, Seghier, et al., 2019). In order to test the effects of tDCS combined with passive mobilisation on the connections in our model, we ran three

separate hierarchical PEB analyses (Zeidman, Jafarian, Seghier, et al., 2019), starting from the 12 neural models (DCMs) estimated per participant (i.e., one per CF-fMRI run).

(1) To assess the effects of a single tDCS session, we first built 3 *within-subject* PEBs (1st-level) per participant encoding the differences between pre- and post- stimulation (pre-tDCS < post-tDCS) for each polarity on the first MRI session. We then entered these into 3 *within-subject* PEBs (2nd level) for each participant that encoded comparisons between polarities (Anodal > Sham, Anodal > Cathodal, Cathodal > Sham) on the differences between pre- and post tDCS. Finally, we specified 3 group (*between-subject*) PEBs encoding the commonalities across participants for each 2nd-level PEB, and included sex, age, and handedness score as regressors of non-interest (3rd level). The 3 final PEBs therefore encode increases (i.e., pre-tDCS<post-tDCS) in effective connectivity that are greater after anodal tDCS as compared to sham (i.e., anodal > sham), after anodal tDCS as compared to cathodal tDCS, or after cathodal tDCS as compared to sham respectively.

(2) To assess the cumulative effects of 5 tDCS sessions, we replicated the above steps by encoding the differences between the pre-tDCS run in Day1-MRI and the post-tDCS run in Day5-MRI for the 1st level of the hierarchy 2nd and 3rd level PEBs were as above.

(3) Finally, to establish whether the responsiveness to tDCS increases after multiple sessions, we replicated the 1st and 2nd level steps in (1) above for the data on Day5-MRI. Then created a further *within-subject* PEB modelling the differences between sessions (Day1 < Day5) for each individual participant (3rd level). Finally, a between subjects PEB modelled group effects (mean across participants), and included sex, age, and handedness score as regressors of no interest (4th level).

Finally, we used Bayesian Inference to invert the model for each subject and obtain an estimate of the parameters that best explain the data, while minimising complexity. First, we applied Bayesian Model Reduction (BMR) on the final 3 PEBs above (i.e., those encoding group commonalities), to reduce connections that were not adding to the model evidence. Finally, we

used Bayesian Model Average (BMA) to estimate the average parameters across participants for each connection that remained switched on. We used a threshold of a posterior probability > 95%, as we have previously done (Chapter 4).

In addition, to assess the stability of our parameters across sessions, we created 3 PEBS modelling the average across sessions on the baseline pre-tDCS run on Day 1 for each polarity (i.e., run unaffected by any stimulation or passive mobilisation) and used BMR and BMA to estimate parameters as above.

5.3.8. Motion tracking

We analysed the motion data for the CF-fMRI task with a custom MATLAB 2017b script, as we did in our previous study (Chapter 4). We first low-pass filtered the data at 15Hz and calculated the Euclidean distance of the x-y position. To identify the onset and the end of each movement in the arrays containing our motion tracking data, we used the MATLAB function *findchangepts*, which can detect abrupt signal changes given a vector x with N elements and returns the index at which the mean of x changed most significantly. When more than two changes were identified, we used the first and last ones to determine the beginning and end of the movement. We excluded movements where no change was detected, which was usually due to participants not responding to that specific stimulus (on average we removed <1 movement per session, maximum of 12). For each movement we calculated velocity and acceleration at each timepoint, and then derived the mean velocity and peak acceleration. We then averaged those session means to give the mean velocity and peak acceleration for the whole run. We also derived reaction times, defined as the time interval between the auditory stimulus and onset of the movement, identified as per above.

We calculated the means of those values across each subject/run and excluded measurement errors, defined as values with a z-score > 3.0, that were present due to the joystick being incorrectly calibrated. Out of 264 runs (per analysis), we removed 14 from the reaction times analysis, 1 from the mean velocity analysis and 36 from the peak acceleration analysis. Finally, for each of the three metrics (i.e., reaction time, mean velocity and peak acceleration) we

computed three Bayesian repeated measures ANOVAs on JASP, v. 0.16.3 (JASP Team, 2020) to emulate the DCM analyses above:

(1) A Polarity (anodal, cathodal and sham) x Time (pre- vs post-tDCS) ANOVA on the data from Day1-MRI tested the effects of a single tDCS session.
(2) A Polarity x Multiple session time (Day1-MRI pre-tDCS vs Day5-MRI post-tDCS) ANOVA tested the effects of 5 sessions.
(3) Polarity x Time x Day (Day1-MRI vs Day5-MRI) ANOVA tested whether within-session responsiveness to tDCS is affected by the number of sessions.

For each ANOVA, we calculated the evidence in the data for including the interaction (e.g., polarity x time) as a predictor (BF_{incl}); that is, whether the models including the interaction explain the data significantly better than those without it (van den Bergh et al., 2020). We interpreted $BF_{incl} > 3$ as substantial evidence in the data for including the interaction, $BF_{incl} > 10$ as strong evidence, and $BF_{incl} > 100$ as very strong evidence, as per standard guidelines on interpreting Bayes factors (Schönbrodt & Wagenmakers, 2018). Importantly, for $BF_{incl} < 3$, we reported the exclusion Bayes factor (BF_{excl}) instead, which quantifies the opposite effect (the evidence for models excluding the interaction as compared to those including it).

5.3.9. Blinding

To test the success of our blinding protocol, we used McNemar's test on participants' responses as to whether they believed they had / had not received real tDCS on days 1 and 5 (MRI sessions).

5.4. Results

5.4.1. Task activation across sessions

The RFX second-level analysis of brain activation during the active movements to command across sessions showed statistically significant clusters (FWE-corrected $p<0.05$) in all of four ROIs considered in our analyses (see **Table 5.1** and **Figure 5.3**).

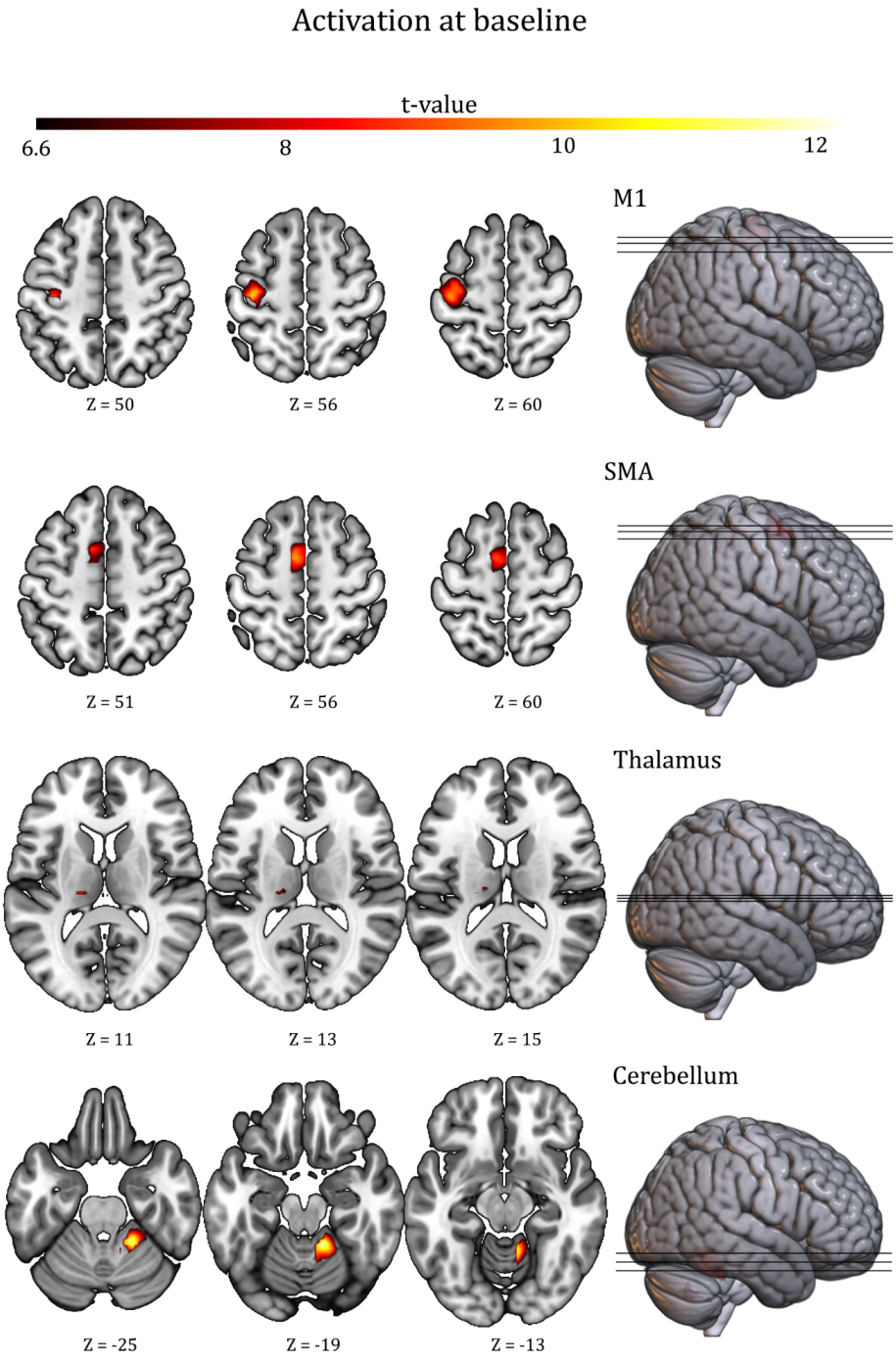


Figure 5.3. Activation at baseline. Brain activation at the group level (RFX, 1-sample t-test) for the command-following task. The general linear model included differences between 'move' and 'rest' blocks on a multi-session 1st level (FFX) model for each subject - using all 12 MRI runs. The activation maps are shown at $p<0.05$ FWE-corrected for M1, SMA, cerebellum and thalamus ROIs, and rendered

on a standard template (152 template in MRIcroGL). Z indicates the Montreal Neurological Institute z coordinate.

Table 5.1: *Canonical activation during command-following.*

Region	**Cluster P**	**Cluster size**	**Peak P**		**F**	**MNI coordinates**
	FWE-corrected	*in mm3*	*Peak FWE-corrected*	*uncorrected*		*[x;y;z]*
Cerebellum	<0.001	3969	<0.001	<0.001	11.871	**[12;-46;-19]**
			<0.001	<0.001	11.337	[9;-52;-13]
	<0.001	729	<0.001	<0.001	9.465	[12;-58;-43]
	<0.001	162	0.005	<0.001	7.399	[27;-49;-46]
M1	<0.001	5697	<0.001	<0.001	10.570	**[-36;-19;56]**
			<0.001	<0.001	9.695	[-27;-19;74]
			<0.001	<0.001	9.174	[-33;-13;65]
	0.026	27	0.008	<0.001	7.126	[-42;-1;20]
SMA	<0.001	3834	<0.001	<0.001	9.812	**[-6;-1;56]**

			0.004	<0.001	7.450	[-9;8;44]
Thalamus	0.002	297	<0.001	<0.001	9.506	**[-18;-22;11]**

Results from the random effect group analyses (RFX, 1-sample t-test) for the command-following task, including all 12 MRI sessions per participant. Results survived a threshold of FWE-corrected $p < 0.05$. We used the peak coordinates for each region (highlighted in bold) as a starting point to extract the time series for the DCM analyses. Abbreviations: FWE, family wise error; M1, primary motor cortex; SMA, supplementary motor area.

5.4.2. Effects of M1-tDCS on motor-network dynamics

5.4.2.1. Effects of one M1-tDCS session (Day1-MRI)

A single anodal M1-tDCS session (**Figure 5.5**, panel A) increased excitation from M1 to SMA, when compared to both cathodal- and sham-tDCS, and from thalamus to M1 as compared to cathodal tDCS only. Additionally, when compared to sham only, anodal tDCS decreased M1 self-inhibition as well as excitation from SMA to thalamus. In turn, a single session of cathodal tDCS, increased cerebellar self-inhibition, when compared to both anodal and sham, and thalamic self-inhibition when compared to sham only. Both anodal and cathodal tDCS increased excitation from SMA to M1 and inhibition from cerebellum to M1, although these changes were more pronounced for cathodal and anodal tDCS respectively. Similarly, both polarities increased inhibition from thalamus to SMA and cerebellum, as well as from cerebellum to SMA, with no differences between polarities in this case. In terms of task modulations on each self-connection (matrix B), we found no significant effects for any polarity. See **Figure 1, Appendix C** for baseline (pre-tDCS) connectivity values.

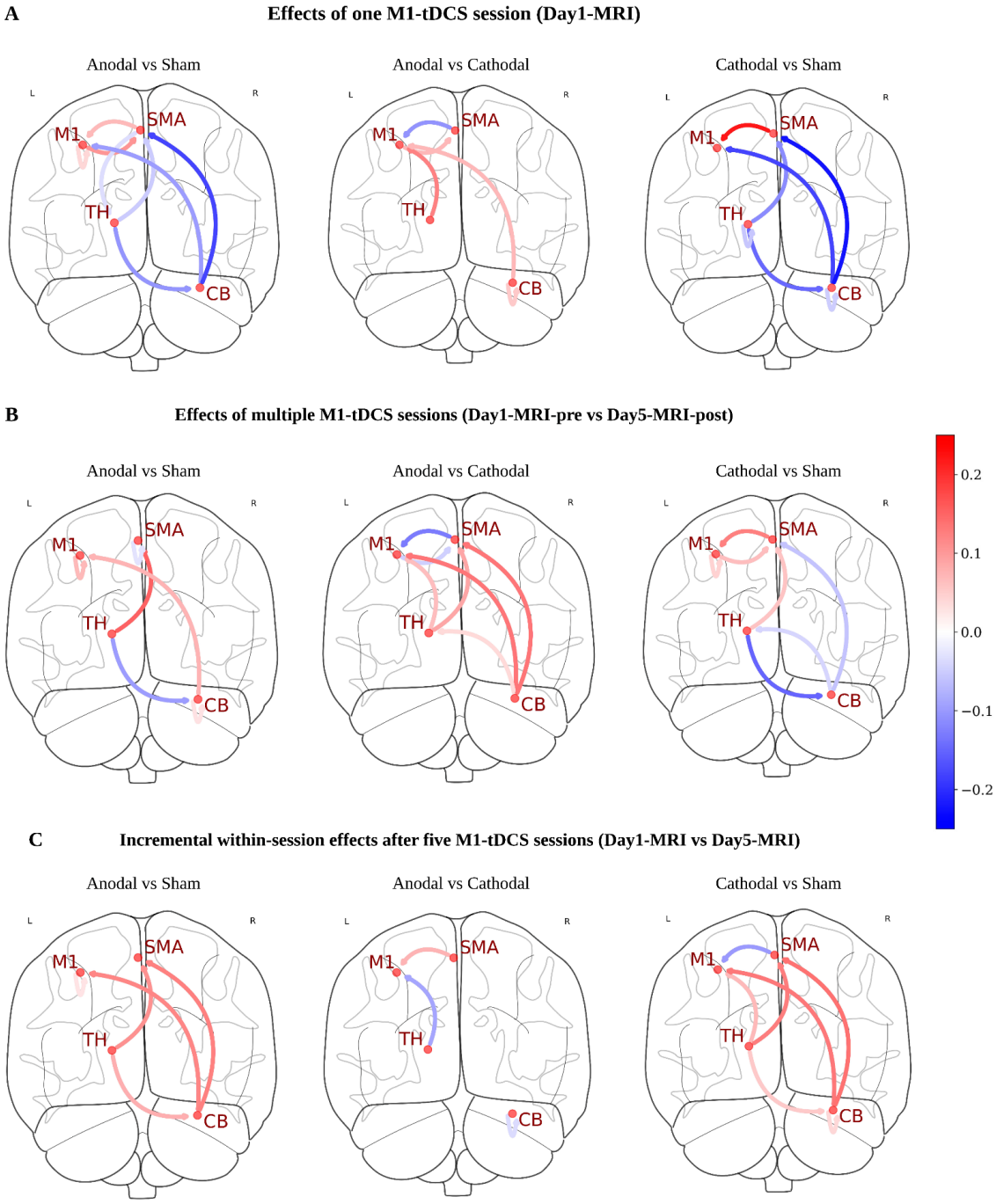


Figure 5.4. Effects of M1-tDCS on neural dynamics. Results from our Parametric Empirical Bayes (PEB) analyses on Day1-MRI (A), Day1-MRI-pre vs Day5-MRI-post (B) and pre- vs post- on Day1-MRI vs Day5-MRI (C). Blue lines indicate decreases and red lines indicate increases in connectivity strength. Notice that we converted self-connections from their original unitless log-scale values to Hertz and added 0.5 to obtain the direction and magnitude of the self-connectivity change and display it in a way that is comparable with between region connections.

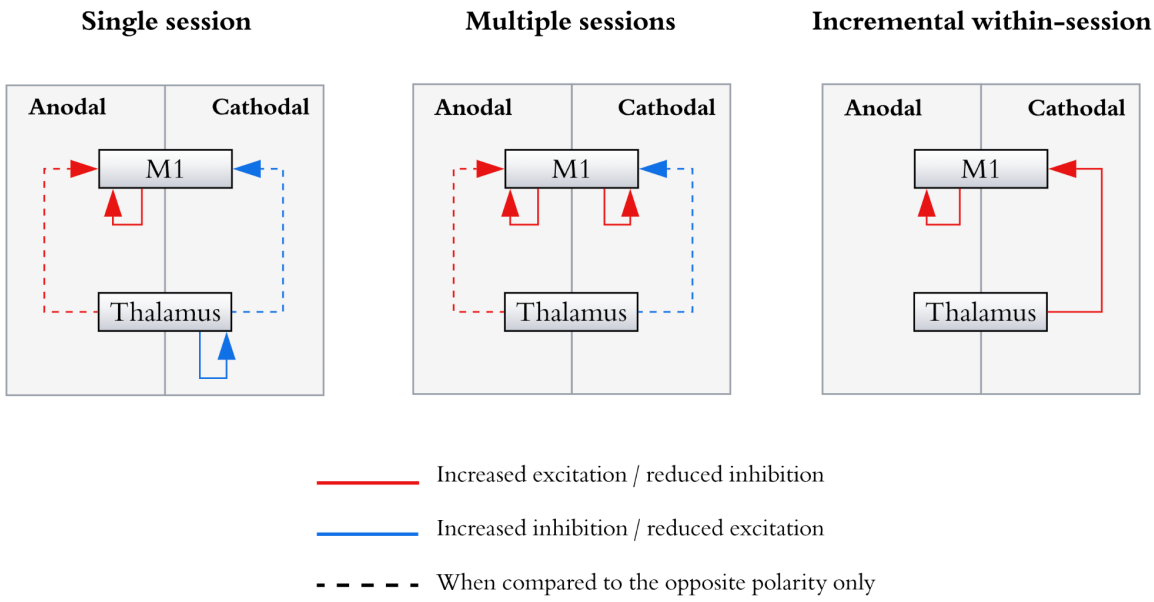


Figure 5.5. Effects of M1-tDCS on thalamo-M1 coupling. Summary results for the thalamus-M1 complex after 1 session (left), 5 sessions (middle), and when comparing within-session changes between day 1 and day 5 (right). Dashed lines represent effects that were only significant in the comparison between polarities (but not when the polarity was compared to sham).

5.4.2.2. Effects of multiple M1-tDCS sessions (Day1-MRI-pre vs Day5-MRI-post)

After 5 sessions, anodal tDCS increased excitation f$rom thalamus to M1 when compared to cathodal tDCS only. It also increased self-inhibition in SMA and reduced self-inhibition in the cerebellum as compared to sham only. Finally, it increased excitation from cerebellum to M1 when compared to both cathodal and sham. Both anodal- and cathodal tDCS increased excitation from thalamus to SMA, although this was significantly stronger for anodal stimulation. Similarly, both polarities reduced M1 self-inhibition and excitation from thalamus to cerebellum compared to sham, with no significant difference between polarities.

In turn, cathodal tDCS increased excitation between M1 and SMA (in both directions) and inhibition from cerebellum to thalamus and SMA, both as compared to anodal tDCS and sham. As above, we found no significant effects in task modulations for either polarity.

5.4.2.3. Incremental within-session effects after five M1-tDCS sessions (Day1-MRI vs Day5-MRI)

Compared to the first session, the fifth session of anodal M1-tDCS (**Figure 5.5**, panel B) reduced M1 self-inhibition as compared to sham only. In addition, both polarities increased excitation from thalamus to SMA and from cerebellum to M1, and reduced inhibition from thalamus to cerebellum and cerebellum to SMA, with no differences across polarities. In turn, the fifth session of cathodal tDCS reduced thalamo-M1 inhibition, and decreased cerebellar self-inhibition and excitation from SMA to M1. All of these were polarity specific, i.e., significant both when compared to anodal tDCS and sham. As above, we found no significant effects in task modulations for either polarity.

5.4.3. Effects of M1-tDCS on behavioural metrics

We found substantial evidence in support of the lack of an interaction ($BF_{excl} > 3$), for reaction times and mean velocity on Day1-MRI and Day1-MRI pre vs Day5-MRI post, as well as for peak acceleration on Day1-MRI only. In addition, we found anecdotal evidence (i.e., $BF_{excl} = 1$-3) for the lack of an interaction on mean velocity for Day1-MRI vs Day5-MRI and peak acceleration for the comparisons Day1-MRI pre vs Day5-MRI post and Day1-MRI vs Day5-MRI. We report means and standard deviations for each condition in **Table 1, Appendix C**, along with the BF_{excl} values and their respective prior and posterior inclusion probability, for all ANOVAS performed. Single-subject values are in **Figure 2, Appendix C**.

5.4.4. Efficacy of blinding protocol

We found no significant differences in the number of times that participants perceived sham and anodal/cathodal stimulation as real stimulation for either Day1-MRI (χ^2=9, p=0.82) or Day1-MRI (χ^2=11, p=0.20).

5.5. Discussion

This study focused on characterising the effects of tDCS paired with passive mobilisation on thalamo-cortical coupling during a motor command-following task; a circuit with an established mechanistic role in the behavioural responsiveness in PDOC (Fernandez-Espejo et al., 2015.). We have previously shown that one anodal M1-tDCS session administered at rest can reduce thalamic self-inhibition during command-following. However, against prediction, these changes were not followed by increased excitation towards M1 (Chapter 4). Here, we demonstrated that, when paired with passive mobilisation, one session of anodal M1-tDCS can indeed increase thalamus to M1 excitation, (and reduce M1 self-inhibition as a result), during the same command following task. This suggests that pairing passive mobilisation with stimulation could have greater therapeutic effects in PDOC, particularly in those patients whose diminished responsiveness is linked to reduced thalamo-cortical connectivity (Fernandez-Espejo et al., 2015; Stafford et al., 2019b). We have previously shown that both an excitatory engagement of the thalamus and thalamus to M1 coupling are necessary for the execution of voluntary motor responses to command in PDOC (Fernandez-Espejo et al., 2015). It is also well known that damage to the thalamus and / or its cortical projections are common in PDOC, and that these abnormalities correlate with the level of reduced responsiveness in these patients (Fernandez-Espejo et al., 2011, 2015; Schiff, 2010; Stafford et al., 2019b). As individual patterns of damage are highly heterogeneous across PDOC patients, one could speculate that, depending on whether the primary damage affects mostly the thalamus or its connections to M1, different patients may benefit most from stimulation being delivered at rest (as discussed inChapter 2) or combined with passive mobilisation (as reported here) respectively. Further studies in PDOC patients themselves are required to ascertain this.

Leaving implications for clinical improvements aside momentarily, our previous study (Chapter 4) revealed unexpected effects after one session of cathodal M1-tDCS, which, against predictions, led to an increase in excitation from thalamus to M1. We attributed this to a compensatory mechanism to overcome the strong inhibition in M1 that followed this polarity and keep performance at a baseline level. In contrast, here we found that anodal and cathodal stimulation showed opposing effects over this connection (i.e., excitatory for anodal and inhibitory for cathodal), in line with our predictions and existing literature. Pairing tDCS with a relevant task is indeed regarded as best practice (Pruski & Cantarero, 2020). In fact, there is much evidence that the effect of tDCS is greatly dependent on the neural state during stimulation, and that using a task that engages the relevant neural circuit can increase the spatial precision of tDCS on the target networks (Li et al., 2019). This can be of even greater importance in patients like those in PDOC, where gross brain abnormalities interfere with an accurate identification of the targets at the scalp level (Chapter 2). Despite this, to our knowledge, all previous tDCS studies in PDOC administered the stimulation at rest (Chapter 2). While this is unsurprising, due to the patients' inability to engage in an active task, we here provide an alternative passive task (for protocols targeting motor areas) that is suitable in this cohort.

Importantly, we know that multiple sessions of tDCS can lead to more robust clinical improvements in PDOC (see Chapter 2 for a review). This is indeed a well-documented phenomenon in therapeutic tDCS applications across clinical conditions(Fregni et al., 2021). Our study offers a window into the neural underpinnings of the cumulative effects of multi-session tDCS, and revealed a somewhat complex picture, particularly for cathodal stimulation. First, after 5 tDCS sessions, anodal stimulation continued to increase thalamus to M1 excitation and to decrease M1 inhibition as compared to baseline. Similarly, cathodal tDCS decreased thalamus to M1 excitation both after 1 and 5 sessions (although significantly less so after 5). However, after 5 sessions, cathodal tDCS also decreased M1 inhibition, and did so at a similar level to anodal tDCS. Moreover, after 5 sessions, cathodal tDCS lost the influence on increasing thalamic self-inhibition that it had after 1. Crucially, the baseline (pre-tDCS) connectivity within and between these two regions was very stable across polarity sessions (see **Figure S5.1**). There were other effects outside these key areas of interest (thalamus, M1 and their connection) that only became apparent or changed tone after 5 sessions of either polarity.

For example, the thalamus changed from inhibiting SMA after one session of either anodal or cathodal tDCS to exciting it after 5 sessions of either polarity. In turn, 5 sessions of anodal tDCS were required to reduce cerebellar self-inhibition, while the effects of cathodal tDCS over the cerebellum in session 1 disappeared after 5 sessions. Looking at the baseline connectivity, it becomes clear that the existing neural state modulates the effect of each polarity to bring the network to an optimal level that maintains behavioural performance. Overall, our results suggest that future research should not necessarily expect opposing effects for the two polarities across the network of interest, nor linear, incremental effects after multiple sessions. The comparison of within-session effects sheds further light into this (**Figure 5**, panel C). For example, anodal tDCS had had a stronger effect on decreasing M1 self-inhibition on the fifth session as compared to the first, suggesting a potentiation of the events (rather than a simple accumulation). In contrast, the increased excitation from thalamus to M1 related to this polarity did not exhibit significant within-session differences (i.e., it was similar in sessions 1 and 5). Finally, the inhibitory effect of cathodal tDCS over this connection was smaller in the fifth session as compared to the first.

Most of our knowledge about tDCS comes from studies focusing on local effects over M1, and much less is understood about how the modulations propagate across other regions in the motor network. It is thus not surprising that the local changes on self-inhibition we identified here are consistent with prior literature, while long-range changes appeared more complex. There is now substantial evidence that anodal tDCS over M1 increases cortical excitability (Horvath et al., 2015; Yamaguchi et al., 2020), and this modulation of neural activity is associated with changes in synaptic plasticity (Monte-Silva et al., 2013b), including early- (e-LTP) and late long-term potentiation (l-LTP) when an appropriate task is used. Crucially, l-LTP requires repeated sessions of stimulation and can lead to structural plasticity that may contribute to more robust tDCS aftereffects (Lu et al., 2019). Furthermore, both anodal and cathodal tDCS have a similar impact on synaptic plasticity (Lu et al., 2019), consistent with our changes after 5 sessions showing reduced M1 self-inhibition for both polarities (albeit stronger for anodal). While it is possible that e-LTP and l-LTP may be one of the mechanisms explaining the local effects on M1 in our current study, especially as we did not find an effect of anodal tDCS on M1 self-connectivity when delivering tDCS at rest in our previous study (Chapter 4), the relationship between synaptic mechanisms and effective connectivity metrics is not well

understood. In fact, DCM does not model the activity of individual neurons, which are characterised by fast dynamics, but slower dynamics - in the scale of seconds - that arise from the synergy of several neuronal populations instead (Zeidman, Jafarian, Corbin, et al., 2019c). Therefore, the comparison between DCM results and neuronal models is not straightforward. Within the DCM framework, a reduction in self-inhibition reflects a lowered rate of decay of neuronal activity, which in turn indicates increased susceptibility to afferent inputs into that region (Zeidman, Jafarian, Corbin, et al., 2019c). In our case, the reported reduction in M1 self-inhibition would make M1 more sensitive to the other nodes in the network (including the excitation coming from thalamus). This way, even when the increase in excitation from thalamus to M1 seemed to be maintained (rather than enhanced) across the sessions, the enhanced responsiveness in M1 to this thalamic excitation after 5 sessions would predict a stronger clinical effect. Importantly, within our network, M1 represents the final motor output for the control of muscles, due to its projections to the spinal cord (Harrison & Murphy, 2013). As such, increasing M1 excitability via a combination of reduced M1 self-inhibition and increased thalamo-M1 excitation might successfully facilitate the initiation of movements in those PDOC patients where the cortico-thalamic tracts are partially spared.

It is worth highlighting here that we designed our command-following task to emulate those used in clinical settings to evaluate residual awareness in PDOC (Fernandez-Espejo & Owen, 2013) and, as a result, our task is insensitive to tDCS-related modulations of behaviour in healthy participants. Indeed, consistently with our previous study (Chapter 4), we found no effect of tDCS on behavioural measures in our cohort. Therefore, further studies in PDOC are required to confirm whether the neural effects reported here indeed translate into clinically meaningful changes in patients. If successful, an increase in thalamo-cortical excitation in PDOC could improve patients' behavioural responsiveness and impact their quality of life by facilitating engagement with rehabilitation as a result (Elliott & Walker, 2005). Additionally, an improvement in responsiveness would also decrease misdiagnosis levels, especially in those patients with CMD, by uncovering patients' real level of awareness.

5.6. Conclusions

Overall, we showed that anodal tDCS coupled with passive mobilisation of the thumb has short- and long-range effects on motor-network dynamics during command-following. Specifically, it can reduce M1 self-inhibition and increase excitation from thalamus to M1. These effects are enhanced after 5 sessions of stimulation. While we tested our protocol on healthy participants, we designed it to be easily integrated into PDOC care as part of routine physical therapy.

Note that the appendix to this chapter can be found at the end of the thesis (Appendix C).

Chapter 6

EXPLORING THE RELATIONSHIP BETWEEN ELECTRIC FIELD CHARACTERISTICS AND TDCS-INDUCED CONNECTIVITY CHANGES IN THE MOTOR NETWORK

6.1. Introduction

I have discussed in Chapter 1 and Chapter 3 that the great variability in the outcomes of studies investigating tDCS in PDOC is linked to multiple factors, among which the high heterogeneity of PDOC patients' brain abnormalities. The inter-individual differences in brain lesions and atrophies severely limits the precision of manual electrode placements, reduces the amount of current reaching brain areas and impacts current direction, significantly limiting the reproducibility of tDCS studies (Nasimova & Huang, 2022). I have argued that, considering the uncertainty related to which brain areas are being reached by the current - a problem that is certainly exacerbated by the overall lack of spatial specificity of tDCS - it becomes rather challenging to associate any observed effect of the stimulation to the region being targeted (Chapter 2).

One feasible approach to address the above issue is the utilisation of individualised finite element models (FEM), derived from MRI scans, to predict tDCS-induced current flows (Albizu et al., 2020; Nasimova & Huang, 2022). These have been made possible by recent improvements in tissue segmentation algorithms and the development of open-source software with automated modelling pipelines, such as SimNIBS (Windhoff et al., 2013) and ROAST (Y. Huang et al., 2018, 2019).

Briefly, these automated pipelines start from individual MRI images of a human head, which are segmented into different tissues. Virtual tDCS electrodes are then placed on the segmented mask, which is then tessellated into a mesh and a FEM is solved in order to estimate the electric field intensity and direction (Y. Huang et al., 2018, 2019).

Interestingly, the accuracy of computational models of TES has been recently confirmed by MRI electrical impedance tomography (Kasinadhuni, 2017; Opitz et al., 2018) and intracranial recordings (Göksu et al., 2018; Y. Huang et al., 2017), hence proving their reliability.

As pointed out by (Albizu et al., 2020), electric field distribution in computationally-derived tES models show great variability across individuals, in line with the variability observed in the outcomes of tDCS studies. Previous studies used tES computational models to compute the electric field in specific ROIs, and correlate electric field models-derived measures (e.g., median electric field intensity in a specific ROI or current direction) with different clinical outcomes (for a review see (Indahlastari et al., 2021; Nasimova & Huang, 2022)). Some studies also used tES models to calculate the dose of the stimulation or optimise its montage ((Indahlastari et al., 2021; Nasimova & Huang, 2022). Measures derived from tES computational models have also been used to predict tDCS-induced changes in fMRI data. For example, (Halko et al., 2011) found a positive correlation ($r = 0.308$) between maximum electric field intensity in the occipital cortex and fMRI BOLD activation related to a visual motion perception task in the occipital lobe, in a stroke patient. Using a similar approach, but focusing on fMRI functional connectivity rather than brain activation, (Indahlastari et al., 2021) found that the amount of current within the left DLPFC ROI positively correlated with functional connectivity changes between the left DLPFC and the left ventrolateral prefrontal cortex (VLPFC) ROIs, in a task performed pre and after tDCS, which targeted working-memory (i.e., an fMRI N-Back task, as published in (Nissim et al., 2019)). The authors did not find the same correlation for the N-Back task in the sham condition. Another study from the same research group applied supervised machine-learning to the same fMRI N-Back dataset, to predict treatment response from electric field intensity and direction, as quantified by tES computational models (Albizu et al., 2020). The authors were able to predict tDCS treatment response with 86% accuracy. Lastly, a study by (Antonenko et al., 2019) investigated the relationship between tDCS-induced changes in rs-fMRI measures and electric field measures derived from tES computational models. The authors found a positive correlation between electric field measures and sensorimotor network connectivity strength as measured with an ICA-based approach.

Overall, these studies indicate that MRI-derived electric field models might have a great prognostic value, and, on the basis of this, could represent an important tool to maximise tDCS

effects in PDOC patients. In fact, precise tES computational models incorporating patients' tissue abnormalities and atrophies could help shed light on the great variability observed in tDCS responsiveness in this clinical group and guide the choice of montage to maximise tDCS effectiveness, as I have previously argued (Chapter 2).

In my previous neuroimaging studies on healthy subjects (Chapter 4, Chapter 5), I targeted thalamo-cortical connectivity and demonstrated that tDCS can alter effective connectivity within the motor network during command-following, which is disrupted in PDOC patients.

Here, I pooled the data from the three experiments (Chapter 4 and Chapter 5), and used MRI-derived electric-field models to investigate inter-individual variability in effective connectivity changes following tDCS. I focused on current density computed from MRI-derived E-field models, as this measure was successfully used in the past to classify responders to tDCS (Albizu et al., 2020) and predict functional connectivity changes following tDCS (Indahlastari et al., 2021).

I restricted the analyses of the electric fields characteristics to three motor network areas, and focused on changes in thalamo-cortical effective connectivity following one session of anodal-M1-tDCS administered at rest (*Experiment 1*), one session of cathodal-cerebellar-tDCS administered at rest (*Experiment 2*), and single and multiple sessions of anodal-M1-tDCS administered during passive mobilisation (*Experiment 3*).

6.2. Methods

Structural MRI imaging and effective-connectivity data used in the analyses of the current chapter were sourced from the fMRI-tDCS experiments discussed in Chapter 3 (*Experiment 1* and *Experiment 2*) and Chapter 4 (*Experiment 3*). The main steps of the analysis are summarised in **Figure 6.1**. Detailed information about participant recruitment and demographics, screening for MRI and tDCS safety, MRI acquisition and fMRI paradigm, passive mobilisation (*Experiment 3* only) and tDCS set-ups can be found in the two above mentioned chapters. As the analyses in the current chapter focus on MRI-derived current density models and effective connectivity changes following tDCS, I will briefly highlight the

differences among the three studies in terms of MRI acquisition, fMRI preprocessing and PEB comparisons, which were also summarised in **Table 3.1**.

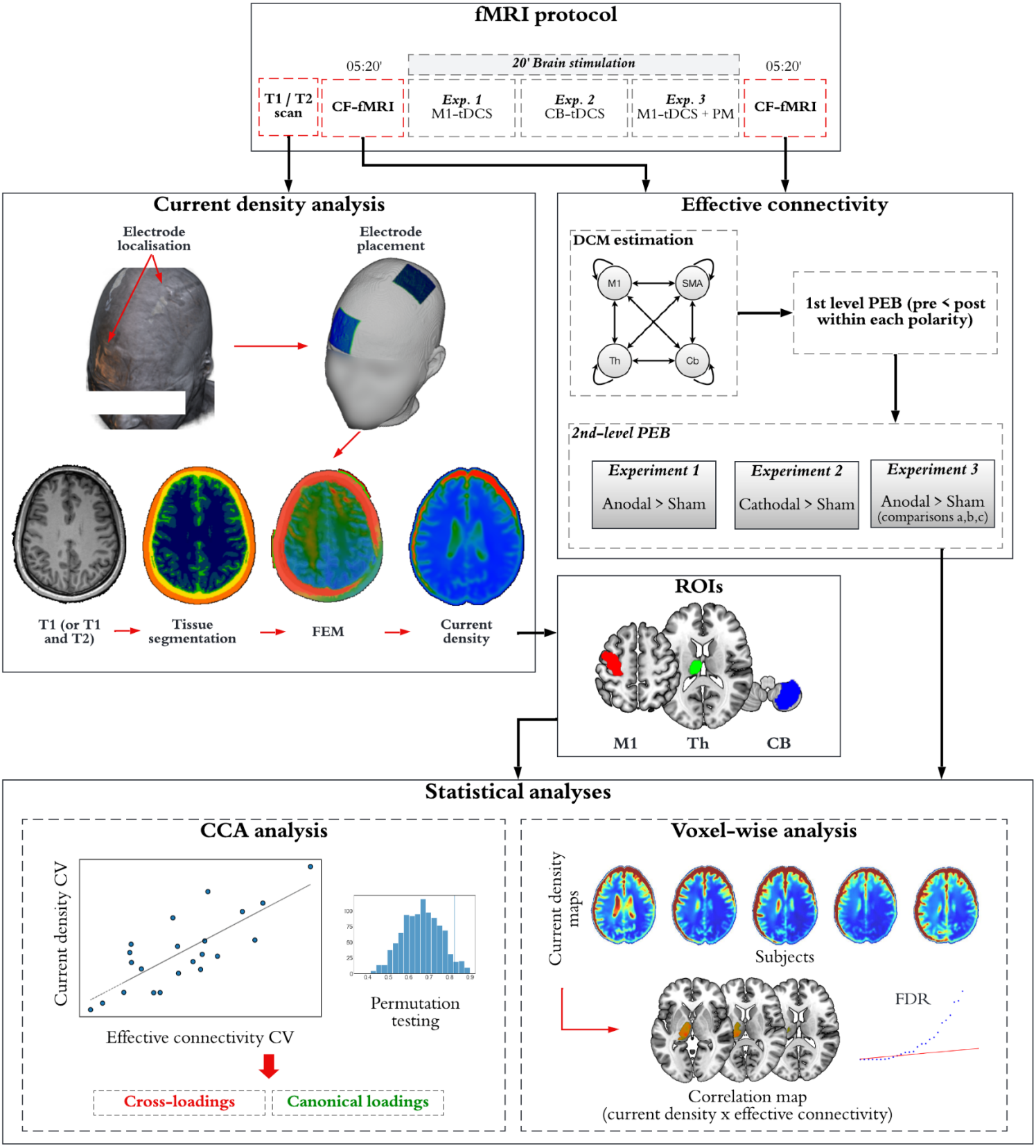

fMRI protocol
05:20'
20' Brain stimulation
05:20'
T1 / T2 scan
CF-fMRI
Exp. 1 M1-tDCS
Exp. 2 CB-tDCS
Exp. 3 M1-tDCS + PM
CF-fMRI
Current density analysis
Electrode localisation
Electrode placement
T1 (or T1 and T2)
Tissue segmentation
FEM
Current density
Effective connectivity
DCM estimation
M1
SMA
Th
Cb
1st level PEB (pre < post within each polarity)
2nd-level PEB
Experiment 1
Anodal > Sham
Experiment 2
Cathodal > Sham
Experiment 3
Anodal > Sham
(comparisons a,b,c)
ROIs
M1
Th
CB
Statistical analyses
CCA analysis
Current density CV
Effective connectivity CV
Permutation testing
Cross-loadings
Canonical loadings
Voxel-wise analysis
Current density maps
Subjects
FDR
Correlation map
(current density x effective connectivity)

Figure 6.1. Diagram representing the fMRI protocol (top), the current-density computation pipeline through ROAST (middle-left), the effective connectivity analysis using DCM and PEB (middle-right), and the two main statistical analyses of the correlation between current density and effective-connectivity changes, namely the CCA analysis (bottom-left) and the voxel wise analysis (bottom-right). For an in detailed explanation of *Experiment 3* comparisons a, b and c, see section *MRI acquisition, fMRI preprocessing and effective-connectivity analysis* below.

6.2.1. MRI acquisition, fMRI preprocessing and effective-connectivity analysis

Structural and functional MRI data from *Experiment 1* and *Experiment 2* was collected using a Philips Achieva 3T MRI scanner, whereas data from Experiment 3 was collected using a Siemens MAGNETOM Prisma 3T. Structural data (i.e., T1- and T2-weighted images) for each experiment was acquired at the beginning of the first experimental session and used for co-registration. Details about MRI acquisition were reported in **Table 3.1**. For the purpose of the present study, structural data from each subject was used to construct computational models of tDCS-induced electric fields. As discussed below, T2-weighted images (T2-w) were used only for Experiment 3, due to the presence of artefacts in T2-images from *Experiment 1* and *2*.

With respect to the fMRI preprocessing, fMRI data was preprocessed following a standard preprocessing pipeline in all three experiments (as reported in Chapter 4 and Chapter 5), with the only difference being the implementation of an additional independent component analysis (ICA) based denoiser in *Experiment 1* and *2* but not in *Experiment 3*.

As regards to the effective-connectivity changes following tDCS, the data used in the current chapter was derived from single-subject 2nd-level PEBs used in Chapter 3 and 4 to estimate the group averages encoding the following pairwise interactions (at the individual level):

1) *Experiment 1*: Anodal versus Sham (i.e., encoding the interaction pre-tDCS < post-tDCS x anodal > sham);

2) *Experiment 2*: Cathodal versus Sham (i.e., encoding the interaction pre-tDCS < post-tDCS x cathodal > sham);

3) *Experiment 3* (detailed information about how comparisons *a* and *c* are made is provided in Chapter 5, section 3.7):

    a) Anodal versus Sham for Day1-MRI only (i.e., encoding the comparison Day1-MRI pre vs Day1-MRI post stimulation);

    b) Anodal versus Sham for Day5-MRI only (i.e., encoding the comparison Day5-MRI pre vs Day5-MRI post stimulation);

    c) Anodal versus Sham Day1-MRI VS Day5-MRI (i.e. encoding the comparison Day1-MRI pre vs Day5-MRI post).

The above resulted in 21 single-subject PEBs for *Experiment 1* (encoding anodal vs sham), 21 for *Experiment 2* (encoding cathodal vs sham), and 44 for *Experiment 3* (encoding the interactions *a*, *b* and *c* explained above), which were used both in the canonical correlation analysis (CCA) as well as in the voxel-wise correlation analyses discussed below. Note that each single-subject 2nd-level PEB can be interpreted as the increases/decreases of one/five sessions of anodal/cathodal tDCS as compared to one session of sham tDCS. Importantly, diagonal entries in the PEB matrices used in the present study were converted to Hz and centred on zero, so that positive values represent a decrease in self-connectivity, and negative values represent an increase.

It is also worth mentioning that, as regards to *Experiment 3*, the group averages for Anodal versus Sham (Day5-MRI only, i.e., comparison *b*) were not estimated in Chapter 5, as the focus of that experiment was on the differences between a single and multiple tDCS sessions. However, in this chapter I used the PEB encoding the pairwise interactions for Day1-MRI and Day5-MRI separately, to avoid adding an extra level of complexity to the CCA and voxel-wise correlation analyses.

Noticeably, I decided to focus the analyses only on the connectivity between M1 and thalamus (as well as their self-connectivities), which appears to have a crucial role in supporting purposeful movements in response to command (Fernández-Espejo et al., 2015) and was the target of our previous studies (Chapter 4, Chapter 5). Importantly, this was also done to limit

the number of multiple comparisons in the CCA as well as in the voxel-wise correlation analysis.

6.2.2. T1-w and T2-w images cleaning

For the tissue segmentation algorithm used in the computational modelling to work, T1-w and T2-w images must not contain external objects. However, in *Experiment 1* and *Experiment 3*, in order to get a reference of the position of the electrode over the motor cortex in the MRI structural images, a skin-marker localization device (in this case a 1000mg cod liver oil capsule) was taped on the electrode over M1 (an example is provided in **Figure 6.1**). Note that the marker was not used in *Experiment 2* as participants would have rested their heads on it. As mentioned in section 6.2.4, this allowed us to accurately define the position of the target electrode and obtain more precise current-density models. Moreover, in some T1-w images, tDCS electrodes and traces of the 10-20 conductive paste were also visible. As such, the cod liver oil capsule, the 10-20 conductive paste and tDCS electrodes were manually removed from T1-w and T2-w images, prior to tissue segmentation, using the open-source *ITK-snap* software (Yushkevich et al., 2016).

6.2.3. Computational modelling

All the model construction analyses were run on a DELL XPS 9560 Windows PC, using SPM12 (www.fil.ion.ucl.ac.uk/spm) on MATLAB 2018b, and the Realistic vOlumetric-Approach to Simulate Transcranial Electric Stimulation (ROAST; https://www.parralab.org/roast/) toolbox (Y. Huang et al., 2019). ROAST is an end-to-end pipeline that relies on open-source software and custom scripts to estimate computational models of how tDCS-induced current flows in the brain (Huang et al., 2018, 2019), starting from the cleaned individual T1-w images in Nifti format (Larobina & Murino, 2014). In Experiment 3, I also used T2-w images, to improve the quality of the head meshes, and hence increasing the accuracy of the electric field models (Van Hoornweder et al., 2022). In order to

create anatomical valid head models, ROAST runs several operations on the subjects' T1- and T2-w images.

6.2.4. Tissue segmentation and electrode placements

The first step in ROAST's pipeline is tissue segmentation, through the segmentation algorithm included in SPM12 (Ashburner & Friston, 2005), which creates probabilistic maps of 6 different brain tissues: white matter (WM), grey matter (GM), skull, scalp, CSF) and air cavities. ROAST then post-processes SPM segmented tissue maps, with a custom touch-up script that aims at smoothing SPM segmentations, filling holes in the CSF and removing disconnected voxels (Y. Huang et al., 2019). The outcomes of this ROAST touch-up procedure are discrete tissue segmentation maps, where each voxel is assigned to a single tissue type only. Following tissue segmentation, ROAST uses a Matlab script developed by (Y. Huang et al., 2013) to place virtual electrodes on the segmented tissue maps. ROAST allows electrode placement to be done with two different approaches: one can either use locations from standard EEG montage systems (e.g. 10-20, BioSemi-256 etc.) or input arbitrary locations on the scalp using subject-specific coordinates in the MRI voxel space (Y. Huang et al., 2019). In order to reach more accurate electric-field (E-field) models, I opted to use arbitrary locations, specific for each participant.

To accurately identify the coordinates of the two tDCS electrodes in each participants' anatomical scan, I used the software MRIcroGl (Rorden & Brett, 2000), which allows to visualise a three-dimensional render of an anatomical image, along with the canonical multi-planar view, and to select any voxel in the 3D space and display the respective MRI volume space coordinates. By visualising the anatomical scans with MRIcroGl it was possible to identify the outline of the electrodes on the scalp, and then approximately identify, manually, the coordinates of the centres of the electrodes, which were finally fed to ROAST in order to place the electrodes on the segmented tissue maps (see Fig xx, middle-left box for an example). Importantly, ROAST also allows for the specification of the size of the electrodes, and the thickness of the paste layer, which here were 50x50mm and 3mm respectively.

6.2.5. Model parameters and solution

After tissue segmentation, ROAST assigns default isotropic conductivity values to each tissue type, and to the electrodes. The following default values were used: grey matter: 0.276 S/m; white matter: 0.126 S/m; CSF: 1.65 S/m; bone: 0.01 S/m; skin: 0.465 S/m, air: 2.5e-14 S/m, electrodes: 5.9e7 S/m, and paste 0.3 S/m (Y. Huang et al., 2019). ROAST also requires the specification of amount of current going into the anode and out of the cathode, and, in line with the methods used in the 3 Experiments, I used +1mA (anode) and -1mA (cathode) for *Experiment 1* and *Experiment 3,* and +1.85mA (anode) and -1.85mA (cathode) for *Experiment 2*.

Lastly, ROAST creates a finite element meshing, using the Matlab toolbox iso2mesh (Fang and Boas, 2009), and uses the open-source solver getDP (Dular et al., 1998) to solve the models for voltage, and calculate the direction and intensity of the electric field at each voxel (E-field magnitude) (Huang et al., 2019). Importantly, all outputs generated by ROAST - including tissue segmentations and electric-field and voltage maps - are in each individual participant's native space. In order to move the electric-field maps from the native space to the MNI space, I first used SPM12 procedures to normalise the anatomical scan of each participant, and then used the normalisation parameters estimated on the anatomical scans to normalise ROAST outputs. Generated electric-field maps for each subject are displayed in **Figure D2.**

6.2.6. Current density computation

Following normalisation and resampling of E-field models, I computed current density maps using Python libraries Numpy (Harris et al., 2020) and Nilearn (Abraham et al., 2014). Specifically, current density (***J***) at each voxel was computed starting from its respective E-field (**E**) and tissue conductivity (σ) values, using the function the function $J = \sigma E,$ in accordance with Ohm's law. According to (Albizu et al., 2020), current density is a useful metric for determining the dosage of current (A/m^2) induced in the brain by tDCS. Additionally, current density can be scaled - by modulating the intensity of the stimulation (i.e., increasing / decreasing the input current) - which might be useful for the purpose of individualised dosing

calculations (Albizu et al., 2020), a fundamental matter in the field of PDOC and rehabilitation (Chapter 3).

Current density volumes of each subject were then restricted to CSF, grey and white matter, using each participant's normalised segmented map. Lastly, current density maps were smoothed by applying a full-width at half maximum (FWHM) Gaussian smoothing kernel with Nilearn, with a kernel size of 4x4x4mm.

6.2.7. Statistical analyses

6.2.7.1. ROIs

All statistical analyses were restricted to two regions of interest (ROIs) in *Experiment 1* and *3*, namely the left motor cortex (M1), the left thalamus, and to 3 ROIs in *Experiment 2*, namely the left M1, the left thalamus and the right cerebellum. All ROIs were obtained from the Automated Anatomical Labelling Atlas 3 (Rolls et al., 2020). Note that all analyses were performed masking out voxels that were not segmented as white matter, grey matter or CSF. This was done to exclude from the analyses voxels that were assigned to air or bone tissue, which might be present in the M1 ROIs and bias the results.

6.2.7.2. Descriptive analysis of electrode placement and current density

To assess inter-individual variability in tDCS-induced current density, I calculated current density median values, for each participant, within the M1 and thalamus ROI for Experiments 1 and 3, and within M1, thalamus and Cerebellar ROI for *Experiment 2*. In line with Indahlastari et al. (2021), I focused on median values as they represent a measure of central tendency, and I avoided mean values as these are heavily influenced by partial volumes effects - that is, outliers due to high current density values at the boundary between CSF and grey matter (Indahlastari et al., 2019; Sadleir et al., 2012).

For exploratory purposes, I assessed inter-individual variability in the placement of the target electrode within each experiment, by first deriving the average position of the target electrode

at the group level (in the MNI space) and then calculating the average of the Euclidean distance between each participant's target electrode coordinates and the average position. Additionally, for *Experiment 1* and *3* only, I calculated the average Euclidean distance between the target electrode and the M1 ROI centroid (MNI coordinates: x = -38.4; y = -7.5; z = 49.2). Importantly, this allowed us to verify whether there were substantial differences between *Experiment 1* and *Experiment 3* in terms of electrode positions and their distance from the motor cortex, as different procedures were used for the placement of the target electrode in the two experiments (i.e. a TMS-guided approach in *Experiment 1*, and a manual placement with a standard EEG cap in *Experiment 3*; for more details see Chapter 4 section 3.3 and Chapter 5 and section 3.3, respectively).

6.2.7.3. Canonical Correlation Analysis between current density measures and effective connectivity changes

In order to investigate the relationship between effective connectivity changes following tDCS (as measured by PEB) and tDCS-induced current density in the aforementioned ROIs, I followed two different approaches: CCA and voxel-wise correlation analysis. I used CCA to correlate median and maximum values of the smoothed current densities within each ROI, with the effective connectivity changes following Anodal (*Experiment 1* and *3*) or Cathodal stimulation (*Experiment 2*). Note that for *Experiment 3* three separate CCA analyses were performed, one for Day1-MRI, one for Day5-MRI, and finally one for Day1-MRI pre versus Day5-MRI post. Detailed explanation of the interpretation of the effective connectivity data used in these analyses is provided above (section 2.1).

CCA analysis is a powerful multivariate tool which is used to investigate the relationship between two sets of data, each containing multiple measurements (Zhuang et al., 2020). The output of the CCA analysis are canonical variates (CV), linear combinations of the features within each data set, that maximise the correlation across sets (Zhuang et al., 2020). Here, the first set of variables consisted of the current density metrics of each subject (medians and max values of each ROI), while the second set consisted of the effective connectivity changes between M1 and thalamus (and their self-connectivities) as estimated with PEB.

Similarly to (O'Donnell et al., 2021), to test the significance of our canonical variates, I performed a randomisation test with 1000 permutations, in which I shuffled the rows (i.e., participants) of the current density metrics with respect to the effective connectivity values. At each permutation, I conducted a CCA analysis and recorded the highest correlation between pairs of canonical variates (i.e., the first canonical variate). After this procedure, I obtained a distribution of 1000 possible correlations between our canonical variates, under the null hypothesis that no relationship between the two sets of variables exists. Finally, the *P*-value associated with our observed CV pair was calculated as the proportion of correlations in the permutation test that are larger than the observed one. For CV pairs whose correlation was significant after the permutation test, I then correlated each feature in each set (i.e., current density metrics or effective-connectivity changes) with the canonical variate of the other set, and obtained the so-called cross-loadings. The cross-loadings are useful in that they quantify how much each feature in one set of variables contributes to the linear combination of the features in the other set of variables (i.e. the canonical variate). Moreover, I also calculated the canonical loadings, which represent the correlation between each feature in a variable set and that variable set canonical variate. (i.e. they quantify how much each feature contributes to the linear combination of all features).

6.2.7.4. Voxel-wise correlation analysis

Following the CCA analysis on the median current density values, I also performed an exploratory voxel-wise correlation analysis between current density maps and effective connectivity changes following tDCS (i.e., the same single-subject PEB comparisons as per above). The voxel-wise analysis was performed in Python using the libraries Numpy (Harris et al., 2020) and Nilearn (Abraham et al., 2014).

Specifically, for each ROI independently, I correlated participants' current density values in each voxel, with participants' changes in effective connectivity in the four connections selected (M1 and thalamus self-inhibitions, as well as their connectivities). This procedure resulted in 12 voxel-wise correlation analyses for *Experiment 1* and *2*, and 36 for *Experiment 3* (i.e., 12 for each PEB interaction). The p-value maps associated with each correlation were then

adjusted using the False Discovery Rate correction (FDR) (Benjamini & Yekutieli, 2001) as implemented by the Python library Statsmodels (Seabold & Perktold, 2010).

6.3. Results

6.3.1. Current density estimates and electrode placement variability

Median and max current density values within each ROI included in the analyses, for each experiment independently, are reported in **Table 6.1**. Median current density values only are reported in **Figure 6.2**.

In *Experiment 1*, target electrode positions (i.e., the electrode over the left M1) varied on average 19.2mm ± 12.7 across participants, from the average position (average MNI coordinates: x = -48; y = -20 ; z = 70). In *Experiment 2,* target electrode positions (i.e., the electrode over the right cerebellum) varied on average 19.3mm ± 9.6 (average MNI: x = 41; y = -91 ; z = -20). In *Experiment 3* target electrode positions (i.e., the electrode over the left M1) varied 16.4mm ± 10.8 (average MNI: x = -58; y = -19 ; z = 48). Lastly, the distance between the target electrode and the M1 ROI was on average 32.5mm ± 13.3 and 29.2 ± 6.5, for *Experiment 1* and *Experiment 3* respectively.

To help with the interpretation of the results related the non-targeted region included in this analyses (i.e., the thalamus), a one-way-between-subject ANOVA was run to assess whether there was a statistically significant difference in thalamic current density medians across experiments. No main effect of Experiment was found on thalamic current density medians ($F = 2.503$, $p = 0.090$, $\eta^2 = 0.076$).

Table 6.1. *Current density median and max values for the three experiments, for the three ROIs included in the analyses.*

Experiment	Region		
	M1	**Thalamus**	**Cerebellum**
Experiment 1	Median: 0.051 ± 0.005 A/m^2 Max: 1.430 ± 0.540 A/m^2	Median: 0.014 ± 0.002 A/m^2 Max: 0.053 ± 0.016 A/m^2	Median: 0.014 ± 0.002 A/m^2 Max: 0.119 ± 0.032 A/m^2
Experiment 2	Median: 0.018 ± 0.003 A/m^2 Max: 0.076 ± 0.013 A/m^2	Median: 0.016 ± 0.002 A/m^2 Max: 0.066 ± 0.021 A/m^2	Median: 0.064 ± 0.010 A/m^2 Max: 1.537 ± 0.554 A/m^2
Experiment 3	Median: 0.054 ± 0.007 A/m^2 Max: 1.529 ± 0.597 A/m^2	Median: 0.016 ± 0.003 A/m^2 Max: 0.079 ± 0.227 A/m^2	Median: 0.015 ± 0.0015 A/m^2 Max: 0.143 ± 0.034 A/m^2

Abbreviations: M1, motor cortex.

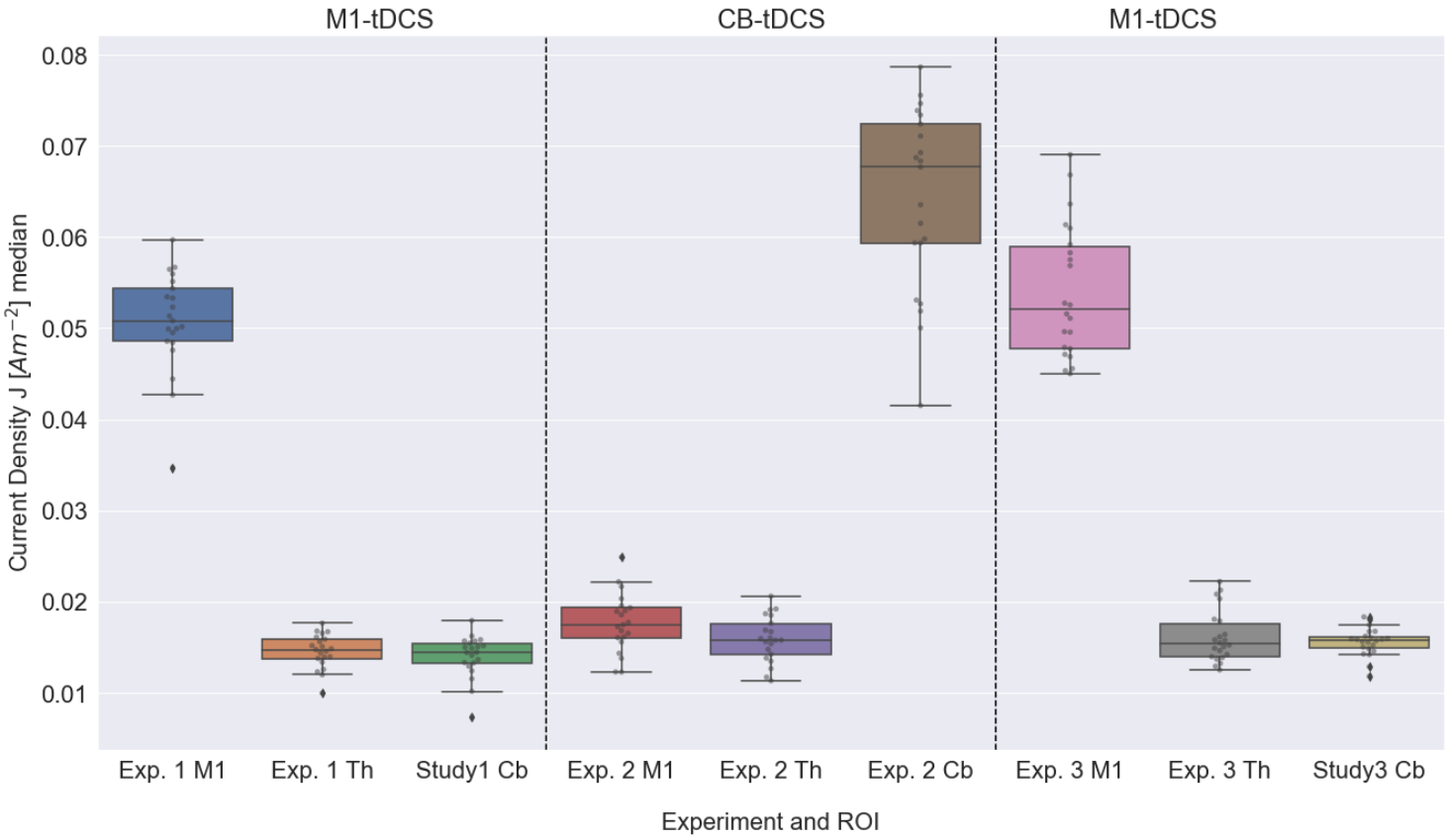


Figure 6.2. Box plots displaying median current density values per subject, for each experiment and ROI. Abbreviations: Exp, experiment; M1, motor cortex; Th, thalamus; Cb, cerebellum.

6.3.2. CCA analysis

Our CCA approach resulted in only one significant correlation, specifically between the first pair of canonical variates for *Experiment 3* comparison *c* (Day5-MRI) ($r = 0.824$, $p_{corr} = 0.046$; **Figure 6.3**). Non significant correlations are reported in **Table D2**.

Cross- and canonical loadings are reported in **Table 6.2**, along with the respective p-values. The first current-density canonical variate significantly correlated with the self-connectivity in M1 ($r = 0.695$, $p < 0.000$), whereas the first effective-connectivity canonical variate significantly correlated with both median ($r = 0.432$, $p = 0.045$) and max ($r = 0.470$, $p = 0.027$) current density in the thalamic ROI. As regards to the canonical loadings, the self-connectivity in M1 and the thalamus-to-M1 connectivity positively correlated with the effective

connectivity CV (r = 0.843 p < 0.000, and r = 0.448 p = 0.036, respectively). Additionally, maximum values of M1 current density (r = 0.488, p = 0.021), maximum thalamic current density (r = 0.570, p = 0.006), and median thalamic current density (r = 0.523, p = 0.012), all positively correlated with the current density canonical variate.

Table 6.2. Cross- and canonical loadings from the CCA analysis for *Experiment 3* (Day5-MRI).

Variable set	**Feature**	**Effective connectivity CV**	**Current density CV**
Effective connectivity variable set	M1 ←→ M1	**0.843 (p < 0.000)**	**0.695 (p < 0.000)**
	Th ←→ Th	0.127 (p = 0.572)	0.105 (p = 0.642)
	M1 → Th	-0.138 (p = 0.540)	-0.114 (p = 0.614)
	Th → M1	**0.448 (p = 0.036)**	0.369 (p = 0.090)
Current density variable set	M1 median CD	0.335 (p = 0.128)	0.406 (p = 0.061)
	M1 max CD	0.402 (p = 0.063)	**0.488 (p = 0.021)**
	Th median CD	**0.432 (p = 0.045)**	**0.523 (p = 0.012)**
	Th max CD	**0.470 (p = 0.027)**	**0.570 (p = 0.006)**

Correlation between each feature and the respective and opposite variable set are reported, along with the p-value. Significant loadings (p < 0.05) are reported in bold. Cross-loading are highlighted in red, whereas canonical loadings are highlighted in green. Abbreviations: CD, current density; CV, canonical variate; M1, motor cortex; Th, thalamus.

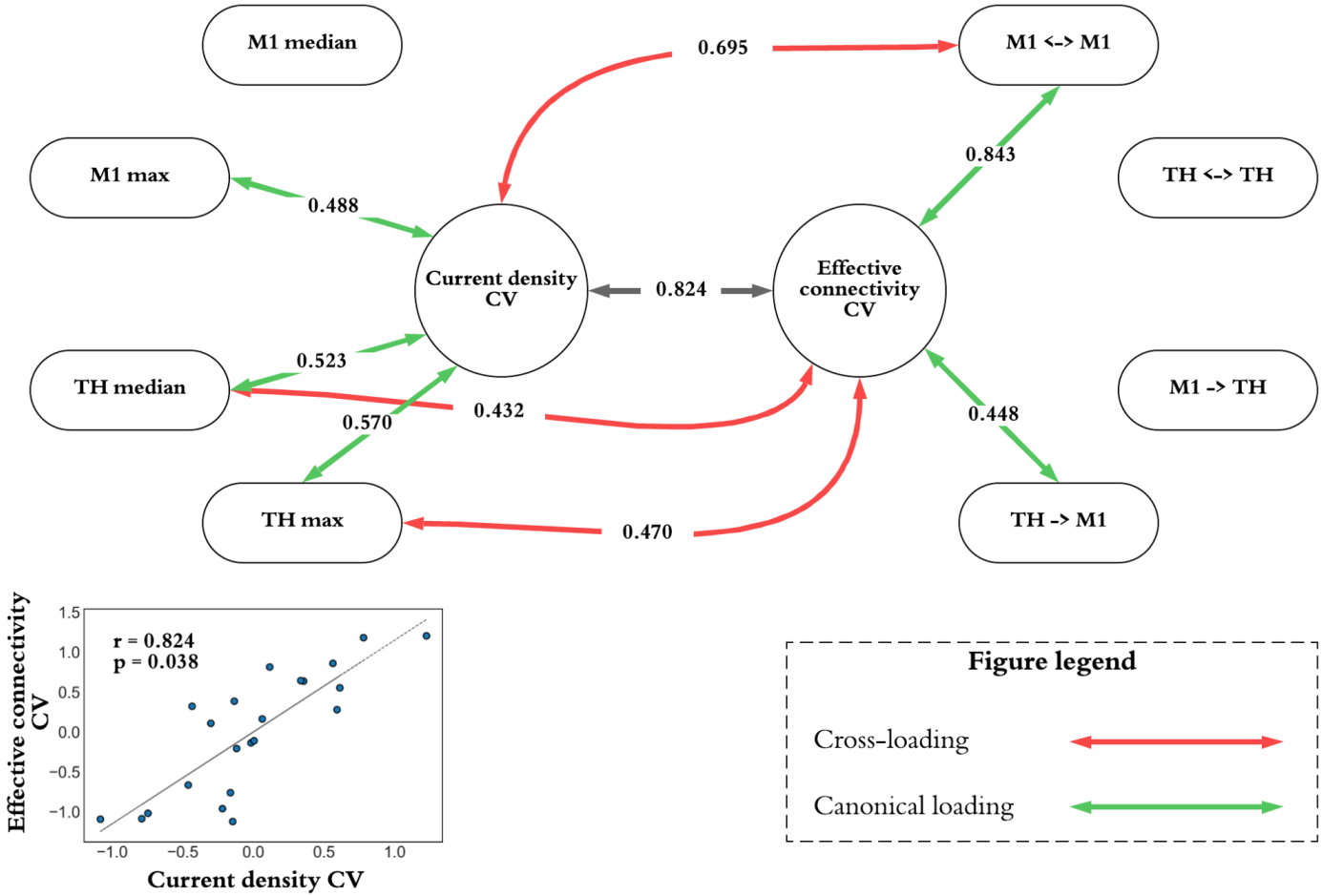


Figure 6.3. CCA results for *Experiment 3*, (Day5-MRI). Individual features of each variable set are represented by rounded rectangles. The first canonical variate for each variable set is represented by circles. The correlation between canonical variates is represented as a dark grey arrow, and is also displayed at the bottom left of the figure. Cross- and canonical loadings are shown as red and green arrows respectively, and their associated Pearson's R is reported. Note that loadings whose associated p-value was > 0.05 were not displayed (but are reported in **Table 6.2**.

6.3.3. Voxel-wise analysis

Results for the voxel-wise correlation analyses that resulted in significant correlations ($p < .05$ FDR corrected) are reported in **Table 6.3**. I observed significant correlations between current density in the thalamus and in the cerebellum ROIs, and M1 self-connectivity (number of significant voxels: 6373 and 11082 respectively) in *Experiment 2*. Lastly, a significant correlation was also observed between current density in the thalamus and M1 self-connectivity (number of significant voxels: 5530) in *Experiment 3* after one tDCS session (Day1-MRI). Importantly, when accounting for multiple-multiple comparisons by applying the FDR correction on the peak p-values (**Table 6.3**), no significant correlations are observed.

Table 6.3. *Voxel-wise correlation analysis results.*

Experiment	**ROI**	**N. of significant voxels**	**Connection**	**Peak R**	**Peak p-value (FDR)**	**Peak MNI coordinates**
Experiment 2	cerebellum	11082	M1 ←→ M1	-0.805	0.016	39; -40; -53
	thalamus	6373	M1 ←→ M1	-0.653	0.031	-12; -24; 0
Experiment 3, Day1-MRI	thalamus	5530	M1 ←→ M1	-0.729	0.020	-7; -9; -4

Three out of 32 voxel-wise correlation analyses resulted in significant correlations between current density and effective-connectivity. For each voxel-wise analysis I reported the ROI and effective-connectivity measure, along with the peak correlation coefficient R with its associated FDR-corrected p-value and MNI coordinates.

6.4. Discussion

The main goal of this study was to investigate the relationship between the amount of tDCS-induced current reaching key regions of the motor network, and the tDCS-related changes in effective connectivity. In order to disentangle this relationship, I first used CCA to fully utilise the common information within each modality (i.e., current density / effective connectivity). I then used voxel-wise correlation analysis to assess the presence of ROI-specific patterns of correlations.

In our CCA analysis, I found a significant correlation between current-density and effective-connectivity CVs only for *Experiment 3* (Day5-MRI), where the canonical variate for the effective-connectivity variables positively correlated with current density in the thalamus (**Figure 6.3**). Moreover, in the same comparison, I found that the combined variable for current-density positively correlated with self-connectivity in M1. This suggests that (thalamo-cortical) effective-connectivity overall is most strongly related to current density in the thalamus, and that current density overall is most strongly related to effective-connectivity in M1 self-inhibition. Interestingly, the CCA analysis uncovered that, even though the thalamus is not the primary target of our stimulation protocol, and a substantially inferior amount of current density was observed within the thalamic ROI as compared to M1 (with median current density values of 0.016 A/m^2 in the thalamus versus 0.054 A/m^2 in M1), the amount of current within the thalamic region seems to contribute more to the linear combination of the effective connectivity variable than that in M1. In particular, given the direction of the correlation between current density in the thalamus and the canonical variate for the effective connectivity variable, increasing current density in the thalamus would result in an overall increase in thalamocortical connectivity and/or reduction in self-inhibition. While these findings are interesting, it is important to note that the values of the median current density estimated within thalamic ROI in the three experiments (0.014 A/m^2 for Experiment 1, and 0.016 A/m^2 *Experiment 2* and *3*) correspond to an average median electric field magnitude of 0.10 ± 0.14 mV/mm (*Experiment 1*), 0.10 ± 0.17 mV/mm (*Experiment 2*) and 0.10 ± 0.18 mV/mm (*Experiment 3*) (**Table D.1**). Noticeably, these values fall below what recent evidence suggests to be necessary to elicit neuronal spiking and subthreshold currents in the cortex (i.e., 1 mV/mm) (Vöröslakos et al., 2018). Importantly, this observation applies to the targeted areas as well (**Table D.1**).

In fact, it has been pointed out that the stimulation intensities commonly used in tDCS research might not create enough current in the cortex to modulate neuronal functioning, and that current intensities as high as 4mA-6mA might be actually needed (Underwood, 2016; Vöröslakos et al., 2018). However, in contrast to the above findings, other studies reported physiological changes even with low intensity stimulations (for a review see (Filmer et al., 2020). For instance, an in-vitro study on rat hippocampal slices observed modulations of carbachol-induced gamma oscillations with alternating currents of 0.2 V/m (Reato et al., 2010b). Moreover, several studies on non-human primates (such as macaque monkeys) have reported physiological modulations of neuronal activity in the cortex (i.e., either timing or amount of spiking) with currents of as low as ~ 0.4 V/m (as reviewed by (Filmer et al., 2020). This was recently estimated to be achieved even with stimulations of 1mA (Y. Huang et al., 2017). Even though - with respect to the stimulated regions - the electric current models generated in the present study are in line with results from (Y. Huang et al., 2017), the electric field magnitudes within the thalamic ROI still fall slightly under 0.4 V/m (**Table D.1**). As such, it is possible that the observed correlation between current-density and effective-connectivity CVs in *Experiment 3* (Day5-MRI) is spurious, or, alternatively, that the present study adds up to the above evidence that lower currents can induce changes in neuronal activity.

Considering the role of thalamo-cortical connectivity in PDOC who lack behavioural responsiveness (Fernández-Espejo et al., 2015; Stafford et al., 2019c), these findings might suggest that, when administering M1-tDCS to PDOC patients, optimising tDCS montages so that the current that reaches the thalamus is maximised, might increase the effects of M1-tDCS on thalamo-cortical connectivity. However, it is important to notice that many PDOC patients have widespread atrophies that result in increased CSF volumes (Arnts et al., 2020), due to lost brain tissue being replaced by CSF (Indahlastari et al., 2020).

CSF is highly conductive, and its architecture might severely impact the shape of tDCS-induced current flow (Bikson et al., 2012) and reduce the overall amount of current delivered to brain areas (Mahdavi & Towhidkhah, 2018). Thus, I expect much lower electric-field amplitudes in subcortical structures of PDOC patients as compared to healthy subjects, which might in turn limit the translation of our findings to the patients. This notwithstanding, similar levels of current density in the left thalamic ROI were observed between the experiments targeting M1 (*Experiment 1* and *3*) and that targeting the right cerebellum (*Experiment 2*)

(**Table 6.1**). Hence, it is possible that, depending on the specific neuroanatomy of the patient, cerebellar cathodal-tDCS might represent a better therapeutic option, in that it might allow higher current density in the thalamus. Noticeably, the segmentation algorithm used by ROAST is tailored at the healthy brain, meaning that other procedures would have to be used to derive FEMs in PDOC, and segmentations should be visually checked and potentially manually corrected for each individual patient.

On the other hand, the presence of a significant correlation in the CCA analysis for *Experiment 3* only might be due to the inclusion of passive mobilisation, which enhanced tDCS effects on the motor-network causal architecture. Noticeably, this could have also been partially driven by the slightly higher current density observed in the thalamus in *Experiment 3* as compared to *Experiment 1* (**Table 6.1**), although proper statistical analyses were not run.

Similarly, in *Experiment 3*, the lack of findings following one tDCS session (Day1-MRI) might be attributed to the different effects that a single and multiple tDCS sessions have on motor network effective connectivity (see Chapter 5, section 4.2).

Finally, the results from the present study suggest that current density can predict thalamo-cortical effective connectivity changes following multiple sessions of anodal-tDCS, but cannot predict neither changes following single anodal-tDCS sessions (either administered at rest or paired with passive mobilisation), nor the changes following multiple anodal-tDCS sessions (i.e. *Experiment 3* Day1-MRI pre-tDCS vs Day5-MRI post-tDCS). This finding may be linked to the non-linearity of tDCS effects (Esmaeilpour et al., 2018) and might point out to the fact that current density measures have a stronger correlation with tDCS long-term effects rather than short-term ones, which might be due to the latter being more variable in nature.

However, in contrast to the CCA findings, the exploratory voxel-wise correlation analyses showed a different picture, reporting negative correlations between M1 self-connectivity and median current density in the thalamus (*Experiment 2* and *Experiment 3* Day1-MRI) and the cerebellum (*Experiment 2* only). In *Experiment 2*, the negative correlation observed in the voxel-wise analysis suggests that the more current reaches the cerebellum or the thalamus, the more self-inhibition is observed in M1, after cathodal-tDCS.

Interestingly, the correlation between these two regions - the cerebellum and M1 - was anticipated, owing to the inhibitory effect that the former area exerts on the latter, through dentate-thalamo-cortical connections (Galea et al., 2009a).

Overall, while this finding provides evidence of a network effect of tDCS, the direction of the relationship is of difficult interpretation due to the nature of the measure chosen, in that the electric field (or current density) vector after inverting the tDCS montage is simply the inverse vector (i.e., the magnitude remains constant):

$$\sqrt{X_{Cathodal}{}^{2} + Y_{Cathodal}{}^{2} + Z_{Cathodal}{}^{2}} = \sqrt{(-X_{Anodal})^{2} + (-Y_{Anodal})^{2} + (-Z_{Anodal})^{2}}$$

As such, other characteristics of the electric field, such as current density direction (i.e., (Albizu et al., 2020) or electric field orientation relative to grey matter surface (i.e., (Nandi et al., 2022), would provide more insights into the relationship between the tDCS-induced electric field and effective-connectivity changes following stimulation.

In *Experiment 3*, the voxel-wise correlation analyses suggested that higher current-density values in the thalamus correspond to higher values in M1 self-inhibition following one anodal-tDCS session. By contrast, in my previous chapter investigating the effects of multiple tDCS sessions on motor network effective connectivity, I had found that, at the group level, anodal-tDCS decreases M1 self-inhibition (Chapter 5). Again, while interpreting the direction of this correlation is challenging, it suggests a network effect of tDCS, and highlights that, when investigating inter-individual variability in responsiveness to tDCS, it is important to also consider regions that are not the primary target of the stimulation.

Surprisingly, the above correlations were not observed in the CCA, and, on the other hand, the voxel-wise analysis did not report any significant correlation in *Experiment 3* Day5-MRI.

This discrepancy suggest that, with multiple tDCS sessions, the combination of the information contained in the current-density maps in the M1 and thalamic ROIs (as done in the CCA), is

more informative in explaining effective-connectivity changes following tDCS than when considering those ROIs independently from each other (as done in the voxel-based correlation analysis). Importantly, the lack of findings in the voxel-wise analysis might also be related to a lack of statistical power, due to multiple comparison corrections.

Additionally, it is important to highlight that, when accounting for multiple multiple-comparisons, no significant correlations were observed in the voxel based analysis. Hence, the observed correlations in the voxel-based analysis might be, in fact, spurious. Overall, the voxel-based and canonical correlation approaches results are not mutually exclusive, in that the two methods investigate different aspects of the association between effective connectivity following tDCS and current density. Specifically, while the former uncovers univariate associations, the latter unveils joint multivariate relationships among multiple sets of features (while avoiding corrections for multiple comparisons typical of univariate methods), which are normally overlooked by univariate methods (Zhuang et al., 2020).

The strengths of the work presented in this chapter are two-fold: first, the analyses were performed independently in three fMRI studies, each adopting a different stimulation protocol (see **Table 3.1**). As such, I could explore the relationship between tDCS-induced current density and effective connectivity in two different tDCS montages, one targeting the left M1 (*Experiment 1* and *3*) and one targeting the right cerebellum (*Experiment 2*). This allowed for a more varied assessment of the relationship. Second, previous literature mainly focused on the relationship between tDCS-induced electric fields and neuroimaging or behavioural measures gathered after one single tDCS session (Nasimova & Huang, 2022). Opposedly, here I also explored such a relationship after multiple tDCS sessions (i.e., *Experiment 3*, *Day1-MRI vs Day5-MRI* and *Day5-MRI*). As a consequence, it is possible to interpret the analyses for *Experiment 3* in terms of the relationship between the amount of tDCS-induced current and changes in effective connectivity that are potentially related to mechanisms of structural plasticity (i.e., long-term potentiation).

However the findings from the present chapter should be interpreted in light of several limitations. Firstly, automated tissue segmentation routines as the ones used by ROAST have only a certain degree of accuracy (Kazemi & Noorizadeh, 2014), and misclassification of tissue will therefore reflect on FEM results, as current density measures are directly derived from tissue types - and, therefore, conductivities - assigned to each voxel (Albizu et al., 2020).

Another limitation to consider is related to the inter-session within-subject variability in the electrode montage (i.e., anode and cathode positioning). In fact, the coordinates used for the electrode placements needed to estimate the computational models of the electric field were derived from the first MRI session of each participant, which might have not been the session where the participant received the anodal (for *Experiment 1* and *3*) or the cathodal (for *Experiment 2*) simulation, due to the randomisation of the conditions in the experiment design. This particular choice was motivated by the fact that T1-weighted scans were not collected in each MRI session. However, I expect differences in electrode positioning across different sessions of the same participant to be only marginal.

Importantly, another limitation related to the computational models used in the present study is linked to the usage of both T1- and T2-weighted scans. In fact, I used both images only for *Experiment 3*, due to artefacts in T2-weighted images of *Experiment 1* and *3*. However, recent evidence suggests that including both T1- and T2-weighted structural MRI scans allows for more precise electric field models, owing to a better representation of both cerebrospinal fluid and bones at the SPM12 tissue segmentation stage (Van Hoornweder et al., 2022). Importantly, this might have contributed to the lack of findings in the CCA of *Experiment 1* and *2*.

In addition to the above, another factor that might have limited the results of this study is the usage of template ROIs for the estimation of current density median and max values, as opposed to using the VOIs included in the DCM models (Chapter 4 section 3.7.1 for *Experiment 1* and *Experiment 2*, Chapter 5 section 3.7 for *Experiment 3*). In brief, the DCM models were not estimated on the fMRI time-series of the entire ROIs, but on smaller volumes, whose location was defined via looking at nearest local maxima (to the group peak activation) in each individual run. As such, investigating the relationship between current density and connectivity in these subject- and run-specific VOIs might have provided a more straightforward link between the two variables.

Lastly, it is worth mentioning that the present analyses focused solely on current density magnitude and did not assess current direction. However, current direction relative to the grey matter surface is well known to influence tDCS effects (Radman et al., 2009). As such, to fully investigate the relationship between tDCS-induced electric field and changes in effective connectivity, future research should include as electric field characteristic either the electric

field direction (Albizu et al., 2020), or the orientation of the electric field relative the grey matter such as the normal and tangential components of the current (i.e., (Nandi et al., 2022).

To conclude, while applications of tDCS in PDOC - and in general - continue to grow, their therapeutic potential is still limited by the heterogeneity of the effects of the stimulation (Chapter 2; Evans, 2020). Most of the variability observed in tDCS effectiveness is thought to be related to inter-individual anatomical differences (Evans, 2020). Consequently, optimal treatment responses cannot be achieved with fixed-dose tDCS (that is, applying the same stimulation parameters to all patients). To this regard, MRI-derived FEMs estimating tDCS-induced electric fields represent a viable approach to determine optimal tDCS parameters, and ensure that enough current is delivered to those brain regions involved in the treatment response. Here, I assessed the relationship between FEM derived measures and changes in thalamo-cortical connectivity following three different tDCS protocols. I found significant correlations between current density metrics and effective-connectivity changes following tDCS, in two out of the three experiments included in the analyses.

While the reported findings are mixed, this study serves as a proof of concept study suggesting that differences in tDCS-induced connectivity changes might be reduced by using individualised stimulation parameters based on FEMs. Specifically, by computing a FEM of a patient's brain, one could determine the best stimulation parameters to achieve desired current density in a specific region (Evans et al., 2020). In this case, reducing inter-individual variability and enhancing the desired effects of tDCS on thalamo-cortical connectivity could be particularly beneficial for improving treatment prospects of PDOC patients.

Note that the appendix to this chapter can be found at the end of the thesis (Appendix D).

Chapter 7

TDCS COMBINED WITH PASSIVE MOBILISATION IN PDOC: A MULTI-MODAL MULTI-SESSION CASE STUDY

7.1. Introduction

Even though our results on healthy participants represent a good proof-of-concept for the stimulation of the motor cortex in PDOC patients, the protocol had yet to be tested in a clinical setting. The aim of the case study presented in this chapter was to apply and evaluate the methodologies developed in this thesis on a PDOC patient, while also incorporating additional techniques (such as EEG) to fully assess the patient's clinical condition.

It was also fundamental to test the safety of our protocol, as well as the patient's tolerability of multiple MRI and tDCS sessions. Moreover, as part of our stimulation protocol, manual passive mobilisation had to be administered with the brain stimulation, even during the MRI sessions. To the best of our knowledge, no study assessed the feasibility of such a combination on PDOC patients, hence it was important to test that as well.

Aside from MRI, EEG also has an important role in the diagnosis and prognosis of patients with DOC, particularly due to EEG being bedside-applicable, less invasive and less expensive as compared to fMRI methods. fMRI applicability in PDOC patients is in fact more limited than EEG, in that it cannot be applied to patients who are unable to be transported to the scanner, as well as to those with ferromagnetic implants, or those who present frequent involuntary movements (Formaggio et al., 2020). As such, another scope of the present case study was to include EEG in order to increase clinical applicability of our methods.

Here, I report the result for the first patient who took part in a multi-modal crossover sham- and polarity-controlled feasibility study, combining fMRI, EEG, motion-tracking and behavioural assessments of consciousness, to evaluate the effects of multiple sessions of M1-tDCS coupled with passive mobilisation, on patients' responsiveness and brain dynamics (Fernández-Espejo et al., 2020). Specifically, I used fMRI to characterise changes in brain activity and effective connectivity following tDCS intervention, in line with our previous studies (Chapter 4 and Chapter 5), as discussed in the general methods of this thesis (Chapter

3). Additionally, I also assessed the presence of covert awareness with fMRI mental-imagery and command-following tasks. The role of fMRI mental-imagery tasks in the evaluation of covert cognition, and their relevance to PDOC differential diagnosis have been widely discussed in Chapter 1.
As well as completing the examinations described (on healthy controls) in the two empirical studies reported in Chapter 4 and Chapter 5, in this case study I also investigated tDCS-related changes in patient's resting-state fMRI (rs-fMRI) derived functional networks, resting-state EEG (rs-EEG) power spectra and graph-theoretical metrics, and finally EEG event-related desynchronisation (ERD) in response to a motor-imagery task. These methods were introduced in section 1.5.2.

The combination of active and passive MRI- and EEG-based active and passive tasks allows to better characterise tDCS-induced changes in brain activity and functional connectivity, and link those changes to behavioural measures (i.e. motion tracking and CRS-R), as well as thoroughly assess patient's signs of residual awareness with multiple approaches.
As the protocol is designed to target specifically CMD patients, if the patient is covertly aware, I hypothesise to observe: 1) changes in brain activation during the active conditions of the fMRI tasks (both in the command-following and motor-imagery tasks), 2) detectable ERDs in the EEG command-following task, 3) an increase in fMRI motor-network effective connectivity in the fMRI command-following task of the anodal stimulation condition as compared to sham, and 4) an increase in CRS-R scores in relation to the active stimulation conditions.
On the contrary, if the patient is not covertly aware, my hypotheses are more exploratory in nature, and I expect to observe some changes in functional connectivity measures during/following the active tDCS sessions, such as: 1) an increase in fMRI functional connectivity within the motor network and DMN at rest, 2) changes in EEG resting-state derived metrics that reflect an improvement in consciousness.

7.2. Methods

7.2.1. Ethics Statement

The West Midlands – Coventry and Warwickshire Research Ethics Committee (NHS Health Research Authority) provided ethical approval for this study (19/WM/0180). The patient's legal representative provided informed written consent allowing the participation of the patient in the study. The patient was pre-screened to confirm MRI and tDCS safety prior to the beginning of the study.

7.2.2. Eligibility Screening

Eligibility criteria for the participation in the present feasibility study were to be aged 18-years or older, having a consensus clinical diagnosis of PDOC from any aetiology (i.e. traumatic or non-traumatic injury) and being medically stable, with no need of mechanical support (such as respirators, etc.). On the other hand, exclusion criteria included having scalp skin sores or other skin damages at the EEG electrode sites, having metallic implants in the face or skull, having had a craniectomy, not showing evidence of auditory startle in clinical observations, or having absent brainstem auditory evoked potentials, and being MRI incompatible (having metal plates incompatible with the MRI scanner, acemaker, being unable to lay flat for long time periods, having aneurysm clips, neurostimulators, brain/subdural electrodes, etc.).

7.2.3. Patient description and clinical assessment

The patient was a right-handed 27-year-old man who suffered a sustained cardiorespiratory arrest, presumed to be following a near-drowning. Before receiving cardiopulmonary resuscitation (CPR), the patient was submerged in the water for about 8-10 minutes. At the time of admission, the patient was unconscious with miotic pupils and not reactive to light, and a first computed tomography (CT) showed diffuse cerebral oedema. Moreover, pupillary and corneal reflexes were absent but oculocephalic reflexes were present, as well as abnormal flexion to pain. Subsequent electroencephalography (EEG) revealed a low voltage background,

with no epileptiform activity. The first neurological assessment showed a low awareness state, and the patient was initially treated with amantadine. One month post injury, the patient was diagnosed with unresponsive wakefulness syndrome (UWS) with stimulus-sensitive myoclonus movements. A first Magnetic Resonance Imaging (MRI) evaluation (five-month post injury), identified a severe cerebral atrophy and gliosis, predominantly affecting the supratentorial parenchyma, as well as a hypoxia in the basal ganglia and thalami, and ex-vacuo dilatation of the ventricles (**Figure 7.1**). Seven months post injury the patient was discharged home and remained in a low awareness state, although some possible improvements were observed by his caregivers: the patient was able to turn his head and eyes to localise sound and touch for a few seconds, and spontaneous movements of fingers were reported, however not in response to command. Prior to the cardiac arrest, the patient had a history of paranoid schizophrenia and depression, although this was well controlled and the patient was about to reduce medication at the time of the incident. Ten months post injury the patient was transferred to the Wellington Hospital's Acute Neurological Rehabilitation Centre (London, UK), where detailed neurological assessments and longitudinal assessments of awareness using the CRS-R were conducted. These resulted in a diagnosis of UWS, with CRS-R scores around 5-7 out of 23. The patient had been able to turn his head and gaze to voice, which appears to be more frequent with familiar voices, and he responded to auditory startle. Further MRI examination confirmed profound hypoxic-ischaemic encephalopathy and longstanding secondary degenerative changes. Additionally, EEG examination showed highly abnormal and generalised low amplitude mixed frequency activity, which was unresponsive to external stimulation and in line with the severe cerebral dysfunction. Lastly, the patient was affected by generalised dystonia involving the face, axial muscles, upper and lower limbs, with his lower limbs being in fixed abduction.

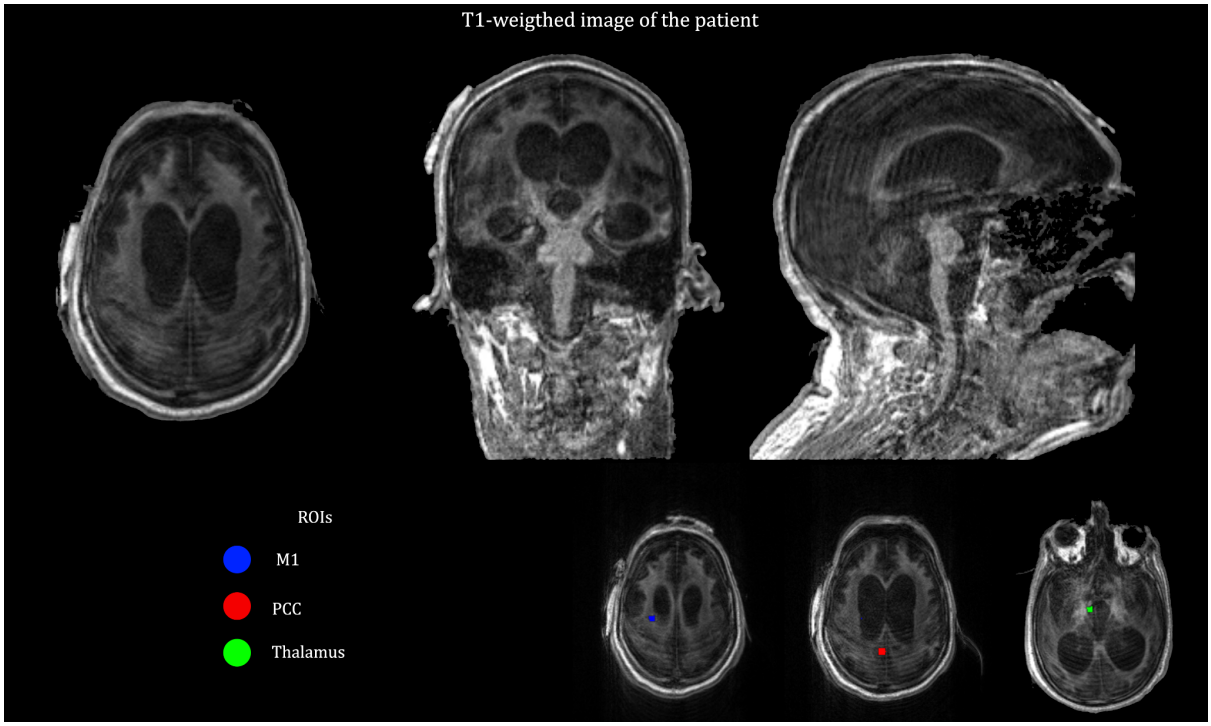


Figure 7.1. T1-weighted image of the patient. Bottom: manually selected ROIs for the DCM analyses (M1 and thalamus) and for the rs-fMRI analyses (M1, thalamus and PCC). The active and return electrodes are visible from the T1-image.

7.2.4. Experimental Procedure

The experimental procedure used in the present case study is also described in detail in our previous study protocol ((Fernández-Espejo et al., 2020). We used a sham- and polarity-controlled blind crossover design (**Figure 7.2**). The experiment involved 3 testing weeks in which the patient received either anodal, cathodal or sham tDCS, coupled with passive mobilisation of the right thumb. Each testing week included 5 consecutive daily sessions of stimulation of the same polarity. Testing weeks were spaced out by at least 7 days of rest (7 days between the first and second testing weeks, and 14 days between the second and third testing weeks). I administered the first (Day1-MRI) and fifth (Day5-MRI) tDCS with passive mobilisation sessions of each testing week within the MRI scanner (six MRI sessions in total), where the patient also performed a command-following task (see section *fMRI paradigm* below) and resting-state task, both before and after the stimulation. The second, third and fourth tDCS sessions were delivered at the bedside in the patient's room (Day2-bedside, Day3-

bedside and Day4-bedside respectively). In addition to the MRI sessions, our experiment also included six EEG sessions (two sessions per polarity): the first EEG session was run the week before each testing week, which served as a baseline for the second EEG session, happening on the fourth day of each testing week (that is, Day4-bedside), following brain stimulation. Importantly, no tDCS was administered during the baseline EEG session. Similarly to the MRI sessions, in the EEG sessions the patient also performed a simple command-following task, during which I also recorded motion-tracking data to assess potential motor behaviours associated with the task. In addition to the active-task, I also collected EEG resting-state data. Lastly, throughout the course of the experiment I administered the CRS-R 36 times (12 assessments per polarity), to evaluate potential behavioural changes. Importantly, all instructions used in the experiment were translated from English to the patients' native language (Greek), and so were the CRS-R evaluations.

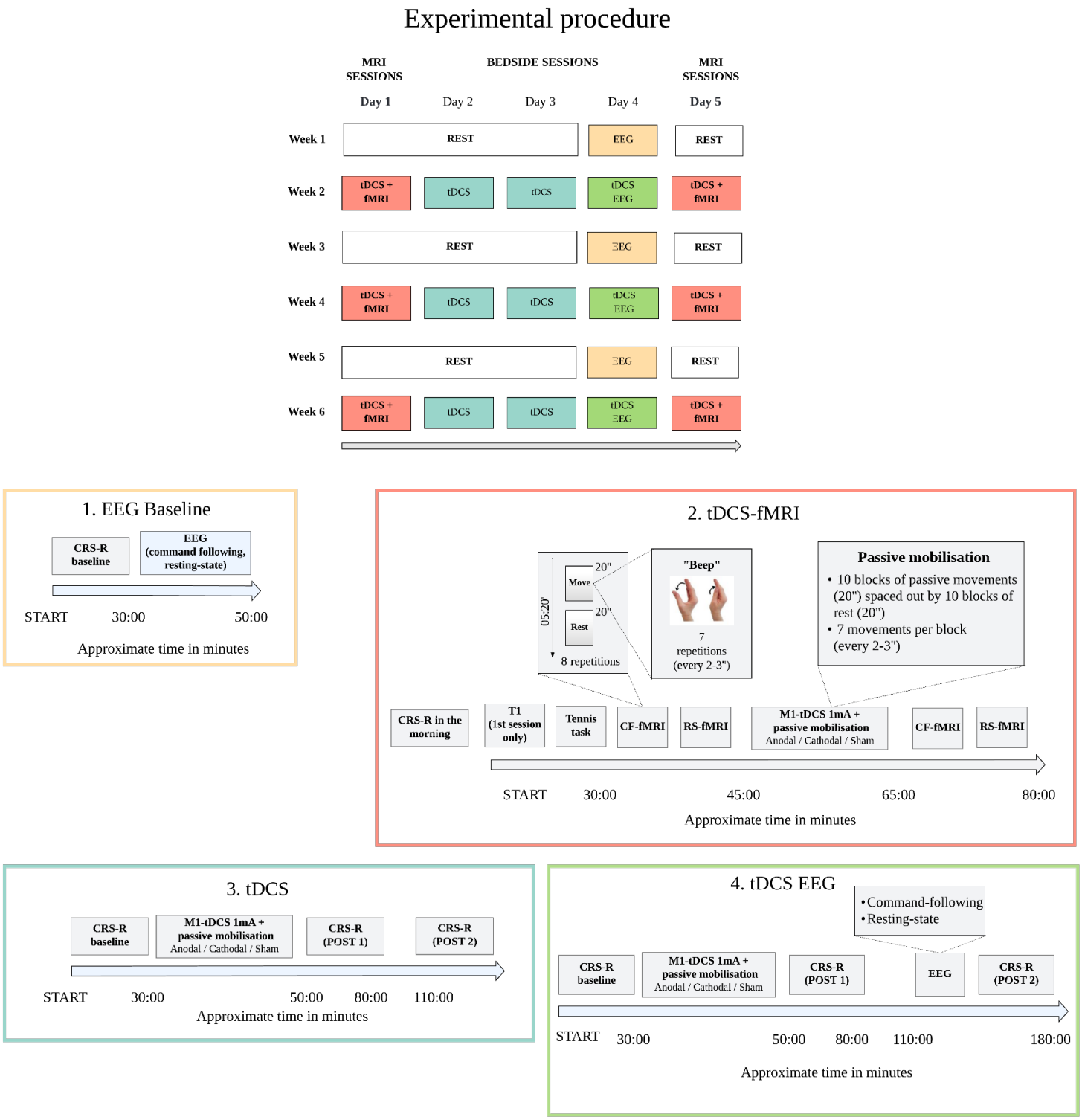


Figure 7.2. Experimental procedure. Top left: organisation of the testing weeks. EEG command-following and resting-state baselines were collected during the resting weeks (panel 1, EEG baseline), after a CRS-R assessment. During each testing week, the patient received five daily tDCS sessions. In the first and last sessions (tDCS + fMRI), the tDCS stimulation was carried out within the MRI scanner

(panel 2, tDCS-fMRI), and was preceded by a CRS-R assessment. In the second and third sessions, the tDCS stimulation was performed after a CRS-R assessment, which was also performed straight after the stimulation, and after half an hour (panel 3, tDCS). During the fourth session (panel 4, tDCS EEG), a CRS-R assessment was performed before the tDCS session. After the session, another CRS-R assessment was carried out, followed by an EEG session, after which a last CRS-R assessment was performed.

7.2.5. MRI acquisition

MRI-data were acquired in a 3T scanner (Siemens Skyra Magnetom) at the on-site MRI department of the Wellington Hospital, London (UK). fMRI data was acquired in 6 experimental sessions, using gradient-echo echo planar imaging (EPI) sequences. The fMRI parameters for all fMRI tasks (see fMRI paradigm below) were the same: TR = 1770 ms, TE = 35, 63 slices, matrix size = 84x84, slice thickness = 2.5mm), with the only difference across tasks being the number of volumes (command-following task: 225 volumes; tennis-task: 200 volumes; resting-state task: 170 volumes; tDCS with passive mobilisation: 678 volumes). In addition to the functional scans, I also acquired a high-resolution (1x1x1 mm) T1-weighted image (TR = 4, TE = 2, matrix size = 208x256x256), used for head anatomical reference and co-registration.

7.2.6. fMRI paradigm

At the beginning of each fMRI session, the patient was asked to perform a well-established motor-imagery tennis-task, adapted from (Owen et al., 2006), to detect the presence of covert command-following (Schiff, 2015b). The motor-imagery task fMRI paradigm utilised a block design with five 30-s active blocks, where the patient was asked to imagine himself playing tennis (cued by the word “tennis”), spaced out by five 30-s rest blocks, where the patient was asked to relax (cued by the word “relax”). In total, I collected 150s of active data and 150s of rest data. Following the tennis-task, the patient performed a motor command-following task (CF-task) and a resting-state scan. Both acquisitions were performed before and after the stimulation coupled with passive mobilisation of the thumb. Similarly to the tennis-task, the

CF-task also had a block design, with five 30-s active blocks spaced out by five 30-s rest blocks. In each active block, the patient was asked to try to move his right thumb five times (cued by the sentence "try to move your thumb"), with random interstimulus intervals of 6 ± 1 seconds. Each rest block was prompted by the word "relax". Noticeably, the same command-following task was used in our previous research to assess the effects of tDCS on the motor areas and on the thalamo-cortical axis (Chapter 4, Chapter 5). In the resting-state scan, the patient was asked to remain still and not think about anything in particular for five minutes.
As previously mentioned, I administered passive mobilisation to the patient's right thumb during brain stimulation. The design of the passive mobilisation was the same used in our previous study assessing the effects of multiple M1-tDCS sessions on healthy participants (Chapter 5), however, in the current case study passive movements were performed manually by the main researcher, instead of via an automatic passive-mobilisation device. Note that this choice was guided by the presence of limb rigidity in PDOC patients, which makes it particularly challenging to develop a custom-made and MRI-compatible device for administering passive mobilisation, akin to that used in Chapter 5.

Similarly to the motor-imagery and command-following fMRI-tasks used here and in Chapter 3 and 4, the tDCS with passive-mobilisation fMRI paradigm also had a block design, with 30 20-s "passive movement" blocks (with 7 movements per block, for a total of 210 passive movements administered during the 20 minutes of stimulation), spaced out by "relax" blocks of 20-s. Importantly, in contrast to my previous studies (Chapter 4, Chapter 5), in this case I did not record thumb movements in the scanner in any of the fMRI tasks. As I also highlight below, this was due to the presence of limb and hand rigidity in PDOC patients, which makes it difficult to use an MRI-compatible joystick for motion-tracking as I have done on healthy subjects.
Prior to each fMRI task, the patient listened to the task instructions (see **Table F1**). Auditory stimuli and instructions were played using MRI-compatible ear plugs with 30dB of noise suppression.

7.2.7. EEG and motion-tracking acquisition

EEG data was acquired at bedside, using the 128 channels Hydrocel Geodesic Sensor Net (Electrical Geodesics, Inc., Eugene, OR, USA) and Net Amps 400 amplifier, at a sampling of 1000 Hz, through the software Net Station Acquisition v5.4 (Eugene, OR). EEG impedance of all channels was inspected prior to the beginning of the experiment and kept below 50 kΩ and data was referenced to Cz at acquisition.

Motion-tracking data was acquired during the EEG active-task (see EEG paradigm below) using a Polhemus Patriot two-sensor 6DOF tracker (Colchester, VT), with an update rate of 60Hz. The Patriot sensors were secured to the patient's right thumb and index finger using paper tape, whereas the source sensor was placed on the overbed table next to the patient's bed, ensuring minimal interference of metallic objects in the line-of-sight with the sensors.

7.2.8. EEG paradigm

Each EEG session included a motor command-following task and a period of resting-state. The full instructions given prior to the beginning of each task can be found in **Table E1**. The command-following task was composed of 36 "move" trials and 36 "relax" trials, in alternating order, and had a total duration of about 9.6 minutes. Each "move" trial began with the instruction "Try to move your right thumb". Each instruction had a duration of 3.4 seconds and was followed by between 4- and 7-seconds of silence (randomly selected from a uniform distribution shuffled prior to the beginning of the experiment). After this period of silence, each "move" trial was followed by a "relax" trial, starting with the instruction "Stay Still" (lasting 1.8 seconds), and followed by between 3.5 to 4.5 seconds of silence (mean: 4 ± 0.4, randomly selected from a uniform distribution shuffled prior to the beginning of the experiment). After the command-following task, I asked the patient to try to remain still and not to think about anything in particular, and recorded five minutes of resting-state data.

7.2.9. Electrical Stimulation and Passive Mobilisation

Electrical stimulation was administered using a NeuroConn DC-STIMULATOR-MR for the MRI sessions and a DC-STIMULATOR for all the other sessions carried out at bedside (neuroCare Group GmbH, Germany). I used two squared electrodes (5x5 cm2) and a thin layer of electro-conductive Ten20® paste in order to increase conductivity. Electrodes were secured to the patient's scalp using rubber bandages provided with the NeuroConn stimulators. The active electrode was placed on the left motor cortex (left M1) whereas the reference electrode was placed over the right orbitofrontal area (Fp2 in the standard 10-20 system). To place the electrode over the left M1, I first identified the midpoint between inion and nasion, and then the midpoint between the left ear and the previously identified position. The resulting location roughly corresponds to the position C3 in the standard 10-20 system. Importantly, in the anodal session I placed the anode over C3 and the cathode over Fp2, whereas in the cathodal session I reversed this montage. In both anodal and cathodal sessions I stimulated the patient for 20 minutes at 1mA, and used a 30 seconds ramp-up period and a 30 seconds ramp-down. In the sham session, I randomly used anodal or cathodal montage, but stimulated only for 30 seconds, also using ramp-up and ramp down periods of 30 seconds, in line with well known protocols to ensure blinding (A. J. Woods et al., 2016b).

During all tDCS sessions (both at bedside and in the MRI scanner), I also administered passive mobilisation of the right thumb, in order to enhance tDCS effects on neural networks (Bolognini et al., 2009c). As mentioned above, differently from the experiment reported in Chapter 4, passive mobilisation to the patient was performed manually by a trained researcher, who was delivering full abduction-adduction of the participant's thumb. Passive movements were triggered by "beeps" played to the main researcher via MRI-compatible headphones during the MRI sessions, and through laptop speakers during the bedside sessions.

7.2.10. CRS-R assessment

Neurobehavioural assessment of the patient was carried out using the CRS-R, a standardised scale specifically developed for use in DOC patients (Giacino et al., 2004). The CRS-R assessments were administered either by a lead clinical neuropsychologist or a trained speech-

therapist. During each testing week, a total of 12 CRS-R assessments were carried out at different times. Specifically, CRS-R evaluations were carried out: prior to the first EEG session and prior to each tDCS session, and following tDCS sessions on the second, third and fourth day of each testing week (both right after the stimulation and after 60'). Importantly, on the second EEG session of each testing week (fourth day), the second CRS-R assessment following brain stimulation was administered after the EEG data collection. Moreover, administering the behavioural assessment after the MRI sessions was avoided, as this would likely be affected by fatigue.

7.2.11. fMRI preprocessing

The preprocessing of the fMRI data was performed using SPM12 on MATLAB 2018b (www.fil.ion.ucl.ac.uk/spm). First, I visually inspected the anatomical scan and all the functional scans acquired, and manually reoriented them. I then realigned and resliced all functional scans to the first image acquired, in order to control for motion artefacts and have all scans in the same space. Noticeably, volumes where realignment exceeded either a 2mm translation or a 2° rotation were subsequently excluded from the brain activation analysis. Following realignment, I applied a rigid-body transformation to co-register structural and functional data. Importantly, fMRI data was not normalised, as spatial normalisation of brains with structural lesions is greatly limited by the lack of correspondence between the patient's brain and the standardised template image used as a reference (Crinion et al., 2007). In addition to the above steps, I further preprocessed the resting-state data to improve its signal-to-noise ratio, performing the following operations using the Python library Nilearn (Abraham et al., 2014): dropping the first four volumes to remove high intensity signals usually present in the first seconds of an fMRI scan, detrending of the data to achieve stationary time-series by removal of scanner-induced drifts in the signal, low- and high- pass filtering (at 0.1 Hz and 0.001 Hz respectively) to preserve low-frequency connectivity signals, confounds removal (including 6 motion parameters output from the realignment and an extra regressor containing the list of volumes that exceeded the translation or rotation limits highlighted above), and standardisation. Finally, all functional images were smoothed with an 8mm Gaussian kernel.

7.2.12. fMRI motor-imagery, command-following and passive-mobilisation tasks analyses

Single-participant fixed-effect analysis was performed using a GLM in which I modelled each scan to belong to the "active" condition (i.e. blocks of "tennis", for the tennis-task, blocks of "move" for the command-following task, and blocks of "passive movements" for the passive mobilisation task) or to the rest condition. Importantly, I also included the realignment parameters as covariates of interest to account for residual motion related variance. Moreover, I also used a high-pass filter with a cut-off period of 80 seconds in order to remove slow-signal drifts from the functional time series. Finally, I set linear contrasts to obtain estimates of the effects of interest within each session, and I reported statistically significant voxels (i.e. surviving a family-wise error (FWE) corrected threshold of $p<0.05$ and an uncorrected threshold of $p<0.001$) in three regions of interest (ROIs): the left supplementary motor area (SMA), the left precentral gyrus (M1) and the left thalamus. Noticeably, for the motor-imagery task I focused only on SMA, as motor and spatial imagery tasks are known to be associated with fMRI activity predominantly within this area (Boly et al., 2007b; Monti et al., 2010; Owen et al., 2006). ROIs were extracted from the Automated Anatomical Labelling 3 (AAL3) Atlas (Rolls et al., 2020). In order to transform the ROIs from the MNI space to the native space, I first transformed the patient's anatomical scan used for coregistration to the MNI space (using the function SPM normalise) and applied the inverse of the transformation matrix to the ROIs. As mentioned above, normalisation procedures tend to perform poorly in the presence of structural abnormalities (Crinion et al., 2007). However, using large ROIs limited this issue, and, upon visual inspection, the resulting masks were found to be acceptably accurate.

7.2.13. Analysis of brain dynamics

In addition to the fMRI brain activation analyses, I also performed an exploratory effective connectivity analysis on the command-following task data, using the dynamic causal modelling (DCM) approach (Zeidman, Jafarian, Corbin, et al., 2019a), similarly to our previous study (Chapter 4).

I began the DCM analysis by visually selecting on the patient's anatomical scan (AC - PC oriented) the coordinates for the left M1, the left SMA and the left thalamus VOIs. I identified the left M1 and left SMA by using the central sulcus and the longitudinal fissure as anatomical landmarks, and by looking at the position of the tDCS electrode.

To identify the left thalamus, I first located the brain stem, then moved upwards on the Z plane and used the third ventricle as a guide until the remaining tissue of the thalamus was visible. Noticeably, I acknowledge that the presence of motion artefacts and extensive brain atrophies have impacted the precision of the manual selection of the VOIs.

Importantly, differently from the experiments reported in Chapter 4 and 5, as this was an exploratory analysis, I opted to exclude the cerebellum from the present DCM analysis in order to simplify the model and focus on thalamo-cortical connectivity only.

Once I identified the coordinates, I extracted the time series from spherical volumes centred on the aforementioned coordinates and with a radius of 4mm. Following time series extraction, I specified DCM models for each command-following task fMRI session, using the same DCM parameters adopted in Chapter 4, with the sole difference being the number of regions included in the model: one-state per region, bilinear modulatory effects, mean-centred inputs.

Finally, I specified multiple hierarchical models using the parametric empirical bayes (PEB) approach as in Chapter 4, and the same hierarchical structure adopted in Chapter 5, section 3.7.4. In brief, I ran three separate analyses, one assessing the effects of tDCS on Day1-MRI, one assessing the effects of multiple sessions (Day1-MRI pre vs Day5-MRI post) and finally one comparing the effects of one versus multiple sessions (Day1-MRI vs Day5-MRI). The posterior probability threshold for the PEB matrices in this study was set at a lower level of 0.55%, compared to 0.95% of the previous studies (Chapter 4, Chapter 5), to reflect the exploratory nature of the research. Lastly, I converted the self-connections (i.e. the diagonal elements in each DCM matrix) from their original unitless log-scale values to Hertz, and zero-centred them, to obtain the direction and magnitude of the change.

7.2.14. fMRI resting-state analyses

Seed-to-voxel connectivity analyses were performed on the resting-state time-series with the Python library Nilearn (Abraham et al., 2014). Seed-voxel connectivity substantially consists of extracting the BOLD time-course from a seed (or ROI) which is then used to calculate correlations with all the other voxels in the brain. The obtained correlation map of a single seed represents the pattern of correlation between a seed (i.e. the time-series resulting from the average of all voxels within the seed) and the entire brain (i.e. all the other voxels in the brain).

Here, I used three predefined seeds (i.e. spheres with a radius of 4mm), namely the left M1, the left thalamus and the PCC (these seeds are reported in **Figure 7.1**). The former two ROIs are included in order to look at the connectivity in the motor regions and, specifically, in the thalamo-cortical axis, as I had previously done (Chapter 3; Chapter 4). As mentioned above, the PCC represents a key region in the DMN and was therefore included in order to assess non-motor specific changes in brain connectivity.

The coordinates for the left M1 and left thalamus seeds were the same used in the DCM analyses described above. In order to define the coordinates of the PCC seed, I followed guidelines from (Coulborn et al., 2021) whereby I first moved 6mm in the x-axis from the anterior-commissure-posterior-commissure (AC-PC) and then identified the space between the marginal and parieto-occipital sulci, in the sagittal view. Finally, to identify the z coordinate of the PCC seed, I used a reference line crossing the upper boundary of the corpus callosum. The seed-to-voxel correlation analysis then extracts the time-series from the above-mentioned seeds, and computes the average time-series within each seed. These average time-series are then correlated to all the BOLD time-series at each voxel and seed-to-voxel correlation maps are produced (i.e. maps of Pearson's r correlation coefficient). Finally the seed-to-voxel correlation maps were converted to t-statistics and thresholded at $p < 0.001$ uncorrected (t-critical = 3.35).

7.2.15. EEG command-following preprocessing

The EEG command-following data preprocessing and ERD analysis was performed using the MNE-python library (v 1.0.3) (Gramfort, 2013). Firstly, data was filtered offline with a high-

pass cutoff of 1Hz and and a low-pass cutoff of 100Hz. Specifically, I used the overlap-add FIR filtering offered by the MNE method *filter()*, with an automatic filter length, a phase of zero, a hamming window and a "firwin" filter design. Moreover, in order to remove power line noise with minimal disruption to the signal, I also applied a zero-phase notch filter at 50 and 100Hz. I then segmented the data into 72 10-s long epochs around the "move" events (from -4s to 6s after the onset of each instruction), and trials containing obvious muscular artefacts were visually identified and removed (bad epochs). I then identified bad channels using the Random Sample Consensus (RANSAC) approach (Bigdely-Shamlo et al., 2015; Fischler & Bolles, 1981) implemented by the python-library Autoreject (Jas et al., 2017). In brief, Autoreject's implementation of RANSAC detects outlier electrodes by randomly creating subsets (inliers) of electrodes (25% of the total sensors) and interpolating the remaining ones from the inlier electrodes. This procedure is repeated 50 times, resulting in 50 time-series per electrode. Finally, RANSAC computes the median at each time point between these time series and correlates it with the real data: if the correlation is less than 0.75, the sensor is then considered an outlier (Jas et al., 2017).

After following the preprocessing steps discussed above, the resulting number of epochs included in the analyses of the six EEG command-following sessions was on average 22.5 ± 4, with 16.3 ± 5.1 channels being marked as bad per session.

Following filtering and bad channels removal, I referenced the data to a common average reference using MNE-python method *set_eeg_reference()*, which computes the average of the signal among all EEG channels and subtract it from the signal at every channel and for every time point. Following these procedures, in order to attenuate artefacts in the signal resulting from eye movements and blinks, I applied the Infomax algorithm (Amari et al., 1995), implemented in MNE-python, to the segmented data (after excluding bad trials and bad channels defined as per above). Clear components containing eye blinks were then visually identified and removed from the raw epoched data. Lastly, I performed the following operations on the cleaned epoched data: I applied a low pass filter with cutoff of 40 Hz, I interpolated electrodes that had been marked as bad, and finally re-referenced the data to common average.

7.2.16. Motion-tracking data preprocessing

Motion-tracking data from the two Polhemus Patriot sensors was used to calculate the euclidean distance between the electrodes at each timepoint. Euclidean distance time-series were then low-pass filtered at 25 Hz and displayed for exploratory purposes. In addition to this visual exploratory analysis, I calculated the coefficient of variation (CV) for each Euclidean distance time-series (that is, the ratio of the standard deviation to the mean: $\frac{s}{\mu} \times 100$), as an attempt to capture changes in movement variability across different sessions, that could be related to the brain stimulation. Moreover, I also calculated CVs for each trial "move" and each trial "rest" and ran a permutation test to assess whether there was a significant difference between variability of the signals for the move versus rest conditions.

7.2.17. EEG command-following spectral analysis

The power spectrum analysis was performed with a sliding time window approach on the single trials (Tallon-Baudry & Bertrand, 1999), using MNE-python function *tfr_multitaper(),* following recommendations by (Ferrante et al., 2022). The analysis was performed separately for each EEG command-following session, and, as this was an exploratory analysis, I did not run any statistical analysis. The analysis was targeted at frequencies between 8 and 30Hz (in 1Hz steps), and used a sliding time window of 500ms. Before calculating the discrete Fourier transform used to estimate the spectral power, a single discrete prolate spheroidal taper was multiplied to each time window, resulting in a spectral smoothing of ± 3Hz. The power for each frequency of interest was then estimated as the squared modulus of the Fourier transform and then the power estimates per trial were averaged. The relative change in power was obtained with respect to a baseline of -1 to -0.5s. More specifically, I used a *log-ratio* baseline correction which divides by the mean of baseline values and takes the log. Lastly, the change in power of each EEG channel in the mu (8-13 Hz) and beta (13-30 Hz) bands were averaged at each time point.

To assess whether a statistically significant difference in power was present within each EEG active session, I first started by creating two clusters of electrodes, left and right central (Figure E.2). I then computed the Time-Frequency Representations (TFR) as per above, using the

multitaper method and logratio baseline correction, for the mu and beta bands separately, per trial, and averaged across the clusters of electrodes separately. Lastly, for each EEG session, the TFR data was cropped to a specified time window (after baseline to 4s) and a 1-sample permutation t-test was run (p-value 0.05), to test the significant difference between baseline and movement periods (i.e., difference different from 0). In total, 24 1-sample permutation t-tests were run (four per EEG session). TFRs averaged per electrode cluster are reported in Figure E.3.

7.2.18. EEG resting-state preprocessing and analysis

EEG resting-state data was analysed in MATLAB using the publicly available MOHAWK toolbox https://github.com/srivaschennu/MOHAWK (Chennu et al., 2014, 2017; Delorme & Makeig, 2004; Oostenveld et al., 2011) following the same preprocessing and feature extraction procedures as done in previous studies of resting-state EEG and DOC patients (Chennu et al., 2014, 2017; O'Donnell et al., 2021). In brief, resting-state EEG data was first filtered between 0.5 and 45Hz and then segmented into 10-s epochs. Following filtering and epoching, electrodes and epochs with excessive artefacts were removed in a semi-automated manner, combining visual inspection of the data and ICA.

Lastly, the EEG data was then re-referenced to a common average reference. Following this standard preprocessing pipeline, MOHAWK performs EEG feature extraction (spectral phase, power and graph-analysis) for five frequency bands: delta (0-4 Hz), theta (4-8 Hz), alpha (8-13 Hz), beta (13-30 Hz) and gamma (30-45 Hz). Noticeably, MOHAWK restricts the analysis to 91 channels out of the original 128 channels present in the Geodesic GSN-HydroCel-128 montage. For each frequency band, connectivity between all channels is estimated using the debiased weighted phase lag index (dWPLI) (Vinck et al., 2011). dWPLI is an improved version of the phase lag index (PLI) (Stam et al., 2007), which is supposedly less sensible to uncorrelated noise sources and volume conduction, and has increased statistical power to detect changes in phase-synchronisation (Vinck et al., 2011). The dWPLI connectivity analysis

outputs five 91x91 channel-pair matrices per EEG resting-state session, which are then used for the calculation of graph-derived metrics at each frequency band.

Importantly, the graph-derived metrics are calculated upon graph binarisation, which is performed at proportional network densities ranging from 100% to 10% in steps of 0.25 (i.e. all connections are kept, or only the strongest 10% of the connections are kept). In line with (O'Donnell et al., 2021), I averaged graph metrics over network density thresholds from 90% to 10%, and I focused on those graph metrics and spectral measures that have been observed to provide some diagnostic and/or prognostic information with regards to DOC patients: relative alpha and delta power (average across all channels), median connectivity (dWPLI) across all channels (alpha and delta bands), modular span in the alpha band, standard deviation of the participation coefficient across all channels in the alpha band, clustering coefficient in the delta band (mean across all channels) and modularity in the delta band. Briefly, modular span is a novel graph-derived measure that was introduced by (Chennu et al., 2014) and measures the average weighted topographical distance (in centimetres, over the scalp) spanned by a module in a network. Instead, modularity quantifies the degree to which nodes in the graph can be divided into smaller, highly connected and topologically distinct modules (i.e. modules with relatively few inter-modular connections) (Chennu et al., 2014). Following a graph decomposition into modules, participation coefficient then quantifies network centrality in terms of inter-modular connectivity, that is, nodes that link many modules together will have a high participation coefficient (Chennu et al., 2014). Lastly, clustering coefficient quantifies the amount of connected triangles in a network, hence capturing local efficiency (Stam et al., 2007).

7.3. Results

Since this is a single-subject case study, no comparisons across conditions were run (with the exception of the PEB analyses). Instead, first-level results are reported and tDCS effects are discussed qualitatively. I will first discuss the fMRI and EEG baseline results, and then move on to describing the effects of tDCS.

7.3.1. fMRI assessment of consciousness at baseline

In comparison to the rest condition, neither the fMRI motor-imagery task (i.e., the tennis task) nor the command-following task (i.e. thumb movements) elicited any significant activation at p<0.05 FWE corrected. However, after lowering the threshold to p < 0.001 uncorrected, few significant clusters could be observed (**Figure 7.3**, **Table 7.1** and **7.2**). In particular, compared to the rest condition, the motor imagery task (imagine playing tennis) led to significant clusters of activation (p < 0.001 uncorrected) within the SMA ROI only in one session (Cathodal Day-1) out of the total 6.

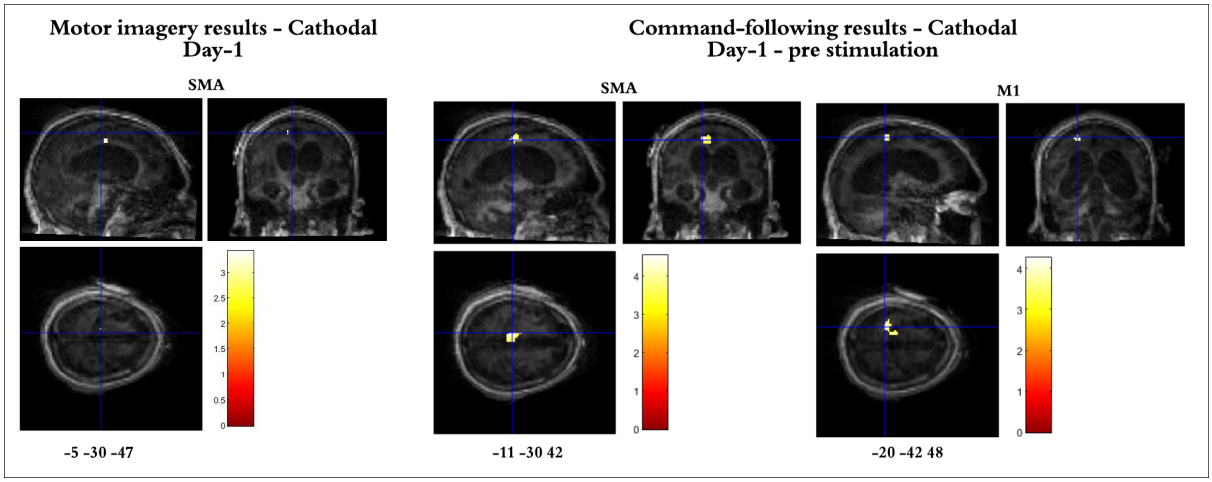


Figure 7.3. Brain activation results for the motor-imagery task (SMA ROI) and command-following task (SMA and M1 ROIs). Results are shown at p < 0.001 uncorrected. Colour bars represent the t-statistic.

Table 7.1. *Brain activation during motor-imagery (Cathodal Day-1).*

Region	**Cluster Size (mm3)**	**Peak P *uncorrected***	**Peak stat. (T)**	**Coordinates (X Y Z)**

SMA	109	< 0.001	3.39	-6; -22; 40
	31	< 0.001	3.19	-11; -27; 47

Notes: coordinates are reported in the patient's volume space. Results are reported at $p < 0.001$ uncorrected.

Table 7.2. *Brain activation during command-following (Cathodal Day-1, before stimulation).*

Region	**Cluster Size (mm3)**	**Peak P *uncorrected***	**Peak stat. (T)**	**Coordinates (X Y Z)**
M1	562	< 0.001	4.26	-21; -42; 48
	78	< 0.001	3.69	-26; -20; 42
	78	< 0.001	3.52	-13; -27; 47
	15	< 0.001	3.19	-16; -37; 43
	15	< 0.001	3.19	-26; -25; 45
	15	< 0.001	3.14	-18; -30; 45
SMA	1031	< 0.001	4.53	-11; -30; 43

	187	< 0.001	3.57	-1; -5; 34

Notes: coordinates are reported in the patient's volume space. Results are reported at $p < 0.001$ uncorrected.

7.3.2. EEG ERDs assessment of consciousness at baseline

From a visual inspection of the ERD results in each EEG baseline session, I could not observe any difference in the magnitude of the *mu* and *beta* band oscillations before and after the "move" instruction. As such I did not find evidence consistent with specific response to command at baseline. Examples of the results of the EEG ERDs analysis (for anodal stimulation only) can be found in **Figure 7.4**.

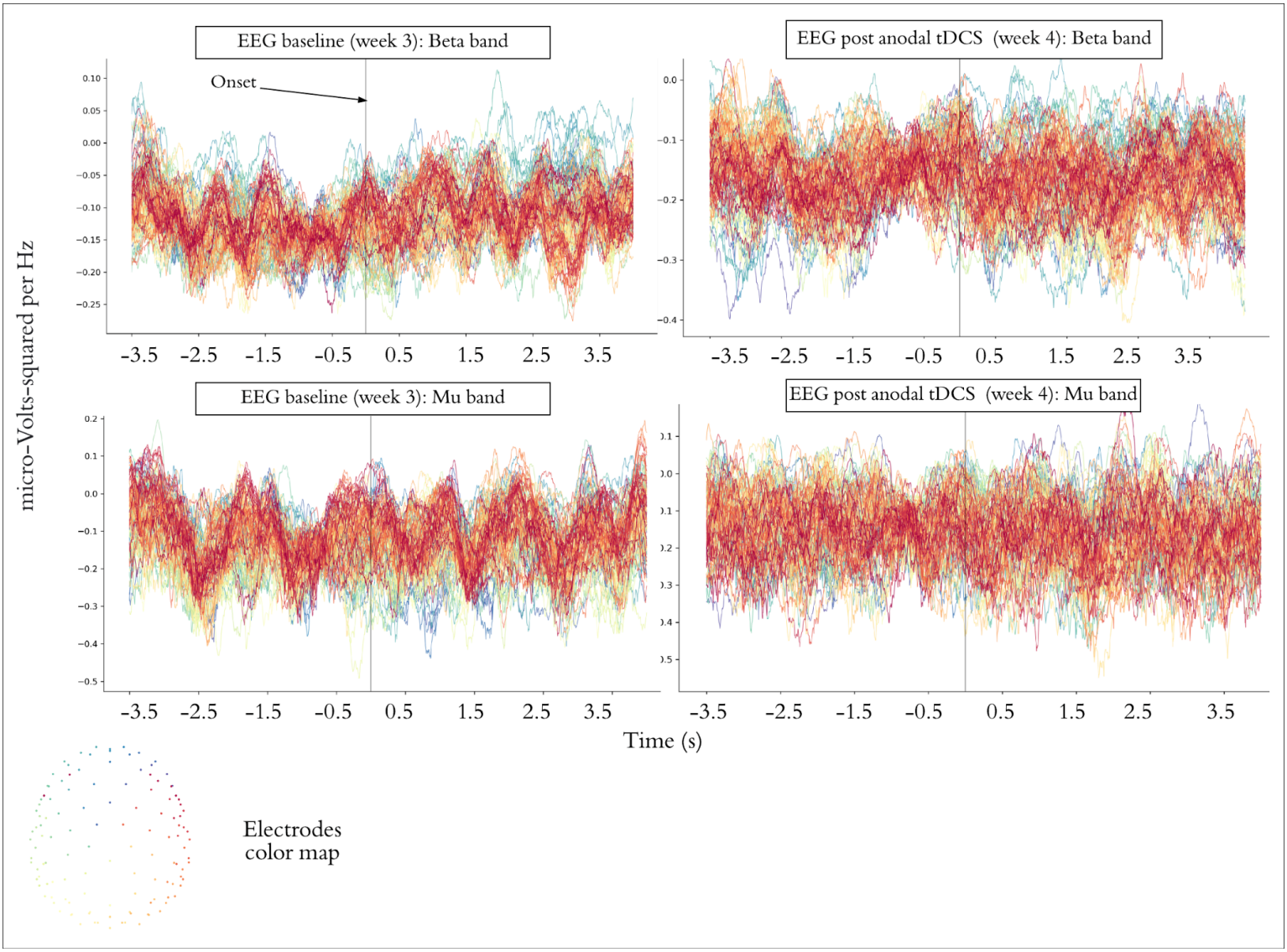


Figure 7.4. Results of the ERD analysis for the EEG command-following task, for the third (EEG baseline) and fourth (EEG post anodal tDCS) weeks of testing (i.e., anodal stimulation). Each line represents one electrode, which colours are represented in the electrodes colour map in the bottom left.

7.3.3. Effects of tDCS on CRS-R

CRS-R scores (single scales and totals) are illustrated in **Figure 7.5**. Total CRS-R scores ranges were 4-9 in the sham testing week, 4-10 in the anodal testing week, and 5-9 in the cathodal testing week. Overall, no particular trends are observed that can be associated with tDCS, however, some small but consistent improvements are present following anodal-tDCS on Day-2, Day-3 and - although less markedly - on Day-4.

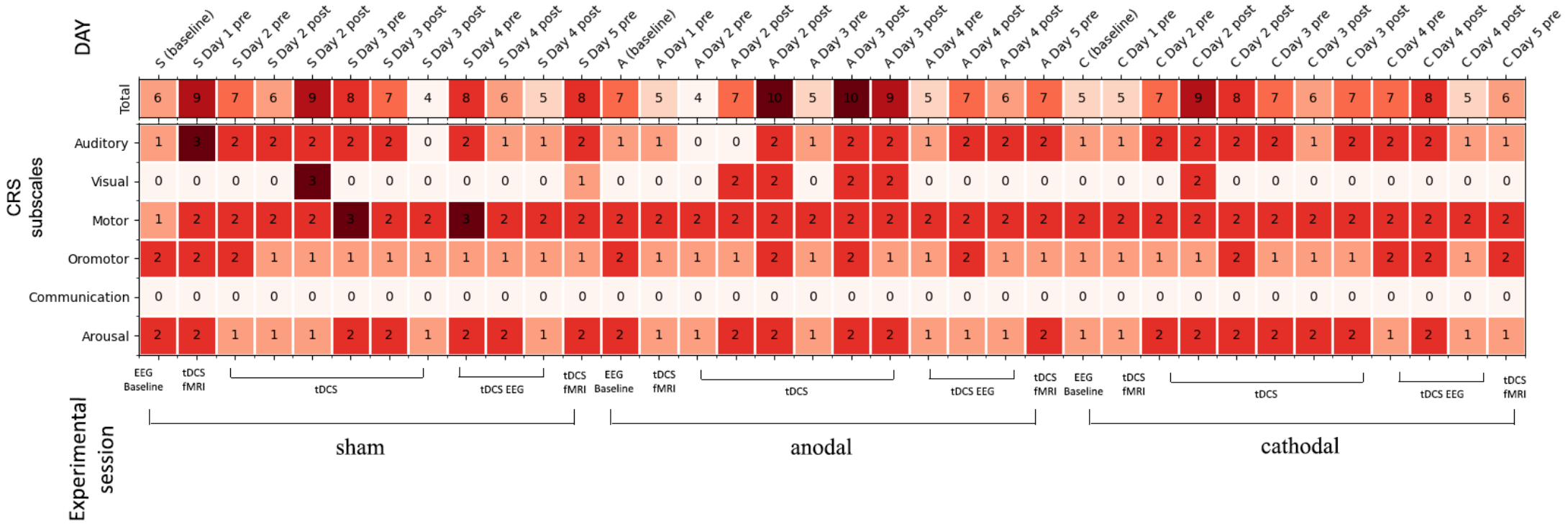


Figure 7.5. CRS-R results. A total of 36 CRS-R assessments were conducted throughout the course of the experiment. The results of each evaluation are presented for each CRS-R subscale individually, as well as for the CRS-R total (top axis). The day of the assessment is reported at the top of the figure. Day 2, 3 and 4 have two "post" CRS-R assessments, as I carried out one assessment right after the stimulation and a last assessment 30' after the stimulation. The day named as "baseline" refers to the baseline EEG sessions, where no tDCS was administered. The experimental sessions are reported at the bottom, following the naming scheme of **Figure 7.2**. Abbreviations: A, anodal; C, cathodal; S, sham.

7.3.4. Effects of M1-tDCS on brain activation and dynamics

With respect to the command-following fMRI task post tDCS, our standard GLM analysis did not reveal any significant cluster for the contrast "move > relax", neither at $p < 0.05$ FWE nor $p < 0.001$ uncorrected.

Passive-mobilisation of the right thumb led to significant clusters ($p < 0.001$ uncorrected) of activation in the SMA ROI only, on Day-5 of the sham stimulation week and Day-1 of anodal stimulation week (**Table 7.3**).

Our three PEB analyses on the command-following fMRI task revealed a decrease in M1 to SMA connectivity following one session of anodal-tDCS as compared to one session of cathodal-tDCS, and an increase in thalamus to SMA connectivity following one anodal-tDCS session as compared to one sham-tDCS. Comparing Day1-MRI pre-stimulation to Day5-MRI post-stimulation did not show any significant change in effective connectivity. Lastly, when comparing the effects of one session to those of five (i.e. Day1-MRI vs Day5-MRI), I observed an increase in the connectivity from M1 to SMA following five anodal-tDCS sessions as compared to five cathodal-tDCS sessions (**Figure 7.6**).

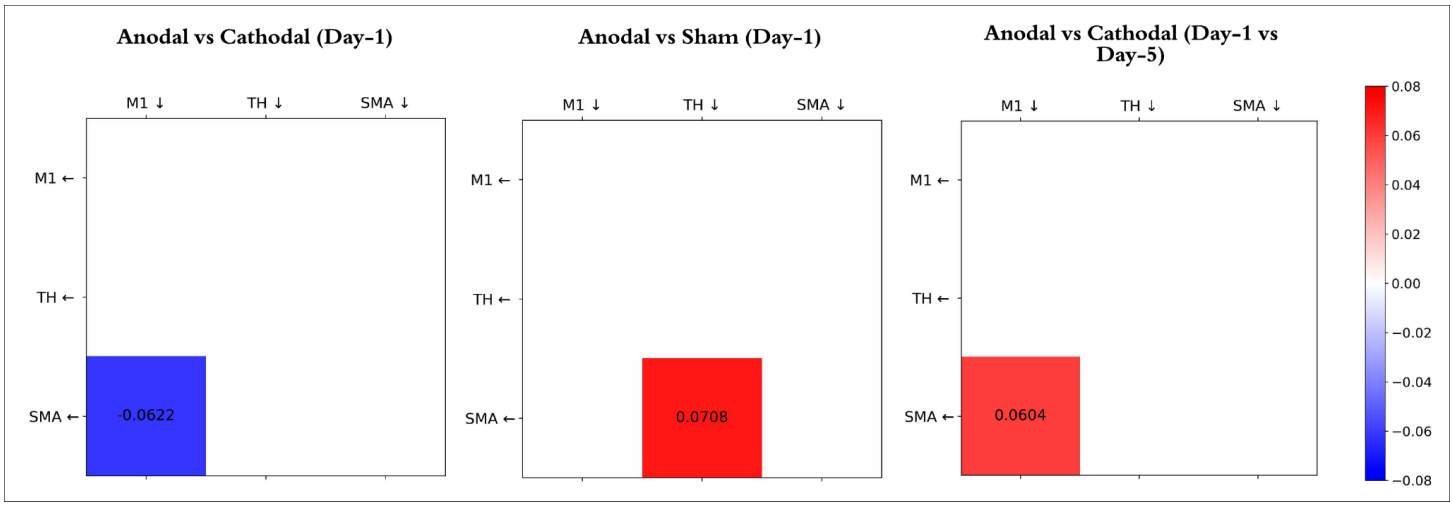


Figure 7.6. The figure shows the effects of M1-tDCS on functional neural dynamics. Connections were

thresholded at a posterior probability of 0.55%. The direction of the connectivity is column to row (e.g., there is a decrease in M1 to SMA connectivity after one anodal tDCS as compared to one cathodal tDCS session).

Table 7.3. *Brain activation during passive-mobilisation.*

Day and stimulation polarity	**Region**	**Cluster Size (mm3)**	**Peak P *uncorrected***	**Peak stat. (T)**	**Coordinates (X Y Z)**
Sham Day-5	SMA	31	< 0.001	3.18	-1; 0; 37
Anodal Day-1	SMA	31	< 0.001	3.27	-9; 7; 36

Notes: coordinates are reported in the patient's volume space. Results are reported at $p < 0.001$ uncorrected.

7.3.5. Effects of M1-tDCS on resting-state fMRI

The seed-to-voxel correlation analysis identified statistically significant clusters for the PCC seed only, in the resting-state session following the first anodal stimulation (i.e. Anodal Day-1, post stimulation), with Perarson's R correlation values ranging from 0.26 to 0.28. From visual inspection of the seed-to-voxel correlation map superimposed on the patient's brain MRI scan, the significant clusters appear to be within the right PCC/precuneus and cerebellar areas (**Figure 7.7**).

Table 7. 4. *Results for the seed-to-voxel correlation analyses (Anodal Day-1, post stimulation).*

Region	**Cluster Size (mm3)**	**Peak P *uncorrected***	**Peak stat. (T)**	**Coordinates (X Y Z)**
PCC	1234	< 0.001	3.61	20 -55 36
	953	< 0.001	3.50	7 -48 33
	-	< 0.001	3.56	8 -52 -19
	515	< 0.001	3.50	34 -30 28
	109	< 0.001	3.43	26 -72 21
	93	< 0.001	3.42	18 -60 34
	15	< 0.001	3.36	28 -62 16

Notes: coordinates are reported in the patient's volume space.

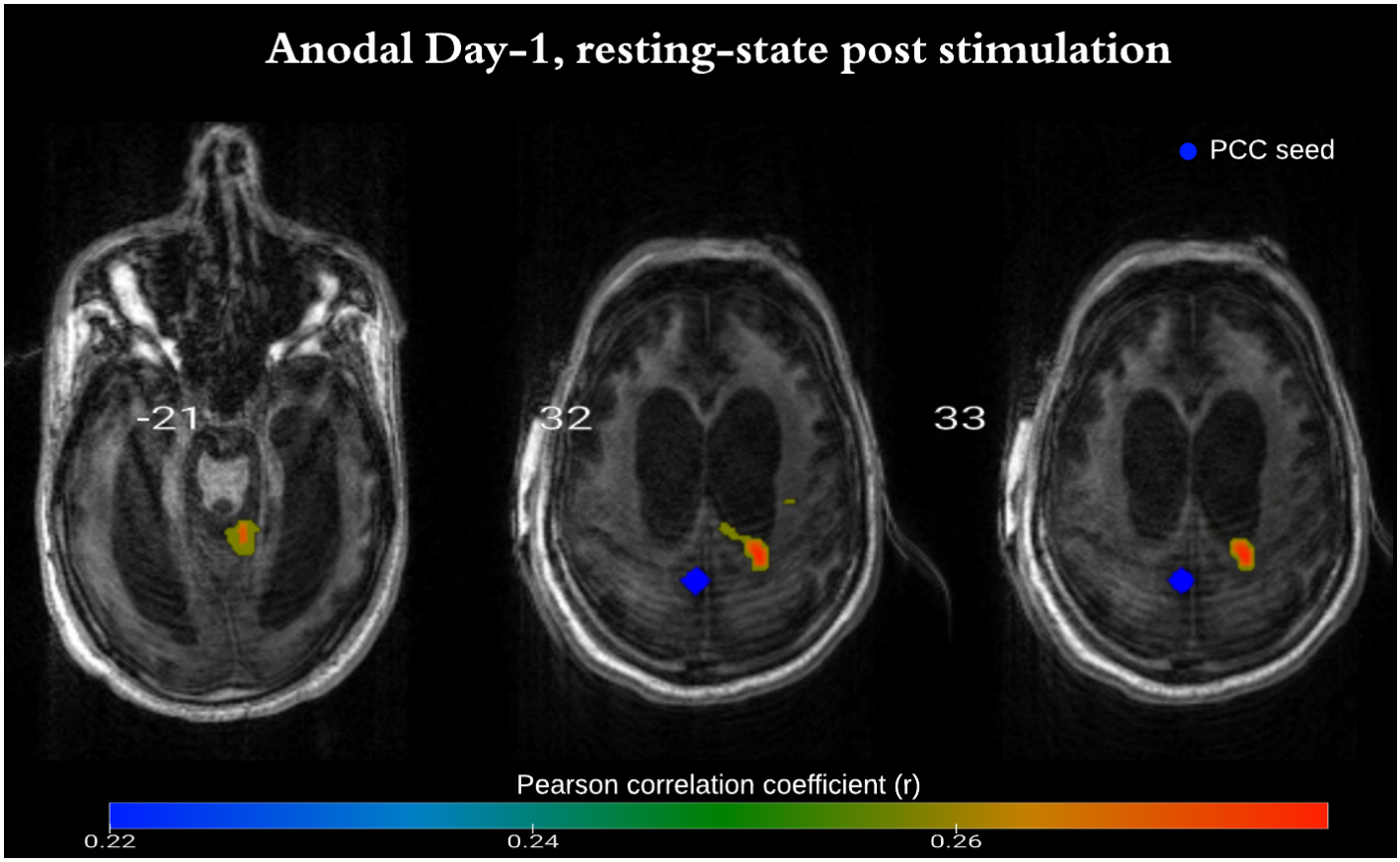


Figure 7.7. Results of the seed-to-voxel connectivity analysis with the left PCC seed (reported in blue) for the resting-state session following the first anodal M1-tDCS (Day-1). The Pearson's r correlation coefficient map was thresholded to display only correlations with an associated p-value of < 0.001 uncorrected.

7.3.6. Effects of M1-tDCS on motor-responses

No motor-response could be observed from visual inspection of the time-series. The coefficients of variation at baseline and after four days of stimulation were 2.90 - 10.80 (sham), 2.56 - 3.34 (anodal), 7.36 - 6.89 (cathodal). Examples of the motion tracking data (for anodal stimulation only) can be found in **Figure 7.8**. Averaged time-series for the motion tracking data, along with standard deviation, are shown in **Figure 1 Appendix E**. Permutation tests to

assess difference in signal variability across the “move” and “relax” trials did not result in any statistically significant difference ($p < 0.05$).

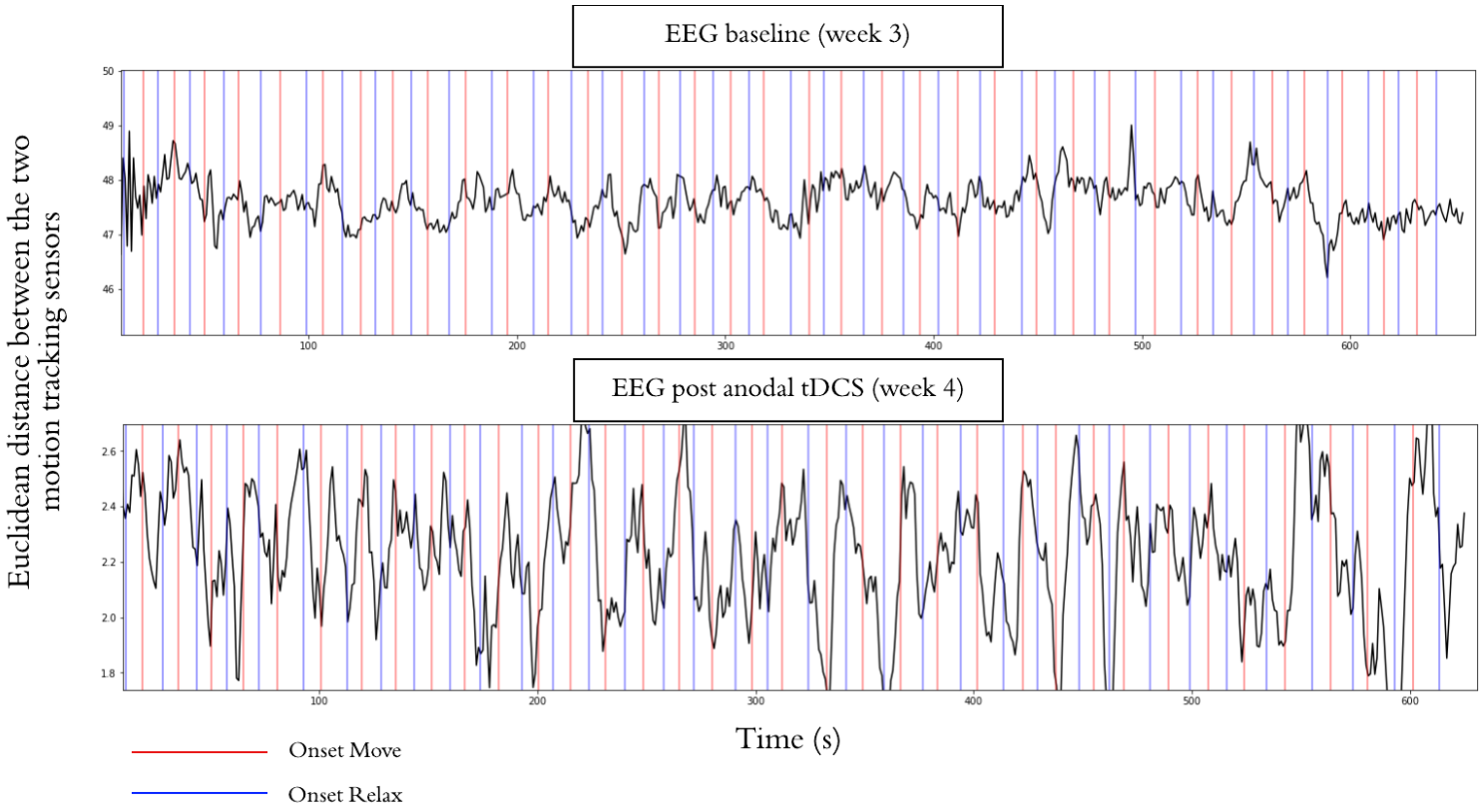


Figure 7.8. Motion tracking data (euclidean distance between the two motion tracking sensors) for the EEG command-following task of week 3 (EEG baseline) and week 4 (after anodal tDCS). The onsets for the instructions “move your thumb” and “relax” are represented as red and blue vertical lines, respectively.

7.3.7. Effects of M1-tDCS on EEG ERDs

I could not observe any difference in the magnitude of the mu and beta band oscillations before and after the "move" instruction in any EEG post-tDCS session. As such, there was no difference in terms of ERDs between the baseline and post-tDCS EEG sessions. I can therefore exclude an effect of tDCS on the patients' response to command as measured with EEG ERDs. This lack of difference in ERDs between baseline and post-tDCS EEG sessions can be observed in **Figure 7.4**.

No significant clusters of activation were found in any of the 1-sample permutation t-tests run. Two examples of permutation t-test maps are reported in Figure E.4.

7.3.8. Effects of M1-tDCS on resting-state EEG spectral power, connectivity and graph-theoretic metrics

Values of relative spectral power, connectivity and graph-derived measures for each EEG resting-state session are shown in **Figure 7.9**. In general, no particular trend can be observed in any of the metrics included in the analyses, due to the great variability across sessions.

However, some noteworthy increases following four sessions of anodal- and cathodal-tDCS were present in the alpha-band median connectivity (from 0.118 to 0.299 for anodal, and from 0.011 to 0.120 for cathodal) and in relative alpha power (from 1.1956 to 1.657 for anodal and from 0.385 to 1.344 for cathodal).

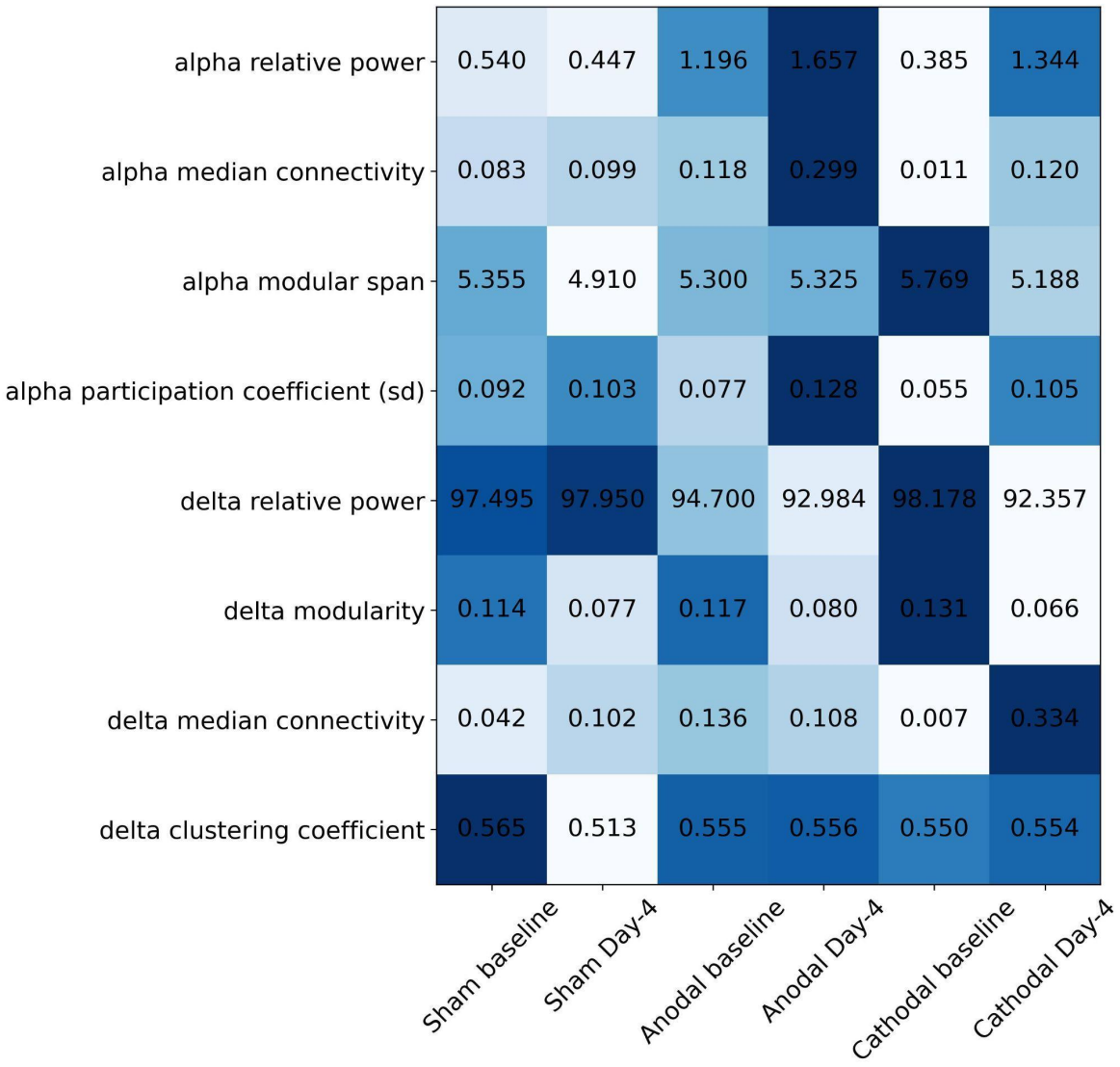


Figure 7.9. Results of the resting-state EEG analyses. Note that *baseline* refers to the EEG baseline (panel 1 in **Figure 7.2**) and Day-4 refers to the EEG session following the fourth day of tDCS stimulation (panel 4 in **Figure 7.2**) .

7.4. Discussion

To the best of our knowledge, this was the first case study on PDOC using a complex multi-modal (fMRI, EEG and motion-tracking) and multi-session tDCS design. As such, this case study serves as a preliminary proof-of-concept that such methods can be safely applied to PDOC patients. In fact, no safety or health concerns occurred during the experiment, and the patient tolerated all tDCS sessions (both in the MRI scanner and at bedside) as well as the fMRI and EEG assessments. Crucially, this indicates that future studies could safely include multiple neuroimaging modalities and assess the effects of multiple tDCS sessions on a larger sample of patients. However, it is important to mention that the Neurological Rehabilitation Centre where the study took place represents an ideal research setting in that both the MRI scanner and EEG device are available at the same location where the patient was hospitalised (i.e., minimal transfer is required for MRI and EEG testing).

The patient included in this case study had a clinical diagnosis of UWS due to severe cerebral atrophy and gliosis. The CRS-R assessments administered during the study kept up with the diagnosis of UWS, with total CRS-R values ranging from 4-10 out of 23, with the communication scale always scoring 0.

The fMRI and EEG results were in line with the diagnosis of UWS and did not provide any evidence of covert cognition. Specifically, the fMRI motor-imagery task did not reveal any consistent cluster of activation within the SMA, in any of the six MRI sessions ($p<0.05$ FWE), which would be instead expected in PDOC patients who retain a certain level of covert cognition (Bodien et al., 2017; Monti et al., 2010; Owen et al., 2006).

In line with the fMRI motor-imagery task, the fMRI command-following task also failed to elicit significant activation within the SMA and M1 ROIs. Despite this, when the statistical threshold was reduced to $p < 0.001$, both tasks revealed significant clusters in one fMRI session (pre-cathodal tDCS). It is however probable that the presence of such clusters in only one fMRI session is a result of the low threshold used and not a true positive finding. This lack of activation during the command-following task might also explain the overall lack of effect of

the stimulation on brain effective-connectivity, with changes in connectivity being present only at low posterior probability thresholds (**Figure 7.6**).

Importantly, the overall lack of positive findings in the motor-imagery and command-following tasks do not necessarily rule out the presence of covert cognition, as false negative findings are not rare in fMRI studies (Owen et al., 2006). For instance, a previous study tested both a hand-squeezing fMRI-task (similar to the command-following task used here) as well as the same fMRI tennis playing paradigm used here, on healthy participants and PDOC patients with behavioural evidence of command-following (MCS+) and without it (coma, UWS, MCS-) (Bodien et al., 2017). The authors reported fMRI covert command-following in 2/3 MCS+ patients and 7/10 healthy controls, using the hand-squeezing task, and in 0/3 MCS+ patients and 9/10 healthy controls, using the tennis playing paradigm. Moreover, another study using a hand-raising fMRI task reported that 1/7 MCS+ patients could adjust their brain activity in response to the commands (F. Wang et al., 2019). These results highlight that fMRI methods for measuring motor imagery frequently fail to detect command following in individuals where this would be expected to be found (i.e., healthy subjects, MCS+ patients). In consideration of the above evidence, the lack of covert command-following in fMRI paradigms cannot rule out the presence of covert awareness, and results from such paradigms should be interpreted with caution.

This notwithstanding, in addition to the above considerations on the fMRI motor-imagery and command-following tasks, it is important to notice that our EEG command-following task also did not show evidence of specific response to command (i.e. ERDs consistently time-locked to the "move" commands), which was also the case for the motion-tracking data (with the latter being expected given diagnosis of the patient). A similar task was previously used by (Cruse et al., 2012) on a UWS patient, and reliable modulations in sensorimotor beta rhythms in response to commands were observed. Furthermore, similar command-following motor tasks were also used by (Cruse et al., 2011), and markers of motor imagery were observed in 9/12 healthy controls. The evidence from the previous two studies highlights that - similarly to fMRI motor-imagery and command-following tasks - in EEG command-following tasks, the lack of ERDs cannot rule out covert awareness. In fact, as observed by (Cruse et al., 2012), ERDs in

motor tasks present great single-subject variability (in terms of frequency bands, time-course and laterality) even in healthy participants, such that reliable mu/bands modulations are not always detectable (Guger et al., 2003). Overall, while the presence of consistent brain responses to command-following tasks - either in their EEG or fMRI implementations - in a PDOC patient would suggest covert awareness, the lack of such responses cannot exclude it. In fact, as also mentioned above, active paradigms are limited by PDOC patients' fluctuations of attention, as well as by the presence of sensory and motor deficits (Duszyk-Bogorodzka et al., 2022). As a result, it can be inferred that some patients may experience difficulty in adhering to task instructions or actively participating in the task, despite maintaining a certain degree of awareness. However, it is important to mention that in the above studies, patients' evaluation of awareness was typically based on one fMRI/EEG session only. Instead, in the present case study, awareness was assessed multiple times during six weeks of testing (i.e., through 6 fMRI motor-imagery tasks, 12 command-following fMRI tasks and 6 command-following EEG tasks). Therefore, even though the above points about negative findings remain valid, it is unlikely that the patient of this case study was covertly aware.

Crucially though, this also implies that the patient supposedly did not perform any command-following task, hence they did not represent an ideal candidate for our stimulation protocol, as I specifically focused on changes in brain activation and dynamics during the command-following task. In fact, our GLM analyses are all centred on the difference in activation between the active versus rest blocks (see section 7.2.12 above). It might be the case that these analyses are less sensitive to the effects of tDCS on brain activation if patients are not performing the task and more emphasis should be placed on alternative measurements (e.g., resting state) in these cases.

Another aspect to consider is related to one clinical feature of the patient, that is the presence of stimulus sensitive myoclonus, which could be interpreted in two ways. In the case that this feature had a brainstem basis, it would predict a response according to our hypotheses explained above. However, if this feature had a cortical basis, the response would be less likely in line with our hypotheses.

Additionally, our intervention protocol is aimed at PDOC patients with CMD specifically, in that it is not meant to restore awareness but rather to bridge the link between the remaining covert function and the external responsiveness.

Some noteworthy changes were observed in the resting-state EEG alpha relative power and connectivity following four sessions of anodal and cathodal stimulation. Even though caution must be taken when interpreting the above results, it is interesting to note that previous authors have consistently observed a positive correlation between alpha relative power and CRS-R scores (Chennu et al., 2014; Rossi Sebastiano et al., 2015; Sitt et al., 2014; Stefan et al., 2018). Alpha relative power also represents a good indicator of recovery in UWS patients (Babiloni et al., 2009; Stefan et al., 2018). Moreover, alpha connectivity is also normally reduced in UWS patients as compared to MCS patients and healthy controls (Chennu et al., 2014; Höller et al., 2014; Sitt et al., 2014), hence, an increase in alpha connectivity might indicate a tendency towards less disrupted alpha oscillations.

In addition to the resting-state EEG results, the fMRI resting-state seed-to-voxel analysis demonstrated significant findings following one anodal-tDCS session, related to the correlation between the left PCC seed and voxels (supposedly) within the right PCC and the cerebellum. As mentioned above, the PCC is a central area in the DMN, a network whose residual functional connectivity has been shown to reflect clinical severity in UWS and MCS patients (Crone et al., 2011; Demertzi et al., 2015; Vanhaudenhuyse et al., 2011). Moreover, DMN resting-state functional connectivity in PDOC patients has been positively associated with the level of consciousness, with the peak of significance for the correlation between connectivity and consciousness being within the PCC area (Vanhaudenhuyse et al., 2010). As such, the above results suggest that anodal-M1 tDCS might also impact PCC functional connectivity and that this could have therapeutic value in some PDOC patients.

On the other hand, the higher connectivity between the PCC seed and the cerebellum might indicate a trend towards an overall increase in cerebellar-DMN coupling. Traditionally, the cerebellum has been mainly studied with regard to motor functions, such as motor learning and control (W. Guo et al., 2015). However, it has been recently observed that the cerebellum is

also functionally coupled with the prefrontal cortex, suggesting that it participates in circuits involved in non-motor functions, including fronto-cerebellar networks interacting with the DMN (Krienen & Buckner, 2009). This notwithstanding, cerebellar-DMN connectivity has not been investigated in PDOC patients, and its clinical significance is unclear.

Overall, the effects of anodal-M1 tDCS on PCC connectivity might be linked to the low spatial resolution of canonical tDCS. In fact, one of the drawbacks of canonical tDCS (as compared to HD-tDCS) is the widespread diffusion of the induced electric field, which goes beyond the stimulated area (as discussed in Chapter 2, sections 2.8.1 and 2.8.2). For instance, a recent study investigating the effects of multiple sessions of tDCS over the left DLPFC in 11 MCS patients found increased rs-fMRI functional connectivity in multiple regions distant from the targeted area, among which the precuneus (Peng et al., 2022). Thus, the presence of more generalistic effects of M1-tDCS (i.e., in the EEG and fMRI resting-state derived measures rather than in the motor-imagery and command-following tasks) could be attributed to the overall lack of spatial specificity of tDCS, as well as to the low precision of electrode placement in patients with brain lesions.

This notwithstanding, due to the patient's widespread brain atrophies and dilation of the ventricles, it is difficult to attribute the above changes in EEG and fMRI resting-state measures to the stimulation of the motor cortex, as the severe brain abnormalities have led to important anatomical changes. That said, as observable from **Figure 7.1**, our selected ROI for the M1 region did roughly sit under the tDCS electrode. However, it is important to notice that functional reorganisations following brain injuries are possible (Reddy et al., 2002) and might further complicate relating the stimulation to the resting-state changes. Moreover, as highlighted by (Marino et al., 2016), the great signal contamination due to artefacts and noise severely limit the study of spontaneous BOLD signal fluctuations in PDOC patients. Moreover, the head-motion artefacts present in the anatomical scan of the patient also makes it hard to identify the location of the significant clusters. Despite these limitations, these findings highlight that even when no changes in motor responsiveness are present, tDCS might still have

an effect on brain activity and dynamics. As such, different tDCS montages might still be beneficial for patients who do not show signs of covert awareness.

It is however critical to consider that, similarly to our previous multi-session tDCS study on healthy participants (Chapter 5), the increased specificity of our stimulation protocol derives from the engagement of the motor areas due to the passive mobilisation administered alongside tDCS (as opposed to tDCS administered at rest, as in Chapter 4. However, in the current case study I only observed neglectable clusters of activations in two out of the six passive-mobilisation sessions carried out in the MRI scanner (as reported in **Table 7.3**). Hence, it is possible that our passive-mobilisation protocol was not sufficient to elicit a response in the motor areas and that, in turn, this might have reduced the effects of tDCS on the thalamo-cortical axis, as also confirmed by an overall lack of effect on motor network effective connectivity. Additionally, it is also likely that the effects of tDCS on this patient might be drastically limited by the severe neuronal loss and consequent lack of neuronal circuitry due to the diffuse brain atrophy and gliosis.

This was the first study administering tDCS in a PDOC patient in the MRI scanner, as well as assessing tDCS effects with fMRI. Overall, while I cannot draw conclusions on the therapeutic value of tDCS from this single-patient case study, I provided evidence for the feasibility of a multi-session and multi-modality tDCS study in PDOC. Moreover, the design of the current study allowed for a detailed characterisation of the effects of tDCS in PDOC through fMRI and EEG active- and passive-tasks, while also evaluating the patients' level of awareness on multiple time-points during the study (hence accounting for normal fluctuations in patients' arousal). Importantly, detecting patients' awareness using also neuroimaging methods helps overcome the limitations of the more broadly used behavioural assessment scales (e.g., the CRS-R), therefore allowing for a more precise characterisation of tDCS effects on consciousness. Our results might influence the design and analysis pipeline of future clinical trials involving a higher number of patients, to better define the neural, behavioural and clinical effects of tDCS on PDOC, as well as the underlying mechanisms behind inter-subject variability in terms of responsiveness to tDCS (Fernández-Espejo et al., 2020). Future research

on larger samples of UWS and MCS patients is needed to determine the real therapeutic value of multiple-sessions of M1-tDCS.

Note that the appendix to this chapter can be found at the end of the thesis (Appendix E).

Chapter 8

GENERAL DISCUSSION

8.1. Summary of aims and results

This work aimed: 1) to explore the effects of different tDCS protocols on thalamo-cortical effective connectivity during command-following, using fMRI (Chapters 4-5), 2) to investigate inter-individual variability in tDCS-induced thalamo-cortical changes through MRI-derived electric field models (Chapter 6), and 3) to test the feasibility of a multi-modal multi-session tDCS intervention on a PDOC patient (Chapter 7).

In Chapter 4, I assessed motor-network effective connectivity changes during a command-following task following a single-tDCS session over the left M1 (*Experiment 1*) and the right cerebellum (*Experiment 2*). Anodal M1-tDCS led to a reduced thalamic self-inhibition (polarity-specific change), and a reduced M1 to thalamus excitation (non-polarity specific). On the other hand, cathodal M1-tDCS led to increased excitation both from thalamus to M1 (non-polarity specific) and from thalamus to SMA (polarity-specific). In turn, anodal cb-tDCS increased thalamic and M1 self-inhibitions (polarity-specific), while also decreasing M1 to thalamus excitation and increasing SMA to thalamus (non-polarity specific). Conversely, cathodal cb-tDCS led to an increase in M1 self-inhibition (non-polarity specific), an increase in thalamus-to-M1 excitation (polarity-specific), and a non-polarity specific increase in SMA to thalamus excitation.

In Chapter 5 (*Experiment 3*), I investigated the same effects, but used a multi-session M1-tDCS protocol, and coupled the stimulation with passive mobilisation of the thumb. A single-session of anodal-tDCS reduced M1 self-inhibition and increased thalamus-SMA inhibition (non-polarity specific), while cathodal-tDCS increased thalamic self-inhibition and thalamus to SMA inhibition. Multiple sessions of tDCS (both polarities) decreased M1 self-inhibition, while reversing the thalamus to SMA effect.

Chapter 6 investigated the relationship between current density injected by the stimulation and the changes in thalamo-cortical connectivity described above. In particular, I focused on a

subgroup of effective-connectivity changes (i.e., only anodal- vs sham-tDCS for *Experiments 1* and *3*, and cathodal- vs sham-tDCS for *Experiment 2*, at the single-subject level), and assessed their relationship with current density. Noticeably, in *Experiment 3*, I considered the same comparisons highlighted above, but substituted the one encoding the incremental effects of multiple sessions with that encoding the differences between pre and post fifth tDCS session (i.e., Day5-MRI only). I first used CCA to investigate the joint multivariate correlations between effective connectivity changes and current density metrics, as whole. Only the CCA of *Experiment 3* Day5-MRI resulted in a significant correlation between the effective connectivity and current density canonical variates. Interestingly, this correlation seems to be mainly mediated by current density in the thalamus (for the current density variable set), and M1 self-inhibition (for the effective connectivity variable set), as shown by their significant cross-loadings. I then used voxel-based correlation analyses to investigate ROI-specific patterns for the same correlations and found significant negative correlations for *Experiment 2,* between current density within the cerebellum and thalamus and M1 self-connectivity, and for *Experiment 3* (after a single tDCS session) between current density within the thalamus and M1 self-inhibition. It is reminded that in the above analyses, self-connectivity values were converted to Hz, such that higher values correspond to lower self-inhibition.

Finally, I investigated the feasibility of assessing the effects of tDCS administered multiple times using a multi-modal approach (behavioural, fMRI and EEG), in a PDOC patient (Chapter 7). Importantly, this matter had not been explored elsewhere. I observed no evidence of covert awareness or improvements in clinical status, nor brain activation or connectivity following multiple tDCS sessions, perhaps to be expected due to the existing severe brain atrophy and gliosis. Nevertheless, this study proved the feasibility of our experimental design and analysis pipelines.

8.2. Interpretation of results

8.2.1. Implications for the understanding of tDCS

8.2.1.1. tDCS and long-range connectivity

Most research on tDCS has focused on the local excitability of targeted areas (Polania et al., 2018; Bikson et al., 2018; Sehatpour et al., 2020), but recent evidence suggests that neuromodulation can affect entire brain networks (for a review see To et al., 2018). Moreover, the therapeutic effects of non-invasive brain stimulation are thought to arise from the interplay between the stimulated target and associated networks (Kunze et al., 2016).

Similarly to recent literature (To et al., 2018; Sehatpour et al., 2020), in the experiments presented, the focus was on network-level effects across distant brain regions. In all experiments, long-range effects of tDCS were observed within the motor-network connectivity during command-following. These findings are therefore in line with previous literature showing network-level effects of tDCS (Mehrkanoon et al., 2016; Breaksper et al., 2017; Sehatpour et al., 2020). Given the above considerations, as well as the long-range effects of tDCS observed in this thesis, the use of neuroimaging methods appear fundamental to characterise the effects of tDCS at the macro-level, both on healthy and clinical populations. With canonical tDCS, it is difficult to understand if long-range effects are a result of the modulating effect of the targeted region on other regions or if the stimulation is affecting multiple regions, due to the low spatial specificity of tDCS. Our analyses in Chapter 6 help shed light into this. Specifically, the voxel-wise correlation analyses showed complex relationships between tDCS-induced current and tDCS-induced changes in coupling. Overall, the findings add to the existing literature reporting significant correlations between electric-field measures and both tDCS outcome measures and inter-subject variability (Nasimova & Huang, 2022). The most interesting finding, supporting the evidence already discussed above, on the long-range effects of tDCS, is that current-density metrics in the targeted regions correlate with effective-connectivity changes of distal areas, as inferable from the canonical-

and cross-loadings in the CCA analysis for *Experiment 3* (**Figure 6.3**) and the significant correlations reported in the voxel-wise analysis for *Experiment 2* and *3* (**Table 6.3**).

Interestingly, in all analyses, M1 self-inhibition appeared to be consistently associated with current density, both when targeting M1 itself - although in *Experiment 3* only - and when targeting the cerebellum. These findings, while supporting network-level effects of tDCS, may indicate that the current magnitude in certain regions may contribute to changes in network causal architecture induced by tDCS.

Moreover, the findings presented in Chapter 6 might also support the idea of compensatory mechanisms arising in response to network perturbations induced by non-invasive brain stimulation (Reato et al., 2010; Jackson et al., 2016). For example, in *Experiment 2* it was observed that the more current reaches the cerebellum (and the thalamus), the greater the self-inhibition in the motor cortex. This finding might be explained in terms of a homeostatic response taking place in the motor cortex. Recent evidence both on motor and non-motor literature also suggest a complex non-linear relationship between tDCS current intensity and MEPs increases or behavioural improvements, such that lower intensities sometimes lead to better outcomes (Dissanayaka et al., 2017; Ehrhardt et al., 2021). Although the underlying reasons have not been investigated systematically, it was suggested that these effects are the results of homeostatic mechanisms arising to balance the over-excitation/over-inhibition induced by tDCS in part of the network (Smucny, 2021). Interestingly, homeostatic responses following tDCS were also found in computational models of tDCS, although in the targeted areas rather than in distal areas (Li et al., 2019). As such, it may be the case that the more current reaches the cerebellum, the greater its inhibition and consequent increase in thalamo-cortical connectivity, which triggers a homeostatic response from the motor cortex.

Importantly, when considering the findings of the current thesis, it must be considered that some of the connectivities that were included in the DCM models, while functionally present, are anatomically mediated by third regions. For example, the dentate nucleus mediates the connectivity between the lateral cerebellum and the ventral anterior and ventral lateral thalamus. These regions are the main thalamic inputs to the neurons that form the corticospinal

tract (CST) in the motor cortex, along with supplementary and premotor areas (Felten et al., 2016). It follows that when interpreting the results from the DCM, one should take into consideration the influence of these intermediary regions in the neural networks under consideration.

Overall, these results may offer valuable information for future studies aiming at optimising tDCS protocols for enhancing the efficacy of stimulation within the motor network.

8.2.1.2. tDCS at rest and coupled with a task

In *Experiment 3* the stimulation was paired with passive mobilisation of the thumb, in an attempt to engage the motor cortex and enhance the effects of tDCS on the activated neuronal populations (see 1.6.3.2). The hypothesis that tDCS enhances the response of the neuronal populations active during motor training (Bolognini et al., 2009; Ehsani et al., 2022; Jin et al., 2019; Morrison-Ham et al., 2022) might therefore explain how the most consistent findings (i.e, that remained significant across sessions) in *Experiment 3* were related to the target of the stimulation, M1, and might also be at the basis of the difference in the findings of the two studies. A speculative explanation of the above discrepancy could therefore be that the greater engagement of the motor area during the stimulation maximised the effects of tDCS on the targeted area, but that the decrease in M1 self-inhibition following anodal-tDCS was still not sufficiently large to affect thalamo-cortical connectivity as predicted. In fact, the thalamus-to-M1 connection did show a trend towards increased excitation, but this was only reflected by the comparison between anodal- and cathodal-tDCS rather than between anodal- and sham-tDCS (**Fig 5.4** and **5.5**). However, a statistical comparison of the results of the two studies is not possible (i.e., two different montages were used and two different MRI scanners and sequence parameters), and it is therefore difficult to establish whether coupling the stimulation with passive mobilisation would translate into greater clinical gains in PDOC patients. This notwithstanding, the literature on tDCS administered during a task rather than at rest would suggest so (see 1.6.3.2 and 1.6.3.3).

Considering the results from *Experiment 1* and those from *Experiment 3* (Day-1), where the target of the stimulation was M1, a discrepancy is present. In fact, the decrease in thalamic self-inhibition following anodal-tDCS was present in *Experiment 1* but not in *Experiment 3* (Day1-MRI). Instead, in *Experiment 3*, a decrease in M1 self-inhibition was observed. This incongruence in findings might be related to differences in the stimulation protocols used in the two experiments: first, in *Experiment 1*, the motor cortex was located using a TMS procedure, whereas in *Experiment 3* it was located using a manual procedure. This led to a slight difference in the average distance of the active electrode to M1 between the two experiments, and a difference in the variability of electrode location, with electrodes in *Experiment 3* also being more laterally distributed (see section 6.3.1, and **Figure 8.1** below). Noticeably, the electrode localisation procedure followed in *Experiment 3*, with C3 used as reference for M1, is more commonly used than that through TMS (Knotkova et al., 2019). This holds true even in the studies of tDCS in PDOC patients (Chapter 2). Considering this, the results of *Experiment 3* are probably more easily comparable to the previous literature on M1-tDCS.

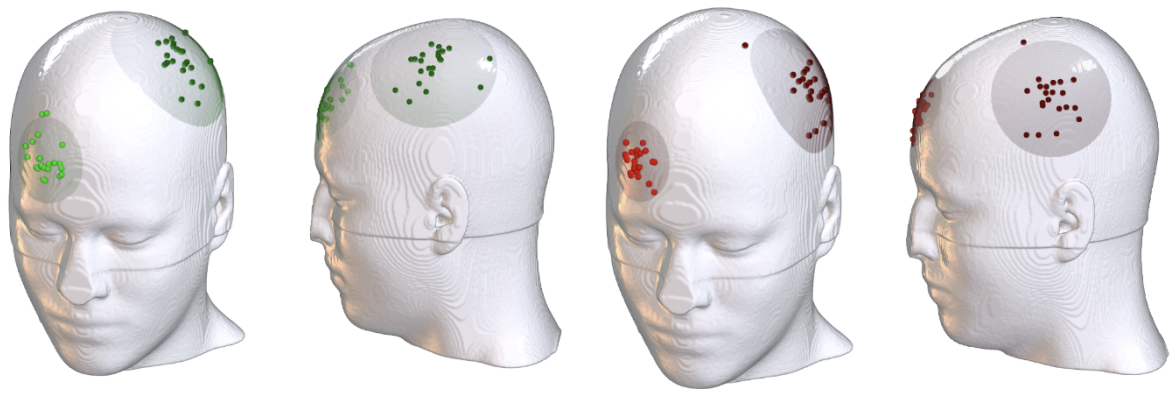


Figure 8.1. Electrode locations in *Experiment 1* (first and second head models) and *Experiment 3* (third and fourth head models). Dots represent the coordinates of the active (left motor cortex) and return electrode (right orbitofrontal cortex) per participant. The ICBM-NY head was used as a template (Y. Huang et al., 2016).

8.2.1.3. tDCS and multiple sessions

The effect of anodal-tDCS on M1 self-inhibition in *Experiment 3* increased following multiple stimulation sessions as compared to a single session. As already stated in section 5.5, the progressive decrease in M1 self-inhibition observed in *Experiment 3* following multiple tDCS sessions, might be the result of both e- and l-LTP mechanisms and might highlight that multiple-sessions of the stimulation protocol used could lead to structural plasticity changes and greater tDCS after-effects (Lu et al., 2019). When considering other connections than M1 self-inhibition, the results of *Experiment 3* expands the literature on the partial non-linearity of the effects of tDCS (Batsikadze et al., 2013; Shilo & Lavidor, 2019). In particular, in Batsikadze et al. (2013) it was found that both anodal and cathodal tDCS at 2 mA increased MEPs, while 1 mA cathodal tDCS decreased corticospinal excitability. Additionally, Shilo & Lavidor (2019) showed that the polarity-dependent effects of tDCS on motor-performance can change direction depending on the duration of the stimulation.

Non-linear effects of tDCS were already observed in studies on cortical excitability, both related to stimulation frequency and duration (Monte-Silva et al., 2010; Monte-Silva et al; 2013) and stimulation intensity (Batsikadze et al., 2013; Jamil et al., 2017). Moreover, non-linear effects were also observed on resting-state effective connectivity during the stimulation itself (Calzolari et al., 2023). Here the non-linearity is linked to the amount of sessions instead. In fact, if the increases or decreases in effective-connectivity induced by tDCS were linear, we would have expected to find similar results (i.e., connectivity changes going in the same direction) when assessing the effects of one session and those of multiple sessions (**Figure 6.4, panels A and B**). This suggests that the enhancements or reduction of coupling in the targeted networks do not necessarily increase with the number of stimulation sessions, and connectivities might instead switch direction. Importantly, in *Experiment 3* fMRI data was collected only during the first and last session, while the sessions were carried out outside the MRI scanner. As such, it is not possible to fully characterise the changes that occurred during the other 3 sessions.

As also highlighted by other authors, this non-linearity is an important matter that points out to the necessity of a more systematic investigation of stimulation parameters (Jamil et al., 2020). Lastly, non-linearity must be also taken into account when developing multi-session stimulation protocols that are based on results from single-session studies.

8.2.2. Implication for PDOC rehabilitation

In the three experiments on healthy individuals, it was found that tDCS modulates the coupling in the pre-mentioned axis during command-following, hence impacting long-range dynamics, other than just self-connectivities of the targeted areas. From a clinical perspective, in *Experiment 1*, our results were only partially satisfactory, in the sense that the expected increase in excitation from the thalamus to M1 was not observed after anodal-tDCS. However, the observed reduction in thalamic self-inhibition still constituted a promising finding in terms of potential implications for PDOC rehabilitation. From a neurobiological standpoint, intrinsic connections modulate the excitatory-inhibitory balance of a given region (Snyder et al., 2021); it follows that a decrease in self-inhibition - as observed in *Experiment 1* - could result in an increased net effect of the extrinsic inputs to that region. In PDOC patients characterised by partial damage of thalamo-cortical fibres, the excessive thalamic inhibition may result from the spared cerebellar-thalamic structural connectivity (leading therefore to an excessive cerebellar-brain inhibition) (Stafford et al., 2019). Therefore, a reduction in thalamic self-inhibition may help compensate for such an excessive thalamic inhibition observed in PDOC, by making the thalamus more prone to the excitatory tone coming from the motor cortex itself, and potentially lead to beneficial therapeutic effects. However, it can also be argued that such a reduction in thalamic self-inhibition might make the thalamus more sensitive to the inhibitory tone of the cerebellum. On the other hand, the increase in thalamo-cortical connectivity expected after anodal-tDCS was observed after cathodal-tDCS instead. As already mentioned, this could be the result of network compensatory mechanisms, which have also been observed in studies conducted on animals (Jackson et al., 2016; Reato et al., 2010), but it may suggest that cathodal-tDCS on M1 might also have a therapeutic value.

Importantly, the above leads to the consideration that, when assessing the effects of tDCS on PDOC patients, including both polarities in the study design might be needed, to better unveil the potential therapeutic effects of tDCS and, overall, to better understand the long-range effects of tDCS. Noticeably however, polarity-controlled designs were rarely used in the literature on tDCS and PDOC (see Chapter 2 and Appendix A).

Leaving the effects of single M1-tDCS session administered at rest aside, in *Experiment 3* the most significant finding was related to M1 self-inhibition, which was progressively reduced after anodal-tDCS. As noted above, this might lead to beneficial effects in PDOC, by making M1 more susceptible to thalamic excitatory inputs.

The same reasoning on the potential therapeutic effects of tDCS on PDOC also applies to the incremental effects that cathodal cerebellar-tDCS had, on the connectivity from thalamus to M1, in *Experiment 2*. Interestingly, in their first-in-man clinical trial, Cain et al. (2022) investigated the effects of MRI-guided low-intensity focused ultrasound (LIFU) over the thalamus, on 11 patients with disorders of consciousness (DOC). The authors found that thalamic LIFU led to increased behavioural responsiveness and that the increased connectivity between the thalamus and the motor cortex is predictive of recovery (Cain et al., 2022). This further highlights the potential for cathodal cerebellar-tDCS to support PDOC rehabilitation.

It must be noted that the results for *Experiment 2* are also partially in line with the CBI hypothesis, in that anodal-tDCS over the cerebellum increased thalamic and M1 self-inhibitions, whereas cathodal-tDCS increased thalamocortical connectivity (Galea et al., 2009). However, recent research on the effects of tDCS on CBI reported a more complex picture than that of Galea et al. (2009), with a varying effect of cerebellar-tDCS on the cerebellar-M1 axis, dependent not only on tDCS polarity but also on the TMS intensity chosen (Batsikadze et al., 2019). Importantly, CBI is relevant for PDOC rehabilitation in that its modulation could help compensate for the reduction in thalamo-cortical coupling.

Overall, while the above effects cerebellar-tDCS on thalamo-cortical connectivity suggest that this specific montage could be used to support PDOC rehabilitation, further research is needed

to confirm these findings in clinical populations, and determine the optimal tDCS parameters. Considering the above, cerebellar-tDCS could represent a viable alternative to M1-tDCS, in several cases:

1) the presence of excessive thalamic inhibition, as reported by neuroimaging assessments;
2) the presence of widespread motor-cortex lesion (as CSF in atrophies might lead to shunting of tDCS-injected current);
3) the patient has not responded to M1-tDCS.

Overall, the results from the studies above were only partially in line with what was predicted, and the potential therapeutic effect of the montages are still uncertain. While it is challenging to establish which montage/protocol would yield to more favourable results, the effectiveness of a particular montage or protocol may vary depending on the skull lesions and atrophies specific to each patient. Additionally, a combined approach that integrates the positive effects of each individual montage on motor network connectivity could potentially lead to greater therapeutic effects. In fact, as also noted by Liu et al. (2022), while studies targeting a single brain region provide important treatment references and explain the rationale behind choosing a specific target area, they might not maximise the therapeutic effect of tDCS. To this regard, more research is being done on the therapeutic effects of multi-site tDCS (i.e., by either targeting multiple areas concurrently, or by administering tDCS multiple times and switching the target), with results on PDOC being largely encouraging (Zhang et al., 2021; Liu et al., 2022; Kumar et al., 2022).

Lastly, given the widespread and heterogeneous CSF abnormalities and brain atrophies following a brain injury (as discussed in section 1.6.4), it is necessary to adopt a more individualised dose-controlled approach to electrode placement in PDOC patients. Considering also the complexity of the relationships between tDCS-induced electric fields and network connectivity modulations, a neuroimaging-guided approach to electrode placement is highly important, especially for treatments targeting long-range connectivities.

Overall, the effects of tDCS on healthy-subject motor-network connectivity reported in this thesis highlight the potential for M1- and cerebellar-tDCS in supporting PDOC rehabilitation, by re-establishing some levels of thalamo-cortical coupling. However, considering the complexity of the effects of tDCS and also the relationship between electric field and connectivity changes mentioned above, multi-imaging, polarity- and sham-controlled studies on clinical populations are needed to fully understand tDCS clinical value in PDOC patients, and to determine the best stimulation protocols.

To conclude, in the case study reported in this thesis no noticeable effects of tDCS were found on either neuroimaging-derived or behavioural metrics. While the findings of a case study should be interpreted with caution, and not used as definitive evidence of treatment efficacy, they are in line with literature suggesting that tDCS efficacy in PDOC is highly dependent on the patient's condition, with patients in MCS showing greater improvements after treatment as compared to those with UWS/VS (Xu et al., 2022).

8.4.4. Challenges of conducting clinical multi-modal multi-session research

The data collection for the case study at the Wellington Hospital presented some additional challenges when compared to that on healthy individuals:

1) Due to the stiffness of the muscles of the patient's arm and akinetic rigidity, reaching the patient's hand and administering passive mobilisation of the thumb while the patient was laying in the MRI bore was challenging, especially considering the duration of the stimulation protocol (20').
2) I contracted Covid-19 in the middle of a testing week, which led to a loss of data and consequent delay in the data collection process, as the entire testing week had to be rescheduled. This highlights the importance of having multiple experimenters available for data collection in such multi-session studies.
3) The multi-session-multi-modal nature of the study made it also challenging to coordinate with the hospital staff to schedule the daily tDCS sessions, as well as EEG

and fMRI sessions, around the patient's routine treatments. To this respect, I highlight the importance of making the medical staff involved with the care of the patient aware of the data collection.

4) Lastly, while all fMRI sessions happened under the supervision of the chief MRI radiologist, during the EEG sessions I was normally supported by the nurse on duty, who was not necessarily trained to set up EEG. This highlights the need of training all nurses assigned to the patient before the data collection, to ensure a faster and accurate montage.

Overall, the above challenges should be considered when designing multi-modal multi-session tDCS studies in clinical settings, especially with patients requiring complex clinical care.

8.4. Limitations of the Research

8.4.1. Limitations of tDCS methods used

The limitations of canonical tDCS (as compared to HD-tDCS) were already discussed (Chapter 4 section 5, Chapter 5 section 5) and concerned mainly the low spatial specificity of the stimulation technique used in the studies, which makes it difficult to establish clear relationships between stimulated area and observed effects. Moreover, in *Experiment 1* and *3*, a relatively low intensity (1mA) was used. ROI metrics derived from single-subject electric-field models used in Chapter 6 showed relatively low electric-field median values in the targeted ROIs (**Table D.1**), falling below what is suggested to be necessary to elicit subthreshold currents in neuronal populations (1 mV/mm) (Vöröslakos et al., 2018). On the other hand, it must be noted that the maximum electric-fields values did approach 1 mV/mm, suggesting that the parts of the ROIs closer to the scalp have been exposed to sufficient current intensity. It must be also considered that the M1 and cerebellar ROI are relatively large ROIs, and median values only describe the central tendency of the electric fields within the region (Indahlastari et al., 2021). In addition, the threshold mentioned above is primarily linked to the

activity of individual neurons, but as pointed out by (Modolo et al., 2018), when targeting neural networks that consist of thousands of neurons, network-wide amplification happens, which enhances weak membrane depolarizations.

In summary, it is difficult to establish whether greater current intensities than 1mA might lead to a greater impact on the motor network connectivity. In fact, several authors have reported non-linear effects of current intensity, as already discussed in section 8.2.1.4, when considering network homeostatic regulation mechanisms in response to tDCS stimulation.

8.4.2. Comparison across studies

When considering the results from the experiments presented in the thesis, it is important to mention that the data was acquired with two different scanners and using different acquisition parameters (**Table 3.1**). This may limit the comparison between studies, and explain some differences between the results of *Experiment 1* and those of *Experiment 3* (Day1-MRI). The same holds true even when considering the results from Chapter 6, where participants' structural MRI scans were used. Related to this, in such analyses T1s plus T2s scans were used to compute the electric-field models in *Experiment 3*, whereas in *Experiment 1* and *2* only T1s were used, which might further limit the comparison between studies. In fact, using only T1-scans might lead to poorer tissue segmentations as compared to combining both T1s and T2s (Van Hoornweder et al., 2022). However, the current density metrics obtained from the ROI analysis in Chapter 6 reported similar current values in *Experiment 1* and *3*, suggesting that the differences in the segmentation procedures did not significantly affect the estimates of current density in the targeted brain regions.

Lastly, different procedures were used in *Experiment 1* and *3* to localise the targeted area (M1) (see section 3.5 for more details), which might further explain the differences found between the two experiments, both in terms of connectivity changes induced by tDCS and correlations between current density and such connectivity changes.

8.4.3. BOLD signal, DCM and hierarchical PEBs

The main neuroimaging method used in the present thesis is fMRI, which relies on changes of BOLD signal. While providing high spatial accuracy, the temporal specificity of fMRI is limited, due to reasons already explained in section 3.1. The consequence of this limitation is that temporal information of the underlying neural processes gets greatly blurred (Glover, 2011). Moreover, BOLD signals might also be affected by artefacts due to signal distortion or signal dropout, especially around parietal areas, and frontal orbital areas (Glover, 2011). It is possible that these limitations also apply to the DCM models built upon the BOLD time-series. Additionally, the DCM models included in the thesis were limited to four brain regions, as the analyses were hypothesis-driven. The effects of tDCS were therefore modelled by DCM only within those four nodes. It cannot be ruled out that an expanded model would lead to a more precise description of the effects of tDCS.

Lastly, in *Experiment 3*, hierarchical PEBs were used, with up to three levels of comparisons. While the PEB approach presents several benefits, such as modelling individual differences in connectivity and accounting for group-level variability (Zeidman et al., 2019), the complexity of such hierarchical models can make it more challenging to interpret the results.

8.5. Conclusions and future directions

Overall, the work presented in this thesis aimed at improving the understanding of the effects of brain stimulation on thalamo-cortical connectivity, while investigating its potential application in the rehabilitation of PDOC. Future research should aim at filling various gaps in the understanding of the effects of tDCS, which were not addressed by the current work.

For instance, in this thesis the effects of tDCS were tested both when the stimulation was administered at rest and when it was paired to a task. However, a direct comparison of the two

stimulation protocols was not made. Interestingly, the literature on the matter is scarce. I argue that studies on healthy subjects, with experimental designs allowing for a proper comparison between rest and task-paired tDCS, are needed, to fully understand the synergic effect of combining tDCS with a task.

Similarly, the literature on the benefits of multiple stimulation sessions is also limited (Hashemirad et al., 2016). Interestingly, though, in PDOC patients multiple sessions seem to be more effective than single ones (Chapter 2, Appendix A), which is reflected by a trend towards switching from single to multiple sessions protocols (Xu et al., 2022). It has been suggested that the prolongation of tDCS after effects following multiple sessions might be linked to neuroplasticity mechanisms, such as l-LTP (Agboada et al., 2020; Monte-Silva et al., 2013). However, the exact processes behind are still unclear, and the mentioned studies have mainly focused on the motor cortex. In fact, findings from tDCS-MEP studies involving M1 do not necessarily generalise to other brain areas (Jamil et al., 2020). Considering this, more studies are needed to understand the underlying mechanisms of multiple tDCS sessions, in the healthy brain first, and also focusing on other areas than the motor cortex.

Importantly, given the non-linearity of tDCS effects present in the literature (Dissanayaka et al., 2017; Ehrhardt et al., 2021) and observed in *Experiment 3*, future experimental designs could incorporate more frequent fMRI or EEG sessions throughout the administration of the intervention, rather than limiting them to the first and last session. By collecting data at multiple time points during the intervention, it will be possible to better characterise the trajectory of the effects of tDCS on brain activity and connectivity, and understand how these evolve over time. This information could help identify when, during the time course of the intervention, tDCS effects reach optimal levels, which may guide the development of more effective protocols. Moreover, for tDCS to be clinically relevant, its effects should be long-lasting. However, long-term effects are rarely investigated. I suggest that future studies - both on healthy individuals and PDOC patients - include proper follow-up sessions where neuroimaging data are also collected, so that the sustainability of the changes in brain activity and connectivity can also be determined.

In addition, to reduce the great inter-subject variability in tDCS effects, future research should adopt neuroimaging-driven approaches to localise stimulation electrodes, as also suggested by Evans et al. (2020, 2022). For instance, it was recently demonstrated that the inter-subject variability in electric-field intensity can be reduced by using structural MRI-derived current flow modelling (as those presented in Chapter 6) and fine-tuning tDCS intensity (Evans et al., 2020). In the case of PDOC patients, given the presence of skull lesions and atrophies, this approach should perhaps be extended to electrode localisation too, in order to reduce the variance in current distribution as well. Importantly, MRI-based current-density models as those shown in this work, can also be used to model electric-fields generated via HD-tDCS montages. As argued in section 2.8.2, this offers a great opportunity to study the potential benefits of HD-tDCS in PDOC patients, and this approach allows for more targeted stimulations and may result in more consistent and reliable effects across individuals. Additionally, MRI current-flow models could also broaden our understanding of how brain lesions and atrophies may impact the distribution and intensity of tDCS-injected current, a matter for which the literature is still limited. Given the heterogeneity of brain lesions in PDOC patients (Jennet et al., 2001, Jellinger 2013), understanding the influence of structural abnormalities on tDCS current might help improve treatment parameters.

Noticeably, the most recent studies regarding tDCS in PDOC adopted a multi-region approach, by either targeting multiple regions at once, or targeting different regions through multiple sessions (for a review see Appendix A). However, such protocols have not been tested systematically on healthy participants yet. I argue that these protocols should be tested on healthy participants first. In fact, without properly testing a protocol on healthy subjects first, using neuroimaging methods, it becomes challenging to explain the mechanisms behind any potential therapeutic effects, which may limit any further optimisation of the intervention. Exploring the effects of a protocol on healthy participants first also helps understand which effects translate to PDOC patients and which do not. Moreover, further research could also explore the effects of combining the two montages used in this thesis, coupled also with passive mobilisation, and verify whether a synergistic effect exists so that the beneficial effects of tDCS on M1 and on the thalamo-cortical axis are enhanced.

APPENDIX

Appendix A

Following the review that constitutes Chapter 2 of this thesis, 8 studies were published assessing the effects of tDCS on PDOC patients. Below I provide a short summary of the methods and outcomes of such studies.

In their multi-session and multi-target control study, Zhang et al. (2021) investigated the effects of 80 tDCS sessions (20', 2mA), administered in two cycles of 4 weeks, over the prefrontal area, the left DLPFC and bilaterally over the fronto-temporo-parietal cortices (FTPCs). The treatment and control groups were constituted by 55 and 50 PDOC patients, respectively. As regards to the stimulation of the FTPC, this was performed one week with the anode over the left FTPC and one week with the anode over the right FTPC. The authors used the CRS-R and EEG-derived metrics as outcome measure, and the modified GOS (mGOS) as a follow up measure (12 months after disease onset), and found greater improvements in CRS-R and mGOS scores in the tDCS group as opposed to the control group. According to the authors, these improvements were also reflected by increased interconnections between the sensorimotor and frontal areas on the affected hemisphere, and the prefrontal-parietal and temporo-parietal cortical networks of the unaffected hemisphere (Zhang et al., 2021).

In another study, Zhang et al. (2022) investigated the effects of multiple sessions (twice a day for 14 consecutive days) of HD-tDCS (20', 2mA) targeted at the posterior parietal lobe, on 42 PDOC patients. In particular, the authors focused on changes in CRS-R scores as well as in EEG spectral energy and other graph theory measures. Overall, the authors reported that 32/42 patients showed an increase in the CRS-R scores after multiple sessions of tDCS as compared to baseline. Moreover, the change in CRS-R scores was used to classify patients in responders (R+) and non responders (R-), the differences in EEG-derived metrics were evaluated between the two groups. Interestingly, the authors reported increased spectral energy in the alpha2 and beta1 bands around the frontal and parietal electrodes. Additionally, the authors also found increased graph-theoretical metrics in the bands alpha1-2 and beta1, as well as increased

normalised spatial complexity in the beta2 band for the R+ group (Zhang et al., 2022). The authors interpret these findings as evidence that improvements in consciousness in R+ patients might be associated with a greater integration in the alpha1 band, as well as stronger isolation in the beta2 band.

Similarly, Han et al. (2022) also investigated the electrophysiological mechanisms underlying multiple sessions of HD-tDCS in PDOC (10 anodal sessions over the left DLPFC for 5 consecutive days, at 2mA for 20'), although in a smaller cohort of patients (N=19). The authors also classified the patients into an R+ and R- group (N=11 and 8, respectively) based on CRS-R changes, and assessed the difference between the two groups in EEG PSD. The PSD analysis of the differences between R+ and R- uncovered increased PSD values following multiple stimulations, mainly in the parieto-occipital region, for the frequency range 6-8Hz. Moreover, consistently with previous studies (Chennu et al., 2014; Thibaut et al., 2018), the authors also reported a positive correlation between theta power and alpha power and CRS-R scores following a single stimulation. These findings are also in line with other studies linking increases in theta, alpha and beta power to improvements in consciousness (Chennu et al., 2017; H. Huang et al., 2020; Sitt et al., 2014). Noticeably, however, the study was not sham controlled.

On the other hand, Liu et al. (2022) explored the potential for tDCS combined with EEG to predict the prognosis (as measured through mGOS at 12 months post onset) of 85 patients in UWS, in a historical controlled trial. The authors used the same multi-session multi-target tDCS approach used by Zhang et al. (2021). First, the authors found that the mGOS improvement was higher for the tDCS group as compared to the control group. Secondly, the authors also found that the prognostic sensitivity for patients in UWS was increased when modelling the mGOS outcome including both clinical parameters (i.e., age, gender, lesion and disease course) and EEG-derived metrics (specifically related to prefrontal-parietal cortical networks).

Similarly to Liu et al. (2022), Guo et al. (2022) assessed the changes in PDOC patients' brain dynamics through EEG, following 14 days HD-tDCS sessions targeted at the precuneus (2mA,

20', 2 sessions per day). The authors collected EEG signals and CRS-R scores before and after the treatment, in 33 PDOC patients (13 in VS/UWS, 20 in MCS). Interestingly, the CRS-R scores of 18 patients increased after the treatment (4 VS/UWS and 14 MCS). Moreover, in line with Liu et al. (2022), Guo et al. (2022) also found that improvements in brain dynamics relate to improvements in consciousness.

Peng et al. (2022), in a sham-controlled study, focused on the effects of 10 sessions of 20' of tDCS over the left DLPFC (preceded by 5 daily sessions of sham tDCS), on 11 MCS patients. The author assessed changes in CRS-R scores and performed a seed-to-voxel connectivity analysis using rs-fMRI data at three time points per patient (baseline, post-sham tDCS and post-real tDCS). The functional connectivity analysis was performed using the following seeds: SMA, precuneus, middle frontal gyrus, angular gyrus, superior temporal gyrus and occipital lobe. Five patients showed CRS-R improvements at two weeks following the last real tDCS sessions. Interestingly, when comparing the functional connectivity results after sham-tDCS with real-tDCS, the authors found increased connectivity for the bilateral SMA, right angular gyrus and right superior temporal gyrus, and increased connectivity of the bilateral occipital lobe and right precuneus when comparing real-tDCS with baseline (Peng et al., 2022). Importantly, as the authors also highlight, these findings are in line with other electrophysiologic and fMRI studies suggesting that the restoration of consciousness is dependent on the collaboration and coordination of multiple brain regions (Peng et al., 2022; Qin et al., 2015).

In a randomised clinical control trial, Kumar et al. (2022) assessed the effects of anodal-tDCS on 40 PDOC patients (n=20 for the experimental group and control group), with the stimulation being targeted at three regions simultaneously, namely the motor area (C3/C4 ipsilesional), the sensory area (P3/P4 ipsilesional) and the left DLPFC (F3). Patients in the stimulation group received 2 daily sessions of tDCS for a week. The multi-target multi-session protocol led to an improvement in GSC scores as well as in the other diagnostic tool used by the authors, the Rancho Los Amigos Scale (RLAS) (Kumar et al., 2022).

Lastly, Barra et al. (2022) compared the effects of tDCS (over the prefrontal cortex, 20' at 2mA) to those of bimastoid transcranial pulsed-current stimulation (tPCS), which is thought to reach deeper brain structures as compared to tDCS. Specifically, tPCS was delivered at random frequencies (ranging between 6-10 Hz) and with a biphasic current of 2mA (peak-to-peak) for 20'. The design of their study was sham-controlled, crossover and double-blind, and the authors administered one session of tDCS, one of tPCS and one of sham-tDCS, with a washout period of 1 week between each condition. Moreover, the authors collected CRS-R scores and EEG-derived metrics (power spectra, graph-theoretical metrics) before and after each session. Interestingly, while tPCS did not lead to neither EEG-metrics changes nor behavioural changes, tDCS improved behavioural responsiveness and increased theta frontal functional connectivity (Barra et al., 2022).

Overall, the studies reviewed above back up the observation already expressed in Chapter 2, that multiple tDCS sessions might be more effective than a single session, in that they more consistently elicit changes in PDOC behavioural responsiveness. Additionally, multi-target protocols - either via simultaneous stimulation of different areas (Kumar et al., 2022), or by targeting different areas across several weeks of stimulation (B. Liu et al., 2022; X. Zhang et al., 2021) - also showed promising results, and are in line with previous evidence highlighting that stimulating multiple brain regions might be more beneficial for rehabilitation, as compared to targeting one region only (Chen et al., 2019). According to Kumar et al. (2022), multi-region stimulation protocols might enhance neurosynaptic pathways and, in turn, lead to a response of the reticular activating system (RAS). Nevertheless, more research is needed to understand the synergistic effects of multi-target tDCS on patients with PDOC.

Lastly, the studies from Liu et al. (2022) and Guo et al. (2022), in addition to confirming the therapeutic effect of multiple sessions of tDCS, also highlighted that tDCS combined with EEG might have an important prognostic value.

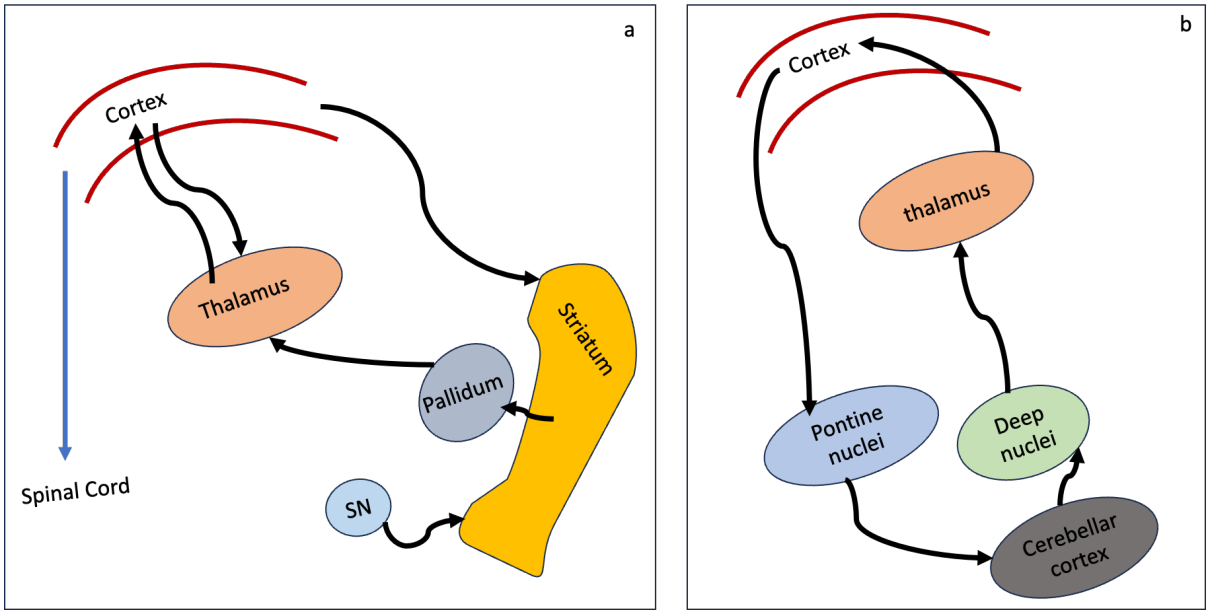


Figure A1. Schematic representation of the cortico-thalamic-cortical (a) and cortico-cerebellar-thalamic (b) loops.

Appendix B

Supplementary tables

Table B1. *Effect of M1-tDCS on brain activation.*

Contrast	Region	Cluster P	Cluster size	Peak P		F / T	MNI coordinates
		FWE-corrected	*in mm3*	*FWE-corrected*	*uncorrected*		*[x;y;z]*
Interaction between polarity and time	*Thalamus*	0.967	54	0.965	<0.001	8.092	[-3;-16;-1]
Greater Increase after anodal as compared to cathodal	*SMA*	0.886	108	0.790	<0.001	3.550	[-9;11;53]
		0.935	54	0.907	<0.001	3.383	[-9;20;56]

Greater increase after cathodal as compared to sham	*Thalamus*	0.935	54	0.443	<0.0001	3.901	[-3;-16;-1]
Greater increase after anodal as compared to sham‡	*Thalamus*	0.999	189	0.993	0.001	3.069	[-15;-25;-1]
		0.998	216	0.999	0.002	2.868	[-6;-13;-1]

Results from the random effect group analyses on the brain activation during thumb movements to command. We include results that survive a threshold of $p<0.001$ uncorrected ($p<0.005$ in the case of ‡). In addition, we do not include spurious single voxel activations. Abbreviations: FWE, family wise error; MNI, Montreal Neurological Institute; SMA, supplementary motor area.

Table B2. *Effects of tDCS on behavioural metrics.*

Metrics	**Polarity**	**Baseline**	**Post-tDCS**	**t** (baseline vs post-tDCS)	**p-Holm (baseline vs post-tDCS)**	**F** (main effect time)	**p** (main effect time)	**F** (interaction)	**p** (interaction)
Experiment 1 - M1-tDCS									
Reaction time ()	**Anodal**	0.29 (± 0.06)	0.27 (± 0.05)	2.389	0.314	3.990	0.063	1.312	0.283

	Cathodal	0.27 (± 0.05)	0.26 (± 0.04)	0.626	1.0				
	Sham	0.28 (± 0.05)	0.28 (± 0.07)	0.102	1.0				
Mean Velocity	**Anodal**	8.39 (± 3.98)	7.59 (± 2.81)	2.697	0.145	04.430	0.051	1.939	0.160
	Cathodal	7.71 (± 4.49)	7.26 (± 3.83)	0.868	1.0				
	Sham	6.96 (± 3.14)	6.99 (± 2.83)	0.120	1.0				
Peak acceleration	**Anodal**	31.05 (± 41.64)	37.31 (± 56.13)	0.312	1.0	0.616	0.444	0.636	0.536
	Cathodal	32.81 (± 38.32)	24.11(± 29.34)	0.325	1.0				
	Sham	77.82 (± 177.01)	111.39 (± 244.91)	1.299	1.0				
Experiment 2 - cb-tDCS									
Reaction time	**Anodal**	0.30 (± 0.04)	0.28 (± 0.04)	3.669	0.008**	21.094	<0.001**	0.951	0.395

	Cathodal	0.29 (±0.03)	0.28 (± 0.04)	1.998	0.601				
	Sham	0.30 (± 0.05)	0.29 (±0.05)	1.885	0.601				
Mean Velocity	**Anodal**	7.44 (± 3.53)	7.78 (± 3.98)	0.626	1.0	0.286	0.598	1.106	0.340
	Cathodal	7.11 (± 3.18)	6.38 (± 2.77)	-1.486	1.0				
	Sham	8.09 (± 2.73)	8.09 (± 2.55)	-0.007	1.0				
Peak acceleration	**Anodal**	39.29 (± 31.94)	39.29 (± 33.62)	0.001	1.0	1.823	0.191	0.404	0.670
	Cathodal	51.19 (± 96.90)	31.74 (± 15.27)	-0.372	1.0				
	Sham	77.82 (± 141.91)	60.96 (± 108.44)	-1.046	1.0				

Statistics for the post hoc (baseline vs post-tDCS) tests, main effect of time, and interaction between polarity (anodal, cathodal, sham) and time (baseline vs post-tDCS) on average reaction time, mean velocity and peak acceleration for Experiment 1 and Experiment 2. p-Holm value adjusted for comparing a family of 15; $p_{(interaction)}$ uncorrected; **p<.01. Abbreviations: ms, milliseconds; cm, centimetres; s, seconds; m, metres.

Table B3. *Blinding*.

Experiment	Active Stimulation	Sham		p
Experiment 1	31/43	15/22	0.9682	0.701
Experiment 2	33/40	13/22	0.0869	0.263

Number of times that each type of stimulation was perceived as real, and statistics for the corresponding McNemar's Test. Active stimulation includes anodal and cathodal sessions.

Supplementary figures

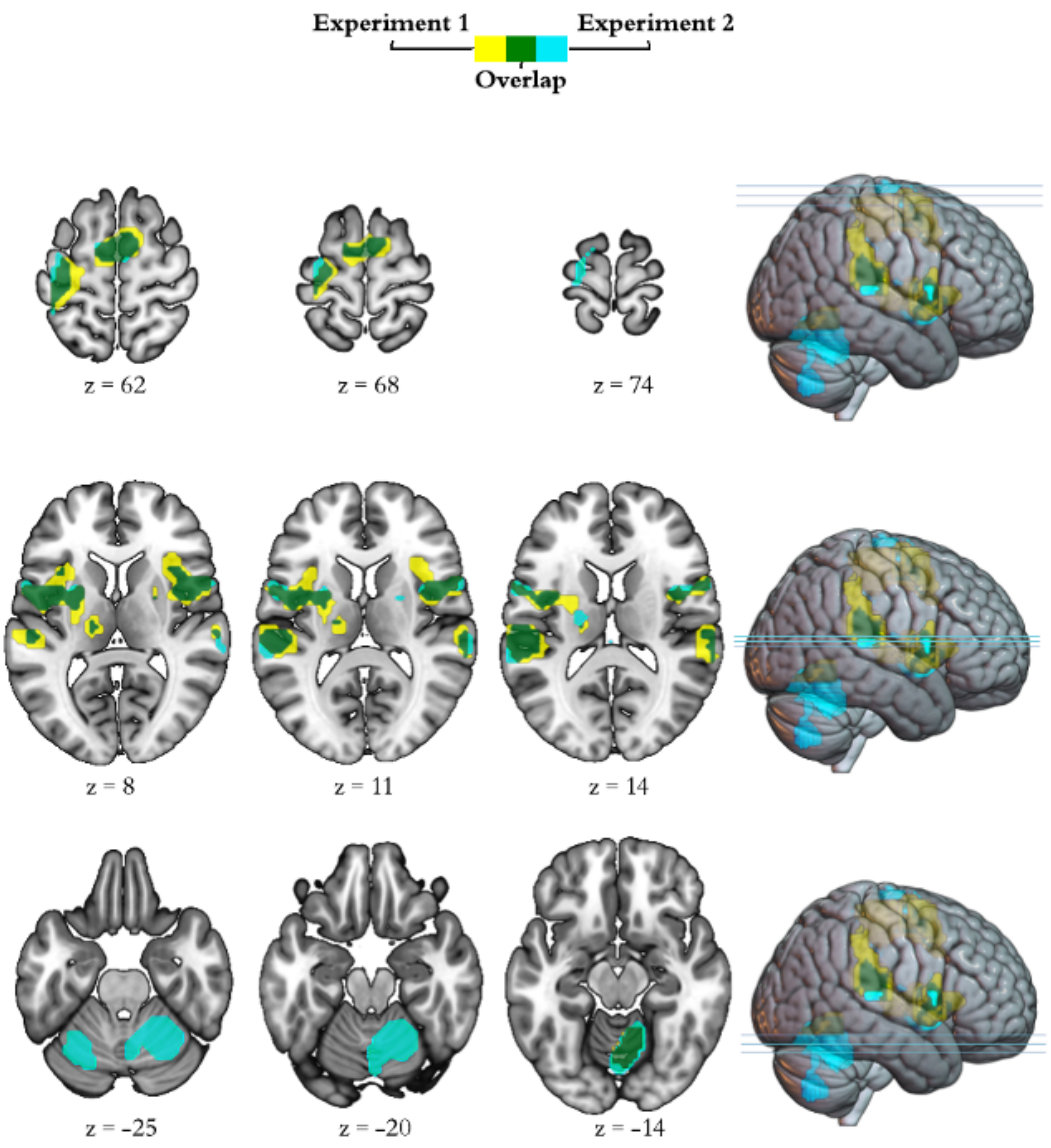


Figure B1. Brain activation during command following across trials. The insets display group general linear model differences between 'move' and 'rest' blocks in Experiment 1 (yellow) and Experiment 2 (light blue), across all trials included in the ANOVA (positive effect of task). The overlap across

experiments appears in green. Activation maps are shown at a FWE p<0.05 and rendered on a standard template (152 template in MRIcroGL). We display whole brain results as per request during peer review. z indicates the Montreal Neurological Institute z coordinate.

Appendix C

Supplementary Tables

Table C1. *Effects of tDCS on behavioural metrics (V2).*

					Analysis of Effects: BF_{excl} (P(excl) → P(excl|data)		
Metrics	**Day**	**Polarity**	**Baseline**	**Post-tDCS**	**Day1-MRI only**	**Day1-MRI pre vs Day5-MRI post**	**Day1-MRI vs Day5-MRI**
Reaction times (*s*)	Day1-MRI	Anodal	0.221 (± 0.032)	0.220 (± 0.044)	4.732 (0.200 → 0.082)	7.689 (0.200 → 0.106)	0.506 (0.053 → < 0.000)
		Cathodal	0.244 (± 0.058)	0.230 (± 0.057)			
		Sham	0.225 (± 0.051)	0.233 (± 0.056)			
	Day5-MRI	Anodal	0.220 (± 0.040)	0.214 (± 0.047)			
		Cathodal	0.231 (± 0.056)	0.230 (± 0.049)			
		Sham	0.217 (± 0.037)	0.214 (± 0.040)			
Mean velocity (*cm*/*s*)	Day1-MRI	Anodal	8.801 (± 5.053)	7.242 (± 3.741)	5.323 (0.200 → 0.090)	3.936 (0.007 → 0.026)	2.227 (0.053 → < 0.000)
		Cathodal	8.910 (± 4.270)	8.196 (± 3.691)			
		Sham	7.924 (± 4.176)	7.881 (± 4.489)			

	Day5-MRI	Anodal	8.463 (± 4.042)	7.880 (± 4.203)			
		Cathodal	8.196 (± 3.828)	9.100 (± 4.367)			
		Sham	8.513 (± 3.756)	8.731 (± 4.573)			
Peak acceleration (m/s^2)	Day1-MRI	Anodal	39.495 (± 24.847)	32.871 (± 15.274)	4.143 (0.200 → 0.076)	1.531 (0.025 → 0.038)	1.066 (0.053 → < 0.002)
		Cathodal	38.049 (± 22.992)	37.162 (± 19.804)			
		Sham	34.160 (± 17.280)	37.660 (± 21.256)			
	Day5-MRI	Anodal	38.837 (± 21.750)	46.071 (± 33.901)			
		Cathodal	42.245 (± 22.053)	46.245 (± 30.373)			
		Sham	35.989 (± 16.956)	29.900 (± 10.887)			

Statistics for the Bayesian repeated measures ANOVAs (Day1-MRI only, Day1-MRI pre vs Day5-MRI post and Day1-MRI vs Day5-MRI), on behavioural metrics. We report exclusion Bayes factors for the interaction effect between the considered factors for each Bayesian ANOVA. Abbreviation: $BF_{exl,}$ Bayesian evidence for the exclusion of the interaction in the model, against the matched model; P(excl), prior inclusion probability; P(excl I data), inclusion probability; cm, centimetres; s, seconds; m, metre.

Supplementary figures

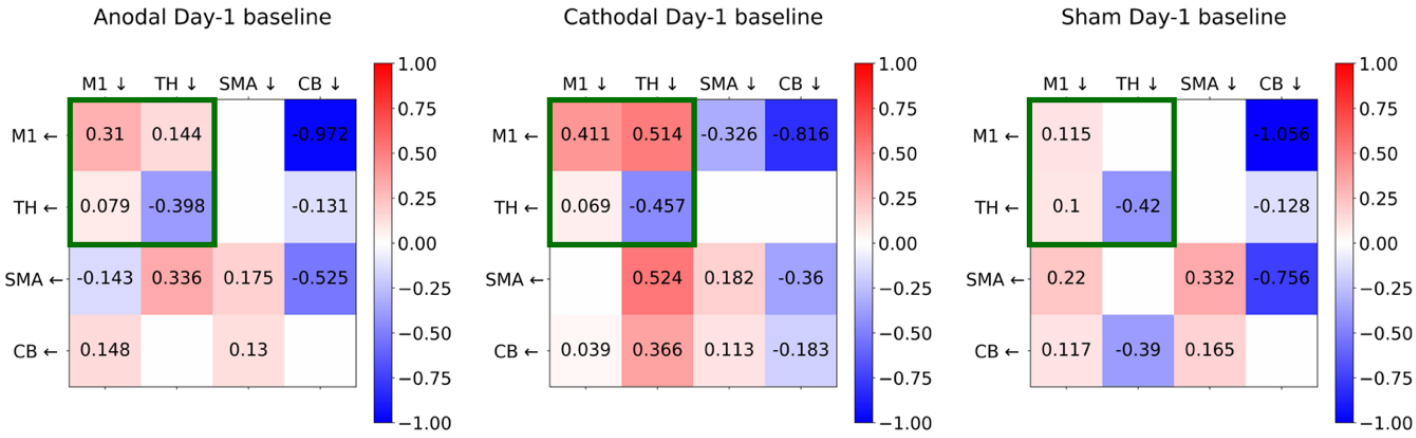


Figure C1. Effective connectivity on the pre-tDCS run on Day1-MRI session. Group average of effective connectivity for the pre-tDCS run on the first session for anodal (left), cathodal (middle), and sham (right) sessions. Arrows represent the direction of the connectivity in each cell. For between-region connections red cells indicate excitatory coupling and blue cells indicate inhibitory coupling. Self-connections are always inhibitory and red/blue cells indicate increased/decreased inhibition respectively. Green boxes highlight the key connections of interest. We display connections that survive a 95% posterior probability threshold for free energy.

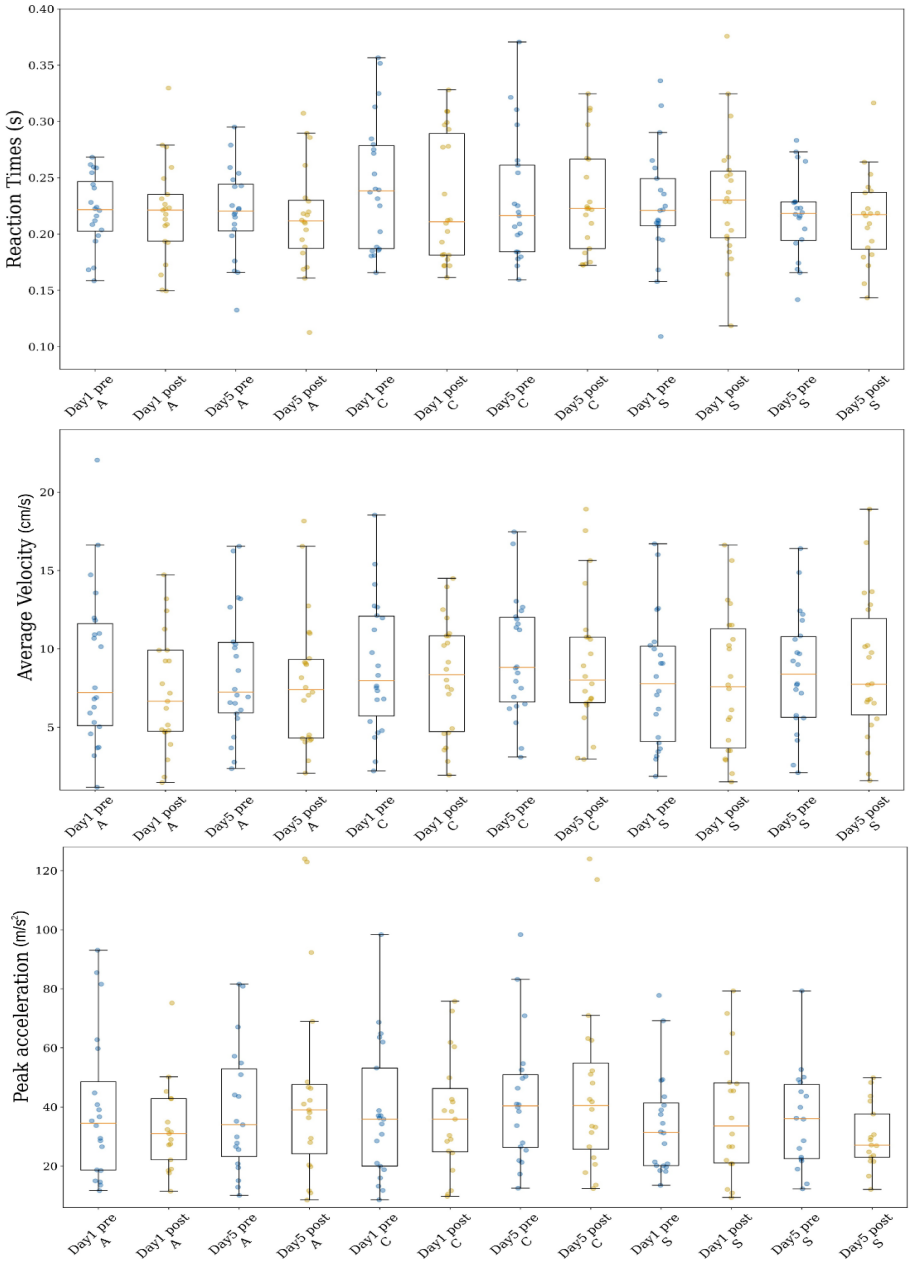


Figure C2. Effects of M1-tDCS on behavioural metrics. Effects of M1-tDCS on behavioural command following. Scatter plots displaying the average values per condition for the reaction times (top figure), average velocity (centre) and peak acceleration (bottom). In each column, each dot represents the averaged value for one participant. Data-points corresponding to measurement errors (defined as values with a Z-score > 3.0) are not displayed. Abbreviations: Day1, first day of the testing week (i.e., Day1-

MRI); Day5, last day of the testing week (i.e., Day5-MRI); A, anodal stimulation; C, cathodal stimulation; S, sham stimulation; pre, before stimulation; post, after stimulation.

Supplementary methods

C-Matrix definition

As we have done in (Chapter 4), to establish the set of driving inputs (C matrix) that best fitted our data, we first created DCM models that included driving inputs to all 4 regions (12 DCM models per participant, one per fMRI run). We then created a second level within-subject PEB per participant, to model the commonalities between all 12 runs. We subsequently entered the resulting 22 PEBs into a third level PEB, to model the similarities across all participants. We included in the model a constant encoding the group mean, as well as the following nuisance regressors: sex, age, and Edinburgh Handedness Inventory score (all mean-centred). To do this, we applied Bayesian Model Reduction (BMR) to iterate over the reduced models, and then used Bayesian Model Average (BMA) to determine the average connectivity parameters (Zeidman, Jafarian, Corbin, et al., 2019c). We used a 95% posterior probability threshold for free energy (i.e., comparing the evidence for all models where a particular connection/input is included versus when it is excluded). Like in our previous study (Chapter 4), this step showed robust support (>95% posterior probability) for the inclusion of driving inputs to cortical regions only (M1 and SMA). We therefore modelled the final DCMs for all participants with all self- and between-region connections (A matrix), modulatory inputs to each self-connection (B matrix) and driving inputs to M1 and SMA (C matrix).

Appendix D

Supplementary tables

Table D1. Electric-field medians and max values.

Experiment	**ROI**	**Median Electric-field (mV/mm)**	**Max Electric-field (mV/mm)**
Experiment 1			
	M1	0.165 ± 0.029	0.886 ± 0.317
	Thalamus	0.101 ± 0.014	0.129 ± 0.017
Experiment 2			
	M1	0.053 ± 0.010	0.084 ± 0.016
	Thalamus	0.102 ± 0.017	0.158 ± 0.028
	Cerebellum	0.203 ± 0.031	0.991 ± 0.344
Experiment 3			
	M1	0.164 ± 0.028	0.943 ± 0.357
	Thalamus	0.103 ± 0.019	0.146 ± 0.027

Electric field (mV/mm) median and max values are reported for each individual ROI used in the CCA and voxel-wise analyses, for each experiment. Abbreviations: M1, motor cortex.

Table D2. CCA correlations and p-values.

Comparison	**r**	**p**
Experiment 1	0.725	0.319

Experiment 2	0.765	0.9
Experiment 3 (Day1)	0.786	0.078
Experiment 3 (Day1-MRI pre vs Day5-MRI post)	0.625	0.998

Supplementary figures

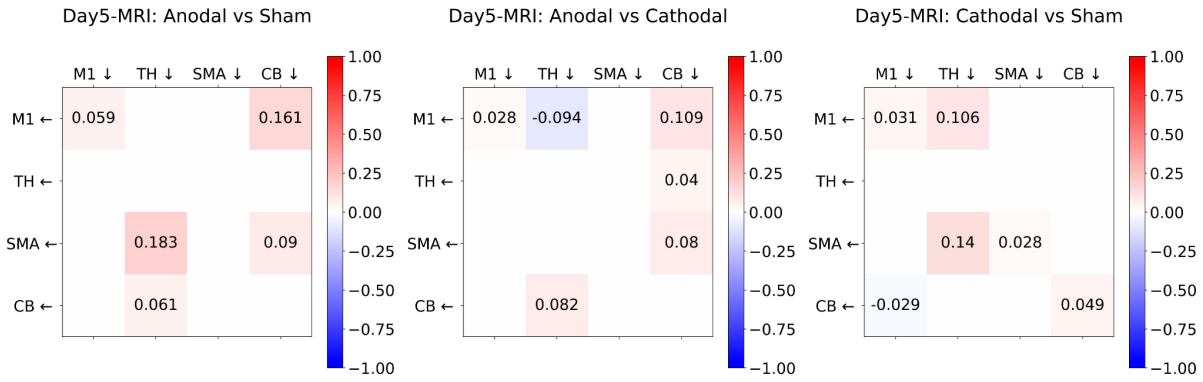
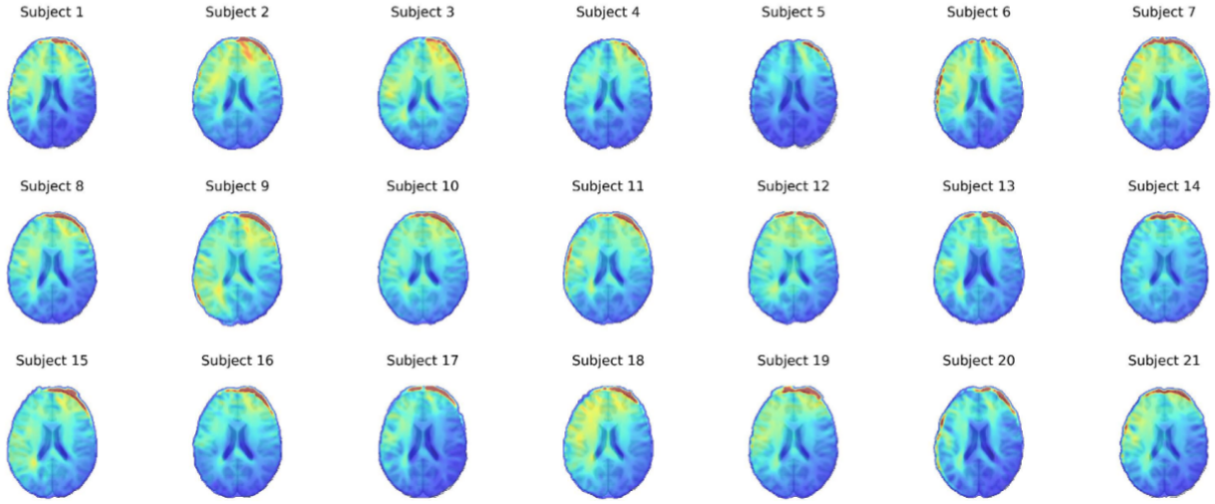
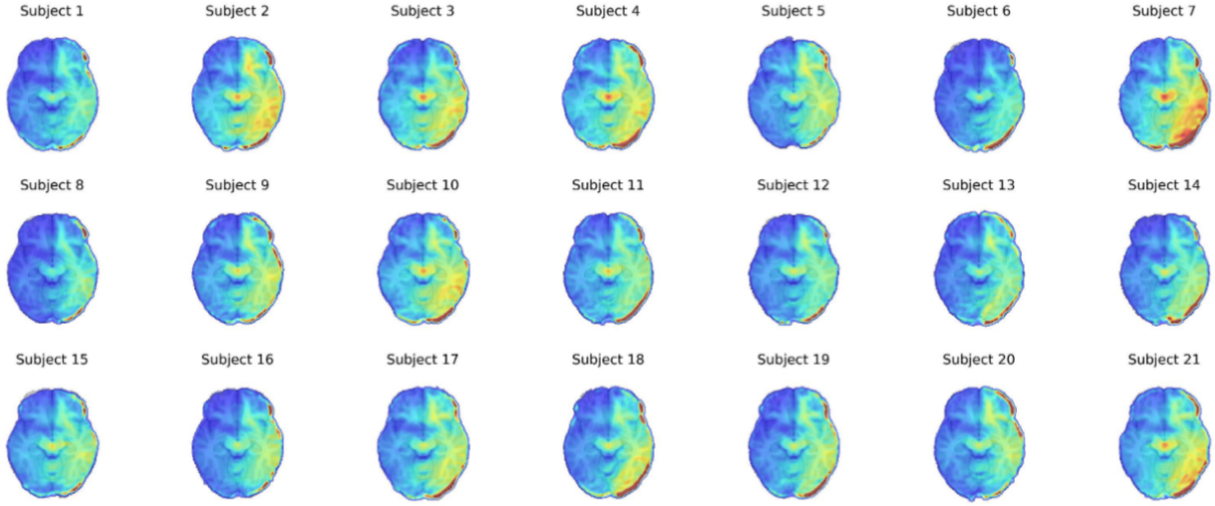


Figure D.1. Additional PEB results: Experiment 3 (Day5-MRI only) PEB results. Results for the 3rd-level PEBs encoding the group-averages for each combined comparison between polarities on Day5-MRI only (i.e., anodal > sham x pre-tDCS < post-tDCS, anodal > cathodal x pre-tDCS < post tDCS, and cathodal > sham x pre-tDCS < post-tDCS). Self-connections (i.e., diagonal entries in the matrices) were converted to Hz multiplying the exponential of the original self-connection by -0.5. Values were then re-centred to zero so that positive values indicate a decrease in self-inhibition and negative values an increase. Note that I included this comparison in the present chapter as it was not reported in Chapter 5, where I focused on the incremental effects of Day5-MRI over Day1-MRI instead. Abbreviations: CB, cerebellum; M1, motor cortex; SMA, supplementary motor area; TH, thalamus.

Experiment 1



Experiment 2



Experiment 3

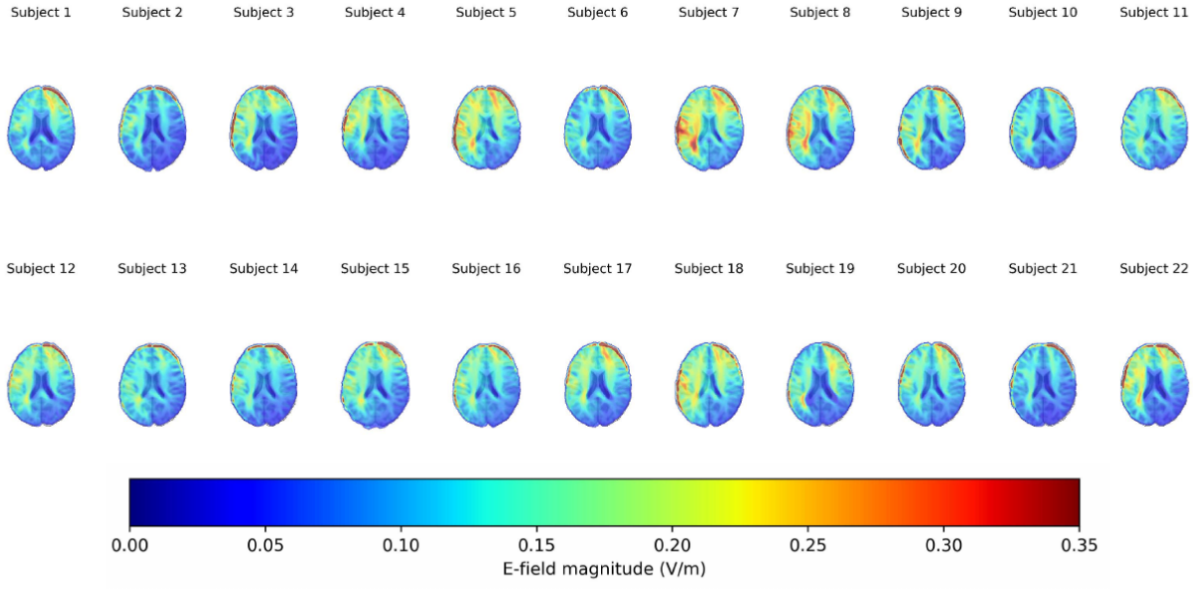


Figure D.2. Axial views of the generated electric-field maps (V/m) for each participant, for Experiments 1, 2 and 3. Slice location used was Z=28 for Experiments 1 and 3, and Z=-13 for Experiment 2.

Appendix E

Supplementary tables

Table E1. *Instructions of the tasks included in the case study.*

Task	**Instructions**
fMRI command-following task	*Every time you hear a 'Try to move your right thumb', try to move your right thumb away from your fingers as fast as you can. Do not worry if you can't produce the movements you would like. Keep on trying to move every time you hear 'Try to move your right thumb'. Stop moving and stay still when you hear the words 'and now stay still'.*
fMRI tennis-task	*When you hear the word 'tennis' we'd like you to imagine you're on a tennis court with a tennis racket in your hand. Imagine that you're playing a vigorous game of tennis, swinging your arm back and forth to hit a ball over and over again. Don't run around but remain in one place and imagine the ball keeps coming directly towards you, for you to hit it as hard as you can. Keep imagining playing tennis until you hear the word 'relax.*
EEG command-following task	*Every time you hear a 'Try to move your right thumb', try to move your right thumb away from your fingers as fast as you can. Do not worry if you can't produce the movements you would like. Keep on trying to move every time you hear 'Try to move your right thumb'. Stop moving and stay still when you hear the words 'and now stay still'.*

EEG and fMRI resting-state tasks	*During the next 5 minutes try to remain still and don't think about anything in particular.*

Table E2. Results from the permutation tests on the coefficients of variation of move vs rest trials per each condition.

Condition	**p-value**	**statistic**
Sham (baseline)	0.099	-0.443
Sham (post-tDCS)	0.929	0.056
Anodal (baseline)	0.781	0.007
Anodal (post-tDCS)	0.202	1.540
Cathodal (baseline)	0.207	-1.552
Cathodal (post-tDCS)	0.645	0.151

Supplementary Figures

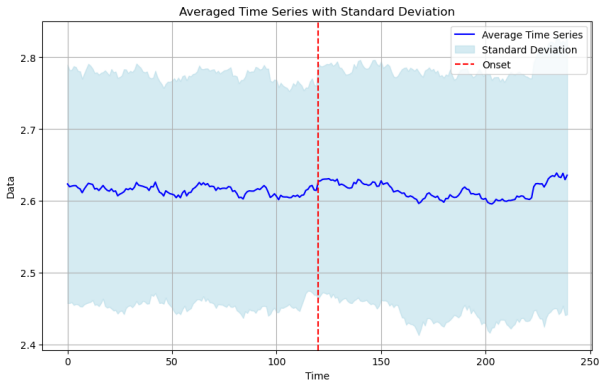
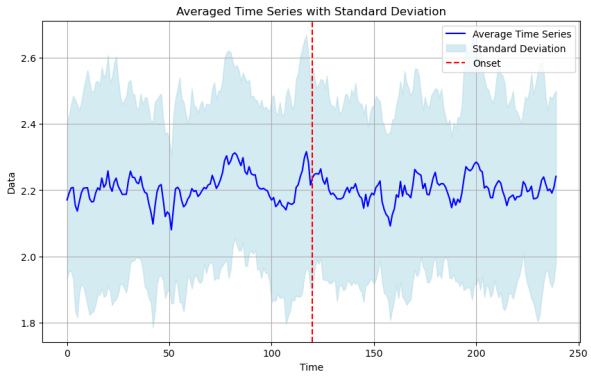
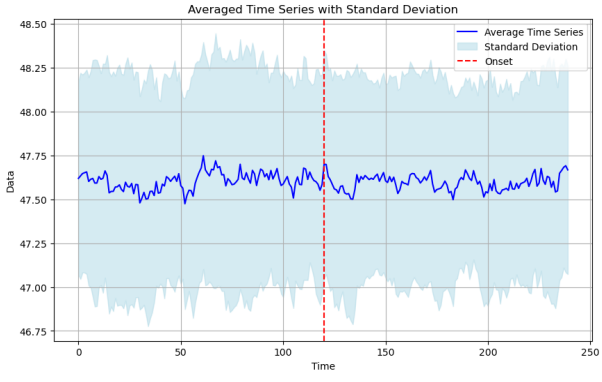
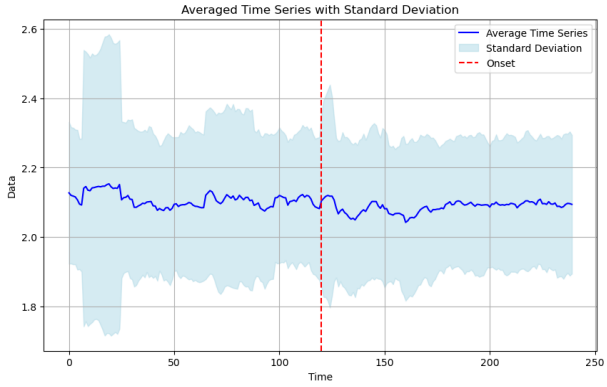
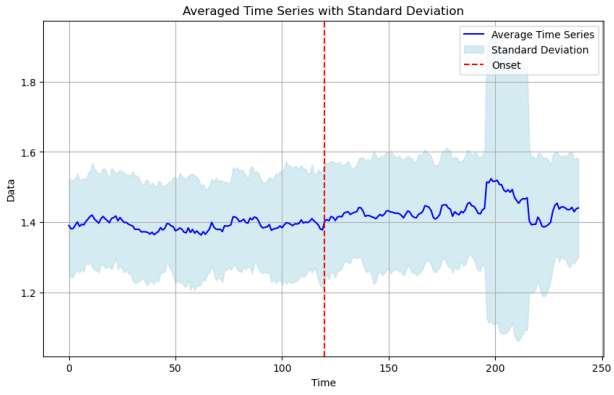
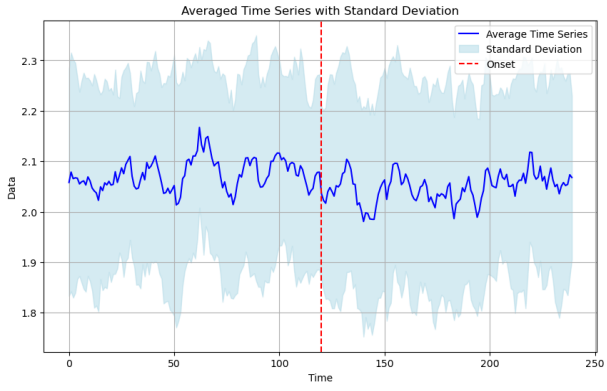
Stimulation	Condition	
	Baseline	Post-tDCS
Sham		
Anodal		
Cathodal		

Figure E.1. Averaged motion-tracking time-series with standard deviation for the EEG active tasks. The onset line corresponds to the onset of the instruction “Move”.

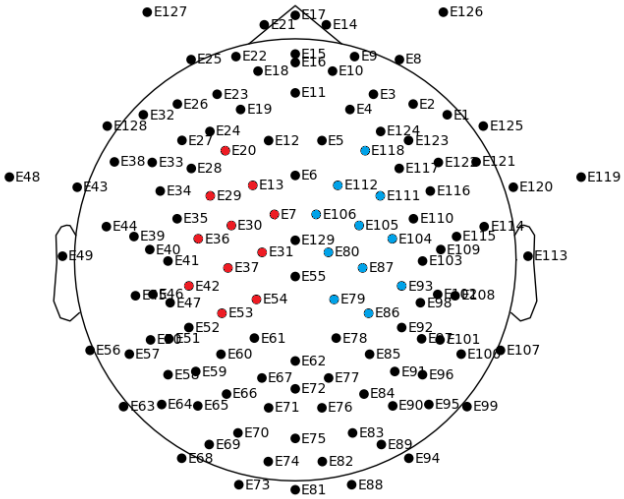
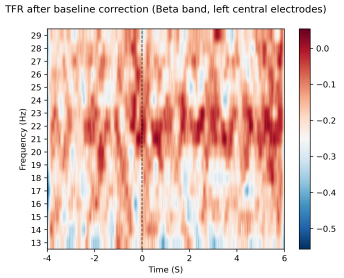
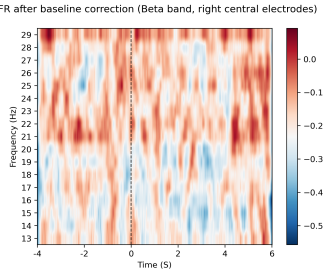
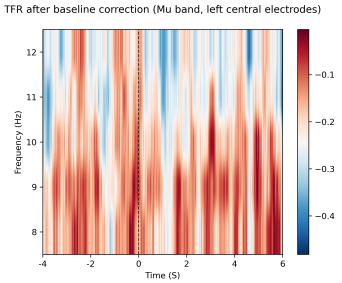
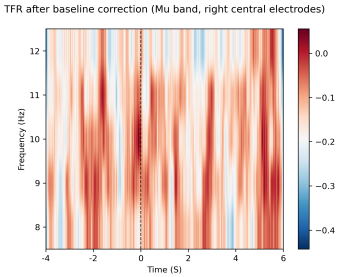
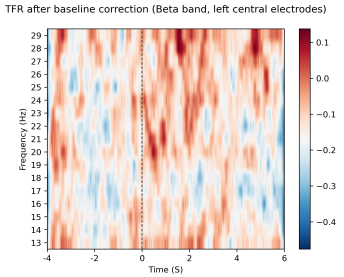
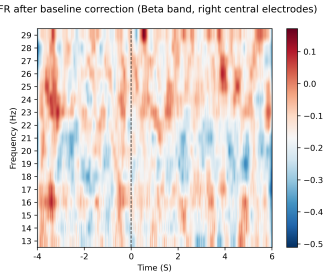
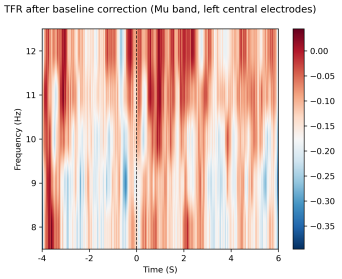
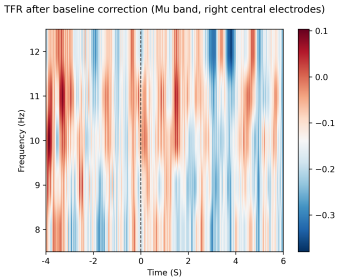
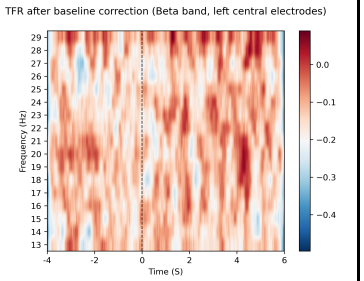
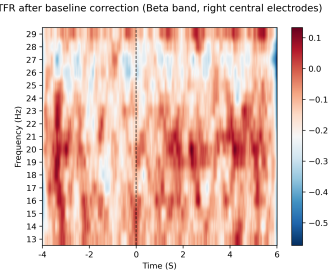
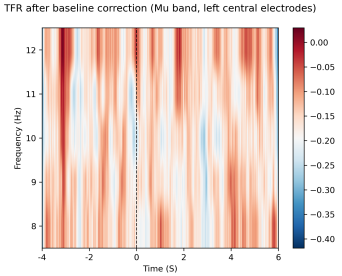
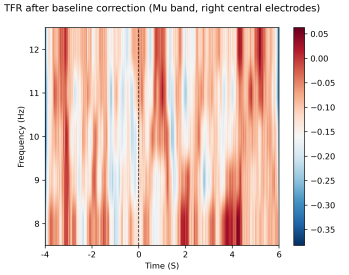
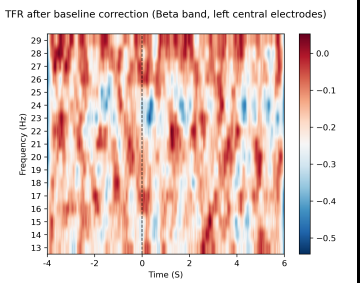
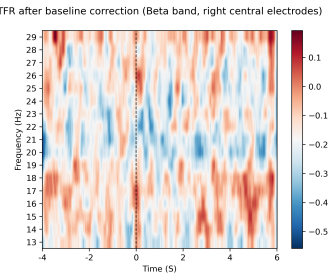
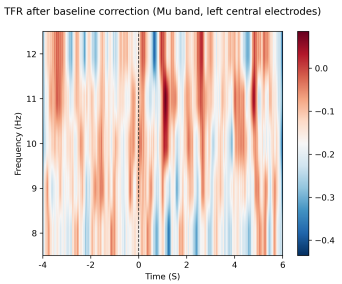
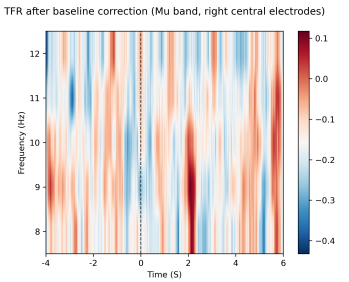
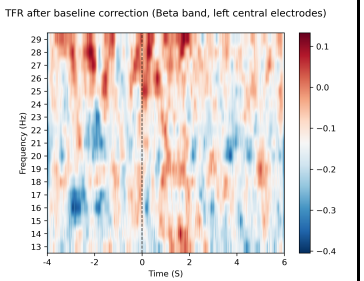
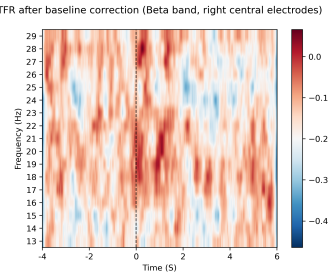
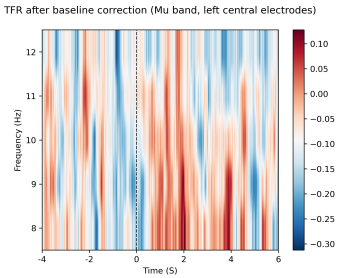
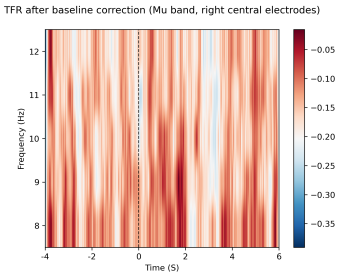


Figure E.2. Left (red) and right (blue) central electrodes selected for the time-frequency permutation test on the EEG active task data.

	Beta band left	Beta band right	Mu band left	Mu Band right
Week 1				
Week 2				

Week 3				
Week 4				
Week 5				

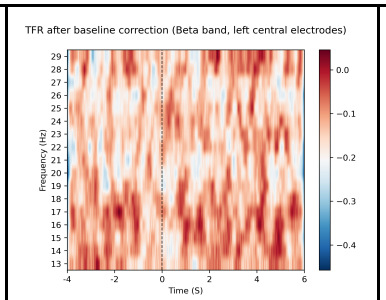
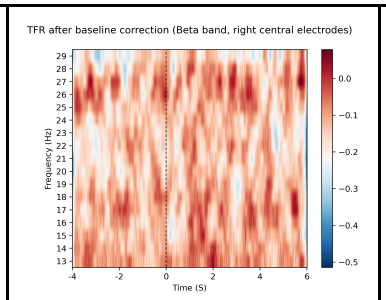
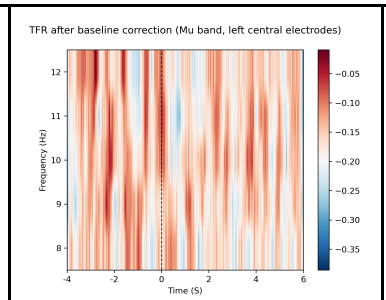
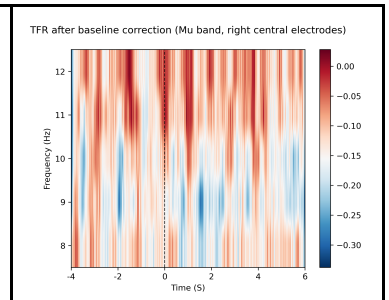
Week 6				

Figure E.3. TFR for each EEG active session, averaged by group of electrodes and by trials, for the frequency bands mu and beta.

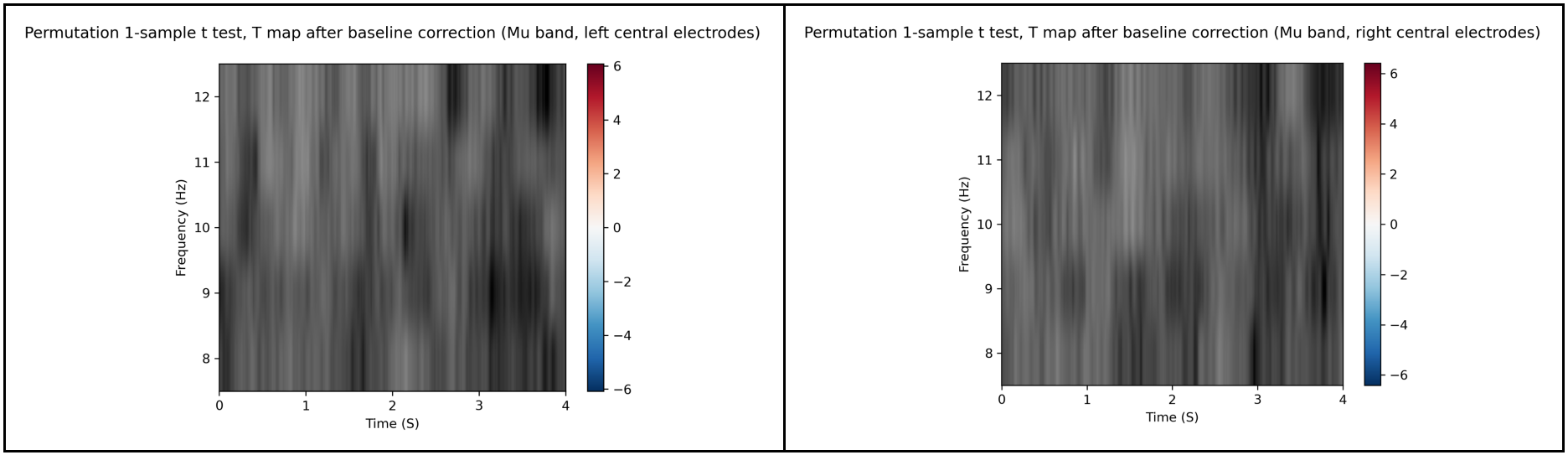


Figure E.4. 1-sample permutation t-test results (i.e., t-maps) for week 2 (after anodal stimulation), for the Mu band, averaged over the left and right central electrodes.

REFERENCES

Abellaneda-Pérez, K., Vaqué-Alcázar, L., Perellón-Alfonso, R., Bargalló, N., Kuo, M.-F., Pascual-Leone, A., Nitsche, M. A., & Bartrés-Faz, D. (2020). Differential tDCS and tACS Effects on Working Memory-Related Neural Activity and Resting-State Connectivity. *Frontiers in Neuroscience*, *13*. https://www.frontiersin.org/articles/10.3389/fnins.2019.01440

Abraham, A., Pedregosa, F., Eickenberg, M., Gervais, P., Mueller, A., Kossaifi, J., Gramfort, A., Thirion, B., & Varoquaux, G. (2014). Machine learning for neuroimaging with scikit-learn. *Frontiers in Neuroinformatics*, *8*. https://doi.org/10.3389/fninf.2014.00014

Agboada, D., Mosayebi-Samani, M., Kuo, M.-F., & Nitsche, M. A. (2020). Induction of long-term potentiation-like plasticity in the primary motor cortex with repeated anodal transcranial direct current stimulation – Better effects with intensified protocols? *Brain Stimulation*, *13*(4), 987–997. https://doi.org/10.1016/j.brs.2020.04.009

Alary, F., Doyon, B., Loubinoux, I., Carel, C., Boulanouar, K., Ranjeva, J. P., Celsis, P., & Chollet, F. (1998). Event-Related Potentials Elicited by Passive Movements in Humans: Characterization, Source Analysis, and Comparison to fMRI. *NeuroImage*, *8*(4), 377–390. https://doi.org/10.1006/nimg.1998.0377

Albizu, A., Fang, R., Indahlastari, A., O'Shea, A., Stolte, S. E., See, K. B., Boutzoukas, E. M., Kraft, J. N., Nissim, N. R., & Woods, A. J. (2020). Machine learning and individual variability in electric field characteristics predict tDCS treatment response. *Brain Stimulation*, *13*(6), 1753–1764. https://doi.org/10.1016/j.brs.2020.10.001

Aloi, D., della Rocchetta, A. I., Ditchfield, A., Coulborn, S., & Fernández-Espejo, D. (2021a). Therapeutic Use of Transcranial Direct Current Stimulation in the Rehabilitation of Prolonged Disorders of Consciousness. *Frontiers in Neurology*, *12*. https://doi.org/10.3389/fneur.2021.632572

Aloi, D., Jalali, R., Tilsley, P., Miall, R. C., & Fernández-Espejo, D. (2022a). TDCS modulates effective connectivity during motor command following; a potential therapeutic target for disorders of consciousness. *NeuroImage*, *247*, 118781. https://doi.org/10.1016/j.neuroimage.2021.118781

Amari, S., Cichocki, A., & Yang, H. H. (1995). *A New Learning Algorithm for Blind Signal Separation*. 7.

Ammann, Claudia, Danny Spampinato, and Javier Márquez-Ruiz. 2016. 'Modulating Motor Learning through Transcranial Direct-Current Stimulation: An Integrative View'. *Frontiers in Psychology* 7 (December). https://doi.org/10.3389/fpsyg.2016.01981.

Angelakis, E., Liouta, E., Andreadis, N., Korfias, S., Ktonas, P., Stranjalis, G., & Sakas, D. E. (2014). Transcranial direct current stimulation effects in disorders of consciousness. *Archives of Physical Medicine and Rehabilitation*, *95*(2), 283–289.

Angius, L., Hopker, J., & Mauger, A. R. (2017). The Ergogenic Effects of Transcranial Direct Current Stimulation on Exercise Performance. *Frontiers in Physiology*, *8*. https://doi.org/10.3389/fphys.2017.00090

Antal, A., Alekseichuk, I., Bikson, M., Brockmöller, J., Brunoni, A. R., Chen, R., Cohen, L. G., Dowthwaite, G., Ellrich, J., Flöel, A., Fregni, F., George, M. S., Hamilton, R., Haueisen, J., Herrmann, C. S., Hummel, F. C., Lefaucheur, J. P., Liebetanz, D., Loo, C. K., … Paulus, W. (2017a). Low intensity transcranial electric stimulation: Safety, ethical, legal regulatory and application guidelines. *Clinical Neurophysiology: Official Journal of the International Federation of Clinical Neurophysiology*, *128*(9), 1774–1809. https://doi.org/10.1016/j.clinph.2017.06.001

Antal, A., Terney, D., Poreisz, C., & Paulus, W. (2007). Towards unravelling task-related modulations of neuroplastic changes induced in the human motor cortex: Effect of tDCS is modified by mental activity and exercise. *European Journal of Neuroscience*, *26*(9), 2687–2691. https://doi.org/10.1111/j.1460-9568.2007.05896.x

Antonenko, D., Thielscher, A., Saturnino, G. B., Aydin, S., Ittermann, B., Grittner, U., & Flöel, A. (2019). Towards precise brain stimulation: Is electric field simulation related to neuromodulation? *Brain Stimulation*, *12*(5), 1159–1168. https://doi.org/10.1016/j.brs.2019.03.072

Arnts, H., van Erp, W. S., Sanz, L. R. D., Lavrijsen, J. C. M., Schuurman, R., Laureys, S., Vandertop, W. P., & van den Munckhof, P. (2020). The Dilemma of Hydrocephalus in Prolonged Disorders of Consciousness. *Journal of Neurotrauma*, *37*(20), 2150–2156. https://doi.org/10.1089/neu.2020.7129

Ashburner, J., & Friston, K. J. (2005). Unified segmentation. *NeuroImage*, *26*(3), 839–851. https://doi.org/10.1016/j.neuroimage.2005.02.018

Babiloni, C., Sarà, M., Vecchio, F., Pistoia, F., Sebastiano, F., Onorati, P., Albertini, G., Pasqualetti, P., Cibelli, G., Buffo, P., & Rossini, P. M. (2009). Cortical sources of resting-state alpha rhythms are abnormal in persistent vegetative state patients. *Clinical Neurophysiology*, *120*(4), 719–729. https://doi.org/10.1016/j.clinph.2009.02.157

Bai, Yang, Xiaoyu Xia, Jiannan Kang, Yi Yang, Jianghong He, and Xiaoli Li. 2017. 'TDCS Modulates Cortical Excitability in Patients with Disorders of Consciousness'. *NeuroImage: Clinical* 15: 702–9. https://doi.org/10.1016/j.nicl.2017.01.025.

Bai, Yang, Xiaoyu Xia, Yong Wang, Yongkun Guo, Yi Yang, Jianghong He, and Xiaoli Li. 2018. 'Fronto-Parietal Coherence Response to TDCS Modulation in Patients with Disorders of Consciousness'. *International Journal of Neuroscience* 128 (7): 587–94. https://doi.org/10.1080/00207454.2017.1403440.

Bai, Yang, Yajun Lin, and Ulf Ziemann. 2020. 'Managing Disorders of Consciousness: The Role of Electroencephalography'. *Journal of Neurology*, September. https://doi.org/10.1007/s00415-020-10095-z.

Barra, A., Rosenfelder, M., Mortaheb, S., Carrière, M., Martens, G., Bodien, Y. G., Morales-Quezada, L., Bender, A., Laureys, S., Thibaut, A., & Fregni, F. (2022). Transcranial Pulsed-Current Stimulation versus Transcranial Direct Current Stimulation in Patients with Disorders of Consciousness: A Pilot, Sham-Controlled Cross-Over Double-Blind Study. *Brain Sciences*, *12*(4), Article 4. https://doi.org/10.3390/brainsci12040429

Bastani, A., & Jaberzadeh, S. (2012). Does anodal transcranial direct current stimulation enhance excitability of the motor cortex and motor function in healthy individuals and subjects with stroke: A systematic review and meta-analysis. *Clinical Neurophysiology*, *123*(4), 644–657. https://doi.org/10.1016/j.clinph.2011.08.029

Bastos, A. M., & Schoffelen, J.-M. (2016). A Tutorial Review of Functional Connectivity Analysis Methods and Their Interpretational Pitfalls. *Frontiers in Systems Neuroscience*, *9*. https://doi.org/10.3389/fnsys.2015.00175

Batsikadze, G., Moliadze, V., Paulus, W., Kuo, M.-F., & Nitsche, M. A. (2013). Partially non-linear stimulation intensity-dependent effects of direct current stimulation on motor cortex excitability in humans: Effect of tDCS on cortical excitability. *The Journal of Physiology*, *591*(7), 1987–2000. https://doi.org/10.1113/jphysiol.2012.249730

Batsikadze, G., Rezaee, Z., Chang, D.-I., Gerwig, M., Herlitze, S., Dutta, A., Nitsche, M. A., & Timmann, D. (2019). Effects of cerebellar transcranial direct current stimulation on cerebellar-brain inhibition in humans: A systematic evaluation. *Brain Stimulation*, *12*(5), 1177–1186. https://doi.org/10.1016/j.brs.2019.04.010

Baudewig, J., Nitsche, M. A., Paulus, W., & Frahm, J. (2001). Regional modulation of BOLD MRI responses to human sensorimotor activation by transcranial direct current stimulation. *Magnetic Resonance in Medicine : Official Journal of the Society of Magnetic Resonance in Medicine / Society of Magnetic Resonance in Medicine*, *45*(2), 196–201.

Beckmann, C. F., & Smith, S. M. (2004). Probabilistic independent component analysis for functional magnetic resonance imaging. *IEEE Transactions on Medical Imaging*, *23*(2), 137–152. https://doi.org/10.1109/TMI.2003.822821

Benjamini, Y., & Yekutieli, D. (2001). The Control of the False Discovery Rate in Multiple Testing under Dependency. *The Annals of Statistics*, *29*(4), 1165–1188.

Berker, Archy O. de, Marom Bikson, and Sven Bestmann. 2013. 'Predicting the Behavioral Impact of Transcranial Direct Current Stimulation: Issues and Limitations'. *Frontiers in Human Neuroscience* 7. https://doi.org/10.3389/fnhum.2013.00613.

Berlingeri, Manuela, Francesca Giulia Magnani, Gerardo Salvato, Mario Rosanova, and Gabriella Bottini. 2019. 'Neuroimaging Studies on Disorders of Consciousness: A Meta-Analytic Evaluation'. *Journal of Clinical Medicine* 8 (4): 516. https://doi.org/10.3390/jcm8040516.

Bestmann, Sven, Archy O. de Berker, and James Bonaiuto. 2015. 'Understanding the Behavioural Consequences of Noninvasive Brain Stimulation'. *Trends in Cognitive Sciences* 19 (1): 13–20. https://doi.org/10.1016/j.tics.2014.10.003.

Bigdely-Shamlo, N., Mullen, T., Kothe, C., Su, K.-M., & Robbins, K. A. (2015). The PREP pipeline: Standardized preprocessing for large-scale EEG analysis. *Frontiers in Neuroinformatics*, *9*. https://doi.org/10.3389/fninf.2015.00016

Bikson, M., Brunoni, A. R., Charvet, L. E., Clark, V. P., Cohen, L. G., Deng, Z.-D., Dmochowski, J., Edwards, D. J., Frohlich, F., Kappenman, E. S., Lim, K. O., Loo, C., Mantovani, A., McMullen, D. P., Parra, L. C., Pearson, M., Richardson, J. D., Rumsey, J. M., Sehatpour, P., … Lisanby, S. H. (2018). Rigor and reproducibility in research

with transcranial electrical stimulation: An NIMH-sponsored workshop. *Brain Stimulation*, *11*(3), 465–480. https://doi.org/10.1016/j.brs.2017.12.008

Bikson, M., Rahman, A., Datta, A., Fregni, F., & Merabet, L. (2012). High-Resolution Modeling Assisted Design of Customized and Individualized Transcranial Direct Current Stimulation Protocols. *Neuromodulation: Technology at the Neural Interface*, *15*(4), 306–315. https://doi.org/10.1111/j.1525-1403.2012.00481.x

Bikson, Marom, and Jacek Dmochowski. 2020. 'What It Means to Go Deep with Non-Invasive Brain Stimulation'. *Clinical Neurophysiology* 131 (3): 752–54. https://doi.org/10.1016/j.clinph.2019.12.003.

Blumenfeld, H. (2023). Brain Mechanisms of Conscious Awareness: Detect, Pulse, Switch, and Wave. *The Neuroscientist*, *29*(1), 9–18. https://doi.org/10.1177/10738584211049378

Bodien, Y. G., Giacino, J. T., & Edlow, B. L. (2017). Functional MRI Motor Imagery Tasks to Detect Command Following in Traumatic Disorders of Consciousness. *Frontiers in Neurology*, *8*, 688. https://doi.org/10.3389/fneur.2017.00688

Boggio, P. S., Castro, L. O., Savagim, E. A., Braite, R., Cruz, V. C., Rocha, R. R., Rigonatti, S. P., Silva, M. T. A., & Fregni, F. (2006). Enhancement of non-dominant hand motor function by anodal transcranial direct current stimulation. *Neuroscience Letters*, *404*(1–2), 232–236. https://doi.org/10.1016/j.neulet.2006.05.051

Bolognini, N., Pascual-Leone, A., & Fregni, F. (2009a). Using non-invasive brain stimulation to augment motor training-induced plasticity. *Journal of NeuroEngineering and Rehabilitation*, *6*(1), Article 1. https://doi.org/10.1186/1743-0003-6-8

Bolognini, N., Pascual-Leone, A., & Fregni, F. (2009b). Using non-invasive brain stimulation to augment motor training-induced plasticity. *Journal of Neuroengineering and Rehabilitation*, *6*(1), 8.

Bolognini, Nadia, Giuseppe Vallar, Carlotta Casati, Lydia Abdul Latif, Rasheda El-Nazer, Julie Williams, Elisabetta Banco, et al. 2011. 'Neurophysiological and Behavioral Effects of TDCS Combined With Constraint-Induced Movement Therapy in Poststroke Patients'. *Neurorehabilitation and Neural Repair* 25 (9): 819–29. https://doi.org/10.1177/1545968311411056.

Boly, M., Coleman, M. R., Davis, M. H., Hampshire, A., Bor, D., Moonen, G., Maquet, P. A., Pickard, J. D., Laureys, S., & Owen, A. M. (2007a). When thoughts become action: An fMRI paradigm to study volitional brain activity in non-communicative brain injured patients. *NeuroImage*, *36*(3), Article 3. https://doi.org/10.1016/j.neuroimage.2007.02.047

Bolzoni, Francesco, Lars-Gunnar Pettersson, and Elzbieta Jankowska. 2013. 'Evidence for Long-Lasting Subcortical Facilitation by Transcranial Direct Current Stimulation in the Cat: Subcortical Effects of TDCS'. *The Journal of Physiology* 591 (13): 3381–99. https://doi.org/10.1113/jphysiol.2012.244764.

Bornheim, Stephen, Jean-Louis Croisier, Pierre Maquet, and Jean-François Kaux. 2020. 'Transcranial Direct Current Stimulation Associated with Physical-Therapy in Acute Stroke Patients - A Randomized, Triple Blind, Sham-Controlled Study'. *Brain Stimulation* 13 (2): 329–36. https://doi.org/10.1016/j.brs.2019.10.019.

Boscolo Galazzo, I., Storti, S. F., Formaggio, E., Pizzini, F. B., Fiaschi, A., Beltramello, A., Bertoldo, A., & Manganotti, P. (2014). Investigation of brain hemodynamic changes induced by active and passive movements: A combined arterial spin labeling–BOLD fMRI study. *Journal of Magnetic Resonance Imaging*, *40*(4), 937–948. https://doi.org/10.1002/jmri.24432

Bourdillon, P., Hermann, B., Sitt, J. D., & Naccache, L. (2019). Electromagnetic Brain Stimulation in Patients With Disorders of Consciousness. *Frontiers in Neuroscience*, *13*, 223. https://doi.org/10.3389/fnins.2019.00223

Breakspear, M. (2017). Dynamic models of large-scale brain activity. *Nature Neuroscience*, *20*(3), 340–352. https://doi.org/10.1038/nn.4497

Bruno, Marie-Aurélie, Steve Majerus, Mélanie Boly, Audrey Vanhaudenhuyse, Caroline Schnakers, Olivia Gosseries, Pierre Boveroux, et al. 2012. 'Functional Neuroanatomy Underlying the Clinical Subcategorization of Minimally Conscious State Patients'. *Journal of Neurology* 259 (6): 1087–98. https://doi.org/10.1007/s00415-011-6303-7.

Buch, E. R., Santarnecchi, E., Antal, A., Born, J., Celnik, P. A., Classen, J., Gerloff, C., Hallett, M., Hummel, F. C., Nitsche, M. A., Pascual-Leone, A., Paulus, W. J., Reis, J., Robertson, E. M., Rothwell, J. C., Sandrini, M., Schambra, H. M., Wassermann, E. M., Ziemann, U., & Cohen, L. G. (2017). Effects of tDCS on motor learning and memory formation: A consensus and critical position paper. *Clinical Neurophysiology*, *128*(4), 589–603. https://doi.org/10.1016/j.clinph.2017.01.004

Bullmore, E., & Sporns, O. (2009). Complex brain networks: Graph theoretical analysis of structural and functional systems. *Nature Reviews Neuroscience*, *10*(3), Article 3. https://doi.org/10.1038/nrn2575

Cain, J. A., Spivak, N. M., Coetzee, J. P., Crone, J. S., Johnson, M. A., Lutkenhoff, E. S., Real, C., Buitrago-Blanco,

M., Vespa, P. M., Schnakers, C., & Monti, M. M. (2022). Ultrasonic Deep Brain Neuromodulation in Acute Disorders of Consciousness: A Proof-of-Concept. *Brain Sciences*, *12*(4), Article 4. https://doi.org/10.3390/brainsci12040428

Calzolari, S., Jalali, R., & Fernández-Espejo, D. (2023). Characterising stationary and dynamic effective connectivity changes in the motor network during and after tDCS. *NeuroImage*, *269*, 119915. https://doi.org/10.1016/j.neuroimage.2023.119915

Cao, B., Chen, Y., Yu, R., Chen, L., Chen, P., Weng, Y., Chen, Q., Song, J., Xie, Q., & Huang, R. (2019). Abnormal dynamic properties of functional connectivity in disorders of consciousness. *NeuroImage: Clinical*, *24*, 102071. https://doi.org/10.1016/j.nicl.2019.102071

Cao, J., Zhao, Y., Shan, X., Wei, H., Guo, Y., Chen, L., Erkoyuncu, J. A., & Sarrigiannis, P. G. (2022). Brain functional and effective connectivity based on electroencephalography recordings: A review. *Human Brain Mapping*, *43*(2), Article 2. https://doi.org/10.1002/hbm.25683

Carrière, Manon, Sepehr Mortaheb, Federico Raimondo, Jitka Annen, Alice Barra, Maria C. Binda Fossati, Camille Chatelle, et al. 2020. 'Neurophysiological Correlates of a Single Session of Prefrontal TDCS in Patients with Prolonged Disorders of Consciousness: A Pilot Double-Blind Randomized Controlled Study'. *Brain Sciences* 10 (7): 469. https://doi.org/10.3390/brainsci10070469.

Cavaliere, C., Aiello, M., Di Perri, C., Amico, E., Martial, C., Thibaut, A., Laureys, S., & Soddu, A. (2016). Functional Connectivity Substrates for tDCS Response in Minimally Conscious State Patients. *Frontiers in Cellular Neuroscience*, *10*. https://doi.org/10.3389/fncel.2016.00257

Cavinato, Marianna, Clara Genna, Emanuela Formaggio, Caterina Gregorio, Silvia F. Storti, Paolo Manganotti, Emanuela Casanova, Roberto Piperno, and Francesco Piccione. 2019. 'Behavioural and Electrophysiological Effects of TDCS to Prefrontal Cortex in Patients with Disorders of Consciousness'. *Clinical Neurophysiology* 130 (2): 231–38. https://doi.org/10.1016/j.clinph.2018.10.018.

Chalmers, D. J., & Cruz, S. (2016). *FACING UP TO THE PROBLEM OF CONSCIOUSNESS*.

Chen, C., Fang, Y., Wang, X., Bao, S.-C., Tang, Z., & Tong, R. K. (2019). Excitation Comparison between Multi-site Stimulation using Network-based tDCS and Focal Stimulation using High-definition tDCS. *2019 41st Annual International Conference of the IEEE Engineering in Medicine and Biology Society (EMBC)*, 6884–6887. https://doi.org/10.1109/EMBC.2019.8857287

Chennu, S., Annen, J., Wannez, S., Thibaut, A., Chatelle, C., Cassol, H., Martens, G., Schnakers, C., Gosseries, O., Menon, D., & Laureys, S. (2017). Brain networks predict metabolism, diagnosis and prognosis at the bedside in disorders of consciousness. *Brain*, *140*(8), 2120–2132. https://doi.org/10.1093/brain/awx163

Chennu, S., Finoia, P., Kamau, E., Allanson, J., Williams, G. B., Monti, M. M., Noreika, V., Arnatkeviciute, A., Canales-Johnson, A., Olivares, F., Cabezas-Soto, D., Menon, D. K., Pickard, J. D., Owen, A. M., & Bekinschtein, T. A. (2014). Spectral Signatures of Reorganised Brain Networks in Disorders of Consciousness. *PLoS Computational Biology*, *10*(10), Article 10. https://doi.org/10.1371/journal.pcbi.1003887

Cherian, I., Beltran, M., Landi, A., Alafaci, C., Torregrossa, F., & Grasso, G. (2018). Introducing the concept of "CSF-shift edema" in traumatic brain injury. *Journal of Neuroscience Research*, *96*(4), 744–752. https://doi.org/10.1002/jnr.24145

Chhatbar, Pratik Y., Steven A. Kautz, Istvan Takacs, Nathan C. Rowland, Gonzalo J. Revuelta, Mark S. George, Marom Bikson, and Wuwei Feng. 2018. 'Evidence of Transcranial Direct Current Stimulation-Generated Electric Fields at Subthalamic Level in Human Brain in Vivo'. *Brain Stimulation* 11 (4): 727–33. https://doi.org/10.1016/j.brs.2018.03.006.

Chye, L., Nosaka, K., Murray, L., Edwards, D., & Thickbroom, G. (2010). Corticomotor excitability of wrist flexor and extensor muscles during active and passive movement. *Human Movement Science*, *29*(4), Article 4. https://doi.org/10.1016/j.humov.2010.03.003

Claassen, J., Doyle, K., Matory, A., Couch, C., Burger, K. M., Velazquez, A., Okonkwo, J. U., King, J.-R., Park, S., Agarwal, S., Roh, D., Megjhani, M., Eliseyev, A., Connolly, E. S., & Rohaut, B. (2019). Detection of Brain Activation in Unresponsive Patients with Acute Brain Injury. *New England Journal of Medicine*, *380*(26), Article 26. https://doi.org/10.1056/NEJMoa1812757

Clemens, Benjamin, Stefanie Jung, Gianluca Mingoia, David Weyer, Frank Domahs, and Klaus Willmes. 2014. 'Influence of Anodal Transcranial Direct Current Stimulation (TDCS) over the Right Angular Gyrus on Brain Activity during Rest'. Edited by Andrea Antal. *PLoS ONE* 9 (4): e95984. https://doi.org/10.1371/journal.pone.0095984.

Cohen Kadosh, Roi, Sonja Soskic, Teresa Iuculano, Ryota Kanai, and Vincent Walsh. 2010. 'Modulating Neuronal Activity Produces Specific and Long-Lasting Changes in Numerical Competence'. *Current Biology* 20 (22): 2016–20. https://doi.org/10.1016/j.cub.2010.10.007.

Coulborn, S., Taylor, C., Naci, L., Owen, A. M., & Fernández-Espejo, D. (2021). Disruptions in Effective Connectivity within and between Default Mode Network and Anterior Forebrain Mesocircuit in Prolonged Disorders of Consciousness. *Brain Sciences*, *11*(6), 749. https://doi.org/10.3390/brainsci11060749

Crinion, J., Ashburner, J., Leff, A., Brett, M., Price, C., & Friston, K. (2007). Spatial normalization of lesioned brains: Performance evaluation and impact on fMRI analyses. *NeuroImage*, *37*(3), 866–875. https://doi.org/10.1016/j.neuroimage.2007.04.065

Crone, J. S., Ladurner, G., Höller, Y., Golaszewski, S., Trinka, E., & Kronbichler, M. (2011). Deactivation of the Default Mode Network as a Marker of Impaired Consciousness: An fMRI Study. *PLoS ONE*, *6*(10), e26373. https://doi.org/10.1371/journal.pone.0026373

Cruse, D., Chennu, S., Chatelle, C., Bekinschtein, T. A., Fernández-Espejo, D., Pickard, J. D., Laureys, S., & Owen, A. M. (2011). Bedside detection of awareness in the vegetative state: A cohort study. *The Lancet*, *378*(9809), 2088–2094. https://doi.org/10.1016/S0140-6736(11)61224-5

Cruse, D., Chennu, S., Fernández-Espejo, D., Payne, W. L., Young, G. B., & Owen, A. M. (2012). Detecting Awareness in the Vegetative State: Electroencephalographic Evidence for Attempted Movements to Command. *PLoS ONE*, *7*(11), Article 11. https://doi.org/10.1371/journal.pone.0049933

Cummiford, C. M., Nascimento, T. D., Foerster, B. R., Clauw, D. J., Zubieta, J.-K., Harris, R. E., & DaSilva, A. F. (2016). Changes in resting state functional connectivity after repetitive transcranial direct current stimulation applied to motor cortex in fibromyalgia patients. *Arthritis Research & Therapy*, *18*. https://doi.org/10.1186/s13075-016-0934-0

DaSilva, Alexandre F., Mariana E. Mendonca, Soroush Zaghi, Mariana Lopes, Marcos Fabio DosSantos, Egilius L. Spierings, Zahid Bajwa, Abhishek Datta, Marom Bikson, and Felipe Fregni. 2012. 'TDCS-Induced Analgesia and Electrical Fields in Pain-Related Neural Networks in Chronic Migraine'. *Headache: The Journal of Head and Face Pain* 52 (8): 1283–95. https://doi.org/10.1111/j.1526-4610.2012.02141.x.

Daskalakis, Z. J., Paradiso, G. O., Christensen, B. K., Fitzgerald, P. B., Gunraj, C., & Chen, R. (2004). Exploring the connectivity between the cerebellum and motor cortex in humans: Mechanisms of cerebellar inhibition. *The Journal of Physiology*, *557*(2), Article 2. https://doi.org/10.1113/jphysiol.2003.059808

Datta, Abhishek, Varun Bansal Bs, Julian Diaz Bs, Jinal Patel, Davide Reato, and Marom Bikson. n.d. 'Gyri-Precise Head Model of Transcranial Direct Current Stimulation: Improved Spatial Focality Using a Ring Electrode versus Conventional Rectangular Pad', 8.

Delorme, A., & Makeig, S. (2004). EEGLAB: An open source toolbox for analysis of single-trial EEG dynamics including independent component analysis. *Journal of Neuroscience Methods*, *134*(1), 9–21. https://doi.org/10.1016/j.jneumeth.2003.10.009

Demertzi, A., Antonopoulos, G., Heine, L., Voss, H. U., Crone, J. S., de Los Angeles, C., Bahri, M. A., Di Perri, C., Vanhaudenhuyse, A., Charland-Verville, V., Kronbichler, M., Trinka, E., Phillips, C., Gomez, F., Tshibanda, L., Soddu, A., Schiff, N. D., Whitfield-Gabrieli, S., & Laureys, S. (2015). Intrinsic functional connectivity differentiates minimally conscious from unresponsive patients. *Brain*, *138*(9), 2619–2631. https://doi.org/10.1093/brain/awv169

Demertzi, A., Tagliazucchi, E., Dehaene, S., Deco, G., Barttfeld, P., Raimondo, F., Martial, C., Fernández-Espejo, D., Rohaut, B., Voss, H. U., Schiff, N. D., Owen, A. M., Laureys, S., Naccache, L., & Sitt, J. D. (2019). Human consciousness is supported by dynamic complex patterns of brain signal coordination. *Science Advances*, *5*(2), eaat7603. https://doi.org/10.1126/sciadv.aat7603

Di Perri, C., Stender, J., Laureys, S., & Gosseries, O. (2014). Functional neuroanatomy of disorders of consciousness. *Epilepsy & Behavior*, *30*, 28–32. https://doi.org/10.1016/j.yebeh.2013.09.014

Dissanayaka, T., Zoghi, M., Farrell, M., Egan, G. F., & Jaberzadeh, S. (2017). Does transcranial electrical stimulation enhance corticospinal excitability of the motor cortex in healthy individuals? A systematic review and meta-analysis. *European Journal of Neuroscience*, *46*(4), 1968–1990. https://doi.org/10.1111/ejn.13640

Du, T., Mestre, H., Kress, B. T., Liu, G., Sweeney, A. M., Samson, A. J., Rasmussen, M. K., Mortensen, K. N., Bork, P. A. R., Peng, W., Olveda, G. E., Bashford, L., Toro, E. R., Tithof, J., Kelley, D. H., Thomas, J. H., Hjorth, P. G., Martens, E. A., Mehta, R. I., … Nedergaard, M. (2022). Cerebrospinal fluid is a significant fluid source for anoxic cerebral oedema. *Brain*, *145*(2), 787–797. https://doi.org/10.1093/brain/awab293

Dubreuil-Vall, L., Chau, P., Ruffini, G., Widge, A. S., & Camprodon, J. A. (2019). TDCS to the left DLPFC modulates cognitive and physiological correlates of executive function in a state-dependent manner. *Brain Stimulation: Basic, Translational, and Clinical Research in Neuromodulation*, *12*(6), 1456–1463. https://doi.org/10.1016/j.brs.2019.06.006

Dular, P., Geuzaine, C., Henrotte, F., & Legros, W. (1998). A general environment for the treatment of discrete problems and its application to the finite element method. *IEEE Transactions on Magnetics*, *34*(5), 3395–3398. https://doi.org/10.1109/20.717799

Duszyk-Bogorodzka, A., Zieleniewska, M., & Jankowiak-Siuda, K. (2022). Brain Activity Characteristics of Patients With Disorders of Consciousness in the EEG Resting State Paradigm: A Review. *Frontiers in Systems Neuroscience*, *16*, 654541. https://doi.org/10.3389/fnsys.2022.654541

Edlow, Brian L, Camille Chatelle, Camille A. Spencer, Catherine J. Chu, Yelena G. Bodien, Kathryn L. O'Connor, Ronald E. Hirschberg, et al. 2017. 'Early Detection of Consciousness in Patients with Acute Severe Traumatic Brain Injury'. *Brain* 140 (9): 2399–2414. https://doi.org/10.1093/brain/awx176.

Ehrhardt, S. E., Filmer, H. L., Wards, Y., Mattingley, J. B., & Dux, P. E. (2021). The influence of tDCS intensity on decision-making training and transfer outcomes. *Journal of Neurophysiology*, *125*(2), 385–397. https://doi.org/10.1152/jn.00423.2020

Ehsani, F., Mortezanejad, M., Yosephi, M. H., Daniali, S., & Jaberzadeh, S. (2022). The effects of concurrent M1 anodal tDCS and physical therapy interventions on function of ankle muscles in patients with stroke: A randomized, double-blinded sham-controlled trial study. *Neurological Sciences*, *43*(3), 1893–1901. https://doi.org/10.1007/s10072-021-05503-9

Elliott, L., & Walker, L. (2005). Rehabilitation interventions for vegetative and minimally conscious patients. *Neuropsychological Rehabilitation*, *15*(3–4), 480–493.

Estraneo, Anna, Angelo Pascarella, Pasquale Moretta, Orsola Masotta, Salvatore Fiorenza, Grazia Chirico, Emanuela Crispino, Vincenzo Loreto, and Luigi Trojano. 2017. 'Repeated Transcranial Direct Current Stimulation in Prolonged Disorders of Consciousness: A Double-Blind Cross-over Study'. *Journal of the Neurological Sciences* 375 (April): 464–70. https://doi.org/10.1016/j.jns.2017.02.036.

Evans, C., Zich, C., Lee, J. S. A., Ward, N., & Bestmann, S. (2022). Inter-individual variability in current direction for common tDCS montages. *NeuroImage*, *260*, 119501. https://doi.org/10.1016/j.neuroimage.2022.119501

Evans, Carys, Clarissa Bachmann, Jenny S.A. Lee, Evridiki Gregoriou, Nick Ward, and Sven Bestmann. 2020. 'Dose-Controlled TDCS Reduces Electric Field Intensity Variability at a Cortical Target Site'. *Brain Stimulation* 13 (1): 125–36. https://doi.org/10.1016/j.brs.2019.10.004.

Fang, Q., & Boas, D. A. (2009). Monte Carlo Simulation of Photon Migration in 3D Turbid Media Accelerated by Graphics Processing Units. *Optics Express*, *17*(22), 20178. https://doi.org/10.1364/OE.17.020178

Felten D. L. O'Banion M. K. Maida M. S. & Netter F. H. (2016). Netter's atlas of neuroscience (Third). Elsevier. Retrieved September 9 2023 from https://www.clinicalkey.com/dura/browse/bookChapter/3-s2.0-C20130139700.

Fernandez-Espejo, D., & Owen, A. M. (2013). Detecting awareness after severe brain injury. *Nature Reviews Neuroscience*, *14*(11), 801–809.

Fernández-Espejo, D., Aloi, D., Rocchetta, A. I. della, Hoad, D., Greenwood, R., Playford, E. D., & Cruse, D. (2020). *Exploring the neural, behavioural, and clinical effects of transcranial direct current stimulation in patients with a Prolonged Disorder of Consciousness; protocol for a double-blind randomised crossover feasibility study* [Preprint]. In Review. https://doi.org/10.21203/rs.3.rs-15515/v1

Fernandez-Espejo, D., Bekinschtein, T., Monti, M. M., Pickard, J. D., Junque, C., Coleman, M. R., & Owen, A. M. (2011). Diffusion weighted imaging distinguishes the vegetative state from the minimally conscious state. *NeuroImage*, *54*(1), 103–112.

Fernandez-Espejo, D., Junque, C., Bernabeu, M., Roig-Rovira, T., Vendrell, P., & Mercader, J. M. (2010). Reductions of thalamic volume and regional shape changes in the vegetative and the minimally conscious states. *Journal of Neurotrauma*, *27*(7), 1187–1193.

Fernández-Espejo, D., Rossit, S., & Owen, A. M. (2015). A Thalamocortical Mechanism for the Absence of Overt Motor Behavior in Covertly Aware Patients. *JAMA Neurology*, *72*(12), 1442. https://doi.org/10.1001/jamaneurol.2015.2614

Fernandez-Espejo, D., Rossit, S., & Owen, A. M. (2015). A Thalamocortical Mechanism for the Absence of Overt Motor Behavior in Covertly Aware Patients. *JAMA Neurology*, *72*(12), 1–9.

Fernández-Espejo, Davinia, and Adrian M. Owen. 2013. 'Detecting Awareness after Severe Brain Injury'. *Nature Reviews Neuroscience* 14 (11): 801–9. https://doi.org/10.1038/nrn3608.
Fernández-Espejo, Davinia, Carme Junque, Montserrat Bernabeu, Teresa Roig-Rovira, Pere Vendrell, and Jose M. Mercader. 2010. 'Reductions of Thalamic Volume and Regional Shape Changes in the Vegetative and the Minimally Conscious States'. *Journal of Neurotrauma* 27 (7): 1187–93. https://doi.org/10.1089/neu.2010.1297.
Fernández-Espejo, Davinia, Stephanie Rossit, and Adrian M. Owen. 2015. 'A Thalamocortical Mechanism for the Absence of Overt Motor Behavior in Covertly Aware Patients'. *JAMA Neurology* 72 (12): 1442. https://doi.org/10.1001/jamaneurol.2015.2614.
Fernández-Espejo, Davinia, Tristan Bekinschtein, Martin M. Monti, John D. Pickard, Carme Junque, Martin R. Coleman, and Adrian M. Owen. 2011. 'Diffusion Weighted Imaging Distinguishes the Vegetative State from the Minimally Conscious State'. *NeuroImage* 54 (1): 103–12. https://doi.org/10.1016/j.neuroimage.2010.08.035.
Ferrante, O., Liu, L., Minarik, T., Gorska, U., Ghafari, T., Luo, H., & Jensen, O. (2022). FLUX: A pipeline for MEG analysis. *NeuroImage*, *253*, 119047. https://doi.org/10.1016/j.neuroimage.2022.119047
Filmer, H. L., Mattingley, J. B., & Dux, P. E. (2019). Modulating brain activity and behaviour with tDCS: Rumours of its death have been greatly exaggerated. *Cortex*. https://doi.org/10.1016/j.cortex.2019.10.006
Filmer, H. L., Mattingley, J. B., & Dux, P. E. (2020). Modulating brain activity and behaviour with tDCS: Rumours of its death have been greatly exaggerated. *Cortex*, *123*, 141–151. https://doi.org/10.1016/j.cortex.2019.10.006
Filmer, Hannah L., Jason B. Mattingley, and Paul E. Dux. 2020. 'Modulating Brain Activity and Behaviour with TDCS: Rumours of Its Death Have Been Greatly Exaggerated'. *Cortex* 123 (February): 141–51. https://doi.org/10.1016/j.cortex.2019.10.006.
Fischler, M. A., & Bolles, R. C. (1981). Random sample consensus: A paradigm for model fitting with applications to image analysis and automated cartography. *Communications of the ACM*, *24*(6), 381–395. https://doi.org/10.1145/358669.358692
Flöel, A. (2014). TDCS-enhanced motor and cognitive function in neurological diseases. *NeuroImage*, *85*, 934–947. https://doi.org/10.1016/j.neuroimage.2013.05.098
Floyer-Lea, A., & Matthews, P. M. (2005). Distinguishable brain activation networks for short- and long-term motor skill learning. *Journal of Neurophysiology*, *94*(1), 512–518.
Formaggio, E., Del Felice, A., Cavinato, M., Storti, S. F., Arcaro, C., Turco, C., Salvi, L., Avesani, R., Piccione, F., & Manganotti, P. (2020). EEG to Identify Attempted Movement in Unresponsive Wakefulness Syndrome. *Clinical EEG and Neuroscience*, *51*(5), 339–347. https://doi.org/10.1177/1550059420911525
Fornacon-Wood, I., Mistry, H., Johnson-Hart, C., Faivre-Finn, C., O'Connor, J. P. B., & Price, G. J. (2022). Understanding the Differences Between Bayesian and Frequentist Statistics. *International Journal of Radiation Oncology*Biology*Physics*, *112*(5), 1076–1082. https://doi.org/10.1016/j.ijrobp.2021.12.011
Fregni, F., El-Hagrassy, M. M., Pacheco-Barrios, K., Carvalho, S., Leite, J., Simis, M., Brunelin, J., Nakamura-Palacios, E. M., Marangolo, P., Venkatasubramanian, G., San-Juan, D., Caumo, W., Bikson, M., Brunoni, A. R., & Neuromodulation Center Working Group. (2021). Evidence-Based Guidelines and Secondary Meta-Analysis for the Use of Transcranial Direct Current Stimulation in Neurological and Psychiatric Disorders. *International Journal of Neuropsychopharmacology*, *24*(4), 256–313. https://doi.org/10.1093/ijnp/pyaa051
Friston, K. (2009). Causal Modelling and Brain Connectivity in Functional Magnetic Resonance Imaging. *PLoS Biology*, *7*(2), e1000033. https://doi.org/10.1371/journal.pbio.1000033
Friston, K. J., Harrison, L., & Penny, W. (2003). Dynamic causal modelling. *NeuroImage*, *19*(4), Article 4. https://doi.org/10.1016/S1053-8119(03)00202-7
Friston, K. J. (2011). Functional and Effective Connectivity: A Review. *Brain Connectivity*, *1*(1), 13–36. https://doi.org/10.1089/brain.2011.0008
Galea, J. M., & Celnik, P. (2009). Brain Polarization Enhances the Formation and Retention of Motor Memories. *Journal of Neurophysiology*, *102*(1), 294–301. https://doi.org/10.1152/jn.00184.2009
Galea, J. M., Jayaram, G., Ajagbe, L., & Celnik, P. (2009a). Modulation of Cerebellar Excitability by Polarity-Specific Noninvasive Direct Current Stimulation. *Journal of Neuroscience*, *29*(28), Article 28. https://doi.org/10.1523/JNEUROSCI.2184-09.2009
Galea, J. M., Jayaram, G., Ajagbe, L., & Celnik, P. (2009b). Modulation of cerebellar excitability by polarity-specific noninvasive direct current stimulation. *The Journal of Neuroscience : The Official Journal of the Society for Neuroscience*, *29*(28), 9115–9122.
Galea, J. M., Vazquez, A., Pasricha, N., de Xivry, J.-J. O., & Celnik, P. (2011). Dissociating the roles of the cerebellum

and motor cortex during adaptive learning: The motor cortex retains what the cerebellum learns. *Cerebral Cortex (New York, N.Y.: 1991)*, *21*(8), 1761–1770. https://doi.org/10.1093/cercor/bhq246

Galea, Joseph M., and Pablo Celnik. 2009. 'Brain Polarization Enhances the Formation and Retention of Motor Memories'. *Journal of Neurophysiology* 102 (1): 294–301. https://doi.org/10.1152/jn.00184.2009.

Gerrard, P., Zafonte, R., & Giacino, J. T. (2014). Coma Recovery Scale–Revised: Evidentiary Support for Hierarchical Grading of Level of Consciousness. *Archives of Physical Medicine and Rehabilitation*, *95*(12), 2335–2341. https://doi.org/10.1016/j.apmr.2014.06.018

Giacino, J. T., Ashwal, S., Childs, N., Cranford, R., Jennett, B., Katz, D. I., Kelly, J. P., Rosenberg, J. H., Whyte, J., Zafonte, R. D., & Zasler, N. D. (2002). *CME The minimally conscious state*. 6.

Giacino, J. T., Kalmar, K., & Whyte, J. (2004). The JFK Coma Recovery Scale-Revised: Measurement characteristics and diagnostic utility11No commercial party having a direct financial interest in the results of the research supporting this article has or will confer a benefit upon the authors or upon any organization with which the authors are associated. *Archives of Physical Medicine and Rehabilitation*, *85*(12), 2020–2029. https://doi.org/10.1016/j.apmr.2004.02.033

Giacino, J. T., Katz, D. I., Schiff, N. D., Whyte, J., Ashman, E. J., Ashwal, S., Barbano, R., Hammond, F. M., Laureys, S., Ling, G. S. F., Nakase-Richardson, R., Seel, R. T., Yablon, S., Getchius, T. S. D., Gronseth, G. S., & Armstrong, M. J. (2018). Comprehensive systematic review update summary: Disorders of consciousness: Report of the Guideline Development, Dissemination, and Implementation Subcommittee of the American Academy of Neurology; the American Congress of Rehabilitation Medicine; and the National Institute on Disability, Independent Living, and Rehabilitation Research. *Neurology*, *91*(10), Article 10. https://doi.org/10.1212/WNL.0000000000005928

Giacino, J. T., Kezmarsky, M. A., DeLuca, J., & Cicerone, K. D. (1991). Monitoring rate of recovery to predict outcome in minimally responsive patients. *Archives of Physical Medicine and Rehabilitation*, *72*(11), 897–901. https://doi.org/10.1016/0003-9993(91)90008-7

Giacino, J. T., Schnakers, C., Rodriguez-Moreno, D., Kalmar, K., Schiff, N., & Hirsch, J. (2009). Behavioral assessment in patients with disorders of consciousness: Gold standard or fool's gold? In *Progress in Brain Research* (Vol. 177, pp. 33–48). Elsevier. https://doi.org/10.1016/S0079-6123(09)17704-X

Giacino, Joseph, Douglas Katz, and John Whyte. 2013. 'Neurorehabilitation in Disorders of Consciousness'. *Seminars in Neurology* 33 (02): 142–56. https://doi.org/10.1055/s-0033-1348960.

Giacino, Joseph T., Douglas I. Katz, Nicholas D. Schiff, John Whyte, Eric J. Ashman, Stephen Ashwal, Richard Barbano, et al. 2018. 'Practice Guideline Update Recommendations Summary: Disorders of Consciousness: Report of the Guideline Development, Dissemination, and Implementation Subcommittee of the American Academy of Neurology; the American Congress of Rehabilitation Medicine; and the National Institute on Disability, Independent Living, and Rehabilitation Research'. *Neurology* 91 (10): 450–60. https://doi.org/10.1212/WNL.0000000000005926.

Giacino, J T, S Ashwal, N Childs, R Cranford, B Jennett, D I Katz, J P Kelly, et al. 2002. 'CME The Minimally Conscious State', 6.

Gill-Thwaites, H., & Munday, R. (2004). The sensory modality assessment and rehabilitation technique (SMART): A valid and reliable assessment for vegetative state and minimally conscious state patients. *Brain Injury*, *18*(12), Article 12. https://doi.org/10.1080/02699050410001719952

Glover, G. H. (2011). Overview of Functional Magnetic Resonance Imaging. *Neurosurgery Clinics of North America*, *22*(2), 133–139. https://doi.org/10.1016/j.nec.2010.11.001

Göksu, C., Hanson, L. G., Siebner, H. R., Ehses, P., Scheffler, K., & Thielscher, A. (2018). Human in-vivo brain magnetic resonance current density imaging (MRCDI). *NeuroImage*, *171*, 26–39. https://doi.org/10.1016/j.neuroimage.2017.12.075

Goldfine, A. M., Victor, J. D., Conte, M. M., Bardin, J. C., & Schiff, N. D. (2011). Determination of awareness in patients with severe brain injury using EEG power spectral analysis. *Clinical Neurophysiology*, *122*(11), Article 11. https://doi.org/10.1016/j.clinph.2011.03.022

Gomez-Tames, Jose. n.d. 'Significant Group-Level Hotspots Found in Deep Brain Regions during Transcranial Direct Current Stimulation (TDCS): A Computational Analysis of Electric Fields', 40.

Gramfort, A. (2013). MEG and EEG data analysis with MNE-Python. *Frontiers in Neuroscience*, *7*. https://doi.org/10.3389/fnins.2013.00267

Griffanti, L., Salimi-Khorshidi, G., Beckmann, C. F., Auerbach, E. J., Douaud, G., Sexton, C. E., Zsoldos, E., Ebmeier,

K. P., Filippini, N., Mackay, C. E., Moeller, S., Xu, J., Yacoub, E., Baselli, G., Ugurbil, K., Miller, K. L., & Smith, S. M. (2014). ICA-based artefact and accelerated fMRI acquisition for improved Resting State Network imaging. *NeuroImage*, *95*, 232–247. https://doi.org/10.1016/j.neuroimage.2014.03.034

Grimaldi, G., Argyropoulos, G. P., Bastian, A., Cortes, M., Davis, N. J., Edwards, D. J., Ferrucci, R., Fregni, F., Galea, J. M., Hamada, M., Manto, M., Miall, R. C., Morales-Quezada, L., Pope, P. A., Priori, A., Rothwell, J., Tomlinson, S. P., & Celnik, P. (2016). Cerebellar Transcranial Direct Current Stimulation (ctDCS): A Novel Approach to Understanding Cerebellar Function in Health and Disease. *The Neuroscientist*, *22*(1), 83–97. https://doi.org/10.1177/1073858414559409

Guger, C., Edlinger, G., Harkam, W., Niedermayer, I., & Pfurtscheller, G. (2003). How many people are able to operate an EEG-based brain-computer interface (BCI)? *IEEE Transactions on Neural Systems and Rehabilitation Engineering*, *11*(2), 145–147. https://doi.org/10.1109/TNSRE.2003.814481

Guo, W., Liu, F., Liu, J., Yu, M., Zhang, Z., Liu, G., Xiao, C., & Zhao, J. (2015). Increased Cerebellar-Default-Mode-Network Connectivity in Drug-Naive Major Depressive Disorder at Rest. *Medicine*, *94*(9), e560. https://doi.org/10.1097/MD.0000000000000560

Guo, Y., Li, R., Zhang, R., Liu, C., Zhang, L., Zhao, D., Shan, Q., Wang, X., & Hu, Y. (2022). Dynamic Changes of Brain Activity in Patients With Disorders of Consciousness During Recovery of Consciousness. *Frontiers in Neuroscience*, *16*, 878203. https://doi.org/10.3389/fnins.2022.878203

Guo, Yongkun, Yang Bai, Xiaoyu Xia, Jinju Li, Xiaoli Wang, Yiwu Dai, Yuanyuan Dang, Jianghong He, Chunying Liu, and Hui Zhang. 2019. 'Effects of Long-Lasting High-Definition Transcranial Direct Current Stimulation in Chronic Disorders of Consciousness: A Pilot Study'. *Frontiers in Neuroscience* 13 (April): 412. https://doi.org/10.3389/fnins.2019.00412.

Halko, M. A., Datta, A., Plow, E. B., Scaturro, J., Bikson, M., & Merabet, L. B. (2011). Neuroplastic changes following rehabilitative training correlate with regional electrical field induced with tDCS. *NeuroImage*, *57*(3), 885–891. https://doi.org/10.1016/j.neuroimage.2011.05.026

Hamada, M., Galea, J. M., Lazzaro, V. D., Mazzone, P., Ziemann, U., & Rothwell, J. C. (2014). Two Distinct Interneuron Circuits in Human Motor Cortex Are Linked to Different Subsets of Physiological and Behavioral Plasticity. *Journal of Neuroscience*, *34*(38), 12837–12849. https://doi.org/10.1523/JNEUROSCI.1960-14.2014

Han, J., Chen, C., Zheng, S., Yan, X., Wang, C., Wang, K., & Hu, Y. (2022). High-Definition Transcranial Direct Current Stimulation of the Dorsolateral Prefrontal Cortex Modulates the Electroencephalography Rhythmic Activity of Parietal Occipital Lobe in Patients With Chronic Disorders of Consciousness. *Frontiers in Human Neuroscience*, *16*, 889023. https://doi.org/10.3389/fnhum.2022.889023

Hannah, R., Iacovou, A., & Rothwell, J. C. (2019). Direction of TDCS current flow in human sensorimotor cortex influences behavioural learning. *Brain Stimulation*, *12*(3), 684–692. https://doi.org/10.1016/j.brs.2019.01.016

Harris, C. R., Millman, K. J., van der Walt, S. J., Gommers, R., Virtanen, P., Cournapeau, D., Wieser, E., Taylor, J., Berg, S., Smith, N. J., Kern, R., Picus, M., Hoyer, S., van Kerkwijk, M. H., Brett, M., Haldane, A., del Río, J. F., Wiebe, M., Peterson, P., … Oliphant, T. E. (2020). Array programming with NumPy. *Nature*, *585*(7825), 357–362. https://doi.org/10.1038/s41586-020-2649-2

Harrison, T., & Murphy, T. (2013). Towards a circuit mechanism for movement tuning in motor cortex. *Frontiers in Neural Circuits*, *6*. https://www.frontiersin.org/articles/10.3389/fncir.2012.00127

Hashemirad, F., Zoghi, M., Fitzgerald, P. B., & Jaberzadeh, S. (2016). The effect of anodal transcranial direct current stimulation on motor sequence learning in healthy individuals: A systematic review and meta-analysis. *Brain and Cognition*, *102*, 1–12.

Hassanzahraee, Maryam. 2020. 'Determination of Anodal TDCS Duration Threshold for Reversal of Corticospinal Excitability: An Investigation for Induction of Counter-Regulatory Mechanisms'. *Brain Stimulation*, 8.

Höller, Y., Thomschewski, A., Bergmann, J., Kronbichler, M., Crone, J. S., Schmid, E. V., Butz, K., Höller, P., Nardone, R., & Trinka, E. (2014). Connectivity biomarkers can differentiate patients with different levels of consciousness. *Clinical Neurophysiology*, *125*(8), Article 8. https://doi.org/10.1016/j.clinph.2013.12.095

Horvath, J. C., Forte, J. D., & Carter, O. (2015). Evidence that transcranial direct current stimulation (tDCS) generates little-to-no reliable neurophysiologic effect beyond MEP amplitude modulation in healthy human subjects: A systematic review. *Neuropsychologia*, *66*, 213–236.

Horvath, Jared C., Olivia Carter, and Jason D. Forte. 2014. 'Transcranial Direct Current Stimulation: Five Important Issues We Aren't Discussing (but Probably Should Be)'. *Frontiers in Systems Neuroscience* 8. https://doi.org/10.3389/fnsys.2014.00002.

Huang, H., Niu, Z., Liu, G., Jiang, M., Jia, Q., Li, X., & Su, Y. (2020). Early Consciousness Disorder in Acute Large Hemispheric Infarction: An Analysis Based on Quantitative EEG and Brain Network Characteristics. *Neurocritical Care*, *33*(2), 376–388. https://doi.org/10.1007/s12028-020-01051-w

Huang, W., Wannez, S., Fregni, F., Hu, X., Jing, S., Martens, G., He, M., Di, H., Laureys, S., & Thibaut, A. (2017). Repeated stimulation of the posterior parietal cortex in patients in minimally conscious state: A sham-controlled randomized clinical trial. *Brain Stimulation: Basic, Translational, and Clinical Research in Neuromodulation*, *10*(3), 718–720. https://doi.org/10.1016/j.brs.2017.02.001

Huang, Wangshan, Sarah Wannez, Felipe Fregni, Xiaohua Hu, Shan Jing, Geraldine Martens, Minhui He, Haibo Di, Steven Laureys, and Aurore Thibaut. 2017. 'Repeated Stimulation of the Posterior Parietal Cortex in Patients in Minimally Conscious State: A Sham-Controlled Randomized Clinical Trial'. *Brain Stimulation* 10 (3): 718–20. https://doi.org/10.1016/j.brs.2017.02.001.

Huang, Y., Datta, A., Bikson, M., & Parra, L. C. (2018). ROAST: An Open-Source, Fully-Automated, Realistic Volumetric-Approach-Based Simulator For TES. *2018 40th Annual International Conference of the IEEE Engineering in Medicine and Biology Society (EMBC)*, 3072–3075. https://doi.org/10.1109/EMBC.2018.8513086

Huang, Y., Datta, A., Bikson, M., & Parra, L. C. (2019). Realistic volumetric-approach to simulate transcranial electric stimulation—ROAST—a fully automated open-source pipeline. *Journal of Neural Engineering*, *16*(5), 056006. https://doi.org/10.1088/1741-2552/ab208d

Huang, Y., Dmochowski, J. P., Su, Y., Datta, A., Rorden, C., & Parra, L. C. (2013). Automated MRI segmentation for individualized modeling of current flow in the human head. *Journal of Neural Engineering*, *10*(6), 066004. https://doi.org/10.1088/1741-2560/10/6/066004

Huang, Y., Liu, A. A., Lafon, B., Friedman, D., Dayan, M., Wang, X., Bikson, M., Doyle, W. K., Devinsky, O., & Parra, L. C. (2017). Measurements and models of electric fields in the in vivo human brain during transcranial electric stimulation. *ELife*, *6*, e18834. https://doi.org/10.7554/eLife.18834

Huang, Y., Parra, L. C., & Haufe, S. (2016). The New York Head—A precise standardized volume conductor model for EEG source localization and tES targeting. *NeuroImage*, *140*, 150–162. https://doi.org/10.1016/j.neuroimage.2015.12.019

Huang, Yu, Anli A Liu, Belen Lafon, Daniel Friedman, Michael Dayan, Xiuyuan Wang, Marom Bikson, Werner K Doyle, Orrin Devinsky, and Lucas C Parra. 2017. 'Measurements and Models of Electric Fields in the in Vivo Human Brain during Transcranial Electric Stimulation'. *ELife* 6 (February): e18834. https://doi.org/10.7554/eLife.18834.

Hummel, F. C., Heise, K., Celnik, P., Floel, A., Gerloff, C., & Cohen, L. G. (2010). Facilitating skilled right hand motor function in older subjects by anodal polarization over the left primary motor cortex. *Neurobiology of Aging*, *31*(12), 2160–2168. https://doi.org/10.1016/j.neurobiolaging.2008.12.008

Indahlastari, A., Albizu, A., Kraft, J. N., O'Shea, A., Nissim, N. R., Dunn, A. L., Carballo, D., Gordon, M. P., Taank, S., Kahn, A. T., Hernandez, C., Zucker, W. M., & Woods, A. J. (2021). Individualized tDCS modeling predicts functional connectivity changes within the working memory network in older adults. *Brain Stimulation*, *14*(5), 1205–1215. https://doi.org/10.1016/j.brs.2021.08.003

Indahlastari, A., Albizu, A., O'Shea, A., Forbes, M. A., Nissim, N. R., Kraft, J. N., Evangelista, N. D., Hausman, H. K., & Woods, A. J. (2020). Modeling transcranial electrical stimulation in the aging brain. *Brain Stimulation*, *13*(3), 664–674. https://doi.org/10.1016/j.brs.2020.02.007

Jackson, M. P., Rahman, A., Lafon, B., Kronberg, G., Ling, D., Parra, L. C., & Bikson, M. (2016). Animal Models of transcranial Direct Current Stimulation: Methods and Mechanisms. *Clinical Neurophysiology : Official Journal of the International Federation of Clinical Neurophysiology*, *127*(11), 3425–3454. https://doi.org/10.1016/j.clinph.2016.08.016

Jacobson, L., Koslowsky, M., & Lavidor, M. (2012). tDCS polarity effects in motor and cognitive domains: A meta-analytical review. *Experimental Brain Research*, *216*(1), 1–10. https://doi.org/10.1007/s00221-011-2891-9

Jacobson, L., Koslowsky, M., & Lavidor, M. (2012). tDCS polarity effects in motor and cognitive domains: A meta-analytical review. *Experimental Brain Research*, *216*(1), Article 1. https://doi.org/10.1007/s00221-011-2891-9

Jaeger, L., Marchal-Crespo, L., Wolf, P., Riener, R., Michels, L., & Kollias, S. (2014). Brain activation associated with active and passive lower limb stepping. *Frontiers in Human Neuroscience*, *8*. https://www.frontiersin.org/articles/10.3389/fnhum.2014.00828

Jalali, R., Chowdhury, A., Wilson, M., Miall, R. C., & Galea, J. M. (2018a). Neural changes associated with cerebellar

tDCS studied using MR spectroscopy. *Experimental Brain Research*, *236*(4), 997–1006. https://doi.org/10.1007/s00221-018-5170-1

Jamil, A., Batsikadze, G., Kuo, H., Meesen, R. L. J., Dechent, P., Paulus, W., & Nitsche, M. A. (2020). Current intensity- and polarity-specific online and aftereffects of transcranial direct current stimulation: An fMRI study. *Human Brain Mapping*, *41*(6), Article 6. https://doi.org/10.1002/hbm.24901

Jamil, Asif, Giorgi Batsikadze, Hsiao-I. Kuo, Ludovica Labruna, Alkomiet Hasan, Walter Paulus, and Michael A. Nitsche. 2017. 'Systematic Evaluation of the Impact of Stimulation Intensity on Neuroplastic After-Effects Induced by Transcranial Direct Current Stimulation: Effects of DC Intensity on Cortical Excitability'. *The Journal of Physiology* 595 (4): 1273–88. https://doi.org/10.1113/JP272738.

Jang, S. H., Ahn, S. H., Byun, W. M., Kim, C. S., Lee, M. Y., & Kwon, Y. H. (2009). The effect of transcranial direct current stimulation on the cortical activation by motor task in the human brain: An fMRI study. *Neuroscience Letters*, *460*(2), 117–120.

Jas, M., Engemann, D. A., Bekhti, Y., Raimondo, F., & Gramfort, A. (2017). *Autoreject: Automated artifact rejection for MEG and EEG data* (arXiv:1612.08194). arXiv. http://arxiv.org/abs/1612.08194

JASP Team. (2020). *JASP (Version 0.14.1)[Computer software]*. https://jasp-stats.org/

Jellinger, Kurt A. 2013. 'Neuropathology of Prolonged Unresponsive Wakefulness Syndrome after Blunt Head Injury: Review of 100 Post-Mortem Cases'. *Brain Injury* 27 (7–8): 917–23. https://doi.org/10.3109/02699052.2013.793395.

Jennet, B. (1972). *PERSISTENT VEGETATIVE STATE AFTER BRAIN DAMAGE: A Syndrome in Search of a Name*.

Jennett, B., J. H. Adams, L. S. Murray, and D. I. Graham. 2001. 'Neuropathology in Vegetative and Severely Disabled Patients after Head Injury'. *Neurology* 56 (4): 486–90. https://doi.org/10.1212/WNL.56.4.486.

Jennett, B. 2002. 'The Vegetative State'. *Journal of Neurology, Neurosurgery & Psychiatry* 73 (4): 355–57. https://doi.org/10.1136/jnnp.73.4.355.

Jin, M., Zhang, Z., Bai, Z., & Fong, K. N. K. (2019). Timing-dependent interaction effects of tDCS with mirror therapy on upper extremity motor recovery in patients with chronic stroke: A randomized controlled pilot study. *Journal of the Neurological Sciences*, *405*, 116436. https://doi.org/10.1016/j.jns.2019.116436

Jöhr, Jane, Floriana Halimi, Jérôme Pasquier, Alessandro Pincherle, Nicholas Schiff, and Karin Diserens. 2020. 'Recovery in Cognitive Motor Dissociation after Severe Brain Injury: A Cohort Study'. Edited by Jose A. Muñoz-Moreno. *PLOS ONE* 15 (2): e0228474. https://doi.org/10.1371/journal.pone.0228474.

Kadosh, R. C., Soskic, S., Iuculano, T., Kanai, R., & Walsh, V. (2010). Modulating Neuronal Activity Produces Specific and Long-Lasting Changes in Numerical Competence. *Current Biology*, *20*(22), 2016–2020. https://doi.org/10.1016/j.cub.2010.10.007

Kahan, J., & Foltynie, T. (2013). Understanding DCM: Ten simple rules for the clinician. *NeuroImage*, *83*, 542–549. https://doi.org/10.1016/j.neuroimage.2013.07.008

Kasinadhuni, A. K. (2017). *Imaging of current flow in the human head during transcranial electrical therapy*. 9.

Kazemi, K., & Noorizadeh, N. (2014). *Quantitative Comparison of SPM, FSL, and Brainsuite for Brain MR Image Segmentation*. Journal of Biomedical Physics and Engineering.

Kekic, M., Boysen, E., Campbell, I. C., & Schmidt, U. (2016). A systematic review of the clinical efficacy of transcranial direct current stimulation (tDCS) in psychiatric disorders. *Journal of Psychiatric Research*, *74*, 70–86. https://doi.org/10.1016/j.jpsychires.2015.12.018

King, J.-R., Sitt, J. D., Faugeras, F., Rohaut, B., El Karoui, I., Cohen, L., Naccache, L., & Dehaene, S. (2013). Information Sharing in the Brain Indexes Consciousness in Noncommunicative Patients. *Current Biology*, *23*(19), Article 19. https://doi.org/10.1016/j.cub.2013.07.075

Knotkova, H., Riggs, A., Berisha, D., Borges, H., Bernstein, H., Patel, V., Truong, D. Q., Unal, G., Arce, D., Datta, A., & Bikson, M. (2019). Automatic M1-SO Montage Headgear for Transcranial Direct Current Stimulation (TDCS) Suitable for Home and High-Throughput In-Clinic Applications. *Neuromodulation: Technology at the Neural Interface*, *22*(8), 904–910. https://doi.org/10.1111/ner.12786

Koh, C.-L., Lin, J.-H., Jeng, J.-S., Huang, S.-L., & Hsieh, C.-L. (2017). Effects of Transcranial Direct Current Stimulation With Sensory Modulation on Stroke Motor Rehabilitation: A Randomized Controlled Trial. *Archives of Physical Medicine and Rehabilitation*, *98*(12), 2477–2484. https://doi.org/10.1016/j.apmr.2017.05.025

Kondziella, D., Friberg, C. K., Frokjaer, V. G., Fabricius, M., & Møller, K. (2016). Preserved consciousness in vegetative and minimal conscious states: Systematic review and meta-analysis. *Journal of Neurology,*

Neurosurgery & Psychiatry, *87*(5), Article 5. https://doi.org/10.1136/jnnp-2015-310958
Koyama, S., Tanaka, S., Tanabe, S., & Sadato, N. (2015). Dual-hemisphere transcranial direct current stimulation over primary motor cortex enhances consolidation of a ballistic thumb movement. *Neuroscience Letters*, *588*, 49–53. https://doi.org/10.1016/j.neulet.2014.11.043
Krienen, F. M., & Buckner, R. L. (2009). Segregated Fronto-Cerebellar Circuits Revealed by Intrinsic Functional Connectivity. *Cerebral Cortex*, *19*(10), 2485–2497. https://doi.org/10.1093/cercor/bhp135
Kronberg, G., Bridi, M., Abel, T., Bikson, M., & Parra, L. C. (2017). Direct Current Stimulation Modulates LTP and LTD: Activity Dependence and Dendritic Effects. *Brain Stimulation*, *10*(1), 51–58. https://doi.org/10.1016/j.brs.2016.10.001
Kumar, J. S., & Bhuvaneswari, P. (2012). Analysis of Electroencephalography (EEG) Signals and Its Categorization–A Study. *Procedia Engineering*, *38*, 2525–2536. https://doi.org/10.1016/j.proeng.2012.06.298
Kumar, R., Yadav, R., Prajapati, H. P., Kumar, S., Potturi, G., & Sharma, R. (2022). Effect of Transcranial direct current stimulation (tDCS) on altered conscious patients after traumatic brain injury & cerebrovascular accident: A randomized clinical control trial. *Neurology Asia*, *27*(2), Article 2. https://doi.org/10.54029/2022nre
Kunze, T., Hunold, A., Haueisen, J., Jirsa, V., & Spiegler, A. (2016). Transcranial direct current stimulation changes resting state functional connectivity: A large-scale brain network modeling study. *NeuroImage*, *140*, 174–187. https://doi.org/10.1016/j.neuroimage.2016.02.015
Kunze, T., Hunold, A., Haueisen, J., Jirsa, V., & Spiegler, A. (2016). Transcranial direct current stimulation changes resting state functional connectivity: A large-scale brain network modeling study. *NeuroImage*, *140*, 174–187. https://doi.org/10.1016/j.neuroimage.2016.02.015
Küper, M., Mallick, J. S., Ernst, T., Kraff, O., Thürling, M., Stefanescu, M. R., Göricke, S., Nitsche, M. A., & Timmann, D. (2019). Cerebellar transcranial direct current stimulation modulates the fMRI signal in the cerebellar nuclei in a simple motor task. *Brain Stimulation*, *12*(5), 1169–1176. https://doi.org/10.1016/j.brs.2019.04.002
Kwon, Y. H., & Jang, S. H. (2011). The enhanced cortical activation induced by transcranial direct current stimulation during hand movements. *Neuroscience Letters*, *492*(2), 105–108. https://doi.org/10.1016/j.neulet.2011.01.066
Laakso, I., Tanaka, S., Koyama, S., De Santis, V., & Hirata, A. (2015). Inter-subject Variability in Electric Fields of Motor Cortical tDCS. *Brain Stimulation*, *8*(5), Article 5. https://doi.org/10.1016/j.brs.2015.05.002
Labruna, Ludovica, Asif Jamil, Shane Fresnoza, Giorgi Batsikadze, Min-Fang Kuo, Benjamin Vanderschelden, Richard B. Ivry, and Michael A. Nitsche. 2016. 'Efficacy of Anodal Transcranial Direct Current Stimulation Is Related to Sensitivity to Transcranial Magnetic Stimulation'. *Brain Stimulation* 9 (1): 8–15. https://doi.org/10.1016/j.brs.2015.08.014.
Lammi, M. H., Smith, V. H., Tate, R. L., & Taylor, C. M. (2005). The minimally conscious state and recovery potential: A follow-up study 2 to 5 years after traumatic brain injury. *Archives of Physical Medicine and Rehabilitation*, *86*(4), Article 4. https://doi.org/10.1016/j.apmr.2004.11.004
Lant, N. D., Gonzalez-Lara, L. E., Owen, A. M., & Fernandez-Espejo, D. (2016). Relationship between the anterior forebrain mesocircuit and the default mode network in the structural bases of disorders of consciousness. *NeuroImage: Clinical*, *10*, 27–35.
Larobina, M., & Murino, L. (2014). Medical Image File Formats. *Journal of Digital Imaging*, *27*(2), 200–206. https://doi.org/10.1007/s10278-013-9657-9
Laureys, S., & Schiff, N. D. (2012). Coma and consciousness: Paradigms (re)framed by neuroimaging. *NeuroImage*, *61*(2), 478–491. https://doi.org/10.1016/j.neuroimage.2011.12.041
Laureys, S., Celesia, G. G., Cohadon, F., Lavrijsen, J., León-Carrión, J., Sannita, W. G., Sazbon, L., Schmutzhard, E., von Wild, K. R., Zeman, A., & Dolce, G. (2010). Unresponsive wakefulness syndrome: A new name for the vegetative state or apallic syndrome. *BMC Medicine*, *8*(1), Article 1. https://doi.org/10.1186/1741-7015-8-68
Laureys, S., Faymonville, M., Luxen, A., Lamy, M., Franck, G., & Maquet, P. (2000). Restoration of thalamocortical connectivity after recovery from persistent vegetative state. *The Lancet*, *355*(9217), Article 9217. https://doi.org/10.1016/S0140-6736(00)02271-6
Laureys, S., Faymonville, M.-E., De Tiège, X., Peigneux, P., Berré, J., Moonen, G., Goldman, S., & Maquet, P. (2004). Brain Function in the Vegetative State. In C. Machado & D. A. Shewmon (Eds.), *Brain Death and Disorders of Consciousness* (Vol. 550, pp. 229–238). Springer US. https://doi.org/10.1007/978-0-306-48526-8_21
Laureys, S. (2005). The neural correlate of (un)awareness: Lessons from the vegetative state. *Trends in Cognitive Sciences*, *9*(12), Article 12. https://doi.org/10.1016/j.tics.2005.10.010

Laureys 2009 Encyclopedia of Neuroscience (2009), Vol. 2, Pp. 1133-114.Pdf'. 2009. In *Encyclopedia of Neuroscience*, 2009th ed., 1133–42. Encyclopedia of Neuroscience.

Laureys S. (2009). Encyclopedia of Neuroscience (2009), vol. 2, pp. 1133-114.pdf. In *Encyclopedia of Neuroscience* (2009th ed., pp. 1133–1142). Encyclopedia of Neuroscience.

Lechinger, J., Bothe, K., Pichler, G., Michitsch, G., Donis, J., Klimesch, W., & Schabus, M. (2013). CRS-R score in disorders of consciousness is strongly related to spectral EEG at rest. *Journal of Neurology*, *260*(9), Article 9. https://doi.org/10.1007/s00415-013-6982-3

Lefaucheur, J.-P., Antal, A., Ayache, S. S., Benninger, D. H., Brunelin, J., Cogiamanian, F., Cotelli, M., De Ridder, D., Ferrucci, R., Langguth, B., Marangolo, P., Mylius, V., Nitsche, M. A., Padberg, F., Palm, U., Poulet, E., Priori, A., Rossi, S., Schecklmann, M., … Paulus, W. (2017). Evidence-based guidelines on the therapeutic use of transcranial direct current stimulation (tDCS). *Clinical Neurophysiology*, *128*(1), 56–92. https://doi.org/10.1016/j.clinph.2016.10.087

Li, L. M., Violante, I. R., Leech, R., Ross, E., Hampshire, A., Opitz, A., Rothwell, J. C., Carmichael, D. W., & Sharp, D. J. (2019). Brain state and polarity dependent modulation of brain networks by transcranial direct current stimulation. *Human Brain Mapping*, *40*(3), 904–915. https://doi.org/10.1002/hbm.24420

Liu, A., Vöröslakos, M., Kronberg, G., Henin, S., Krause, M. R., Huang, Y., Opitz, A., Mehta, A., Pack, C. C., Krekelberg, B., Berényi, A., Parra, L. C., Melloni, L., Devinsky, O., & Buzsáki, G. (2018). Immediate neurophysiological effects of transcranial electrical stimulation. *Nature Communications*, *9*. https://doi.org/10.1038/s41467-018-07233-7

Liu, B., Zhang, X., Li, Y., Duan, G., Hou, J., Zhao, J., Guo, T., & Wu, D. (2022). TDCS-EEG for Predicting Outcome in Patients With Unresponsive Wakefulness Syndrome. *Frontiers in Neuroscience*, *16*, 771393. https://doi.org/10.3389/fnins.2022.771393

Lotze, M., Braun, C., Birbaumer, N., Anders, S., & Cohen, L. G. (2003). Motor learning elicited by voluntary drive. *Brain*, *126*(4), 866–872. https://doi.org/10.1093/brain/awg079

Lu, H., Gallinaro, J. V., & Rotter, S. (2019). Network remodeling induced by transcranial brain stimulation: A computational model of tDCS-triggered cell assembly formation. *Network Neuroscience*, *3*(4), 924–943. https://doi.org/10.1162/netn_a_00097

Luppi, A. I., Craig, M. M., Pappas, I., Finoia, P., Williams, G. B., Allanson, J., Pickard, J. D., Owen, A. M., Naci, L., Menon, D. K., & Stamatakis, E. A. (2019). Consciousness-specific dynamic interactions of brain integration and functional diversity. *Nature Communications*, *10*(1), Article 1. https://doi.org/10.1038/s41467-019-12658-9

Lutkenhoff, E. S., McArthur, D. L., Hua, X., Thompson, P. M., Vespa, P. M., & Monti, M. M. (2013). Thalamic atrophy in antero-medial and dorsal nuclei correlates with six-month outcome after severe brain injury. *NeuroImage: Clinical*, *3*, 396–404. https://doi.org/10.1016/j.nicl.2013.09.010

Mahdavi, S., & Towhidkhah, F. (2018). Computational human head models of tDCS: Influence of brain atrophy on current density distribution. *Brain Stimulation*, *11*(1), 104–107. https://doi.org/10.1016/j.brs.2017.09.013

Maillé, Sébastien, and Michael Lynn. 2020. 'Reconciling Current Theories of Consciousness'. *The Journal of Neuroscience* 40 (10): 1994–96. https://doi.org/10.1523/JNEUROSCI.2740-19.2020.

Maldjian, J. A., Laurienti, P. J., Kraft, R. A., & Burdette, J. H. (2003). An automated method for neuroanatomic and cytoarchitectonic atlas-based interrogation of fMRI data sets. *NeuroImage*, *19*(3), 1233–1239. https://doi.org/10.1016/S1053-8119(03)00169-1

Manto, M., Bower, J. M., Conforto, A. B., Delgado-García, J. M., da Guarda, S. N. F., Gerwig, M., Habas, C., Hagura, N., Ivry, R. B., Mariën, P., Molinari, M., Naito, E., Nowak, D. A., Oulad Ben Taib, N., Pelisson, D., Tesche, C. D., Tilikete, C., & Timmann, D. (2012). Consensus Paper: Roles of the Cerebellum in Motor Control—The Diversity of Ideas on Cerebellar Involvement in Movement. *The Cerebellum*, *11*(2), 457–487. https://doi.org/10.1007/s12311-011-0331-9

Marino, S., Bonanno, L., & Giorgio, A. (2016). Functional connectivity in disorders of consciousness: Methodological aspects and clinical relevance. *Brain Imaging and Behavior*, *10*(2), 604–608. https://doi.org/10.1007/s11682-015-9417-1

Martens, G., Fregni, F., Carrière, M., Barra, A., Laureys, S., & Thibaut, A. (2019). Single tDCS session of motor cortex in patients with disorders of consciousness: A pilot study. *Brain Injury*, *33*(13–14), 1679–1683. https://doi.org/10.1080/02699052.2019.1667537

Martens, G., Kroupi, E., Bodien, Y., Frasso, G., Annen, J., Cassol, H., Barra, A., Martial, C., Gosseries, O., Lejeune, N., Soria-Frisch, A., Ruffini, G., Laureys, S., & Thibaut, A. (2020). Behavioral and electrophysiological effects

of network-based frontoparietal tDCS in patients with severe brain injury: A randomized controlled trial. *NeuroImage : Clinical*, *28*. https://doi.org/10.1016/j.nicl.2020.102426

Martens, G., Lejeune, N., O'Brien, A. T., Fregni, F., Martial, C., Wannez, S., Laureys, S., & Thibaut, A. (2018). Randomized controlled trial of home-based 4-week tDCS in chronic minimally conscious state. *Brain Stimulation: Basic, Translational, and Clinical Research in Neuromodulation*, *11*(5), 982–990. https://doi.org/10.1016/j.brs.2018.04.021

Martens, Géraldine, Eleni Kroupi, Yelena Bodien, Gianluca Frasso, Jitka Annen, Helena Cassol, Alice Barra, et al. 2020. 'Behavioral and Electrophysiological Effects of Network-Based Frontoparietal TDCS in Patients with Severe Brain Injury: A Randomized Controlled Trial'. *NeuroImage: Clinical* 28: 102426. https://doi.org/10.1016/j.nicl.2020.102426.

Martens, Géraldine, Felipe Fregni, Manon Carrière, Alice Barra, Steven Laureys, and Aurore Thibaut. 2019. 'Single TDCS Session of Motor Cortex in Patients with Disorders of Consciousness: A Pilot Study'. *Brain Injury*, September, 1–5. https://doi.org/10.1080/02699052.2019.1667537.

Martens, Géraldine, Nicolas Lejeune, Anthony Terrence O'Brien, Felipe Fregni, Charlotte Martial, Sarah Wannez, Steven Laureys, and Aurore Thibaut. 2018. 'Randomized Controlled Trial of Home-Based 4-Week TDCS in Chronic Minimally Conscious State'. *Brain Stimulation* 11 (5): 982–90. https://doi.org/10.1016/j.brs.2018.04.021.

Mehrkanoon, S., Boonstra, T. W., Breakspear, M., Hinder, M., & Summers, J. J. (2016). Upregulation of cortico-cerebellar functional connectivity after motor learning. *NeuroImage*, *128*, 252–263. https://doi.org/10.1016/j.neuroimage.2015.12.052

Miyaguchi, S., Onishi, H., Kojima, S., Sugawara, K., Tsubaki, A., Kirimoto, H., Tamaki, H., & Yamamoto, N. (2013). Corticomotor excitability induced by anodal transcranial direct current stimulation with and without non-exhaustive movement. *Brain Research*, *1529*, 83–91. https://doi.org/10.1016/j.brainres.2013.07.026

Modolo, J., Denoyer, Y., Wendling, F., & Benquet, P. (2018). Physiological effects of low-magnitude electric fields on brain activity: Advances from in vitro, in vivo and in silico models. *Current Opinion in Biomedical Engineering*, *8*, 38–44. https://doi.org/10.1016/j.cobme.2018.09.006

Monte-Silva, K., Kuo, M.-F., Hessenthaler, S., Fresnoza, S., Liebetanz, D., Paulus, W., & Nitsche, M. A. (2013a). Induction of Late LTP-Like Plasticity in the Human Motor Cortex by Repeated Non-Invasive Brain Stimulation. *Brain Stimulation*, *6*(3), Article 3. https://doi.org/10.1016/j.brs.2012.04.011

Monte-Silva, K., Kuo, M.-F., Liebetanz, D., Paulus, W., & Nitsche, M. A. (2010). Shaping the Optimal Repetition Interval for Cathodal Transcranial Direct Current Stimulation (tDCS). *Journal of Neurophysiology*, *103*(4), 1735–1740. https://doi.org/10.1152/jn.00924.2009

Monti, M. M., Vanhaudenhuyse, A., Coleman, M. R., Boly, M., Pickard, J. D., Tshibanda, L., Owen, A. M., & Laureys, S. (2010). Willful Modulation of Brain Activity in Disorders of Consciousness. *New England Journal of Medicine*, *362*(7), 579–589. https://doi.org/10.1056/NEJMoa0905370

Morrison-Ham, J., Clark, G. M., Ellis, E. G., Cerins, A., Joutsa, J., Enticott, P. G., & Corp, D. T. (2022). Effects of non-invasive brain stimulation in dystonia: A systematic review and meta-analysis. *Neurological Disorders*, *15*.

Morya, E., Monte-Silva, K., Bikson, M., Esmaeilpour, Z., Biazoli, C. E., Fonseca, A., Bocci, T., Farzan, F., Chatterjee, R., Hausdorff, J. M., da Silva Machado, D. G., Brunoni, A. R., Mezger, E., Moscaleski, L. A., Pegado, R., Sato, J. R., Caetano, M. S., Sá, K. N., Tanaka, C., … Okano, A. H. (2019). Beyond the target area: An integrative view of tDCS-induced motor cortex modulation in patients and athletes. *Journal of NeuroEngineering and Rehabilitation*, *16*, 141. https://doi.org/10.1186/s12984-019-0581-1

Morya, Edgard, Kátia Monte-Silva, Marom Bikson, Zeinab Esmaeilpour, Claudinei Eduardo Biazoli, Andre Fonseca, Tommaso Bocci, et al. 2019. 'Beyond the Target Area: An Integrative View of TDCS-Induced Motor Cortex Modulation in Patients and Athletes'. *Journal of NeuroEngineering and Rehabilitation* 16 (1): 141. https://doi.org/10.1186/s12984-019-0581-1.

Mosayebi Samani, M., Agboada, D., Kuo, M., & Nitsche, M. A. (2020). Probing the relevance of repeated cathodal transcranial direct current stimulation over the primary motor cortex for prolongation of after-effects. *The Journal of Physiology*, *598*(4), 805–816. https://doi.org/10.1113/JP278857

Nandi, T., Puonti, O., Clarke, W. T., Nettekoven, C., Barron, H. C., Kolasinski, J., Hanayik, T., Hinson, E. L., Berrington, A., Bachtiar, V., Johnstone, A., Winkler, A. M., Thielscher, A., Johansen-Berg, H., & Stagg, C. J. (2022). TDCS induced GABA change is associated with the simulated electric field in M1, an effect mediated by grey matter volume in the MRS voxel. *Brain Stimulation*, *15*(5), 1153–1162.

https://doi.org/10.1016/j.brs.2022.07.049
Naro, A., Bramanti, A., Leo, A., Bramanti, P., & Calabrò, R. S. (2018). Metaplasticity: A Promising Tool to Disentangle Chronic Disorders of Consciousness Differential Diagnosis. *International Journal of Neural Systems*, *28*(06), Article 06. https://doi.org/10.1142/S0129065717500599
Naro, A., Russo, M., Leo, A., Cannavò, A., Manuli, A., Bramanti, A., Bramanti, P., & Calabrò, R. S. (2016a). Cortical connectivity modulation induced by cerebellar oscillatory transcranial direct current stimulation in patients with chronic disorders of consciousness: A marker of covert cognition? *Clinical Neurophysiology*, *127*(3), 1845–1854. https://doi.org/10.1016/j.clinph.2015.12.010
Naro, Antonino, Margherita Russo, Antonino Leo, Antonino Cannavò, Alfredo Manuli, Alessia Bramanti, Placido Bramanti, and Rocco Salvatore Calabrò. 2016. 'Cortical Connectivity Modulation Induced by Cerebellar Oscillatory Transcranial Direct Current Stimulation in Patients with Chronic Disorders of Consciousness: A Marker of Covert Cognition?' *Clinical Neurophysiology* 127 (3): 1845–54. https://doi.org/10.1016/j.clinph.2015.12.010.
Naro, Antonino, Rocco Salvatore Calabrò, Margherita Russo, Antonino Leo, Patrizia Pollicino, Angelo Quartarone, and Placido Bramanti. 2015. 'Can Transcranial Direct Current Stimulation Be Useful in Differentiating Unresponsive Wakefulness Syndrome from Minimally Conscious State Patients?' *Restorative Neurology and Neuroscience* 33 (2): 159–76. https://doi.org/10.3233/RNN-140448.
Nasimova, M., & Huang, Y. (2022). Applications of open-source software ROAST in clinical studies: A review. *Brain Stimulation*, *15*(4), 1002–1010. https://doi.org/10.1016/j.brs.2022.07.003
Navarro-López, V., Del-Valle-Gratacós, M., Fernández-Vázquez, D., Fernández-González, P., Carratalá-Tejada, M., & Molina-Rueda, F. (2022). Transcranial direct current stimulation in the management of phantom limb pain: A systematic review of randomized controlled trials. *European Journal of Physical and Rehabilitation Medicine*, *58*(5). https://doi.org/10.23736/S1973-9087.22.07439-1
Nissim, N. R., O'Shea, A., Indahlastari, A., Telles, R., Richards, L., Porges, E., Cohen, R., & Woods, A. J. (2019). Effects of in-Scanner Bilateral Frontal tDCS on Functional Connectivity of the Working Memory Network in Older Adults. *Frontiers in Aging Neuroscience*, *11*, 51. https://doi.org/10.3389/fnagi.2019.00051
Nitsche, M. A., & Paulus, W. (2000). Excitability changes induced in the human motor cortex by weak transcranial direct current stimulation. *The Journal of Physiology*, *527*(Pt 3), 633–639. https://doi.org/10.1111/j.1469-7793.2000.t01-1-00633.x
Nitsche, M. A., & Paulus, W. (2001). Sustained excitability elevations induced by transcranial DC motor cortex stimulation in humans. *Neurology*, *57*(10), Article 10. https://doi.org/10.1212/WNL.57.10.1899
Nitsche, M. A., and W. Paulus. 2000. 'Excitability Changes Induced in the Human Motor Cortex by Weak Transcranial Direct Current Stimulation'. *The Journal of Physiology* 527 (3): 633–39. https://doi.org/10.1111/j.1469-7793.2000.t01-1-00633.x.
Nitsche, M. A., Nitsche, M. S., Klein, C. C., Tergau, F., Rothwell, J. C., & Paulus, W. (2003). Level of action of cathodal DC polarisation induced inhibition of the human motor cortex. *Clinical Neurophysiology*, *114*(4), 600–604. https://doi.org/10.1016/S1388-2457(02)00412-1
Nitsche, M. A., Seeber, A., Frommann, K., Klein, C. C., Rochford, C., Nitsche, M. S., Fricke, K., Liebetanz, D., Lang, N., Antal, A., Paulus, W., & Tergau, F. (2005). Modulating parameters of excitability during and after transcranial direct current stimulation of the human motor cortex: Cortical excitability and tDCS. *The Journal of Physiology*, *568*(1), 291–303. https://doi.org/10.1113/jphysiol.2005.092429
Noel, Jean-Paul, Camille Chatelle, Serafeim Perdikis, Jane Jöhr, Marina Lopes Da Silva, Philippe Ryvlin, Marzia De Lucia, José del R. Millán, Karin Diserens, and Andrea Serino. 2019. 'Peri-Personal Space Encoding in Patients with Disorders of Consciousness and Cognitive-Motor Dissociation'. *NeuroImage: Clinical* 24: 101940. https://doi.org/10.1016/j.nicl.2019.101940.
Nonnekes, Jorik, Anass Arrogi, Moniek A. M. Munneke, Edwin H. F. van Asseldonk, Lars B. Oude Nijhuis, Alexander C. Geurts, and Vivian Weerdesteyn. 2014. 'Subcortical Structures in Humans Can Be Facilitated by Transcranial Direct Current Stimulation'. Edited by Jeffrey M. Haddad. *PLoS ONE* 9 (9): e107731. https://doi.org/10.1371/journal.pone.0107731.
Nozari, N., Woodard, K., & Thompson-Schill, S. L. (2014). Consequences of Cathodal Stimulation for Behavior: When Does It Help and When Does It Hurt Performance? *PLoS ONE*, *9*(1), e84338. https://doi.org/10.1371/journal.pone.0084338
Ochi, M., Saeki, S., Oda, T., Matsushima, Y., & Hachisuka, K. (2013). Effects of anodal and cathodal transcranial

direct current stimulation combined with robotic therapy on severely affected arms in chronic stroke patients. *Journal of Rehabilitation Medicine*, *45*(2), 137–140. https://doi.org/10.2340/16501977-1099

Oldfield, R. C. (1971a). The assessment and analysis of handedness: The Edinburgh inventory. *Neuropsychologia*, *9*(1), 97–113. https://doi.org/10.1016/0028-3932(71)90067-4

Oostenveld, R., Fries, P., Maris, E., & Schoffelen, J.-M. (2011). FieldTrip: Open Source Software for Advanced Analysis of MEG, EEG, and Invasive Electrophysiological Data. *Computational Intelligence and Neuroscience*, *2011*, 1–9. https://doi.org/10.1155/2011/156869

Opitz, A., Yeagle, E., Thielscher, A., Schroeder, C., Mehta, A. D., & Milham, M. P. (2018). On the importance of precise electrode placement for targeted transcranial electric stimulation. *NeuroImage*, *181*, 560–567. https://doi.org/10.1016/j.neuroimage.2018.07.027

Opitz, A., Yeagle, E., Thielscher, A., Schroeder, C., Mehta, A. D., & Milham, M. P. (2018). On the importance of precise electrode placement for targeted transcranial electric stimulation. *NeuroImage*, *181*, 560–567. https://doi.org/10.1016/j.neuroimage.2018.07.027

Opitz, Alexander, Erin Yeagle, Axel Thielscher, Charles Schroeder, Ashesh D. Mehta, and Michael P. Milham. 2018. 'On the Importance of Precise Electrode Placement for Targeted Transcranial Electric Stimulation'. *NeuroImage* 181 (November): 560–67. https://doi.org/10.1016/j.neuroimage.2018.07.027.

Opitz, Alexander. n.d. 'Spatiotemporal Structure of Intracranial Electric Fields Induced by Transcranial Electric Stimulation in Humans and Nonhuman Primates'. *Scientific Reports*, 11.

Orban de Xivry, J.-J., & Shadmehr, R. (2014). Electrifying the motor engram: Effects of tDCS on motor learning and control. *Experimental Brain Research*, *232*(11), Article 11. https://doi.org/10.1007/s00221-014-4087-6

Owen, A. M., Coleman, M. R., Boly, M., Davis, M. H., Laureys, S., & Pickard, J. D. (2006). Detecting Awareness in the Vegetative State. *Science*, *313*(5792), 1402–1402. https://doi.org/10.1126/science.1130197

Owen, Adrian M., Nicholas D. Schiff, and Steven Laureys. 2016. 'The Assessment of Conscious Awareness in the Vegetative State'. In *The Neurology of Conciousness*, 155–66. Elsevier. https://doi.org/10.1016/B978-0-12-800948-2.00010-8.

O'Donnell, A., Pauli, R., Banellis, L., Sokoliuk, R., Hayton, T., Sturman, S., Veenith, T., Yakoub, K. M., Belli, A., Chennu, S., & Cruse, D. (2021). The prognostic value of resting-state EEG in acute post-traumatic unresponsive states. *Brain Communications*, *3*(2), fcab017. https://doi.org/10.1093/braincomms/fcab017

Pan, Jiahui, Qiuyou Xie, Pengmin Qin, Yan Chen, Yanbin He, Haiyun Huang, Fei Wang, et al. 2020. 'Prognosis for Patients with Cognitive Motor Dissociation Identified by Brain-Computer Interface'. *Brain* 143 (4): 1177–89. https://doi.org/10.1093/brain/awaa026.

Parkin, B. L., Ekhtiari, H., & Walsh, V. F. (2015). Non-invasive Human Brain Stimulation in Cognitive Neuroscience: A Primer. *Neuron*, *87*(5), 932–945. https://doi.org/10.1016/j.neuron.2015.07.032

Patel, R., Ashcroft, J., Patel, A., Ashrafian, H., Woods, A. J., Singh, H., Darzi, A., & Leff, D. R. (2019). The Impact of Transcranial Direct Current Stimulation on Upper-Limb Motor Performance in Healthy Adults: A Systematic Review and Meta-Analysis. *Frontiers in Neuroscience*, *13*, 1213. https://doi.org/10.3389/fnins.2019.01213

Peng, Y., Zhao, J., Lu, X., Dong, J., Zhang, S., Zhang, J., Liu, H., Zheng, X., Wang, X., Lan, Y., & Yan, T. (2022). Efficacy of Transcranial Direct Current Stimulation Over Dorsolateral Prefrontal Cortex in Patients With Minimally Conscious State. *Frontiers in Neurology*, *13*, 821286. https://doi.org/10.3389/fneur.2022.821286

Pfurtscheller, G., & Neuper, C. (2001). Motor imagery and direct brain-computer communication. *Proceedings of the IEEE*, *89*(7), Article 7. https://doi.org/10.1109/5.939829

Pfurtscheller, G., Brunner, C., Schlögl, A., & Lopes da Silva, F. H. (2006). Mu rhythm (de)synchronization and EEG single-trial classification of different motor imagery tasks. *NeuroImage*, *31*(1), Article 1. https://doi.org/10.1016/j.neuroimage.2005.12.003

Piarulli, A., Bergamasco, M., Thibaut, A., Cologan, V., Gosseries, O., & Laureys, S. (2016). EEG ultradian rhythmicity differences in disorders of consciousness during wakefulness. *Journal of Neurology*, *263*(9), Article 9. https://doi.org/10.1007/s00415-016-8196-y

Pignat, Jean-Michel, Etienne Mauron, Jane Jöhr, Charlotte Gilart de Keranflec'h, Dimitri Van De Ville, Maria Giulia Preti, Djalel E. Meskaldji, et al. 2016. 'Outcome Prediction of Consciousness Disorders in the Acute Stage Based on a Complementary Motor Behavioural Tool'. Edited by Han-Chiao Isaac Chen. *PLOS ONE* 11 (6): e0156882. https://doi.org/10.1371/journal.pone.0156882.

Pincherle, Alessandro, Jane Jöhr, Camille Chatelle, Jean-Michel Pignat, Renaud Du Pasquier, Philippe Ryvlin, Mauro Oddo, and Karin Diserens. 2019. 'Motor Behavior Unmasks Residual Cognition in Disorders of Consciousness:

Motor Behavior in Disorders of Consciousness'. *Annals of Neurology* 85 (3): 443–47. https://doi.org/10.1002/ana.25417.
Pinto, A. D., & Chen, R. (2001). Suppression of the motor cortex by magnetic stimulation of the cerebellum. *Experimental Brain Research*, *140*(4), Article 4. https://doi.org/10.1007/s002210100862
Pistarini, Caterina, and Giorgio Maggioni. 2018. 'Early Rehabilitation of Disorders of Consciousness (DOC): Management, Neuropsychological Evaluation and Treatment'. *Neuropsychological Rehabilitation* 28 (8): 1319–30. https://doi.org/10.1080/09602011.2018.1500920.
Pixa, N. H., & Pollok, B. (2018). Effects of tDCS on Bimanual Motor Skills: A Brief Review. *Frontiers in Behavioral Neuroscience*, *12*, 63. https://doi.org/10.3389/fnbeh.2018.00063
Polanía, R., Nitsche, M. A., & Ruff, C. C. (2018). Studying and modifying brain function with non-invasive brain stimulation. *Nature Neuroscience*, *21*(2), 174–187. https://doi.org/10.1038/s41593-017-0054-4
Polania, R., Paulus, W., & Nitsche, M. A. (2012). Modulating cortico-striatal and thalamo-cortical functional connectivity with transcranial direct current stimulation. *Human Brain Mapping*, *33*(10), 2499–2508.
Polanía, Rafael, Walter Paulus, and Michael A. Nitsche. 2012. 'Modulating Cortico-Striatal and Thalamo-Cortical Functional Connectivity with Transcranial Direct Current Stimulation'. *Human Brain Mapping* 33 (10): 2499–2508. https://doi.org/10.1002/hbm.21380.
Pozeg, P., Jöhr, J., Pincherle, A., Marie, G., Ryvlin, P., Meuli, R., Hagmann, P., Diserens, K., & Dunet, V. (2021). Discriminating cognitive motor dissociation from disorders of consciousness using structural MRI. *NeuroImage: Clinical*, *30*, 102651. https://doi.org/10.1016/j.nicl.2021.102651
Prolonged disorders of consciousness following sudden onset brain injury: National clinical guidelines. (2020, March 6). RCP London. https://www.rcplondon.ac.uk/guidelines-policy/prolonged-disorders-consciousness-following-sudden-onset-brain-injury-national-clinical-guidelines
Pruski, A., & Cantarero, G. (2020). Transcranial Direct Current Stimulation for Motor Recovery Following Brain Injury. *Current Physical Medicine and Rehabilitation Reports*, *8*(3), 268–279. https://doi.org/10.1007/s40141-020-00262-8
Qin, P., Wu, X., Huang, Z., Duncan, N. W., Tang, W., Wolff, A., Hu, J., Gao, L., Jin, Y., Wu, X., Zhang, J., Lu, L., Wu, C., Qu, X., Mao, Y., Weng, X., Zhang, J., & Northoff, G. (2015). How are different neural networks related to consciousness?: Neural Networks. *Annals of Neurology*, *78*(4), 594–605. https://doi.org/10.1002/ana.24479
Radman, T., Ramos, R. L., Brumberg, J. C., & Bikson, M. (2009). Role of cortical cell type and morphology in subthreshold and suprathreshold uniform electric field stimulation in vitro. *Brain Stimulation*, *2*(4), 215-228.e3. https://doi.org/10.1016/j.brs.2009.03.007
Rahman, A., Reato, D., Arlotti, M., Gasca, F., Datta, A., Parra, L. C., & Bikson, M. (2013). Cellular effects of acute direct current stimulation: Somatic and synaptic terminal effects: Somatic and terminal origin of DCS effects. *The Journal of Physiology*, *591*(10), 2563–2578. https://doi.org/10.1113/jphysiol.2012.247171
Rawji, V., Ciocca, M., Zacharia, A., Soares, D., Truong, D., Bikson, M., Rothwell, J., & Bestmann, S. (2018). TDCS changes in motor excitability are specific to orientation of current flow. *Brain Stimulation*, *11*(2), Article 2. https://doi.org/10.1016/j.brs.2017.11.001
Rawji, Vishal, Matteo Ciocca, André Zacharia, David Soares, Dennis Truong, Marom Bikson, John Rothwell, and Sven Bestmann. 2018. 'TDCS Changes in Motor Excitability Are Specific to Orientation of Current Flow'. *Brain Stimulation* 11 (2): 289–98. https://doi.org/10.1016/j.brs.2017.11.001.
Reato, D., Rahman, A., Bikson, M., & Parra, L. C. (2010a). Low-Intensity Electrical Stimulation Affects Network Dynamics by Modulating Population Rate and Spike Timing. *The Journal of Neuroscience*, *30*(45), 15067–15079. https://doi.org/10.1523/JNEUROSCI.2059-10.2010
Reddy, H., De Stefano, N., Mortilla, M., Federico, A., & Matthews, P. M. (2002). Functional Reorganization of Motor Cortex Increases With Greater Axonal Injury From CADASIL. *Stroke*, *33*(2), 502–508. https://doi.org/10.1161/hs0202.103337
Reinhart, R. M. G., Cosman, J. D., Fukuda, K., & Woodman, G. F. (2017). Using transcranial direct-current stimulation (tDCS) to understand cognitive processing. *Attention, Perception, & Psychophysics*, *79*(1), Article 1. https://doi.org/10.3758/s13414-016-1224-2
Reis, J., & Fritsch, B. (2011). Modulation of motor performance and motor learning by transcranial direct current stimulation: *Current Opinion in Neurology*, *24*(6), 590–596. https://doi.org/10.1097/WCO.0b013e32834c3db0
Reis, J., Schambra, H. M., Cohen, L. G., Buch, E. R., Fritsch, B., Zarahn, E., Celnik, P. A., & Krakauer, J. W. (2009). Noninvasive cortical stimulation enhances motor skill acquisition over multiple days through an effect on

consolidation. *Proceedings of the National Academy of Sciences*, *106*(5), 1590–1595. https://doi.org/10.1073/pnas.0805413106
Ridding, M. C., & Ziemann, U. (2010). Determinants of the induction of cortical plasticity by non-invasive brain stimulation in healthy subjects. *The Journal of Physiology*, *588*(13), 2291–2304. https://doi.org/10.1113/jphysiol.2010.190314
Rolls, E. T., Huang, C.-C., Lin, C.-P., Feng, J., & Joliot, M. (2020). Automated anatomical labelling atlas 3. *NeuroImage*, *206*, 116189. https://doi.org/10.1016/j.neuroimage.2019.116189
Rorden, C., & Brett, M. (2000). Stereotaxic Display of Brain Lesions. *Behavioural Neurology*, *12*(4), 191–200. https://doi.org/10.1155/2000/421719
Rossini, P. M., Burke, D., Chen, R., Cohen, L. G., Daskalakis, Z., Di Iorio, R., Di Lazzaro, V., Ferreri, F., Fitzgerald, P. B., George, M. S., Hallett, M., Lefaucheur, J. P., Langguth, B., Matsumoto, H., Miniussi, C., Nitsche, M. A., Pascual-Leone, A., Paulus, W., Rossi, S., … Ziemann, U. (2015). Non-invasive electrical and magnetic stimulation of the brain, spinal cord, roots and peripheral nerves: Basic principles and procedures for routine clinical and research application. An updated report from an I.F.C.N. Committee. *Clinical Neurophysiology : Official Journal of the International Federation of Clinical Neurophysiology*, *126*(6), 1071–1107. https://doi.org/10.1016/j.clinph.2015.02.001
Rossi Sebastiano, D., Panzica, F., Visani, E., Rotondi, F., Scaioli, V., Leonardi, M., Sattin, D., D'Incerti, L., Parati, E., Ferini Strambi, L., & Franceschetti, S. (2015). Significance of multiple neurophysiological measures in patients with chronic disorders of consciousness. *Clinical Neurophysiology*, *126*(3), 558–564. https://doi.org/10.1016/j.clinph.2014.07.004
Rostami, M., Mosallanezhad, Z., Ansari, S., Ehsani, F., Kidgell, D., Nourbakhsh, M. R., Bakhshi, E., & Jaberzadeh, S. (2020). Multi-session anodal transcranial direct current stimulation enhances lower extremity functional performance in healthy older adults. *Experimental Brain Research*, *238*(9), 1925–1936. https://doi.org/10.1007/s00221-020-05827-6
Rostami, M., Mosallanezhad, Z., Ansari, S., Kidgell, D., Rezaeian, T., Bakhshi, E., Ghodrati, M., & Jaberzadeh, S. (2020). The effects of consecutive sessions of anodal transcranial direct current stimulation over the primary motor cortex on hand function in healthy older adults. *Archives of Gerontology and Geriatrics*, *89*, 104063. https://doi.org/10.1016/j.archger.2020.104063
Royal College of Physicians. (2020). *Prolonged disorders of consciousness following sudden onset brain injury: National clinical guidelines—Royal College of Physicians—2020*. Royal College of Physicians.
Royal College of Physicians. 2020. 'Prolonged Disorders of Consciousness Following Sudden Onset Brain Injury: National Clinical Guidelines - Royal College of Physicians - 2020'. Royal College of Physicians.
Rroji, Orjon, Kris van Kuyck, Bart Nuttin, and Nicole Wenderoth. 2015. 'Anodal TDCS over the Primary Motor Cortex Facilitates Long-Term Memory Formation Reflecting Use-Dependent Plasticity'. Edited by Benjamin Thompson. *PLOS ONE* 10 (5): e0127270. https://doi.org/10.1371/journal.pone.0127270.
Salimi-Khorshidi, G., Douaud, G., Beckmann, C. F., Glasser, M. F., Griffanti, L., & Smith, S. M. (2014). Automatic Denoising of Functional MRI Data: Combining Independent Component Analysis and Hierarchical Fusion of Classifiers. *NeuroImage*, *90*, 449–468. https://doi.org/10.1016/j.neuroimage.2013.11.046
Sankarasubramanian, V., Cunningham, D. A., Potter-Baker, K. A., Beall, E. B., Roelle, S. M., Varnerin, N. M., Machado, A. G., Jones, S. E., Lowe, M. J., & Plow, E. B. (2017). Transcranial Direct Current Stimulation Targeting Primary Motor Versus Dorsolateral Prefrontal Cortices: Proof-of-Concept Study Investigating Functional Connectivity of Thalamocortical Networks Specific to Sensory-Affective Information Processing. *Brain Connectivity*, *7*(3), 182–196. https://doi.org/10.1089/brain.2016.0440
Sanz, L. R. D., Thibaut, A., Edlow, B. L., Laureys, S., & Gosseries, O. (2021). Update on neuroimaging in disorders of consciousness. *Current Opinion in Neurology*, *34*(4), Article 4. https://doi.org/10.1097/WCO.0000000000000951
Sasaki, R., Nakagawa, M., Tsuiki, S., Miyaguchi, S., Kojima, S., Saito, K., Inukai, Y., Masaki, M., Otsuru, N., & Onishi, H. (2017). Regulation of primary motor cortex excitability by repetitive passive finger movement frequency. *Neuroscience*, *357*, 232–240. https://doi.org/10.1016/j.neuroscience.2017.06.009
Sattler, Virginie, Blandine Acket, Nicolas Raposo, Jean-François Albucher, Claire Thalamas, Isabelle Loubinoux, François Chollet, and Marion Simonetta-Moreau. 2015. 'Anodal TDCS Combined With Radial Nerve Stimulation Promotes Hand Motor Recovery in the Acute Phase After Ischemic Stroke'. *Neurorehabilitation and Neural Repair* 29 (8): 743–54. https://doi.org/10.1177/1545968314565465.
Saucedo Marquez, C. M., Zhang, X., Swinnen, S. P., Meesen, R., & Wenderoth, N. (2013). Task-Specific Effect of

Transcranial Direct Current Stimulation on Motor Learning. *Frontiers in Human Neuroscience*, *7*. https://doi.org/10.3389/fnhum.2013.00333
Schiff, N. D. (2010). Recovery of consciousness after brain injury: A mesocircuit hypothesis. *Trends in Neurosciences*, *33*(1), 1–9.
Schiff, N. D. (2015a). Cognitive Motor Dissociation Following Severe Brain Injuries. *JAMA Neurology*, *72*(12), 1413–1415.
Schnakers, C., Edlow, B. L., Chatelle, C., & Giacino, J. T. (2016). Minimally Conscious State. In *The Neurology of Conciousness* (pp. 167–185). Elsevier. https://doi.org/10.1016/B978-0-12-800948-2.00011-X
Schnakers, Caroline, Audrey Vanhaudenhuyse, Joseph Giacino, Manfredi Ventura, Melanie Boly, Steve Majerus, Gustave Moonen, and Steven Laureys. 2009. 'Diagnostic Accuracy of the Vegetative and Minimally Conscious State: Clinical Consensus versus Standardized Neurobehavioral Assessment'. *BMC Neurology* 9 (1): 35. https://doi.org/10.1186/1471-2377-9-35.
Schönbrodt, F. D., & Wagenmakers, E.-J. (2018). Bayes factor design analysis: Planning for compelling evidence. *Psychonomic Bulletin & Review*, *25*(1), 128–142. https://doi.org/10.3758/s13423-017-1230-y
Schuyler, B., Ollinger, J. M., Oakes, T. R., Johnstone, T., & Davidson, R. J. (2010). Dynamic Causal Modeling applied to fMRI data shows high reliability. *NeuroImage*, *49*(1), 603–611. https://doi.org/10.1016/j.neuroimage.2009.07.015
Seabold, S., & Perktold, J. (2010). *Statsmodels: Econometric and Statistical Modeling with Python*. 92–96. https://doi.org/10.25080/Majora-92bf1922-011
Sehatpour, P., Dondé, C., Hoptman, M. J., Kreither, J., Adair, D., Dias, E., Vail, B., Rohrig, S., Silipo, G., Lopez-Calderon, J., Martinez, A., & Javitt, D. C. (2020). Network-level mechanisms underlying effects of transcranial direct current stimulation (tDCS) on visuomotor learning. *NeuroImage*, *223*, 117311. https://doi.org/10.1016/j.neuroimage.2020.117311
Seth, A. K., & Bayne, T. (2022). Theories of consciousness. *Nature Reviews Neuroscience*, *23*(7), 439–452. https://doi.org/10.1038/s41583-022-00587-4
Shiel, A., Horn, S. A., Wilson, B. A., Watson, M. J., Campbell, M. J., & Mclellan, D. L. (2000). The Wessex Head Injury Matrix (WHIM) main scale: A preliminary report on a scale to assess and monitor patient recovery after severe head injury. *Clinical Rehabilitation*, *14*(4), 408–416. https://doi.org/10.1191/0269215500cr326oa
Shilo, G., & Lavidor, M. (2019). Non-linear effects of cathodal transcranial direct current stimulation (tDCS) of the primary motor cortex on implicit motor learning. *Experimental Brain Research*, *237*(4), Article 4. https://doi.org/10.1007/s00221-019-05477-3
Sitt, J. D., King, J.-R., El Karoui, I., Rohaut, B., Faugeras, F., Gramfort, A., Cohen, L., Sigman, M., Dehaene, S., & Naccache, L. (2014). Large scale screening of neural signatures of consciousness in patients in a vegetative or minimally conscious state. *Brain*, *137*(8), 2258–2270. https://doi.org/10.1093/brain/awu141
Sitt, J. D., King, J.-R., El Karoui, I., Rohaut, B., Faugeras, F., Gramfort, A., Cohen, L., Sigman, M., Dehaene, S., & Naccache, L. (2014). Large scale screening of neural signatures of consciousness in patients in a vegetative or minimally conscious state. *Brain*, *137*(8), Article 8. https://doi.org/10.1093/brain/awu141
Smucny, J. (2021). What transcranial direct current stimulation intensity is best for cognitive enhancement? *Journal of Neurophysiology*, *125*(2), 606–608. https://doi.org/10.1152/jn.00652.2020
Snider, S. B., & Edlow, B. L. (2020). MRI in disorders of consciousness. *Current Opinion in Neurology*, *33*(6), Article 6. https://doi.org/10.1097/WCO.0000000000000873
Song, S., Zilverstand, A., Gui, W., Li, H., & Zhou, X. (2019). Effects of single-session versus multi-session non-invasive brain stimulation on craving and consumption in individuals with drug addiction, eating disorders or obesity: A meta-analysis. *Brain Stimulation*, *12*(3), 606–618. https://doi.org/10.1016/j.brs.2018.12.975
Stafford, C. A., Owen, A. M., & Fernández-Espejo, D. (2019a). The neural basis of external responsiveness in prolonged disorders of consciousness. *NeuroImage: Clinical*, *22*, 101791. https://doi.org/10.1016/j.nicl.2019.101791
Stagg, C. J., & Nitsche, M. A. (2011). Physiological Basis of Transcranial Direct Current Stimulation. *The Neuroscientist*, *17*(1), 37–53. https://doi.org/10.1177/1073858410386614
Stagg, C. J., Antal, A., & Nitsche, M. A. (2018). Physiology of Transcranial Direct Current Stimulation: *The Journal of ECT*, 1. https://doi.org/10.1097/YCT.0000000000000510
Stagg, C. J., Best, J. G., Stephenson, M. C., O'Shea, J., Wylezinska, M., Kincses, Z. T., Morris, P. G., Matthews, P. M., & Johansen-Berg, H. (2009). Polarity-Sensitive Modulation of Cortical Neurotransmitters by Transcranial

Stimulation. *Journal of Neuroscience*, *29*(16), Article 16. https://doi.org/10.1523/JNEUROSCI.4432-08.2009
Stagg, C. J., Bestmann, S., Constantinescu, A. O., Moreno Moreno, L., Allman, C., Mekle, R., Woolrich, M., Near, J., Johansen-Berg, H., & Rothwell, J. C. (2011). Relationship between physiological measures of excitability and levels of glutamate and GABA in the human motor cortex. *The Journal of Physiology*, *589*(23), 5845–5855. https://doi.org/10.1113/jphysiol.2011.216978
Stagg, C. J., Jayaram, G., Pastor, D., Kincses, Z. T., Matthews, P. M., & Johansen-Berg, H. (2011). Polarity and timing-dependent effects of transcranial direct current stimulation in explicit motor learning. *Neuropsychologia*, *49*(5), Article 5. https://doi.org/10.1016/j.neuropsychologia.2011.02.009
Stagg, C. J., O'Shea, J., Kincses, Z. T., Woolrich, M., Matthews, P. M., & Johansen-Berg, H. (2009). Modulation of movement-associated cortical activation by transcranial direct current stimulation. *The European Journal of Neuroscience*, *30*(7), 1412–1423. https://doi.org/10.1111/j.1460-9568.2009.06937.x
Stam, C. J., Nolte, G., & Daffertshofer, A. (2007). Phase lag index: Assessment of functional connectivity from multi channel EEG and MEG with diminished bias from common sources. *Human Brain Mapping*, *28*(11), 1178–1193. https://doi.org/10.1002/hbm.20346
Stefan, S., Schorr, B., Lopez-Rolon, A., Kolassa, I.-T., Shock, J. P., Rosenfelder, M., Heck, S., & Bender, A. (2018). Consciousness Indexing and Outcome Prediction with Resting-State EEG in Severe Disorders of Consciousness. *Brain Topography*, *31*(5), 848–862. https://doi.org/10.1007/s10548-018-0643-x
Stefan, S., Schorr, B., Lopez-Rolon, A., Kolassa, I.-T., Shock, J. P., Rosenfelder, M., Heck, S., & Bender, A. (2018). Consciousness Indexing and Outcome Prediction with Resting-State EEG in Severe Disorders of Consciousness. *Brain Topography*, *31*(5), Article 5. https://doi.org/10.1007/s10548-018-0643-x
Stiefel, K. M., Merrifield, A., & Holcombe, A. O. (2014). The claustrum's proposed role in consciousness is supported by the effect and target localization of Salvia divinorum. *Frontiers in Integrative Neuroscience*, *8*. https://doi.org/10.3389/fnint.2014.00020
Stoodley, C. J., Valera, E. M., & Schmahmann, J. D. (2012). Functional topography of the cerebellum for motor and cognitive tasks: An fMRI study. *NeuroImage*, *59*(2), 1560–1570. https://doi.org/10.1016/j.neuroimage.2011.08.065
Straudi, S., Bonsangue, V., Mele, S., Craighero, L., Montis, A., Fregni, F., Lavezzi, S., & Basaglia, N. (2019). Bilateral M1 anodal transcranial direct current stimulation in post traumatic chronic minimally conscious state: A pilot EEG-tDCS study. *Brain Injury*, *33*(4), 490–495. https://doi.org/10.1080/02699052.2019.1565894
Stultz, D. J., Osburn, S., Burns, T., Pawlowska-Wajswol, S., & Walton, R. (2020). Transcranial Magnetic Stimulation (TMS) Safety with Respect to Seizures: A Literature Review. *Neuropsychiatric Disease and Treatment*, *Volume 16*, 2989–3000. https://doi.org/10.2147/NDT.S276635
Subha, D. P., Joseph, P. K., Acharya U, R., & Lim, C. M. (2010). EEG Signal Analysis: A Survey. *Journal of Medical Systems*, *34*(2), Article 2. https://doi.org/10.1007/s10916-008-9231-z
Tallon-Baudry, C., & Bertrand, O. (1999). Oscillatory gamma activity in humans and its role in object representation. *Trends in Cognitive Sciences*, *3*(4), 12.
Teasdale, G., & Jennett, B. (1974). ASSESSMENT OF COMA AND IMPAIRED CONSCIOUSNESS. *The Lancet*, *304*(7872), 81–84. https://doi.org/10.1016/S0140-6736(74)91639-0
The Multi-Society Task Force on PVS. (1994). Medical aspects of the persistent vegetative state (I). *New England Journal of Medicine*, *330*, 1499–1508.
Thibaut, A., Bruno, M.-A., Ledoux, D., Demertzi, A., & Laureys, S. (2014a). tDCS in patients with disorders of consciousness: Sham-controlled randomized double-blind study. *Neurology*.
Thibaut, A., Chennu, S., Chatelle, C., Martens, G., Annen, J., Cassol, H., & Laureys, S. (2018). Theta network centrality correlates with tDCS response in disorders of consciousness. *Brain Stimulation*, *11*(6), Article 6. https://doi.org/10.1016/j.brs.2018.09.002
Thibaut, A., M.-A. Bruno, D. Ledoux, A. Demertzi, and S. Laureys. 2014. 'TDCS in Patients with Disorders of Consciousness: Sham-Controlled Randomized Double-Blind Study'. *Neurology* 82 (13): 1112–18. https://doi.org/10.1212/WNL.0000000000000260.
Thibaut, A., Schiff, N., Giacino, J., Laureys, S., & Gosseries, O. (2019). Therapeutic interventions in patients with prolonged disorders of consciousness. *The Lancet Neurology*, *18*(6), 600–614. https://doi.org/10.1016/S1474-4422(19)30031-6
Thibaut, A., Wannez, S., Donneau, A.-F., Chatelle, C., Gosseries, O., Bruno, M.-A., & Laureys, S. (2017). Controlled clinical trial of repeated prefrontal tDCS in patients with chronic minimally conscious state. *Brain Injury*, 1–9.

Thibaut, Aurore, Andrea Piarulli, Géraldine Martens, Camille Chatelle, and Steven Laureys. 2019. 'Effect of Multichannel Transcranial Direct Current Stimulation to Reduce Hypertonia in Individuals with Prolonged Disorders of Consciousness: A Randomized Controlled Pilot Study'. *Annals of Physical and Rehabilitation Medicine* 62 (6): 418–25. https://doi.org/10.1016/j.rehab.2019.05.009.

Thibaut, Aurore, Sarah Wannez, Anne-Francoise Donneau, Camille Chatelle, Olivia Gosseries, Marie-Aurélie Bruno, and Steven Laureys. 2017. 'Controlled Clinical Trial of Repeated Prefrontal TDCS in Patients with Chronic Minimally Conscious State'. *Brain Injury* 31 (4): 466–74. https://doi.org/10.1080/02699052.2016.1274776.

Thomas, C., Datta, A., & Woods, A. (2018). Effect of Aging on Cortical Current Flow Due to Transcranial Direct Current Stimulation: Considerations for Safety. *2018 40th Annual International Conference of the IEEE Engineering in Medicine and Biology Society (EMBC)*, 3084–3087. https://doi.org/10.1109/EMBC.2018.8513014

Threlkeld, Z. D., Bodien, Y. G., Rosenthal, E. S., Giacino, J. T., Nieto-Castanon, A., Wu, O., Whitfield-Gabrieli, S., & Edlow, B. L. (2018). Functional networks reemerge during recovery of consciousness after acute severe traumatic brain injury. *Cortex*, *106*, 299–308. https://doi.org/10.1016/j.cortex.2018.05.004

To, W. T., Eroh, J., Hart, J., & Vanneste, S. (2018). Exploring the effects of anodal and cathodal high definition transcranial direct current stimulation targeting the dorsal anterior cingulate cortex. *Scientific Reports*, *8*(1), 4454. https://doi.org/10.1038/s41598-018-22730-x

Truong, Dennis Q., and Marom Bikson. 2018. 'Physics of Transcranial Direct Current Stimulation Devices and Their History': *The Journal of ECT*, August, 1. https://doi.org/10.1097/YCT.0000000000000531.

Ulam, F, C Shelton, L Richards, L Davis, B Hunter, F Fregni, and K Higgins. 2015. 'Cumulative Effects of Transcranial Direct Current Stimulation on EEG Oscillations and Attention/Working Memory during Subacute Neurorehabilitation of Traumatic Brain Injury', 48.

Unal, G., Ficek, B., Webster, K., Shahabuddin, S., Truong, D., Hampstead, B., Bikson, M., & Tsapkini, K. (2020). Impact of brain atrophy on tDCS and HD-tDCS current flow: A modeling study in three variants of primary progressive aphasia. *Neurological Sciences*, *41*(7), Article 7. https://doi.org/10.1007/s10072-019-04229-z

Underwood, E. (2016). Cadaver study challenges brain stimulation methods. *Science*, *352*(6284), 397–397. https://doi.org/10.1126/science.352.6284.397

Van den Bergh, D., van Doorn, J., Marsman, M., Draws, T., van Kesteren, E.-J., Derks, K., Dablander, F., Gronau, Q. F., Kucharský, Š., Gupta, A. R. K. N., Sarafoglou, A., Voelkel, J. G., Stefan, A., Ly, A., Hinne, M., Matzke, D., & Wagenmakers, E.-J. (2020). A Tutorial on Conducting and Interpreting a Bayesian ANOVA in JASP. *L'Année psychologique*, *120*(1), 73–96. https://doi.org/10.3917/anpsy1.201.0073

Vanhaudenhuyse, A., Demertzi, A., Schabus, M., Noirhomme, Q., Bredart, S., Boly, M., Phillips, C., Soddu, A., Luxen, A., Moonen, G., & Laureys, S. (2011). Two Distinct Neuronal Networks Mediate the Awareness of Environment and of Self. *Journal of Cognitive Neuroscience*, *23*(3), 570–578. https://doi.org/10.1162/jocn.2010.21488

Vanhaudenhuyse, A., Noirhomme, Q., Tshibanda, L. J.-F., Bruno, M.-A., Boveroux, P., Schnakers, C., Soddu, A., Perlbarg, V., Ledoux, D., Brichant, J.-F., Moonen, G., Maquet, P., Greicius, M. D., Laureys, S., & Boly, M. (2010). Default network connectivity reflects the level of consciousness in non-communicative brain-damaged patients. *Brain*, *133*(1), 161–171. https://doi.org/10.1093/brain/awp313

Vanhaudenhuyse, Audrey, Athena Demertzi, Manuel Schabus, Quentin Noirhomme, Serge Bredart, Melanie Boly, Christophe Phillips, et al. 2011. 'Two Distinct Neuronal Networks Mediate the Awareness of Environment and of Self'. *Journal of Cognitive Neuroscience* 23 (3): 570–78. https://doi.org/10.1162/jocn.2010.21488.

Van Hoornweder, S., Meesen, R., & Caulfield, K. A. (2022). On the importance of using both T1-weighted and T2-weighted structural magnetic resonance imaging scans to model electric fields induced by non-invasive brain stimulation in SimNIBS. *Brain Stimulation*, *15*(3), 641–644. https://doi.org/10.1016/j.brs.2022.04.010

Vestito, Lucilla, Sara Rosellini, Massimo Mantero, and Fabio Bandini. 2014. 'Long-Term Effects of Transcranial Direct-Current Stimulation in Chronic Post-Stroke Aphasia: A Pilot Study'. *Frontiers in Human Neuroscience* 8 (October). https://doi.org/10.3389/fnhum.2014.00785.

Vimolratana, O., Lackmy-Vallee, A., Aneksan, B., Hiengkaew, V., & Klomjai, W. (2023). Non-linear dose response effect of cathodal transcranial direct current stimulation on muscle strength in young healthy adults: A randomized controlled study. *BMC Sports Science, Medicine and Rehabilitation*, *15*(1), 10. https://doi.org/10.1186/s13102-023-00621-7

Vinck, M., Oostenveld, R., van Wingerden, M., Battaglia, F., & Pennartz, C. M. A. (2011). An improved index of phase-synchronization for electrophysiological data in the presence of volume-conduction, noise and sample-

size bias. *NeuroImage*, *55*(4), 1548–1565. https://doi.org/10.1016/j.neuroimage.2011.01.055
Vöröslakos, M., Takeuchi, Y., Brinyiczki, K., Zombori, T., Oliva, A., Fernández-Ruiz, A., Kozák, G., Kincses, Z. T., Iványi, B., Buzsáki, G., & Berényi, A. (2018). Direct effects of transcranial electric stimulation on brain circuits in rats and humans. *Nature Communications*, *9*(1), 483. https://doi.org/10.1038/s41467-018-02928-3
Wang, F., Hu, N., Hu, X., Jing, S., Heine, L., Thibaut, A., Huang, W., Yan, Y., Wang, J., Schnakers, C., Laureys, S., & Di, H. (2019). Detecting Brain Activity Following a Verbal Command in Patients With Disorders of Consciousness. *Frontiers in Neuroscience*, *13*, 976. https://doi.org/10.3389/fnins.2019.00976
Wang, J., Hu, X., Hu, Z., Sun, Z., Laureys, S., & Di, H. (2020). The misdiagnosis of prolonged disorders of consciousness by a clinical consensus compared with repeated coma-recovery scale-revised assessment. *BMC Neurology*, *20*(1), Article 1. https://doi.org/10.1186/s12883-020-01924-9
Wang, Y., Wang, J., Zhang, Q.-F., Xiao, K.-W., Wang, L., Yu, Q.-P., Xie, Q., Poo, M.-M., & Wen, Y. (2023). Neural Mechanism Underlying Task-Specific Enhancement of Motor Learning by Concurrent Transcranial Direct Current Stimulation. *Neuroscience Bulletin*, *39*(1), 69–82. https://doi.org/10.1007/s12264-022-00901-1
Wijdicks, E. F. M. (2006). *Clinical Scales for Comatose Patients: The Glasgow Coma Scale in Historical Context and the New FOUR Score*.
Windhoff, M., Opitz, A., & Thielscher, A. (2013). Electric field calculations in brain stimulation based on finite elements: An optimized processing pipeline for the generation and usage of accurate individual head models. *Human Brain Mapping*, *34*(4), 923–935. https://doi.org/10.1002/hbm.21479
Witte, Sara De. 2018. 'Left Prefrontal Neuronavigated Electrode Localization in TDCS_ 10–20 EEG System versus MRI-Guided Neuronavigation', 23.
Woods, A., Antal, A., Bikson, M., Boggio, P., Brunoni, A., Celnik, P., Cohen, L., Fregni, F., Herrmann, C., Kappenman, E., Knotkova, H., Liebetanz, D., Miniussi, C., Miranda, P., Paulus, W., Priori, A., Reato, D., Stagg, C., Wenderoth, N., & Nitsche, M. (2016). A technical guide to tDCS, and related non-invasive brain stimulation tools. *Clinical Neurophysiology : Official Journal of the International Federation of Clinical Neurophysiology*, *127*(2), 1031–1048. https://doi.org/10.1016/j.clinph.2015.11.012
Woods, A. J., Bryant, V., Sacchetti, D., Gervits, F., & Hamilton, R. (2015). Effects of Electrode Drift in Transcranial Direct Current Stimulation. *Brain Stimulation*, *8*(3), Article 3. https://doi.org/10.1016/j.brs.2014.12.007
Wu, Min, Yamei Yu, Lunjie Luo, Yuehao Wu, Jian Gao, Xiangming Ye, and Benyan Luo. 2019. 'Efficiency of Repetitive Transcranial Direct Current Stimulation of the Dorsolateral Prefrontal Cortex in Disorders of Consciousness: A Randomized Sham-Controlled Study'. *Neural Plasticity* 2019 (June): 1–11. https://doi.org/10.1155/2019/7089543.
Wutzl, B., Golaszewski, S. M., Leibnitz, K., Langthaler, P. B., Kunz, A. B., Leis, S., Schwenker, K., Thomschewski, A., Bergmann, J., & Trinka, E. (2021). Narrative Review: Quantitative EEG in Disorders of Consciousness. *Brain Sciences*, *11*(6), Article 6. https://doi.org/10.3390/brainsci11060697
Xu, Z., Zheng, R., Xia, T., Qi, Z., Zang, D., Wang, Z., & Wu, X. (2022). Behavioral effects in disorders of consciousness following transcranial direct current stimulation: A systematic review and individual patient data meta-analysis of randomized clinical trials. *Frontiers in Neurology*.
Yamaguchi, T., Moriya, K., Tanabe, S., Kondo, K., Otaka, Y., & Tanaka, S. (2020). Transcranial direct-current stimulation combined with attention increases cortical excitability and improves motor learning in healthy volunteers. *Journal of NeuroEngineering and Rehabilitation*, *17*(1), 23. https://doi.org/10.1186/s12984-020-00665-7
Yosephi, M. H., Ehsani, F., Zoghi, M., & Jaberzadeh, S. (2018). Multi-session anodal tDCS enhances the effects of postural training on balance and postural stability in older adults with high fall risk: Primary motor cortex versus cerebellar stimulation. *Brain Stimulation*, *11*(6), 1239–1250. https://doi.org/10.1016/j.brs.2018.07.044
Yushkevich, P. A., Gao, Y., & Gerig, G. (2016). ITK-SNAP: An interactive tool for semi-automatic segmentation of multi-modality biomedical images. *2016 38th Annual International Conference of the IEEE Engineering in Medicine and Biology Society (EMBC)*, 3342–3345. https://doi.org/10.1109/EMBC.2016.7591443
Zeidman, P., Jafarian, A., Corbin, N., Seghier, M. L., Razi, A., Price, C. J., & Friston, K. J. (2019a). A guide to group effective connectivity analysis, part 1: First level analysis with DCM for fMRI. *NeuroImage*, *200*, 174–190. https://doi.org/10.1016/j.neuroimage.2019.06.031
Zeidman, P., Kazan, S. M., Todd, N., Weiskopf, N., Friston, K. J., & Callaghan, M. F. (2019). Optimizing Data for Modeling Neuronal Responses. *Frontiers in Neuroscience*, *12*, 986. https://doi.org/10.3389/fnins.2018.00986
Zhang, B., Karri, J., O'Brien, K., DiTommaso, C., Kothari, S., & Li, S. (n.d.). Spasticity Management in Persons with

Disorders of Consciousness. *PM&R*, *n/a*(n/a). https://doi.org/10.1002/pmrj.12458
Zhang, C., Han, S., Li, Z., Wang, X., Lv, C., Zou, X., Zhu, F., Zhang, K., Lu, S., Bie, L., Lv, G., & Guo, Y. (2022). Multidimensional Assessment of Electroencephalography in the Neuromodulation of Disorders of Consciousness. *Frontiers in Neuroscience*, *16*, 903703. https://doi.org/10.3389/fnins.2022.903703
Zhang, R., Zhang, L., Guo, Y., Shi, L., Gao, J., Wang, X., & Hu, Y. (2020). Effects of High-Definition Transcranial Direct-Current Stimulation on Resting-State Functional Connectivity in Patients With Disorders of Consciousness. *Frontiers in Human Neuroscience*, *14*, 560586. https://doi.org/10.3389/fnhum.2020.560586
Zhang, X., Liu, B., Li, Y., Duan, G., Hou, J., & Wu, D. (2021). Multi-Target and Multi-Session Transcranial Direct Current Stimulation in Patients With Prolonged Disorders of Consciousness: A Controlled Study. *Frontiers in Neuroscience*, *15*, 641951. https://doi.org/10.3389/fnins.2021.641951
Zhang, Y., Song, W., Du, J., Huo, S., Shan, G., & Li, R. (2017). Transcranial Direct Current Stimulation in Patients with Prolonged Disorders of Consciousness: Combined Behavioral and Event-Related Potential Evidence. *Frontiers in Neurology*, *8*. https://www.frontiersin.org/articles/10.3389/fneur.2017.00620
Zhao, T., Zhu, Y., Tang, H., Xie, R., Zhu, J., & Zhang, J. H. (2019). Consciousness: New Concepts and Neural Networks. *Frontiers in Cellular Neuroscience*, *13*. https://www.frontiersin.org/articles/10.3389/fncel.2019.00302
Zhavoronkova, L. A., Boldyreva, G. N., Kuptsova, S. V., Sharova, E. V., Smirnov, A. S., & Pronin, I. N. (2017). FMRI responses of the brain during active and passive movements in left-handed subjects. *Human Physiology*, *43*(2), 191–198. https://doi.org/10.1134/S0362119717010108
Zhuang, X., Yang, Z., & Cordes, D. (2020). A technical review of canonical correlation analysis for neuroscience applications. *Human Brain Mapping*, *41*(13), 3807–3833. https://doi.org/10.1002/hbm.25090